A N N U A L R E P O R T

1964

U. S. WATER CONSERVATION LABORATORY
Southwest Branch
Soil and Water Conservation Research Division
Agricultural Research Service
United States Department of Agriculture
Tempe, Arizona

ADMINISTRATIVELY CONFIDENTIAL

This report contains unpublished and confidential information concerning work in progress. The contents of this report may not be published or reproduced in any form without the prior consent of the research workers involved.

4777

LABORATORY STAFF

Professional:

Dr. H. Bouwer, Research Hydraulic Engineer
Mr. K. J. Brust, Agricultural Engineer
Dr. W. L. Ehrler, Research Plant Physiologist
Mr. L. J. Erie, Research Agricultural Engineer
Mr. G. W. Frasier, Agricultural Engineer
Dr. L. J. Fritschen, Research Meteorologist
Mr. I. C. McIlroy, Soil Scientist
Dr. R. D. Jackson, Research Physicist
Mr. L. E. Myers, Research Hydraulic Engineer
Dr. F. S. Nakayama, Research Chemist
Mr. R. J. Reginato, Research Soil Scientist
Dr. J. A. Replogle, Research Agricultural Engineer
Mr. R. C. Rice, Agricultural Engineer
Dr. C. H. M. van Bavel, Research Physicist

Technicians:

E. D. Escarcega, Engineering Draftsman
R. G. Flores, Engineering Draftsman
O. F. French, Hydraulic Engineering Technician
J. L. Gale, Physical Science Aid
J. R. Griggs, Physical Science Technician
A. N. Lehman, Physical Science Aid
L. E. Lisonbee, Physical Science Aid
J. L. MacIntyre, Physical Science Technician
R. B. MacIntyre, Physical Science Aid
J. B. Miller, Physical Science Technician
S. T. Mitchell, Physical Science Technician
K. G. Mullins, Physical Science Technician
B. A. Rasnick, Physical Science Technician
A. F. Sandecki, Physical Science Technician
W. E. Schmidt, Physical Science Technician
D. R. Sowell, Physical Science Aid
B. W. Tilden, Soils Research Helper

Administrative, Clerical and Maintenance:

O. J. Abeyta, Laborer
E. D. Bell, General Machinist
E. E. De La Rosa, Janitor
A. V. Figueroa, Laborer
B. E. Fisher, Library Assistant
D. S. Fry, Clerk-Stenographer
C. E. Hansen, Secretary

Administrative, Clerical and Maintenance (Cont'd):

C. G. Hiesel, General Machinist
R. C. Klapper, Refrigeration & Air Conditioning Mechanic
J. M. R. Martinez, Laborer
R. S. Miller, Administrative Clerk
A. H. Morse, Clerk-Dictating Machine Transcriber
M. E. Olson, Clerk-Stenographer
M. A. Seiler, Clerk-Stenographer
M. F. Witcher, Clerk-Stenographer
M. M. Zamora, Laborer

CHANGES IN PERSONNEL

The Laboratory staff has been strengthened during 1964 by the addition of four new members. They are as follows:

R. G. Flores, Engineering Draftsman
J. L. Gale, Physical Science Aid
A. N. Lehman, Physical Science Aid
R. B. MacIntyre, Physical Science Aid

Mr. I. C. McIlroy, Soil Scientist, joined our staff as a visiting scientist during 1964. He has returned to his native Australia, where he is employed by C. S. I. R. O.

Also during 1964 there were seven resignations. They are as follows:

E. D. Escarcega, Engineering Draftsman (Military Furlough)
L. E. Lisonbee, Physical Science Aid
J. L. MacIntyre, Physical Science Technician
A. F. Sandecki, Physical Science Aid
W. F. Schmidt, Physical Science Technician
D. R. Sowell, Physical Science Aid
B. W. Tilden, Soils Research Helper

The Laboratory staff is now essentially at full strength with one or two exceptions.

TABLE OF CONTENTS [1/]

TITLE	SECTION
Dynamic Similarity in Elbow Flow Meters. J. A. Replogle, K. J. Brust, L. E. Myers	2
Calibration and Evaluation of Net Radiometers. Leo J. Fritschen	6
Soil Treatment to Reduce Infiltration and Increase Precipitation Runoff. L. E. Myers, G. W. Frasier	7
Application of Hexadecanol-Octadecanol Monofilms to Small Ponds. L. E. Myers, G. W. Frasier	9
Field Application of Falling-Head Technique for Seepage Meters and of Double-Tube Method for Hydraulic Conductivity Measurement. H. Bouwer, R. C. Rice	14
Analyzing Ground Water Mound Formation by Resistance Network Analogs. H. Bouwer	15
Components of the Radiation Balance of Field Crops Under Irrigated Conditions. L. J. Fritschen	18
The Use of Salty Well Water for the Pre-Planting Irrigation on Silty Clay Soils. L. J. Erie, O. F. French	22
Consumptive Use of Water by Crops in Arizona. L. J. Erie, O. F. French	23
Theoretical Effect of Soil, Water Table, and Canal Conditions on Seepage from Canals. H. Bouwer	24
Measuring Horizontal and Vertical Hydraulic Conductivity of Soil with the Double-Tube Method. H. Bouwer, R. C. Rice	25
Nondestructive Beta Ray Transmission Method for Measuring Water Content in Plants. F. S. Nakayama, W. L. Ehrler	26
Leaf Temperature Measurements. F. S. Nakayama, W. L. Ehrler	26A
Water Absorption, Transpiration, and Internal Water Balance of Cotton Plants as Affected by Changes in Evaporative Demands. W. L. Ehrler, C. H. M. van Bavel, F. S. Nakayama	29

1/ Research outlines that have been terminated or that are inactive are not listed.

TITLE	SECTION
Quantitative Measurement of Water Flow with Chemical Tracers. J. A. Replogle, K. J. Brust, L. E. Myers	30
Water Vapor Diffusion in Soils. R. D. Jackson	31
Micrometeorological Determinations of Water Loss from Various Surfaces. L. J. Fritschen	32
Direct Measurement of Evapotranspiration and the Energy Balance of Irrigated Crops. C. H. M. van Bavel, I. C. McIlroy	33
Exchange of Water Vapor with Plant Leaves and Its Relation to Stomatal Diffusive Resistance. F. S. Nakayama ...	34
Water Management for the Efficient Irrigation of Safflower. L. J. Erie, O. F. French	35
Clay Dispersants for the Reduction of Seepage Losses from Reservoirs. R. J. Reginato, L. E. Myers	37
Waterborne Sealants to Reduce Seepage Losses from Unlined Channels and Reservoirs. R. J. Reginato, L. E. Myers	38
Crack Sealants for Concrete Lined Canals. R. J. Reginato, L. E. Myers	39
Dispersion and Flocculation of Soil and Clay Materials as Related to the Na and Ca Status of the Ambient Solution. F. S. Nakayama	40
Manuscripts Approved and/or Published in 1964	AI

WORK AND LINE PROJECTS AND RESEARCH OUTLINES 1/

Work Project	Line Project	Research Outline Code No. 2/ Ariz.-WCL	Title
SWC-4			Conservation of Water Supplies for Agricultural Use.
	gG1		Measurement, Evaluation and Control of Seepage Losses.
		14	Field Application of Falling-Head Technique for Seepage Meters and of Double-Tube Method for Hydraulic Conductivity Measurement. H. Bouwer, R. C. Rice.
		24	Theoretical Effect of Soil, Water Table, and Canal Conditions on Seepage from Canals. H. Bouwer.
		25	Measuring Horizontal and Vertical Hydraulic Conductivity of Soil with the Double-Tube Method. H. Bouwer, R. C. Rice.
		37	Clay Dispersants for the Reduction of Seepage Losses from Reservoirs. R. J. Reginato, L. E. Myers.
		38	Waterborne Sealants to Reduce Seepage Losses from Unlined Channels and Reservoirs. R. J. Reginato, L. E. Myers.
		39	Crack Sealants for Concrete Lined Canals. R. J. Reginato, L. E. Myers.
	gG2		Atmospheric and Related Boundary Mechanisms in Water Vapor Losses from Plant, Soil and Water Surfaces.
		6	Calibration and Evaluation of Net Radiometers. L. J. Fritschen.

1/ Research outlines that have been terminated or are inactive are not listed.

2/ Research outline code number also indicates section number.

Work Project	Line Project	Research Outline Code No.	Title
SWC-4	gG2	9	Application of Hexadecanol-Octadecanol Monofilms to Small Ponds. L. E. Myers, G. W. Frasier.
		18	Components of the Radiation Balance of Field Crops Under Irrigated Conditions. L. J. Fritschen.
		32	Micrometeorological Determinations of Water Loss from Various Surfaces. L. J. Fritschen.
		33	Direct Measurement of Evapotranspiration and the Energy Balance of Irrigated Crops. C. H. M. van Bavel, I. C. McIlroy.
	gG3		Measurement, Evaluation and Control of Infiltration to Conserve Water.
		7	Soil Treatment to Reduce Infiltration and Increase Precipitation Runoff. L. E. Myers, G. W. Frasier.
		15	Analyzing Ground Water Mound Formation by Resistance Network Analogs. H. Bouwer.
		22	The Use of Salty Well Water for the Pre-Planting Irrigation on Silty Clay Soils. L. J. Erie, O. F. French.
		40	Dispersion and Flocculation of Soil and Clay Materials as Related to the Na and Ca Status of the Ambient Solution. F. S. Nakayama.
	gG4		Physical Processes in the Soil Affecting Preventable Losses of Water by Surface Evaporation.
		31	Water Vapor Diffusion in Soils. R. D. Jackson.

Work Project	Line Project	Research Outline Code No.	Title
	gG5		Water Measurement and Control for Water Conservation.
		2	Dynamic Similarity in Elbow Flow Meters. J. A. Replogle, K. J. Brust, L. E. Myers.
		30	Quantitative Measurement of Water Flow with Chemical Tracers. J. A. Replogle, K. J. Brust, L. E. Myers.
SWC-5			Irrigation Principles, Requirements, Practices and Facilities for Efficient Use of Water on Farms.
	g2		Irrigation Requirements of Forage and Cultivated Crops in the Southwest.
		35	Water Management for the Efficient Irrigation of Safflower. L. J. Erie, O. F. French.
SWC-11			Soil, Water, and Plant Relations as They Affect Use of Land and Water Resources.
	gG1		Uptake and Disposal of Water by Plants in an Arid Climate.
		23	Consumptive Use of Water by Crops in Arizona. L. J. Erie. O. F. French.
		26	Nondestructive Beta Ray Transmission Method for Measuring Water Content in Plants. F. S. Nakayama, W. L. Ehrler.
		26A	Leaf Temperature Measurements. F. S. Nakayama, W. L. Ehrler.

Work Project	Line Project	Research Outline Code No.	Title
SWC-11	gG1	29	Water Absorption, Transpiration, and Internal Water Balance of Cotton Plants as Affected by Changes in Evaporative Demands. W. L. Ehrler, C. H. M. van Bavel, F. S. Nakayama.
		34	Exchange of Water Vapor with Plant Leaves and Its Relation to Stomatal Diffusive Resistance. F. S. Nakayama.

TITLE: DYNAMIC SIMILARITY IN ELBOW FLOW METERS

LINE PROJECT: SWC 4-gG5 CODE NO.: Ariz.-WCL-2

INTRODUCTION:

Elbow flow meters, while long known to hydraulic engineers, have not been enthusiastically accepted for other than calibrated-in-place uses. This is understandable since various investigators have reported results that appear to be conflicting and somewhat inconsistant. Two or more methods of analysis are seemingly supported by the various data. The usual conclusion to be obtained from the previous work was that uncalibrated elbow flow meters were at best only ± 10 percent accurate. This conclusion might be credited to efforts trying to describe the calibration of elbow meters with an equation of the form

$$Q = a\sqrt{H} \qquad [1]$$

where Q is the discharge, a is a coefficient including elbow geometry effects and calibration effects, and H is the pressure differential between the inside and outside walls of the elbow at the midpoint of the bend. An equation of this form can be derived from analytical considerations that satisfactorily describes the flow relation for the 3-inch elbows tested in this investigation, deviating a maximum of 3.7 percent from calibrated values. However, this square-root relation does not satisfactorily describe the relation for the larger elbows.

The goal of this study was to calibrate a sufficient number of elbows in each size category and establish an empirical relationship capable of predicting the discharge for uncalibrated elbows to within ± 5 percent.

PROCEDURE:

The 37 commercial 90-degree elbows tested in 1963 were calibrated using a triangular weir and a rectangular weir. The triangular weir was checked volumetrically and was used for the 3-inch elbows. The larger elbows were calibrated on a higher capacity system against a rectangular weir for which the calibration was uncertain. Consequently,

after reconstructing the hydraulic facilities of the laboratory to include a constant head tank and weighing tank with beam scales facilities, these larger elbows were spot checked for calibration. Several inconsistancies were noted as a result of the uncertain difficulty in reading the average depth over the weir at high discharges. Ultimately, it was decided to recheck all those elbows associated with the rectangular weir measurements. This is now completed except for four of the 10-inch elbows.

The elbows were installed in essentially the same manner as was used on the previous calibration with approximately 20 diameters of straight pipe upstream and 10 diameters downstream from the elbow. (See Annual Reports for 1962 and 1963.) The discharge rating curves were determined gravimetrically using the recently designed and installed constant head tank and gravimetric weighing system, Figure 1. This system can measure discharges over a wide range of flows from less than 0.01 cfs to 5.7 cfs (the pumping capacity of the system).

An empirical equation of the form

$$Q = aH^E \qquad [2]$$

was selected for each elbow type and size. In this equation Q is the discharge, H is the pressure differential between pressure taps located on the inside and outside of the bend, and a and E are the intercept on the unity axis and the slope, respectively, of a log-log plot of the data for each type and size.

DISCUSSION AND RESULTS:

In all but two cases the developed equation predicted flow rates within 5 percent over the range calibrated. The two cases in point involved two 3-inch elbows manufactured by the Clow Company (elbows No. 7 and No. 8) and a 12-inch elbow manufactured by the Stockham Company (elbow No. 42). Measurements of the physical dimensions of these elbows disclosed variations from the other elbows tested. The 3-inch elbows No. 7 and No. 8 had different radii of curvature and slightly different diameters than the average of the other elbows. To accomodate the observable characteristics of the individual elbows,

a generalized equation of a form similar to that analytically obtainable is

$$Q = K\sqrt{2g}\,\frac{\pi D^2}{4}\sqrt{\frac{R}{2D}}\;H^E \qquad [3a]$$

or

$$Q = 4.45K\,R^{1/2}\,D^{3/2}\,H^E \qquad [3b]$$

where K is a constant determined for each elbow size and type, g is the gravitational constant, D is the measured elbow diameter, and R is the center line radius of curvature. All dimensions are expressed in feet. Q, H, and E are as previously defined. Values of K for each elbow type and size are tabulated in Table 1.

These values are based on average dimensions obtained for all elbows of each size and type tested. Where plaster-casting data were readily available for values of the center-line radius of curvature, they were incorporated into the tabulation. When such information was not yet available, the best values obtainable by measuring observable tangent lengths and face-to-center dimensions were substituted. The structure of equation [3] shows that a 10 percent error in determining the value for R produces a 5 percent error in Q while the same error in D produces 15 percent error in Q. It is fortunate that D is the more easily determined dimension. The exponent, E, was found to have an average value for a large number of elbows given by

$$E = 0.032D + 0.493 \qquad [4]$$

(see Figure 2). Only the values for the alternate flow directions of one elbow of the 10-inch size are shown in Figure 2 since four others remain to be recalibrated.

The 12-inch elbow No. 47 displayed a 10 percent difference between calibration in the alternate directions through the elbow. The pressure readings in one direction for a given discharge were about 9 percent higher than similar readings for the other 12-inch elbows. A plaster cast was made of the inside and outside of the bend. In this manner

an accurate representation was obtained of the flow path along the elbow wall and over the manometer taps. On this particular elbow, the inside bend radius was found to vary considerably from flange to flange. This was made very apparent by plotting a profile of the casting and then folding the plot in such a way that the two halves of the plot could be visually matched. If the elbow radius of curvature were symmetrical with respect to the piezometer tap, the two directions of flow should produce similar results. In elbow No. 42, the two halves were not symmetrical. The center tap was correctly located at the center of the bend, but the two half curves of the inside bend did not have the same curvature. When the two corresponding halves were checked for symmetry by folding the plotted profiles together, as much as 3/16-inch differences were noted between corresponding points of symmetry. When this elbow was further modified by grinding with a power grinder along the inside bend, radical changes in calibration occurred. Similar grinding on the outside bend produced no noticeable change. It is concluded that the condition of the inside bend is critical.

Plaster casts of the inside bend are easily achieved by simply oiling the surface to be cast and trowling a ribbon of casting plaster along the bend an inch or so wide and about 1 inch thick, depending on the elbow size. Before it sets, wire mesh can be pressed into the plaster for reinforcement. The bend profile can be projected onto drawing paper in a number of ways, the simplest is probably with a drawing triangle and pencil. If examination of this inside-bend profile shows it to be reasonably symmetrical, it is likely that the sand mold casting is within the tolerances necessary to meet the qualifications of the calibrations reported herein. If severe asymmetry is noted, the elbow should be discarded for use as a meter unless calibrated in place.

Average calibration equations for each size and type of elbow are presented with the corresponding calibration curve in Figure 3. These were used to establish the universal relation implied by equations [3] and [4]. The envelopes of scatter of each datum point from the respective average calibration equation are shown in

Figures 4 to 9, as a ratio of measured discharge, Q, to computed discharge, Q_{log}, plotted against the measured discharge, Q. The 5 percent limit is also shown. As explained previously, elbows No. 7 and No. 8, which deviate as plotted by as much as 9 percent can be corrected to within 3 percent by considering observable dimensional variations. Table 2 tabulates pertinent dimensional data obtained for selected elbows by using casting plaster. Two of the elbows, No. 21 and No. 42, should not be considered for elbow meters because of their asymmetry. They can be satisfactorily used with equation [3] by inserting the radius of curvature for the elbow-half that appraoches the inside bend manometer tap. The calculated values for "a" in Table 2 are based on K values derived from all elbows of each type and size tested (see Table 1).

Further checks on the effects of disturbances were conducted with the 12-inch and 6-inch elbows. A flow was established through the elbows using the constant head tank as the supply source. The elbow flanges were clamped and the bolts removed. In this way, an offset in the alignment of either face of the elbow could be achieved by slight loosening of the clamps and offsetting the pipe while still maintaining the same discharge. On the 12-inch elbow severe offsets on the order of 1/4 to 1/2 the bolt hole diameter were necessary to produce approximately 1 percent difference in pressure differential. An upstream offset was more sensitive than a downstream offset. On the 6-inch elbow 1/16-inch offsets of the downstream pipe toward the inside bend caused a 0.9 percent increase in differential reading and a 1/16-inch offset to the outside bend caused a 0.3 percent decrease. Similar treatment with the upstream face caused increases in differential in both cases of 0.5 percent and 1.3 percent, respectively.

It was concluded that the sources of error caused by misalignment can be prevented by carefully aligning the flange bolt holes with tight fitting pins or bolts.

It should be emphasized that in all cases where accurately determined dimensions of the elbow were available, agreement with

the general equation, equation [3], was achieved well within the 5 percent goals. (See Table 2.)

SUMMARY AND CONCLUSIONS:

Recently installed hydraulic calibration equipment, including a constant head tank and gravimetric flow measuring system capable of 0.1 percent accuracy, allowed check calibrations of the elbow flow meters of 6-, 10-, and 12-inch sizes. Previous methods were uncertain to the degree of accuracy desired. Four 10-inch elbows remain to be checked.

An empirical equation was developed that represented the 37 elbows tested. The elbows ranged in size from 3 inches to 12 inches. The equation is

$$Q = K\sqrt{2g}\,\frac{\pi D^2}{4}\sqrt{\frac{R}{2D}}\,H^{0.032D + 0.493}$$

where Q is the discharge, K is a constant determined for each elbow size and type, g is the gravitational constant, D is the measured elbow diameter, R is the center-line radius of curvature, and H is the pressure differential between manometer taps located at the mid-point in the inside and outside bends of the elbow.

The increase in the value of the exponent in the above equation with elbow size is believed to be a scale effect associated with the strength of secondary currents induced in the bend.

This equation satisfactorily describes the discharge relationships for all elbows tested for flow velocities in excess of 3 feet per second with an accuracy of $\pm$ 5 percent. On all but the 12-inch elbows, flow rates at lower velocities, usually down to 1 or 1 1/2 feet per second, are satisfactorily described within this same accuracy.

Plaster castings of the inside and outside bends, made by trowling a 1-inch thick ribbon of casting plaster which was reinforced with wire mesh along the flow path that passed over the pressure taps, allowed accurate determination of critical elbow dimensions. The effective radius of curvature could be determined, as well as the degree of symmetry. An elbow that is not symmetrical with respect

to the center of the bend is indicative of a poorly cast elbow and should be discarded for use as an elbow meter. Good agreement with the general equation to better than ± 3 percent accuracy was achieved in all cases where plaster cast dimensions were obtained. Inferred dimensions obtained from manufacturing specifications were inconsistant and appeared to depend on the manufacturer's particular sand mold. The die-cast, plastic elbows proved symmetrical and dimensionally consistant so that uncalibrated similar elbows can be exptected to perform within ± 2 percent.

PERSONNEL: J. A. Replogle, K. J. Brust, L. E. Myers

Table 1. Average dimensions and coefficient, K, for selected elbow sizes.

Nom. size	Type	$\bar{R}$ 1/	$\bar{D}$ 2/	Equation from calibration	K 3/
in		ft	ft		
12	Cast iron	0.856	0.998	$Q = 4.33\ H^{0.522} \pm 0.143$ cfs	1.054
10	Cast iron	0.800	0.830	$Q = 3.06\ H^{0.538} \pm 0.133$ cfs	1.016
6	Cast iron	0.580	0.494	$Q = 1.16\ H^{0.508} \pm 0.052$ cfs	0.980
3	Cast iron	0.351	0.248	$Q = 0.327\ H^{0.498} \pm 0.012$ cfs	1.004
3 long radius	Cast iron	0.528	0.249	$Q = 0.409\ H^{0.498} \pm 0.009$ cfs	1.018
3 short turn	Plastic	0.300	0.256	$Q = 0.300\ H^{0.500} \pm 0.009$ cfs	0.949
3 long turn	Plastic	0.380	0.256	$Q = 0.344\ H^{0.502} \pm 0.008$ cfs	0.969
3 long turn	Plastic reversed	0.380	0.256	$Q = 0.334\ H^{0.499} \pm 0.005$ cfs	0.940

1/ Average center line radius of elbow determined by plaster casting when available or estimated from consideration of measured tangent lengths.

2/ Average diameters of all elbows tested of similar size; determined from end measurements.

3/ K value required to match calibration equation with equation [3].

Table 2. Dimensions of selected elbows obtained with casting plaster.

Elbow number	Size	Radius[1/] inside bend	Radius[1/] outside bend	Center-line radius R	a [3/] (calculated)	a' (calibrated)	ϵ_a [4/]	Remarks
	in	in	in	in			%	
3 cast iron	3	2.57	-	4.07 [2/]	0.326 [5/] 0.326	0.321 [5/] 0.320	+ 1.5 + 1.9	Inside bend circular over 85°. Center tap accurate to ± 0.05".
21 cast iron	6	4.85 3.88	9.83 9.83	7.34 6.86	1.192 1.150	1.161 1.108	+ 2.7 + 3.8	Asymmetrical; R_i varied from 4.85" to 3.00"; ± 0.1" variations.
33 cast iron	10	4.52	14.40	9.46	-	-	-	Calibrated irradically; Burr found near tap.
40 cast iron	12	4.23 4.23	15.94 15.94	10.08 10.08	4.31 4.30	4.24 4.27	+ 1.7 + 0.7	Diameter varied affecting calculated value for "a".
42 cast iron	12	4.30 4.12	16.61 16.61	10.46 10.37	4.39 4.38	4.04 4.51	+ 0.8 - 2.9	Asymmetrical ± 0.2 to 0.25" variations. R_i varied from 4.3" to 4.12".

1/ Based on center 2/3 of bend or 2/3 of half bend if asymmetrical and two values appear in table.
2/ Calculated by adding half of pipe diameter to inside radius.
3/ Calculated from equations [2] and [3] using K from Table 1.
4/ Percent difference, 100(a - a')/a'.
5/ Two values are for alternate flow directions.

Table 2. Continued.

Elbow number	Size	Radius 1/ inside bend	Radius 1/ outside bend	Center-line radius R	a 3/ (calculated)	a' (calibrated)	ϵ_a 4/	Remarks
	in	in	in	in			%	
P_2 ABS plastic	3 long turn	3.00	6.22	4.61	0.346 5/ 0.336	0.338 5/ 0.331	+ 2.4 + 1.5	Symmetrical; center tap off by 0.2"; Reversibility poor, 3.0% difference.
P_3 ABS plastic	3 long turn	2.96	6.14	4.55	0.342 0.334	0.347 0.335	- 1.4 - 0.3	Same as above.
P_4 ABS plastic	3 short turn	2.02	5.19	3.61	0.300 0.300	0.298 0.304	+ 0.6 - 1.3	Very symmetrical. Inside bend center tap mislocated 0.1". Reversibility acceptable.

1/ Based on center 2/3 of bend or 2/3 of half bend if asymmetrical and two values appear in table.
2/ Calculated by adding half of pipe diameter to inside radius.
3/ Calculated from equations [2] and [3] using K from Table 1.
4/ Percent difference, 100(a - a')/a'.
5/ Two values are for alternate flow directions.

SCHEMATIC OF

RECIRCULATING AND FLOW MEASURING SYSTEM

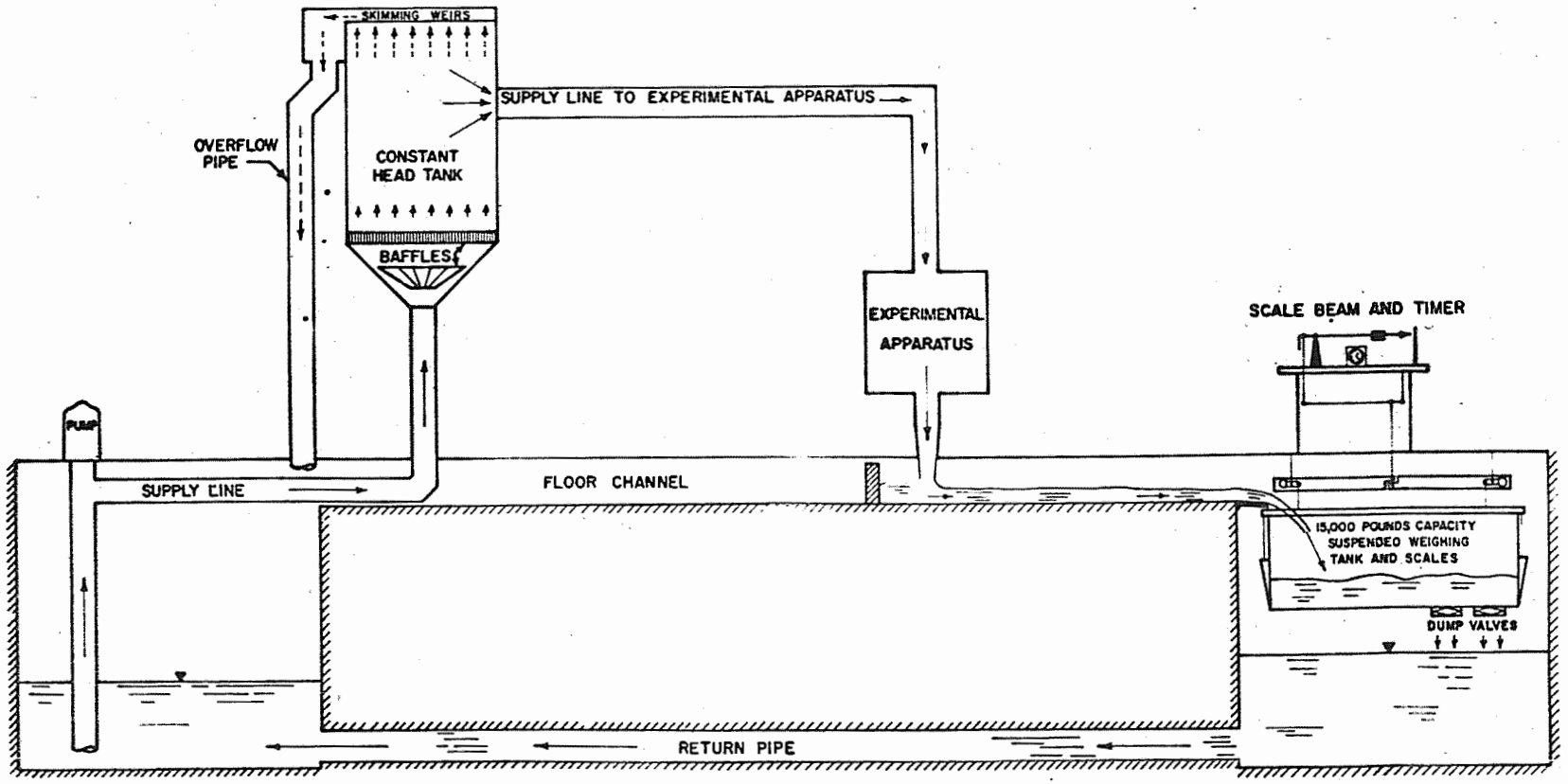

Figure 1. Schematic of recirculating and flow measuring system.

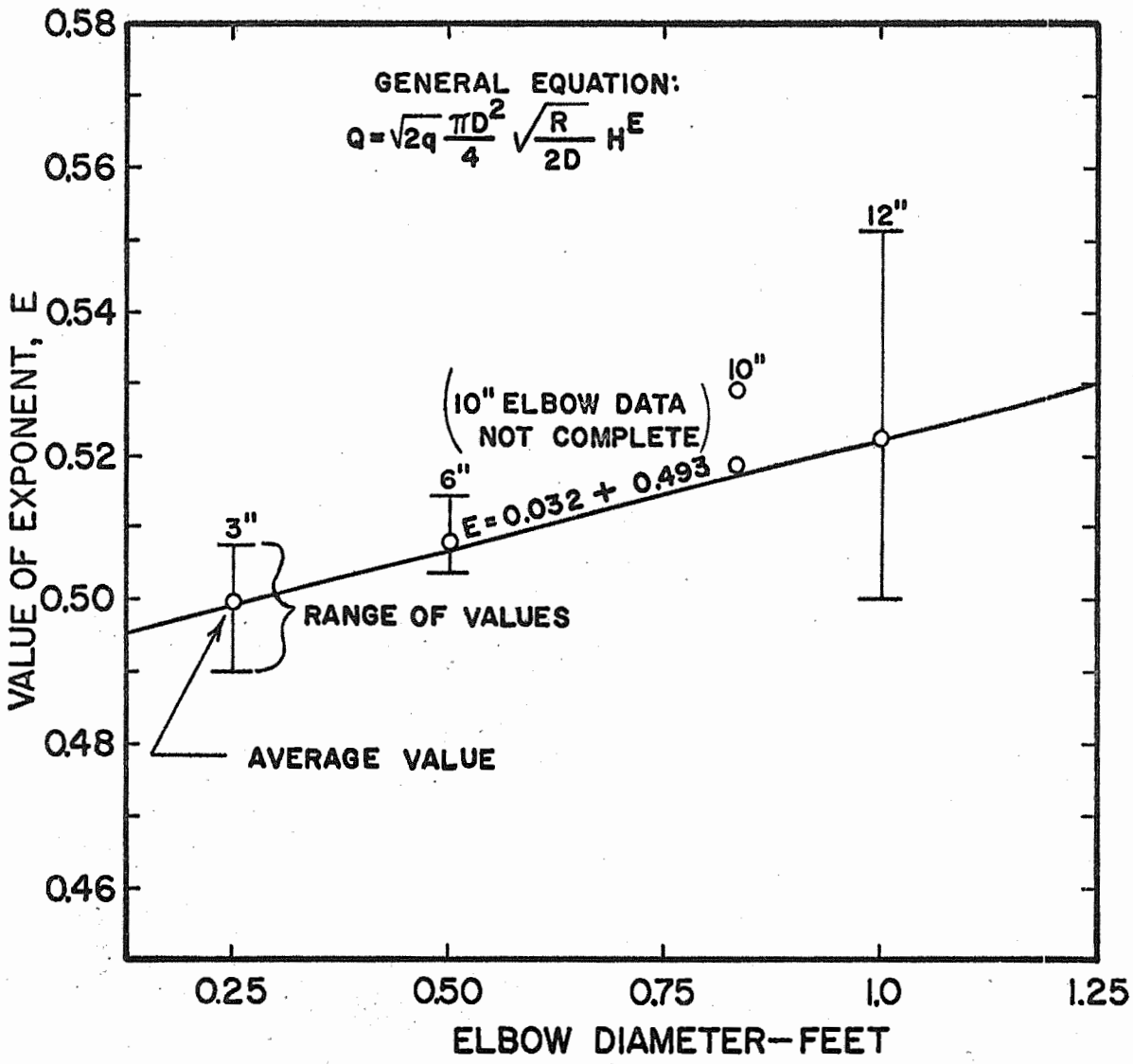

Figure 2. Variation of exponent, E, with elbow meter size.

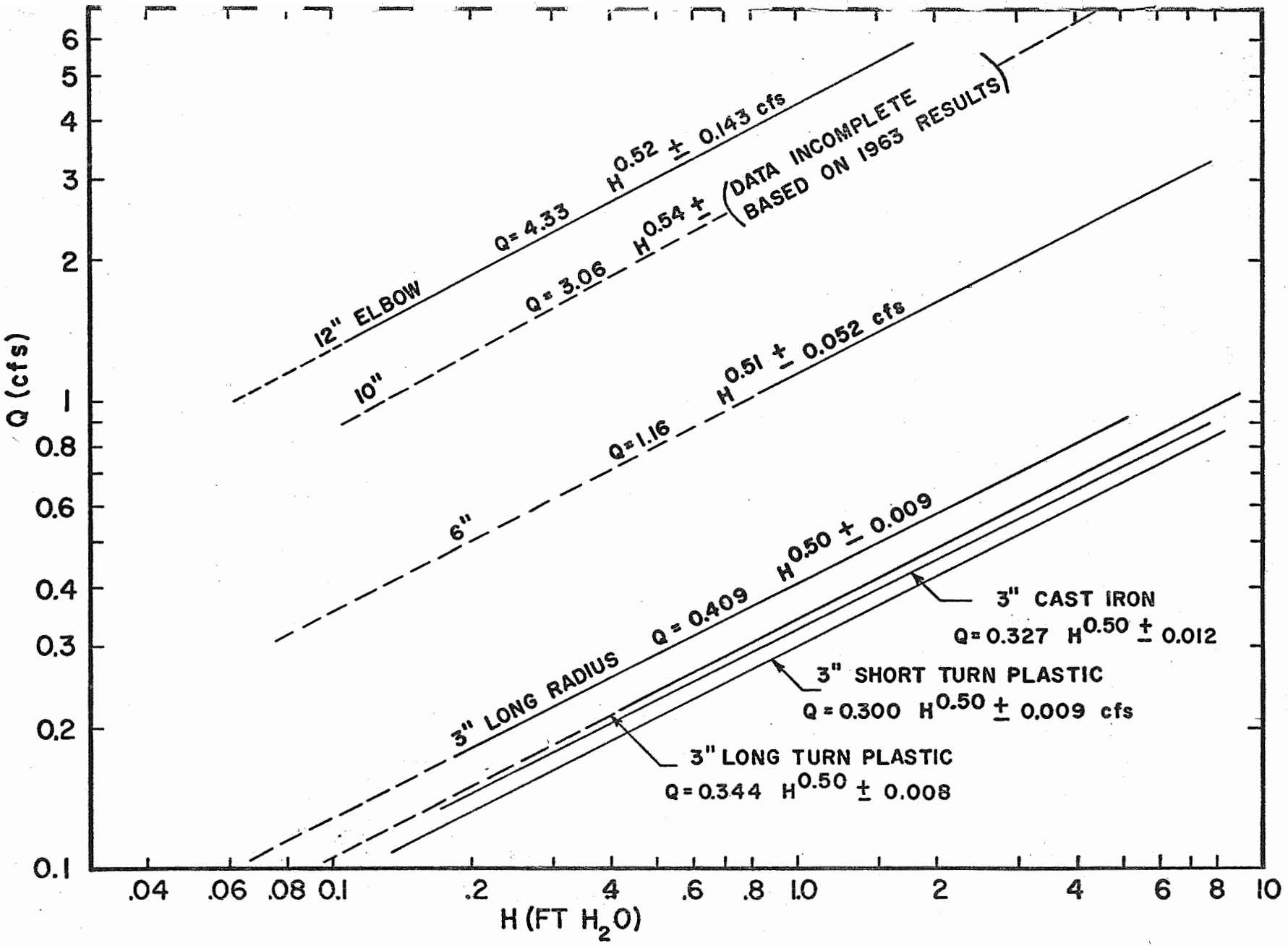

Figure 3. Calibration curves for elbow flow meters.

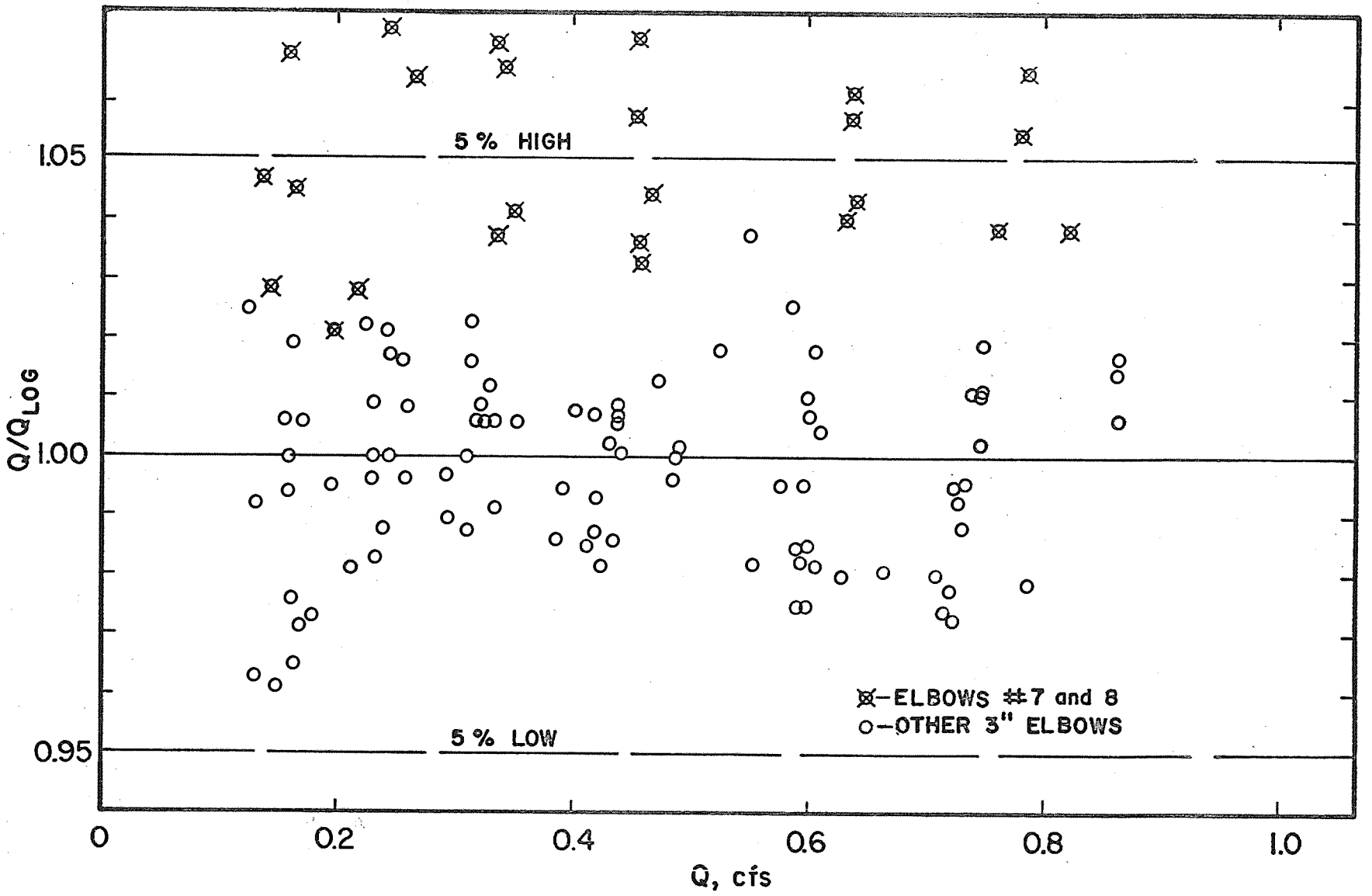

Figure 4. Scatter of calibration data from selected average equation for 3-inch cast iron elbow meters.

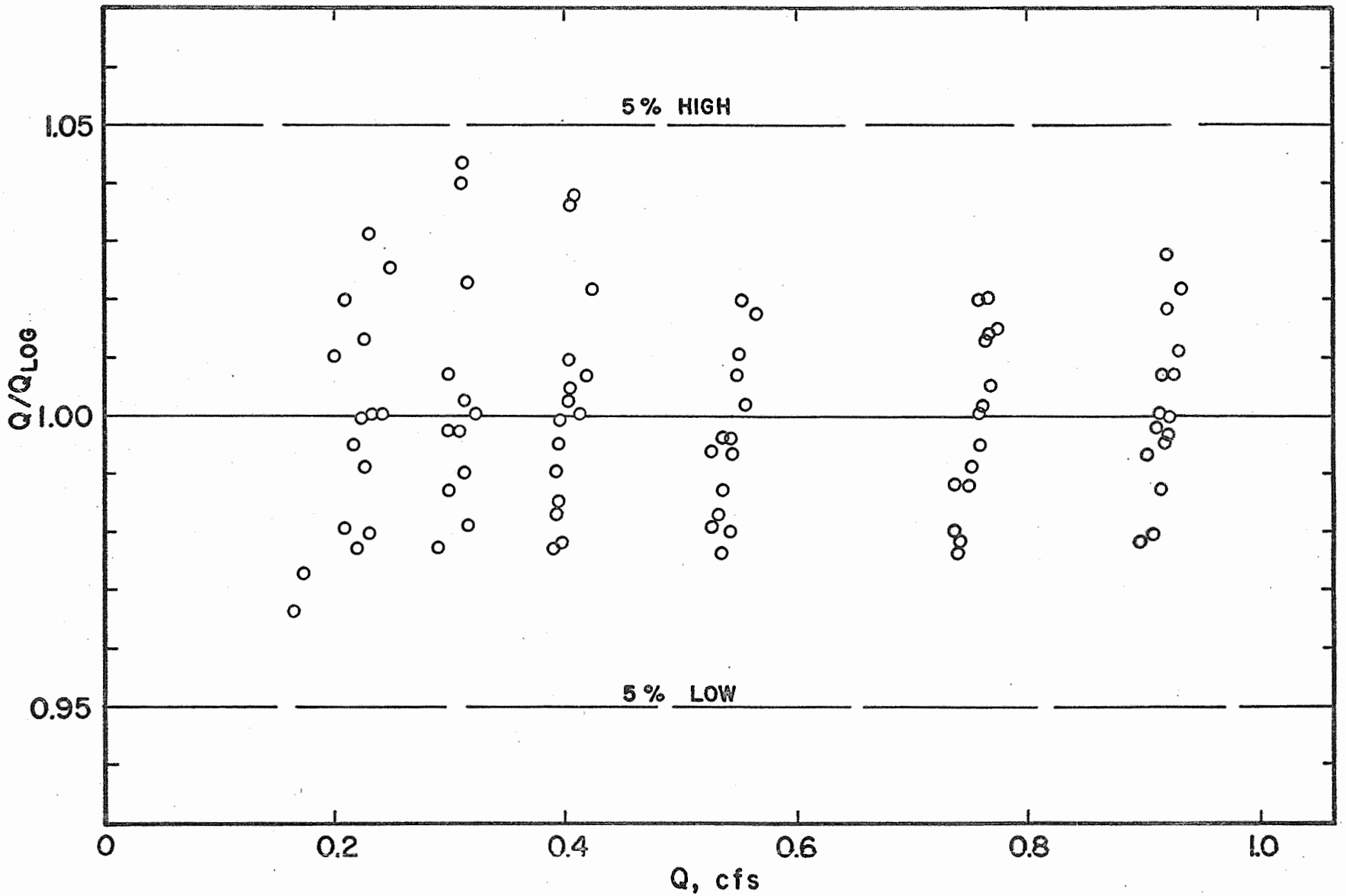

Figure 5. Scatter of calibration data from selected average equation for long radius 5 inch cast iron elbow meters.

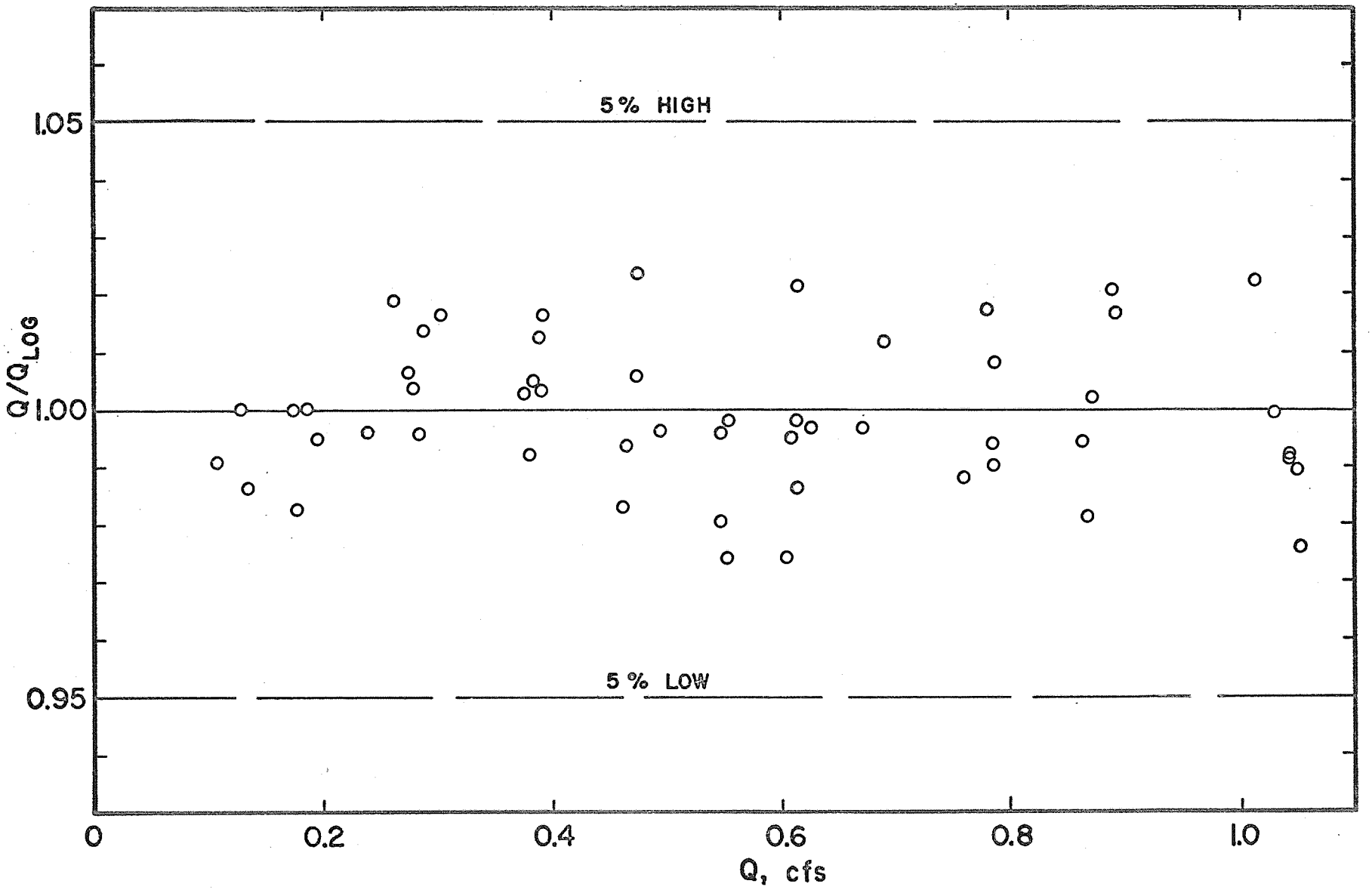

Figure 6. Scatter of calibration data from selected average equation for plastic, short-turn, 3-inch elbow meters.

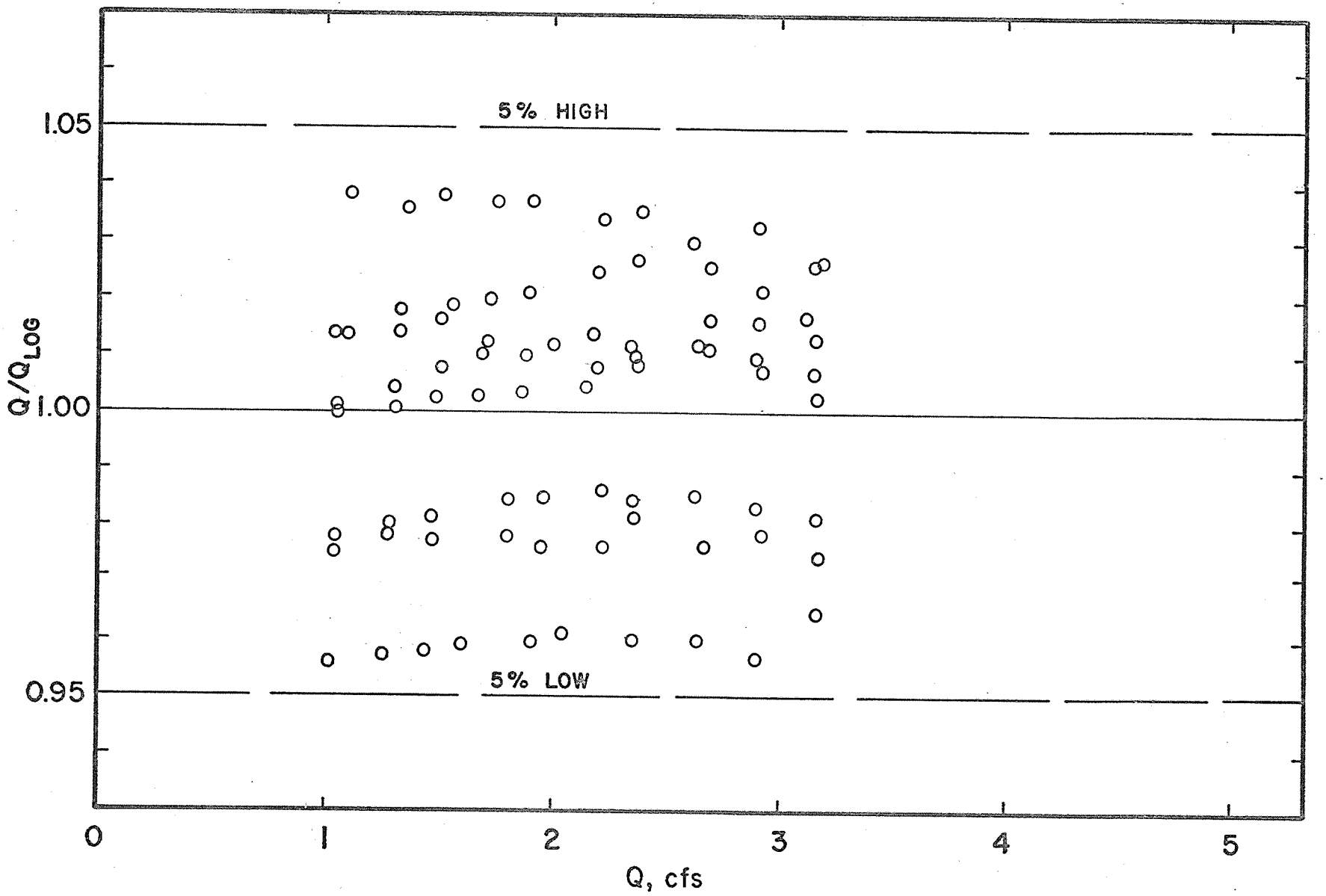

Figure 7. Scatter of calibration data from selected average equation for 6-inch cast iron elbow meters.

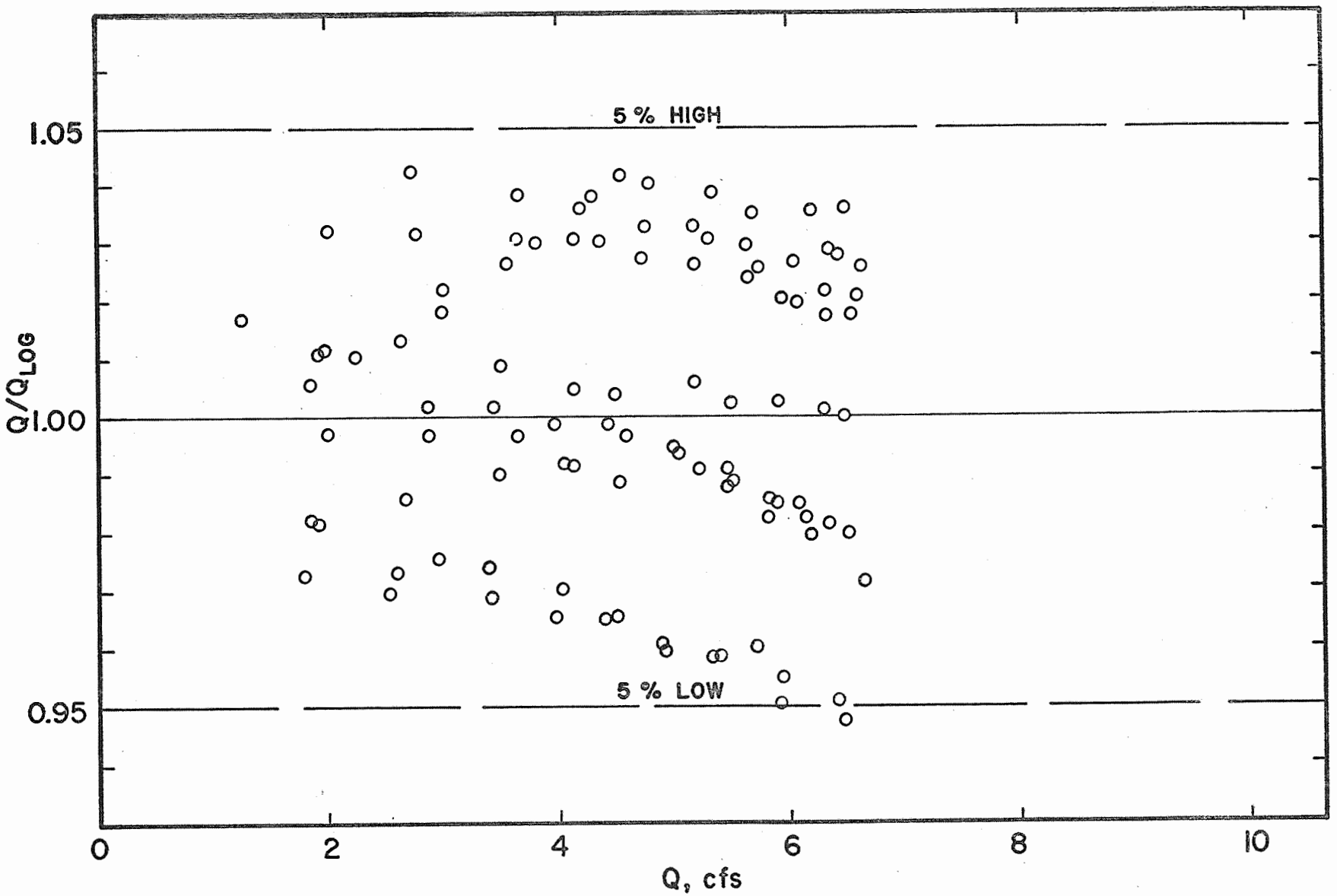

Figure 8. Scatter of calibration data from selected average equation for 10-inch cast iron elbow meters.

Annual Report of the U.S. Water Conservation Laboratory

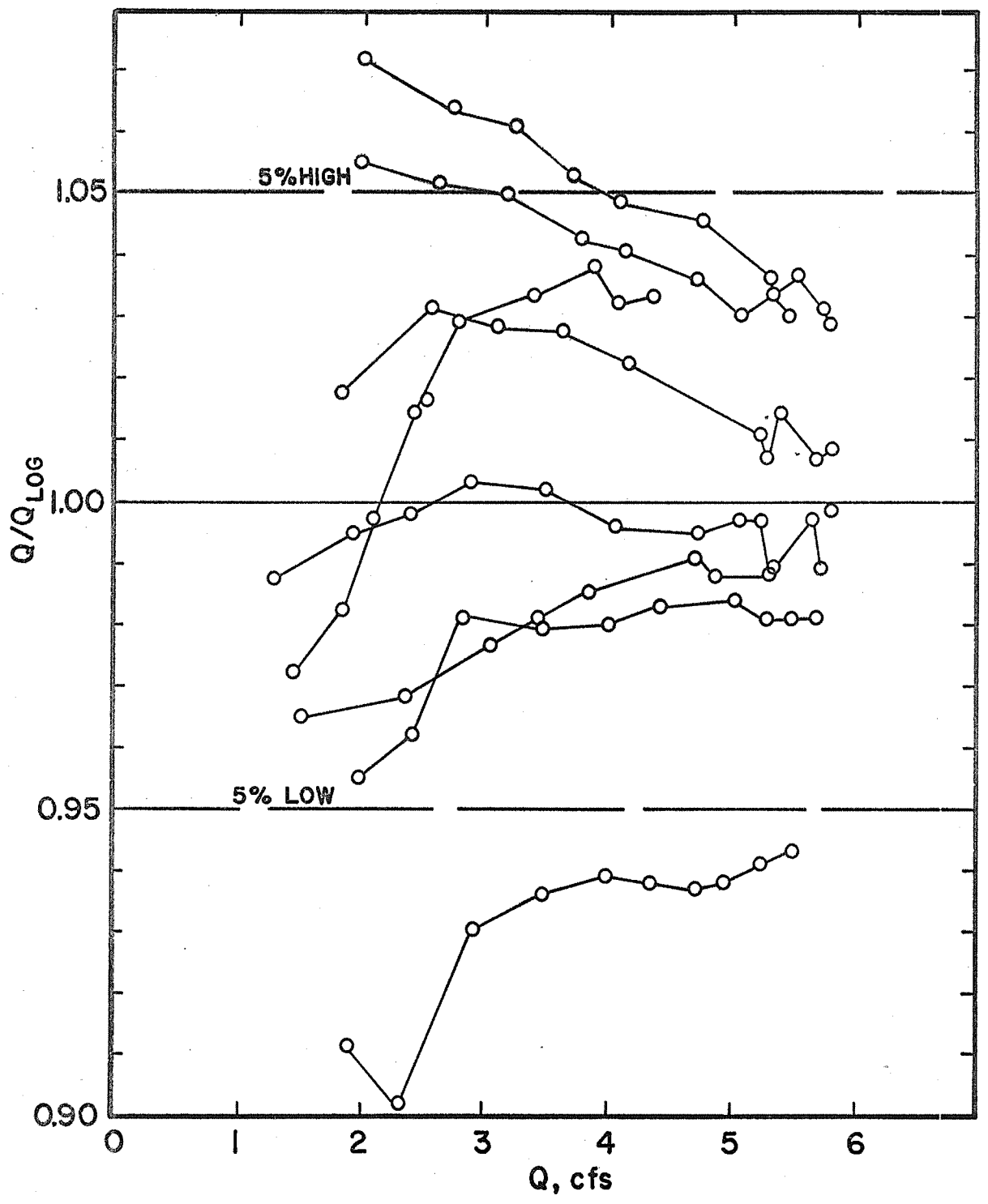

Figure 9. Scatter of calibration data from selected average equation for 12-inch cast iron elbow meters.

TITLE: CALIBRATION AND EVALUATION OF NET RADIOMETERS

LINE PROJECT: SWC 4-gG2 CODE NO.: Ariz.-WCL-6

During the past year the compensated net radiometers (1) have undergone extensive field testing. The net radiometers perform quite satisfactorily. The pressurization system described proved to be very effective even in intense rainstorms, and calibration factors remain unchanged through a season of use. It appears that the polyethylene domes should be replaced after 6 to 9 months' use.

Recently, work has been started to reduce the physical size of the net radiometer, thus facilitating its use in plant canopies. The desirable features would still be retained. The design now being tested includes a transducer, 1.12 inches in diameter. The support frame is being cast from epoxy resins, which reduces the machining time.

REFERENCES:

(1) Fritschen, Leo J.
Miniature net radiometer improvements. Submitted to the Journal of Applied Meteorology.

PERSONNEL: Leo J. Fritschen

TITLE: SOIL TREATMENT TO REDUCE INFILTRATION AND INCREASE PRECIPITATION RUNOFF

LINE PROJECT: SWC 4-gG3 CODE NO.: Ariz.-WCL-7

INTRODUCTION:

Recent laboratory studies of the sprayable asphaltic materials for soil stabilization have been concerned with the asphalt distribution in the soil and with the effect of soil moisture on asphalt penetration and soil strength. A portable testing machine was constructed to measure soil strength in the field for comparison with laboratory results. Laboratory studies also included the use of asphalt for bonding thin plastic films to the soil.

To better obtain rainfall data, preliminary investigations were conducted in developing a storage type, ground level rain gauge. These rain gauges will measure the rainfall which actually reaches the ground and is available for collection by a water harvesting structure.

A new experimental, operational water harvesting structure was constructed in cooperation with the Forest Service near Flagstaff, Arizona. In addition, the Metate, Nelson Road, and Blue Mountain Catchments were given completely new treatments in cooperation with the Bureau of Indian Affairs. We now have six operational catchments under test which involve four different surface treatments and three distinctly different soils.

PART I. SOIL STABILIZATION.

1. Effect of Soil Moisture on Asphalt Penetration.

Procedure. The effect of soil moisture on the depth of penetration of sprayed asphaltic materials into Granite Reef and Control soils was measured. The soils were oven dried at 105 C for 24 hours, then blended in a twin-shell blender with sufficient water to bring the moisture content to the desired level. The 38 × 12 × 5 cm soil trays were filled with 2550 grams of soil and a reinforced board placed on a smooth soil surface. Force was applied to the board with an arbor press to compact the soil to a depth of 4 cm which gave a resulting dry density of 1.4 g per cm^3. The trays were then

covered with a sheet of aluminum foil to prevent moisture loss before treatment. RC-special, MC-250, and RSK-I asphalts, heated to 49 C in an oven, were applied at a rate of 2.45 kg of asphalt per m^2 and allowed to penetrate at an air temperature of 27 C for 24 hours. Penetration was measured by cross-sectioning across the center line of the trays at three locations and the averages recorded.

Results. Treatment and measurement data are presented in Table 1. Penetration of RC-special and MC-250 increased with increasing soil moisture content, with the increase being greater for Granite Reef soil than for Control soil. Penetration into Control soil was doubled by increasing moisture content to 16 percent from 0 percent. Increasing soil moisture content almost completely stopped penetration of RSK-I into both soils.

2. Asphalt Distribution.

Procedure. The effects of soil, asphalt type, and application rate on the vertical distribution of the sprayed asphalt were studied on three different soils with RC-special, MC-70, MC-250, and RSK-I asphalts applied at rates of 1.5 and 2.5 kg per m^2. Soils were compacted into 38 × 12 × 5 cm trays in four increments of 700 g each. The Control and Granite Reef soils were air dried and blended with sufficient quantity of water to bring the moisture content to 10 percent by weight. The Metate soil was compacted into an air-dry state which created an aggregated soil structure similar to dry field conditions. Compaction was done by dropping a 4.1 kg weight six times, from a height of 64 cm, onto a reinforced tamping foot covering the entire soil surface. Asphalts were preheated to 49 C and applied with a Binks external mix spray gun, with the application rate being checked by weighing the boxes before and after treatment. Treated soils were allowed to cure outdoors for 7 days under normal temperature ranges of 21 to 43 C. After curing, the treated soil was sampled in duplicate in 3 mm layers for the full depth of penetration. Twenty grams of each sample was placed in a preweighed 100-ml beaker, allowed to air dry at room temperature 24 C for 48 hours, oven dried for 3 hours at 55 C, and then were weighed.

Next, 60 g of naphtha was added to the asphalt soil sample and it was covered and set aside for 24 hours while the asphalt dissolved from the soil particles. The sample was thoroughly mixed twice during this period. The sample was reweighed, thoroughly mixed, and allowed to stand for 3 minutes before a 20-g aliquot of the asphalt-naphtha was taken and placed in a preweighed beaker for evaporation of the naphtha. The evaporation of the naphtha was done under a ventilated hood for 36 hours, rotating the beakers periodically. The naphtha-asphalt was then placed in a 65 C oven for 1 hour before reweighing. The quantity of asphalt in the original asphalt-soil sample was then calculated from the equation

$$X = (B + X)\frac{D}{C} \quad \text{or} \quad X = \frac{DB}{C}\left(1 - \frac{D}{C}\right)^{-1}$$

where X = total asphalt in sample

B = naphtha added

C = naphtha-asphalt aliquot

D = asphalt residue in aliquot

Results. Distribution data are presented in Table 2. At the low 1.5 kg application rate there was no marked, consistant difference which could be attributed to the type asphalt used. At the high 2.5 kg rate the RC-special tended to penetrate deeper, leaving less asphalt in the surface soil layers, than the RSK-I, with the MC cut-backs in between. There was no significant difference between MC-70 and MC-250 cutback. The low application rate deposited a higher percentage of the asphalt near the soil surface than the high application rate. Penetration was greater and surface asphalt content lower for coarse structured Metate soil than for the sandy loam Granite Reef soil, with loamy sand Control soil in between. These differences are not great, however, and would not significantly affect construction of a sprayed asphalt pavement in the field.

3. Effect of Moisture on Strength of Asphalt Stabilized Soil.

Procedure. The effect of soil moisture on the penetration strength of soil stabilized with RC-special and MC-250 asphalt was investigated

by adding sufficient water to stabilized soil in small trays to raise the moisture content to the desired level. Trays were wrapped air-tight in aluminum foil and the moisture was allowed to equilibrate for 24 hours. The soil strength, in terms of resistance to penetration of a 2.54 cm^2 foot, was measured with the laboratory testing machine. (See Annual Report 1963, WCL-7).

Results. The dry strengths were 15 to 18 kg/cm^2 for the asphalt treated soils compared to 12 on the untreated. The strength values for treated soil dropped 4 to 6 kg/cm^2 at a soil moisture content of 4 percent, but this was not significantly different from the untreated soil at the same moisture content. There was no significant difference between the two asphalts as measured by this test.

4. Field Soil Strength Testing Machine.

Procedure. A portable testing machine was constructed which is capable of providing a constant traverse speed of the testing foot and has loading characteristics equivalent to our laboratory testing machine. A review of commercially available field testing machines failed to provide one with a constant traverse speed at variable loads. Our testing machine was built by constructing a 29.22-cm diameter piston and cylinder arrangement. The piston is moved at a constant rate of 0.6 cm/min in the cylinder by pumping 420 cc/min of light weight hydraulic oil into it with a positive displacement gear pump driven by an electric motor. Fluid pressure in the cylinder is measured with a class AA pressure gauge with a maximum pressure reading of 2.1 kg/cm^2 at an accuracy of $\pm$ 0.01 kg/cm^2. Using a 2.54 cm^2 foot, soil strength in excess of 200 kg/cm^2 can be measured. The piston is mounted in the center of a 1.2 $\times$ 1.8 m platform which is held in place by a counterbalance of four 200-liter drums filled with water. In the field, penetration strength was measured at three locations on each of the plots.

Results. The test locations and results are presented in Table 3. The average pavement strength was 76.0, 41.4, and 16.4 kg/cm^2 for RC-special, modified S-1, and untreated, respectively. The asphalt plots had weathered a minimum of 1 year after an application

rate of 1.47 kg/m^2 of asphalt. Comparing the field results to the strength obtained in the soil trays in the laboratory (Annual Report 1963) shows the laboratory results are representative of the field under the dry soil conditions present at the time of testing.

PART II. THIN FILM BONDING.

The use of thin plastic films bonded to asphalt stabilized soil is quite promising and has several advantages. Runoff water from a film covered surface is clear and of excellent quality. Also, the film protects the asphalt base coat from weathering. Black 1.5-mil polyethylene is relatively low cost and withstands weathering deterioration reasonably well when bonded to the soil surface. Field seaming polyethylene has been a problem in the past, but we have found that for our purposes asphalt compounds are a satisfactory adhesive for constructing polyethylene catchment aprons.

The bonding strength obtained at various curing times and temperatures from asphaltic compounds used with 1.5-mil black polyethylene was evaluated in a laboratory testing machine. The polyethylene was cut into strips 10.2 cm wide and 1.2 m long. The asphalt was applied with a brush at an approximate rate of 0.5 kg asphalt per m^2. Bonding tests were conducted on asphalt treated plywood to reduce sample preparation time and simplify tests. No difference was found in tests using both asphalt treated soil trays and the asphalt treated plywood. All except the 2-hr samples were cured at air temperatures held essentially constant at 27 C for the required time. Samples were then moved into a constant temperature room and allowed to equilibrate to the test temperature for a minimum of 4 hours. The 2-hr samples were placed in the constant temperature room 30 minutes after treatment. All samples were duplicated. The tests consisted of four tests which were designed to fit existing types of film failure in the field and also to correspond as closely as possible to standard ASTM procedures. The tests and results were as follows.

1. Peel Tests.

Procedure. Both 90- and 180-degree peel tests were run with a traverse speed of 5 cm/min at four temperatures and three curing intervals with three asphalt materials. Temperatures were 4, 15, 27, and 49 C. Curing times were 2 hours, 1 day, and 3 days. Asphalts were standard RSK and SS-2 emulsions and SS-2B which is SS-2 modified with butyl latex.

Results. Results are presented in Table 4. All treatments failed at 4 C, indicating that peeling could be a problem at low temperatures. SS-2 and SS-2B had significantly greater initial bonding strength at 27 C than did RSK. RSK was stronger at 15 C than SS-2 or SS-2B but was weaker at 27 C. Bonding strength decreased materially at 49 C as the asphalt softened.

2. Lap Joints.

Procedure. The strengths of the lap joints were measured with the same procedure as described in the 1963 Annual Report with the exception of increasing the traverse speed of the testing machine from 2.5 to 5.0 cm per minute.

Results. The test conditions and results for the lap joint bonding are presented in Table 5. All samples of lap joints at all temperatures provided satisfactory bonds, with the RSK best at 4 and 27 C, and SS-2 and SS-2B best at 49 C. Generally, the longer the cure, the stronger the bond up to the breaking strength of the film. These data indicate that failure of lap joints will not be a problem in the field.

3. Vertical Uplift.

Procedure. The uplift force required to pull bonded polyethylene from the soil was measured by bonding 10.2 × 10.2 cm boards to the top and the bottom of the polyethylene with asphalt. The two boards were then pulled apart in the testing machine and the force required to fail the asphalt on one side of the polyethylene was recorded. The bonding strength on the boards was compared to polyethylene bonded to asphalt stabilized soil in the soil trays.

Results. The vertical uplift bonding strength of the polyethylene bonded to soil and to the plywood board is presented in Table 6. All the vertical uplift tests were conducted at 3 days cure. At 4 C the bonds to the board were over 0.46 kg/cm^2, and the bonds to the soil exceeded the strength of the stabilized base coat. At 49 C in the bonding to the board, the S-1 and SS-2 had strengths in excess of 0.2 kg/cm^2 and the SS-2B had a value of 0.1 kg/cm^2. This should be adequate to prevent film failure in the field by vertical uplift caused by wind.

PART IV. GRANITE REEF TESTING SITE.

Instrumentation to determine wind direction and velocity during rain storms was installed at the Granite Reef testing site the past year. A vector pluviometer was installed to obtain quantitative measurement of the direction the rain comes from. The vector pluviometer consists of four vertical circular openings, 12.7 cm in diameter placed at right angles to each other and facing north, east, south, and west. The rain collected by each opening is stored in a polyethylene bottle and then measured after each rain. To obtain information concerning wind direction and speed, a self-contained recording wind system was designed and installed. The system consists of a directional vane and anemometer with simple signal generators connected to an amplifier and recorder which automatically turn on at the start of a rain. The power supply for the amplifier and recorder is a 110 V A.C. inverter connected to a 12 V battery. The vector pluviometer was installed 15 April 1964 and the wind system in operation 12 September 1964.

1. Small 9.3 m^2 Plots.

Results. Runoff from the 9.3 m^2 plots during 1963 is listed in Table 8. The treatments for the plots are presented in Table 7. The total runoff from the 30-mil butyl sheeting, plot 2, averaged 100 percent of the total rain gauge catch; while from untreated soil, plot 4, the runoff was 31 percent. This high percentage resulted from 80 percent runoff from one high intensity 50 mm storm. Excluding this storm, runoff from the bare soil plot was 15 percent of

rain gauge catch. On 14 April 1964, a modified 1-mil polyethylene sheeting was installed on plot 9. The sheeting was securely fastened with batten strips at the edges, but wind tore the sheet in less than two months. Also on 14 April 1964, plot 8 was covered with 12-mil modified butyl sheeting bonded to the soil with asphalt. There has been no problem with wind and runoff has averaged 100 percent. In July 1964, plot 16 was treated with an MC-250 base coat, and a seal coat of a roofing asphalt clay emulsion. The plot has weathered very well and is giving excellent runoff. Plot 18 was treated in May 1963 with a water repellent designated R-9, and, for the past year, excluding the 50 mm storm, averaged 39 percent runoff as compared to 15 percent from the untreated plot. Runoff including this storm exceeded 51 percent.

2. Large 230 m^2 Plots.

Results. Treatments applied to the 230 m^2 plots are listed in Table 9, and the runoff results are presented in Table 10. The 6-mil polyethylene, plot 1, performed satisfactorily although the runoff was only 95 percent. Observations of the plot during rain showed that wrinkles in the sheeting caused considerable retention.

The smooth, bare plot 2 averaged 35 percent runoff, although the runoff is decreasing as the roughness of the plot increases due to wind erosion of the fine soil particles.

Plot 3, the aluminum foil, still has good appearance, but the runoff has reduced considerably. Close observation shows that many small holes are appearing in the foil and are allowing the water to seep into the soil underneath.

Plot 4, the butyl sheeting standard, has no observed deterioration, and the runoff the past year was 100 percent or over for each storm, with the exception of the first storm of the year. Seasonal runoff averaged 103 percent.

Plot 5, a two-phase asphalt with a modified S-1 base coat and S-1 top coat, has weathered extremely well the past year and averaged 98 percent for the year.

Plot 6, another two-phase treatment using RC-special as a base coat and S-1 and SS-2 modified with butyl latex as a top coat, is also giving us 98 percent runoff. Records for individual storms throughout the year show there may be as much as 30 percent difference in runoff between plots 5 and 6, even though the totals for the year are essentially identical. The differences for individual storms can be explained in that the two plots faced in different directions. Plot 5 slopes to the north, and plot 6 slopes to the east.

Plot 7 is covered with a sheeting of 1-mil white polyvinyl fluoride film manufactured under the trade name of Tedlar. This is asphalt-bonded to the soil which was stabilized with RC-special at a rate of 2 kg of asphalt m^2. The treatment of this plot was finished in February 1964, and has averaged over 100 percent runoff from that time. The sheeting weathers extremely well but is susceptible to mechanical damage. It has been necessary to repair the sheeting three times in the past year due to mechanical damage caused as the sheeting shrinks and longitudinal tears occur.

To help explain differences in the runoff from individual storms between plots 5 and 6, a vector pluviometer (directional rain gauge) was constructed and installed at the Granite Reef testing site. Directional rainfall data from the vector pluviometer are presented in Table 11. The results show that a majority of the storms come from predominantly one or two directions. Although rainfall direction varied considerably from storm to storm the total catch did not vary so much among orifices. Total catch from 27 April through 31 December for orifices facing different directions was: north - 705 ml; east - 777 ml; south - 680 ml, and west - 1028 ml. This is reflected in the almost identical total catch for plots 5 and 6. Plot 5 caught 122.7 mm and plot 6 caught 122.8 mm.

3. Watersheds.

Results. Three 450 m^2 watersheds have been instrumented for the past year. The runoff results are presented in Table 12. Watersheds 1 and 2 are completely untouched as far as smoothing or

clearing of the brush. Watershed 3 has had the brush removed by hand with a minimum of plot disturbance otherwise. The results showed that, for a majority of the storms, there is no runoff from any of the watersheds. Runoff occurs only from high volume, high intensity storms or when the soil is wet from a closely preceding storm. Watershed 3 consistently had more runoff than the other two, averaging 35 percent for the year as compared to approximately 24 and 18 percent for watersheds 1 and 2, respectively.

4. Esso Plots.

A four-plot test unit was constructed in December 1964 at Granite Reef in cooperation with Esso Research Corporation of Linden, New Jersey. Four plots, 7.6 m × 15.2 m each, were built side by side with individual steel tanks for collecting and measuring runoff. The plots are sprayed with varying rates of a one-phase asphalt shipped in from the eastern United States.

PART V. OPERATIONAL FIELD CATCHMENTS.

Nelson Road Catchment. The treatment installed on the Nelson Road Catchment in 1963 had essentailly failed during the winter. In June 1964, the plot was disked, dragged, and rolled with a vibrating roller. A base coat of MC-250 at a rate of 2.5 kg asphalt per yd^2 was applied, and on 25 July a seal coat of clay asphalt emulsion was applied to the catchment at a rate of 1.0 kg of asphalt per m^2. The pavement appeared to be very tough and hard and there were no observable cracks of any kind. A few clods and pieces of old pavement could be picked from the surface, but the base coat underneath was in excellent shape. The asphalt-fiberglas lined pit had recently been retreated with clay emulsion and looked very good. Rainfall had been very low during the summer and the pit contained only a small amount of discolored water.

Blue Mountain Catchment. The Blue Mountain Catchment was initially half-covered with aluminum foil-fiberglas which had been damaged due to plant growth and wind. The undamaged area was cleared and the entire catchment was treated with MC-250 asphalt at a rate of 2.5 gal/yd^2 on 25 August. On 28 September a seal coat of

SS-2 was applied at the rate of 0.5 kg of asphalt per yd^2 to the entire plot and an experimental aluminum compound was applied to half the plot by spraying at a rate of 0.05 kg solution/m^2. The aluminum spray is intended to reduce the coloring of the runoff water and improve durability of the asphalt. This catchment was inspected on 22 October. The aluminum looked very good, and you could feel heat being reflected from the surface. The entire pavement was firm, although the base coat had not completely cured. There were a few sprigs of vegetation growing through the treatment. There had been no rain since the plot had been treated.

Metate Catchment. The two-phase asphalt treatment on the Metate Catchment had failed by the winter of 1963. On 11 May 1964, while the soil was dry, the catchment surface was disked and rolled with a vibrating roller. MC-250 cutback was applied at a rate of 2.5 kg of asphalt per yd^2. The pit was sprayed with MC-250 at 3.0 kg of asphalt per yd^2. On 1 June 1964, 1 1/2-mil polyethylene was bonded to the stabilized soil surface was SS-2 emulsion. The plastic bonded very well. The storage pit for the catchment was lined with 1 ounce fiberglas matting bonded to the base coat with the SS-2 emulsion. The lining was then sealed with asphalt clay emulsion. This catchment was inspected on 20 October and looked very good. There were a few small holes in the polyethylene caused by gravel on the surface when the film was laid. These holes were not being enlarged by wind because the film was well bonded to the soil. There were several yucca sprigs growing through the film but, at present, these were not doing any damage. The pit looked exceptionally good, and the water in the pit was clear. Rainfall had been almost nonexistant and the pit contained only a small amount of water.

Cedar Mesa Catchment. The Cedar Mesa Catchment, which had been covered with 1-mil Tedlar, collected water and was used successfully during the year. The Tedlar is susceptible to mechanical damage, and it had been necessary for the BIA personnel to patch holes. This catchment was inspected on 20 October and appeared in excellent shape. Cattle had gotten into the plot and made small holes in the Tedlar,

but these were easily repaired. The water in the tank was perfectly clear. This will be a successful treatment if mechanical damage by cattle can be prevented.

Hopi No. 1. The catchment on the Hopi Indian Reservation, which had been treated with a two-phase asphalt treatment in 1963, was inspected early in April 1964. The treatment had not been damaged by freezing. Although the surface was still in good condition, the runoff water was discolored. BIA personnel stated that horses would not drink the water although cattle would. Accordingly, on 21 September the catchment was sprayed with clay emulsion at a rate of 1.0 kg of asphalt per yd^2. Inspection of the catchment on 21 October showed good results. The surface coating was tough and in excellent shape. Runoff water from the clay emulsion appeared only slightly discolored. There were a few small yucca sprigs coming through on the plot, but these are being controlled.

Flagstaff Cinders Catchment. This catchment was installed on the cinder flow near Flagstaff, Arizona. The catchment is 45 × 45 m on an 8 percent slope. The plot is constructed on an old cinder flow from local volcanoes in the area. The cinders are estimated to be 15 to 20 feet deep. In their dry, natural state, the cinders are very loose, and a track-type bulldozer was the only machine that could be used to prepare and smooth the site. This presented a problem in obtaining a smooth surface. On 20 June 1964 the catchment surface was sprayed with RSK emulsion at a rate of 2.5 kg of asphalt per yd^2. On 27 June the catchment was sprayed with clay emulsion at a rate of 1.0 kg asphalt per yd^2. At this time the catchment base coat appeared in satisfactory shape, and the seal coat appeared very good after installation. The runoff water is diverted into a 65,000-gallon steel tank, through a 10-inch rigid plastic irrigation pipe, from which pipes will be led out to small watering troughs equipped with float valves. This catchment was inspected on 22 October. It is rough, but the pavement appears to be good and retention is low. The pavement is flexible and gives slightly as loose cinders under the pavement are displaced as you

walk on it. There is absolutely no cracking except for one or two fine hairline cracks in the surface seal coat. There were no cracks in the base coat.

SUMMARY AND CONCLUSIONS:

Tests on field installations of sprayed asphalt pavements have shown bearing strengths remarkably comparable to previous measurements made on soil trays in the laboratory. A testing machine was constructed of a specially machined hydraulic cylinder and matched pump so that piston travel speed equalled that of the head on the laboratory testing machine. The piston device was weighted with drums of water and was used to push our standard square 6.45 cm^2 testing foot into the pavement. Load was measured with a precision pressure gauge on the hydraulic cylinder. Average pavement strengths measured on catchments at the Granite Reef test site were 76.0, 41.4, and 16.4 kg/cm^2 for the RC-special, RSK-I, and untreated plots, respectively. Similar average laboratory measurements for these treatments were > 65.5, 43.8, and 17.8 kg/cm^2, respectively.

Distribution of sprayed asphalt in the vertical profile of an asphalt-soil pavement was investigated in the laboratory with four asphalt compounds, three soils, and two application rates. The asphalts were a special RC cutback, MC-70 and MC-250 cutbacks, and a modified cationic emulsion (RSK-I). Soils were loamy sand, loam and clay loam. Application rates were 1.5 and 2.5 kg/m^2. Penetration and distribution of asphalts sprayed on dry soil was similar with no marked difference attributable to asphalt type. A higher percentage of the applied asphalt remained at the soil surface with the low application rate than with the high rate. The lowest viscosity cutback penetrated slightly farther into the coarsest soil than did the highest viscosity RSK-I material. These tests indicate that in using the four asphalts under field conditions, soil preparation and temperature will control penetration, not asphalt type.

Asphalt was shown to be a satisfactory adhesive for making lap joints in 1.5-mil black polyethylene and for bonding it to soil.

Tests were made with three asphalt emulsions at temperatures ranging from 4 to 40 C. No marked difference in over-all performance of the three emulsions was found. Peel resistance of asphalt-polyethylene bonds was less than 0.01 kg per cm at 4 C and was 0.2 kg per cm at 27 C. Failure by peeling cannot occur until a part of the film has been lifted from the soil surface. Accordingly, the force required to lift a section of bonded film vertically from the base coat was measured. Almost all tests at all temperatures exceeded either the capacity of the testing machine at 0.46 kg per cm^2 or the strength of the asphalt-soil base coat. Similarly, all 5-cm wide lap joints exceeded the strength of the polyethylene. This indicates that failure of lap joints or uplift by wind should not be a problem with asphalt bonded 1.5-mil black polyethylene.

A vector-pluviometer was installed at the Granite Reef test site to obtain information on wind direction during rain storms. Valuable data are being obtained from this simple device which consists of four vertical circular openings placed at right angles to each other and facing north, east, south, and west. Marked differences in the wind direction of individual storms have been found, but differences in seasonal totals are not great. Percent of seasonal catch coming from different directions was as follows: north - 22.1, east - 24.4, south - 21.3, and west 32.2.

Runoff from the 9.3 m^2 butyl covered plot at Granite Reef averaged 100 percent of standard rain gauge catch. Runoff from a similar plot treated with R-9 water repellent on 30 May 1963 exceeded 50 percent. This is remarkable since the plot has a rough surface with less than 3 percent slope. No erosion has been observed.

The 230 m^2 aluminum foil catchment at Granite Reef has developed numerous pinholes and seasonal runoff reduced to 72 percent. Runoff from the 30-mil butyl catchment averaged 103 percent. Two asphalt catchments, now about two years old, have weathered very well. One faces northeast and one faces northwest and catch from different storms has varied by 30 percent. Seasonal totals were almost

identical at 198.3 mm for plot 5 and 198.4 mm for plot 6. The storm differences and seasonal identity agrees with data obtained from the vector pluviometer. Runoff from the plastic film catchments was 101 percent for the Tedlar plot and 95 percent for polyethylene. Wrinkles in the 6-mil polyethylene cause undersirable retention and this will be replaced with 1.5-mil material.

Runoff from bare soil catchments at Granite Reef was considerably higher than usual because of one 50 mm storm which produced unusual runoff from these plots. This 50 mm storm is a once in ten years occurrance. All holding tanks overflowed, and it was necessary to estimate minimum runoff from this one storm by comparison with the bare soil 9.3 m^2 plot. On this basis the total 1964 runoff was as follows:

Untreated plot with brush, average 10 percent slope - 18 to 24 percent,

Cleared plot, no smoothing, average 10 percent slope - 35 percent,

Cleared plot, smoothed with road grader, 5 percent slope - 35 percent.

Runoff from the smoothed plot is gradually decreasing as wind blows away the fine soil and leaves a gravelly surface.

All experimental operational catchments installed in 1963 in cooperation with the Bureau of Indian Affairs, except one, were retreated or resurfaced during 1964. The Tedlar covered Cedar Mesa Catchment was in good condition but had suffered minor damage by cattle walking on it. The asphalt Hopi No. 1 Catchment went through the winter in good shape but was resurfaced with clay-type asphalt emulsion to reduce discoloration of the runoff water. Base coats of RC-special had failed on the Nelson Road and Blue Mountain catchments. These units were disked and retreated with an MC-250 base coat. Nelson Road received an asphalt-clay emulsion seal coat and Blue Mountain received an SS-2 seal coat plus a half-plot top spray of an experimental aluminum compound. A completely new catchment was constructed on loose volcanic cinders near Flagstaff in cooperation with the U. S. Forest Service. The loose cinders were successfully

stabilized with asphalt emulsion and an asphalt-clay emulsion was used as a surface seal. All catchments were inspected in October 1964 and appeared to be in excellent condition.

PERSONNEL: L. E. Myers, G. W. Frasier.

Table 1. Effect of soil moisture on penetration depth of asphalts sprayed on the soil at a rate of 2.5 kg asphalt per m^2.

Soil	Moisture content	Depth of penetration		
		RC-special	MC-250	RSK-I
	percent	cm	cm	cm
Control	0	1.2	1.0	1.5
	8	1.5	1.2	0.1
	16	1.3	1.3	0.1
Granite Reef	0	1.0	0.8	1.3
	8	1.8	1.3	0.1
	16	2.1	1.6	0.1

Table 2. Penetration and distribution of asphalt compounds applied to the surface of three dry test soils.

	Depth from surface	1.5 kg asphalt/m^2				2.5 kg asphalt/m^2			
		Asphalt type				Asphalt type			
		RC-special	MC-70	MC-250	RSK-I	RC-special	MC-70	MC-250	RSK-I
	mm	Percent of total				Percent of total			
Metate Soil	0-3	30.5	22.8	22.6	21.3	17.7	17.4	14.7	15.2
	3-6	30.8	30.8	32.2	29.8	20.8	21.1	20.5	25.4
	6-9	25.6	25.8	26.3	31.0	21.2	20.5	21.4	24.7
	9-12	13.1	20.6	18.9	17.9	15.7	18.3	18.2	18.9
	12-15					10.7	15.6	14.4	15.8
	15-18					9.1	7.1	10.8	
	18-21					4.8			
Control Soil	0-3	33.3	34.5	37.4	38.5	25.5	31.9	28.8	35.5
	3-6	27.1	28.6	30.5	33.2	19.8	25.6	25.7	30.0
	6-9	24.3	24.9	23.2	25.0	18.5	22.2	23.1	23.9
	9-12	15.3	12.0	8.9	3.3	17.9	16.1	17.6	10.6
	12-15					13.9	4.2	4.8	
	15-18					4.4			
Granite Reef Soil	0-3	41.2	38.0	36.4	38.3	26.8	25.6	27.8	24.8
	3-6	34.7	33.1	30.2	34.4	20.5	25.3	25.2	25.3
	6-9	24.1	24.4	26.4	27.3	20.5	22.5	22.9	23.3
	9-12		4.5	7.0		18.1	17.1	17.5	19.5
	12-15					14.1	9.5	6.6	7.1

Table 3. Penetration strength of Granite Reef asphalt sprayed field plots.

Treatment	Soil moisture 1/		Depth of asphalt penetration 1/	Strength 2/			
	0-2.5 cm	2.5-5.0 cm		Field		Laboratory	
	percent	percent	cm	kg/cm^2		kg/cm^2	
RC-special installed April 1963	1.3	1.2	2.5	64.1	Ave. 76.0	> 65.5 3/	
	1.3	1.2	5.0	76.4			
	0.8	1.0	1.2	89.4			
Modified cationic installed Sept. 1962	0.7	1.1	3.7	49.3	Ave. 41.4	58.8	Ave. 43.8
	1.2	1.2	2.5	45.8		28.5	
	1.1	1.0	2.5	29.2		44.2	
Smoothed untreated	3.2	4.0		23.9	Ave. 16.4	13.7	Ave. 17.8 4/
	2.3	4.2		7.4		28.2	
	2.2	3.9		18.0		14.0	

1/ From field samples.

2/ Resistance to penetration of square 2.54 cm^2 foot at 0.6 cm penetration depth.

3/ Dynamometer off scale.

4/ Soil moisture 7 percent average for 5.0 cm depth.

Table 4. Peel resistance of 1.5-mil black polyethylene bonded to plywood with asphalts and cured at 27 C (80 F).

Test temperature		Test angle	RSK			SS-2			SS-2B		
			2 hr	1 day	3 day	2 hr	1 day	3 day	2 hr	1 day	3 day
°F	°C	deg	kg/cm	kg/cm	kg/cm	kg/cm	kg/cm	kg/cm	kg/cm	kg/cm	kg/cm
40	4	90	0.01 1/	0.01	0.01	0.01	0.01	0.01	0.01	0.01	0.01
		180	0.01 1/	0.01	0.01	0.01	0.01	0.01	0.01	0.01	0.01
59	15	90	-	0.23	0.24	-	0.01	0.05	-	0.01	0.03
		180	-	0.24	0.24	-	0.01	0.04	-	0.01	0.05
80	27	90	0.05	0.08	0.17	0.13	0.13	0.17	0.22	0.16	0.22
		180	0.06	0.07	0.13	0.16	0.18	0.16	0.24 2/	0.25 2/	0.23
120	49	90	-	0.01	0.04	-	0.04	0.04	-	0.03	0.07
		180	-	0.01	0.03	-	0.01	0.05	-	0.03	0.05

1/ Asphalt not broken.

2/ Polyethylene failed.

Table 5. Lap joint bonding strength per unit width of 5.1 cm (2 in) laps of 1.5-mil black polyethylene cured at 27 C (80 F).

Test temperature		RSK			SS-2			SS-2B		
		2 hr	1 day	3 day	2 hr	1 day	3 day	2 hr	1 day	3 day
°F	°C	kg/cm	kg/cm	kg/cm	kg/cm	kg/cm	kg/cm	kg/cm	kg/cm	kg/cm
40	4	-	0.29	0.35	-	0.13 1/	0.35	-	0.14 1/	0.21
80	27	0.12 1/	0.18	0.29	0.10 1/	0.10	0.20 1/	0.10 1/	0.13	0.27
120	49	-	0.06	0.15	-	0.10	0.21 2/	-	0.14	0.20 2/

1/ Asphalt not broken.

2/ Polyethylene failed.

Table 6. Vertical uplift resistance of 1.5-mil black polyethylene bonded with asphalt and cured 3 days at 27 C (80 F).

Test temperature		RSK		SS-2		SS-2B	
		Board	Soil	Board	Soil	Board	Soil
°F	°C	kg/cm^2	kg/cm^2	kg/cm^2	kg/cm^2	kg/cm^2	kg/cm^2
40	4	> 0.48 1/	0.31 2/	0.46	0.21 2/	> 0.48 1/	0.26 2/
120	49	0.23		0.24		0.12	

1/ Exceeded capacity of testing machine.

2/ Failure in base coat of asphalt.

Table 7. Treatments on 9.3 m^2 plots at the Granite Reef testing site.

Plot	Treatment date	Treatment
2	18 May 1961	30-mil butyl rubber sheeting
4	15 Sept 1961	Untreated
8	24 Mar 1961	12-mil modified butyl sheeting
16	Base coat 1 July 1964	MC-250 at 2.5 kg asphalt/m^2
	Top coat 10 July 1964	Clay emulsion at 1.0 kg asphalt/m^2
18	30 May 1963	R-9 at 0.113 kg/m^2 upper half R-9 at 0.057 kg/m^2 lower half

Table 8. Runoff results from rainfall on 9.3 m^2 plots at the Granite Reef testing site.

Date	Rainfall			Plot 2 runoff		Plot 4 runoff	
	Intensity						
	Max.	Min.	Total				
1964	mm/hr	mm/hr	mm	mm	%	mm	%
22 Jan	8	2	17.5	17.5	100.1	2.7	15.1
3 Mar	8	2	4.5	4.7	100.4	0	0
23 Mar	3	1	4.1	4.6	112.7	0.1	2.7
27 Apr	2	1	2.8	3.4	123.0	0	0
14 Jul	3	3	11.4	11.1	97.4	0.2	1.9
23 Jul	2	2	2.0	1.9	97.0	0	0
1 Aug	25	25	50.0	44.7 1/	89.5	40.3	80.6
12 Aug	1	1	2.0	2.7	134.0	0	0
13 Aug	15	5	9.0	9.7	107.6	0.9	10.8
26 Aug	20	8	17.2	17.2	100.0	6.5	37.8
13 Sept	3	3	3.0	3.7	122.0	0	0
14 Sept	6	6	7.5	7.5	100.4	2.8	37.3
23 Sept	2	< 1	1.2	1.1	98.3	0	0
16-19 Oct	5	3	5.2	6.0	115.8	0	0
11-15 Nov	3	3	27.7	28.3	102.2	4.6	16.7
18 Nov	2	1	5.3	5.4	101.5	0.3	6.0
18 Dec	4	4	11.2	11.1	98.9	1.4	12.5
27 Dec	20	5	10.8	11.5	106.6	2.7	24.9
31 Dec	2	< 1	10.0	10.8	107.5	0.2	2.2
Total			202.4	202.9	100.2	62.7	31.0

1/ Quantity tank held at time of overflow.

Table 8. Continued.

Date	Plot 8 runoff		Plot 16 runoff		Plot 18 runoff	
1964	mm	%	mm	%	mm	%
22 Jan					13.9	79.1
3 Mar					2.4	54.2
23 Mar					0	0
27 Apr	3.2	115.0			2.5	88.2
14 July	11.1	97.4	10.9	95.6	1.3	11.3
23 July	1.8	91.5	1.7	86.0	0.2	11.0
1 Aug	44.7	89.5	44.7	89.5	44.7	89.5
12 Aug	2.0	102.0	2.0	102.0	1.5	75.0
13 Aug	9.7	107.6	7.5	83.7	4.6	51.3
26 Aug	16.3	94.8	14.5	84.4	10.2	59.4
13 Sept	3.6	118.3	2.9	96.7	0	0
14 Sept	6.7	88.9	5.4	71.7	4.7	63.1
23 Sept	1.0	80.8	1.0	80.8	0	0
16-17 Oct	5.8	111.7	5.3	101.3	0.3	6.2
11-15 Nov	27.4	99.0	24.1	83.3	9.7	34.9
18 Nov	5.8	109.6	5.7	107.4	0.5	10.2
18 Dec	10.5	94.1	11.5	102.7	3.9	34.6
27 Dec	9.0	83.6	10.7	99.5	1.1	10.0
31 Dec	12.8	127.9	9.9	98.9	2.5	24.7
Total	171.4	97.2	157.8	90.9	104.0	51.4

Table 9. Treatments on 230 m^2 plots at the Granite Reef testing site.

Plot	Treatment date	Treatment
1	Base coat 10 Oct 63	RC-special 2.0 kg asphalt/m^2
	Top sheeting 30 Oct 63	6-mil black polyethylene bonded with SS-2B at 0.5 kg asphalt/m^2
2	30 Nov 61	Smoothed untreated
3	19 Jan 62	1-mil aluminum foil
4	30 Nov 61	30-mil butyl rubber sheeting
5	Base coat 18 Sept 62	Modified S-1 at 1.470 kg asphalt/m^2
	Top coat 21 Dec 62	S-1 at 1.035 kg asphalt/m^2
6	Base coat 19 Apr 63	RC-special at 1.470 kg asphalt/m^2
	Top coat South half 8 May 63	SS-2 at 0.654 kg asphalt/m^2 with 3 percent latex
	Top coat North half 9 Jul 63	S-1 at 0.490 kg asphalt/m^2 with 3 percent butyl latex
7	Base coat 12 Feb 64	RC-special at 2.0 kg asphalt/m^2
	Top sheeting 19 Feb 64	1-mil Tedlar PVF film bonded with SS-2B at 0.5 kg asphalt/m^2

Table 10. Runoff results from rainfall on 230 m^2 plots at the Granite Reef testing site.

Date	Rainfall Intensity Max	Min	Total	Plot 1 runoff		Plot 2 runoff		Plot 3 runoff	
1964			mm	mm	%	mm	%	mm	%
22 Jan	8	2	18.0	17.5 1/	97.3	6.2	34.4	14.8	82.4
3 Mar	8	2	4.5	4.4	98.0	0.1	2.5	3.1	70.0
23 Mar	3	1	4.1	4.7	115.0	0.4	8.5	3.5	85.6
27 Apr	2	1	2.8	2.6	94.3	0	0	2.0	71.1
14 July	3	3	11.4	10.3	90.0	0	0	8.2	71.5
23 July	2	2	2.0	1.5	73.0	0	0	1.4	68.5
1 Aug	25	25	50.0	49.5 1/	99.0	41.0 4/	82.0	35.0	70.0
12 Aug	1	1	2.0	1.3	62.0	0	0	1.1	52.5
13 Aug	15	5	9.0	8.3	92.5	1.6	17.6	6.8	75.1
26 Aug	20	8	17.2	16.4	94.8	7.1	41.5	12.4	72.1
13 Sept	3	3	3.0	2.8	92.0	0	0	1.8	59.0
14 Sept	6	6	7.5	7.2	95.3	3.8	50.5	6.6	87.6
23 Sept	2	< 1	1.2	0.9	73.3	0	0	0.8	67.5
16 Oct	5	3	3.0	2.7	90.7	0	0	2.0	65.7
17 Oct	3	1	2.2	1.8	80.5	0	0	1.5	65.9
11 Nov	1	< 1	1.5	1.5	100.0	0	0	1.4	90.7
15 Nov	3	3	26.2	25.7 1/	98.2	7.7	29.4	19.6	74.7
18 Nov	2	1	5.3	4.8	91.1	0	0	2.9	54.7
18 Dec	4	4	11.2	10.5	93.8	1.7	15.0	8.5	76.0
27 Dec	20	5	10.8	10.1	93.9	1.9	17.8	7.4	68.3
31 Dec	2	< 1	10.0	7.7	77.0	0	0	4.2	42.5
Total			202.9	192.2	94.7	70.5	34.7	145.0	71.5

1/ Tank overflowed, runoff estimated by subtracting average retention.

2/ Tank overflowed, runoff estimated at 100 percent.

3/ Quantity tank held at time of overflow.

4/ Tank overflowed, runoff estimated by subtracting infiltration at maximum rate indicated by previous storms.

Table 10. Continued.

Date	Plot 4 runoff		Plot 5 runoff		Plot 6 runoff		Plot 7 runoff	
1964	mm	%	mm	%	mm	%	mm	%
22 Jan	17.8	98.9	18.2	101.2	19.1	106.2		
3 Mar	4.6	102.0	4.0	89.0	4.2	92.0	4.5	101.0
23 Mar	4.8	115.9	3.4	82.4	4.6	111.2	5.0	121.7
27 Apr	3.1	109.6	2.7	96.0	2.7	95.0	2.9	102.5
14 July	11.4	100.0	11.0	96.5	10.3	90.4	10.9	96.0
23 July	2.2	111.0	1.8	91.5	1.7	82.5	2.0	97.5
1 Aug	50.0 2/	100.0	49.7 1/	99.3	49.7 1/	99.3	50.0 2/	100.0
12 Aug	2.0	100.0	1.7	82.5	1.3	65.0	1.8	88.5
13 Aug	9.4	103.8	8.8	97.0	8.8	97.2	9.3	102.8
26 Aug	17.6	102.0	16.2	94.0	16.4	95.3	17.5	101.9
13 Sept	3.3	110.3	2.9	97.3	2.9	95.7	2.9	99.0
14 Sept	7.9	105.9	7.1	95.1	7.5	100.1	7.9	104.7
23 Sept	1.4	114.1	1.0	86.7	0.8	68.0	1.0	80.8
16 Oct	3.2	105.7	2.9	97.3	2.4	81.0	2.9	99.0
17 Oct	2.8	127.3	2.3	104.5	2.2	98.2	2.7	122.3
11 Nov	1.6	104.0	1.3	88.7	0.7	47.3	1.6	104.0
15 Nov	27.9 3/	106.5	25.9 1/	92.8	25.9 1/	92.8	26.2 2/	100.0
18 Nov	5.9	110.6	6.0	112.8	5.7	107.4	5.9	111.5
18 Dec	11.2	100.2	10.7	95.1	11.0	98.2	10.9	97.3
27 Dec	11.1	102.4	10.8	99.8	10.7	98.6	10.7	99.2
31 Dec	10.1	100.9	9.9	99.4	9.8	98.4	10.4	104.2
Total	209.3	103.2	198.3	97.7	198.4	97.8	187.0	101.0

1/ Tank overflowed, runoff estimated by subtracting average retention.

2/ Tank overflowed, runoff estimated at 100 percent.

3/ Quantity tank held at time of overflow.

4/ Tank overflowed, runoff estimated by subtracting infiltration at maximum rate indicated by previous storms.

Table 11. Directional rainfall measurements by vector pluviometer at the Granite Reef testing site.

Date	Total rainfall collected	Collection by orifice facing direction listed							
		N		E		S		W	
1964	ml	ml	%	ml	%	ml	%	ml	%
27 Apr	26	15	57.7	1	3.8	3	11.6	7	26.9
14 July	179	57	31.8	63	35.2	24	13.4	35	19.6
23 July	21	2	9.6	18	85.7	0	0	1	4.7
1 Aug	779	119	15.2	125	16.0	91	11.6	444	56.9
12 Aug	11	1	9.1	7	63.6	0	0	3	27.3
13 Aug	192	83	43.2	72	37.5	10	5.2	27	14.1
26 Aug	339	106	31.3	105	31.0	57	16.8	71	20.9
13 Sept	23	2	8.7	3	13.0	0	0	18	78.3
14 Sept	236	41	17.4	40	17.0	124	52.5	31	13.1
23 Sept	1	0	0	1	100.0	0	0	0	0
16 Oct	24	0	0	10	41.7	8	33.3	6	25.0
17 Oct	44	5	11.4	30	68.2	6	13.6	3	6.8
11 Nov	2	0	0	0	0	0	0	2	100.0
15 Nov	587	65	11.1	166	28.3	191	32.5	165	28.1
18 Nov	86	10	11.6	34	39.5	13	15.2	29	33.7
18 Dec	288	116	40.3	3	38.9	112	1.0	57	19.8
27 Dec	213	30	14.0	22	10.0	41	20.0	120	56.0
31 Dec	139	53	38.0	77	55.0	0	0	9	7.0
Total	3190	705	22.1	777	24.4	680	21.3	1028	32.2

Table 12. Runoff results from 450 m^2 watersheds at the Granite Reef testing site.

Date	Rainfall Intensity Max	Rainfall Intensity Min	Rainfall Total	Watershed 1 runoff		Watershed 2 runoff		Watershed 3 runoff	
1964	mm/hr	mm/hr	mm	mm	%	mm	%	mm	%
23 Jan	8	2	18.0	2.9	16.3	2.1	11.6	2.8	15.3
3 Mar	8	2	4.5	0	0	0	0	0	0
23 Mar	3	1	4.1	0	0	0	0	0	0
27 Apr	2	1	2.8	0	0	0	0	0	0
14 July	3	3	11.4	0	0	0	0	0	0
23 July	2	2	2.0	0	0	0	0	0	0
1 Aug	25	25	50.0	31.3 1/	62.5	22.9 1/	45.8	45.5 1/	91.0
12 Aug	1	1	2.0	0	0	0	0	0	0
13 Aug	15	5	9.0	0.8	8.9	0.5	6.0	1.9	21.6
26 Aug	20	8	17.2	4.8	27.7	3.4	19.8	6.8	39.5
13 Sept	3	3	3.0	0	0	0	0	0	0
14 Sept	6	6	7.5	2.2	29.7	2.1	28.0	4.2	55.7
23 Sept	2	< 1	1.2	0	0	0	0	0	0
16 Oct	5	3	3.0	0	0	0	0	0	0
17 Oct	3	1	2.2	0	0	0	0	0	0
11 Nov	1	< 1	1.5	0	0	0	0	0	0
15 Nov	3	3	26.2	3.6	13.7	3.2	12.4	6.0	22.7
18 Nov	2	1	5.3	0	0	0	0	0	0
18 Dec	4	4	11.2	1.7	15.2	1.2	10.3	2.5	22.1
27 Dec	20	5	10.8	1.3	12.2	0.2	1.6	0.8	7.6
31 Dec	2	< 1	10.0	0.1	0.9	0	0	0.3	2.5
Total			202.9	48.7	24.0	36.6	18.0	70.8	34.9

1/ Overflowed, runoff estimated by comparison with untreated 9.3 m^2 plot.

TITLE: APPLICATION OF HEXADECANOL-OCTADECANOL MONOFILMS TO SMALL PONDS

LINE PROJECT: SWC 4-gG2 CODE NO.: Ariz.-WCL-9

INTRODUCTION:

See Annual Report 1963.

Laboratory studies have shown that long-chain alkanols can be applied to the water surface at a continuous controlled rate by dispersing them in a matrix of material which dissolves when placed in water. As the matrix dissolves, discrete particles of alkanol are released to form an evaporation retarding film on the water surface. Particle release rate can be controlled by using matrix formulations of varying solubility or by varying the surface area exposed to the water.

Continuing studies were also made with floating granular materials which reduced evaporation by lowering the water temperature. Previous floating powders used would sink during a rain storm. The new granular materials are of foamed plastic which does not sink when wetted.

PROCEDURE:

Procedures were the same as outlined in the 1963 Annual Report with the following additions.

The matrix-alkanol mixtures were prepared in two ways: First, by mixing molten alkanol into heated matrix material with mixing continued until cooling produced a paste or solid; second, by mixing powdered alkanol into fluid matrix materials. Delayed setting gels were particularly convenient for the second method of formulation.

Size of alkanol particles was measured with a microscope and a calibrated optical grid.

The rate of film release was measured in a 17.5 × 60-cm plexiglass tray using 25 C tap water with talcum powder as an indicator. A 0.10-g piece of matrix alkanol mixture was placed in one end of the tray and the film spreading rate was measured after initial coverage of 175 cm^2 area.

RESULTS AND DISCUSSION:

Matrix-Alkanol Materials:

Matrix materials tested included sugar syrups, gum tragacanth, hydroxyethyl cellulose, gelatin and bentonite. Gelatin and bentonite

interfered with film spreading and were discarded. The other materials were satisfactory and could easily be formulated to release alkanol and form surface films at varying rates as indicated in Table 1. All mixtures except number 3 were floated or suspended at the water surface. Number 3 rested on the tray bottom and the released alkanol particles floated to the water surface to produce a film at the rate of 440 cm^2 min^{-1}. Film release rates varied from 50 to 3,800 cm^2 min^{-1}. The latter mixture contained a spreading agent and the alkanol particles were about 15-25μ average diameter. Another mixture without a spreading agent and with 150-200μ particle size released film at a rate of 3,030 cm^2 min^{-1}.

Alkanol particle size is important because of its effect on rate of film formation and on particle buoyancy. The desirability of small particle size to increase surface area and rate of film formation by a given quantity of alkanol is well-known. Particle buoyancy proved important during tests of release beneath the water surface. Mixtures 3 and 6 were heavier than water and sank to the bottom of containers to release alkanol particles beneath the water surface. The 15-25μ particles from mixture 6 never floated to the surface and did not form a film. The 40-70μ particles from mixture 3 readily floated to the surface and created a film. Alkanol particle size can be controlled during the formulation process. The simplest method is to mix alkanol ground to the desired size into fluid matrix materials at temperatures below the melting point of the alkanol. When formulations are prepared with melted alkanol, the particle size can be controlled by varying temperature and mixing shear. For example, mixing molten alkanol into matrix material which is at a temperature just below the melting point of the alkanol produces larger particles than those obtained when both materials are at temperatures above the alkanol melting temperature.

Evaporation reduction with m-a mixtures was tested in June 1964 on outdoor water tanks 274 cm in diameter by 91 cm deep, set in the ground so that the tops are approximately flush with a surrounding grass lawn. Untreated evaporation rates were about 7.2 mm day^{-1}. About 50 g

of m-a mixture 6 was suspended at the water surface with a small float and reduced evaporation about 50 percent for a 2-day period. Wave action disintegrated the material and the test was discontinued. Mixture 3 was placed in a test tube, 2.2 cm in diameter and 17 cm long, which was suspended from a float with the open end about 0.5 cm beneath the water surface. Over a 2-week period alkanol particles were released at a reasonably constant rate of about 0.5 g actual alkanol per day and evaporation was reduced about 40 percent. This reduction was accomplished in spite of the presence of a heavy film of dust and algae on the water surface. Indicator oils showed that this dust and algae film could not be displaced until alkanol film pressures exceeded 30 dynes cm^{-1}.

Floating Granular Materials:

The floating granular materials under investigation are chopped styrofoam and small foamed plastic beads. Sizes are highly variable, but the chopped pieces average about 10 mm square and the beads are about 1 mm in diameter. Both materials are white and reduce evaporation by reflecting incoming radiation and reducing the water temperature. Comparative tests were conducted by applying 4 kg of the materials to separate 274 cm-diameter tanks and comparing evaporation losses with two untreated tanks. During the period 30 October through 13 November 1964, when untreated evaporation was 47 mm, the beads reduced evaporation by 42 percent and the chopped material reduced it by 60 percent. A long-term trial is now under way to determine the effect of weathering on evaporation reduction by these materials.

SUMMARY AND CONCLUSIONS:

A new method was developed for continuously applying evaporation retardants to a water surface without using any mechanical devices. Long-chain alkanols were dispersed in a water soluble matrix so that discrete particles of alkanol were released at a controlled rate as the matrix material dissolved when placed in water. Several saccharides proved satisfactory as matrix materials. Particle release rates were controlled by varying both the formulation and the area of matrix-alkanol material exposed to the water. Film release from 0.10-g

pieces of m-a material were varied from 50 to 3800 cm^2 min^{-1} by changing the formulation.

The size of the alkanol particles proved important in its effect on particle buoyancy as well as on rate of film release from a given quantity of alkanol. Spherical particles of 15-25μ average diameter did not float to the surface when released under water. Similar particles of 40-70μ or larger readily floated to the surface and produced a film. Particle size can be controlled during the formulation process. The simplest method is to use powdered alkanol, ground to the desired size, mixed into a fluid matrix material. Delayed setting gels are particularly convenient for this procedure.

Evaporation reduction by an m-a material was tested in June 1964 on 274-cm diameter outdoor tanks. Untreated evaporation rates averaged 7.2 mm day^{-1}. The mixture was placed in a 2.2 × 17 cm glass test tube suspended from a float with the open end 0.5 cm below the water surface. Over a 2-week period about 0.5 g alkanol per day was released at a reasonably constant rate and evaporation was reduced by 40 percent.

Granular foamed plastic materials proved effective in reducing evaporation from the 274-cm diameter tanks. Chopped styrofoam, about 10 mm square, and foamed beads, about 1 mm diameter, were used. Both materials are white and reduce evaporation by reflecting incoming radiation and reducing water temperature. During the period 30 October through 13 November 1964, when untreated evaporation was 47 mm, 4 kg of the beads reduced evaporation 42 percent. The same amount of chopped material reduced evaporation 60 percent.

PERSONNEL: L. E. Myers, G. W. Frasier

Table 1. Rate of film release from various matrix-alkanol mixtures.

Mix	Matrix material		Alkanol		Mixing temperature	Film release 2/
	Type	Amount	Amount	Particle size		
		Percent by weight	Percent by weight	μ	Degrees C	$cm^2\ min^{-1}$
1	glucose syrup sp. gr. 1.39	64	36	150-200	24	50
2	gum tragacanth 2 percent gel	61	39	150-200	24	250
3	sucrose syrup sp. gr. 1.47	71	29	40-70	60	440
4	glucose syrup sp. gr. 1.32	53	47	150-200	24	1700
5	Natrosol hydroxyethyl cellulose 4 percent gel	70	30	150-200	24	3030
6	sucrose syrup sp. gr. 1.40	73 1/	25	15-25	60	3800

1/ Plus 2 percent alkyl quaternary ammonium chloride emulsifier.

2/ Rate of film generation by a 0.10-g piece of m-a material.

TITLE: FIELD APPLICATION OF FALLING-HEAD TECHNIQUE FOR SEEPAGE METERS AND OF DOUBLE-TUBE METHOD FOR HYDRAULIC CONDUCTIVITY MEASUREMENTS

LINE PROJECT: SWC 4-gG1 CODE NO.: Ariz.-WCL-14

INTRODUCTION:

The field application of the falling-head seepage meter technique was continued in 1964 with a demonstration for the Soil Conservation Service in the Loveland, Colorado area. Further cooperation was extended the Arizona State Office of Soil Conservation Service in an investigation of seepage losses from the Highline Canal near Safford, Arizona.

Most of the work on the double-tube method was in relation to the measurement of horizontal and vertical hydraulic conductivity (see WCL-25). A double-tube test, however, was carried out on laboratory grounds for a period of 32 days to investigate long-term behavior of the measured hydraulic conductivity and infiltration rates.

PROCEDURE:

The seepage meter applications were carried out according to the standard procedure as discussed in previous annual reports. The long term double-tube test was carried out on the Bermuda lawn immediately south of the hydraulics laboratory in the month of November. The hole was approximately three feet deep. Installation of equipment and collection of data were carried out according to procedures outlined in previous reports. Phoenix city water was used for the water supply. Several measurements of the hydraulic conductivity K and the infiltration rate I from the inner tube were made each day. From the 11th day on, the salt content of the water was determined from electrical conductivity measurements. On the 30th day, the sodium adsorption ratio of the water was increased from two to twenty by the addition of NaCl to determine its effect on K and I.

RESULTS AND DISCUSSION:

For a detailed discussion of the results of the seepage work in Colorado and Arizona, reference is made to the reports prepared for these measurements. The results of the Colorado measurements are summarized in Table 1, and those of Arizona in Table 2.

The results of the long-term double-tube tests are summarized in Figure 1. For the first five days, K remained relatively constant between 3.2 and 4.4 cm/day. After this, K increased in irregular fashion to a value of approximately 800 cm/day after 32 days. A more or less similar pattern was exhibited by the infiltration rate I, but after 24 days, I began to decrease. The salt content of the water showed a slight increase, which may have been at least in part responsible for the increase in K, as indicated by the parallel trends in salt content and K. The change in sodium adsorption ratio by the addition of sodium chloride, however, appeared to have little effect on K. In the last few days of the test, very small H_b-values were observed, which together with the absence of effects of the NaCl-addition indicated that channels or other free passages had been formed in the soil. These channels permitted the water to move rather freely between the inner and the outer tube. The decrease in I after 25 days is difficult to explain. One possibility is that the wetting front may have encountered slowly permeable material.

After termination of the test, the auger hole bottom was examined. Numerous worms were found at the bottom and in the soil below it. When the double-tube equipment was installed, the soil was dry and no worms were encountered. Evidence of worms working their way up to the auger hole bottom was also found in the presence of channels below the hole bottom which were filled with the sand used to cover the hole bottom for protection of the soil surface. It is, therefore, concluded that the increase in K and I can also be attributed to worm activity.

SUMMARY AND CONCLUSIONS:

The usefulness of the seepage meter in routine seepage investigations was again demonstrated in 1964 by cooperative work with the Soil Conservation Service in Colorado and Arizona. A long-term double-tube test was carried out for 32 days on the Bermuda lawn behind the laboratory. The hydraulic conductivity remained essentially constant at approximately 4 cm/day for the first five days. After this, K increased in irregular fashion to about 800 cm/day

after 32 days. This increase may be due in part to a gradual increase in the salt content of the water from approximately 400 to 700 ppm, and in part to worms which were encountered at and below the auger hole bottom at the termination of the test. The infiltration rate exhibited an increase up to the 25th day, after which a decrease to a much smaller value took place. This decrease may have been caused by backup effects due to the wetting front reaching restricting layers in the soil. Where the effect of water quality on hydraulic conductivity is to be studied in the field with the double-tube method, care should be taken to avoid worm and other biological activities.

PERSONNEL: Herman Bouwer and R. C. Rice.

Table 1. Seepage rates and hydraulic conductivity information, Highline Canal, Safford, Arizona.

Test	r_v in	$\overline{H}$ in/min	I_s ft/day	H_b in	d in	H_w in	K ft/day	I_s/K	r_s hr
1	0.95	1.3	6.0	25	0.5	28			8.3
2a	0.59	0.35	0.60	18	1.5	34	0.059	10	
2b	0.59	0.16	0.28	8.0	2.5	34	0.093	3.0	
3a	0.59	0	0	0	1.5	35	7.8	0	
3b	1.95	0	0	0	1.5	26	65	0	
4a	0.59	0.23	0.40	0.20	1.75	25	6.8	0.06	
4b	0.59	0.82	1.4	0.40	2.0	25	12	0.12	
5a	0.11	0.29	0.018	0.40	1.5	26	0.15	0.12	
5b	0.11	0.84	0.051	0.30	1.75	19	0.57	0.09	
6a	1.95	0	0	0	2.5	13	126	0	
6b	1.95	0	0	0	2.0	14	78	0	
7a	0.11	0.48	0.029	4.2	1.0	20	0.023	1.2	
8a	0.95	0.85	3.9	5.0	1.5	19	2.7	1.5	
8b	0.95	0.80	3.7	1.3	2.5	18	9.7	0.38	
9b	0.11	0.42	0.026	0.60	1.5	20	0.15	0.18	
10a	0.95	0	0	0	1.0	16	21	0	
10b	0.11	0.43	0.027	0.75	1.0	16	0.12	0.22	
11a	0.11	1.24	0.076	1.7	1.5	10	0.15	0.50	
11b	0.95	0	0	0	1.0	9	7.8	0	

Table 2. Calculation of seepage rates, Loveland, Colorado

Test No.	R_c in	R_v in	$\bar{\bar{H}}$ in/min	I_s ft/day
1	5	0.11	2.6	0.16
2	5	1.5	0	0
3	5	0.11	0.14	0.008
4	5	0.11	0.27	0.016
5	5	0.11	0.25	0.015
6	5	1.5	0.70	7.9
7	5	0.95	0.50	2.3
8	5	0.95	0.90	4.1
9	5	0.59	1.2	2.1

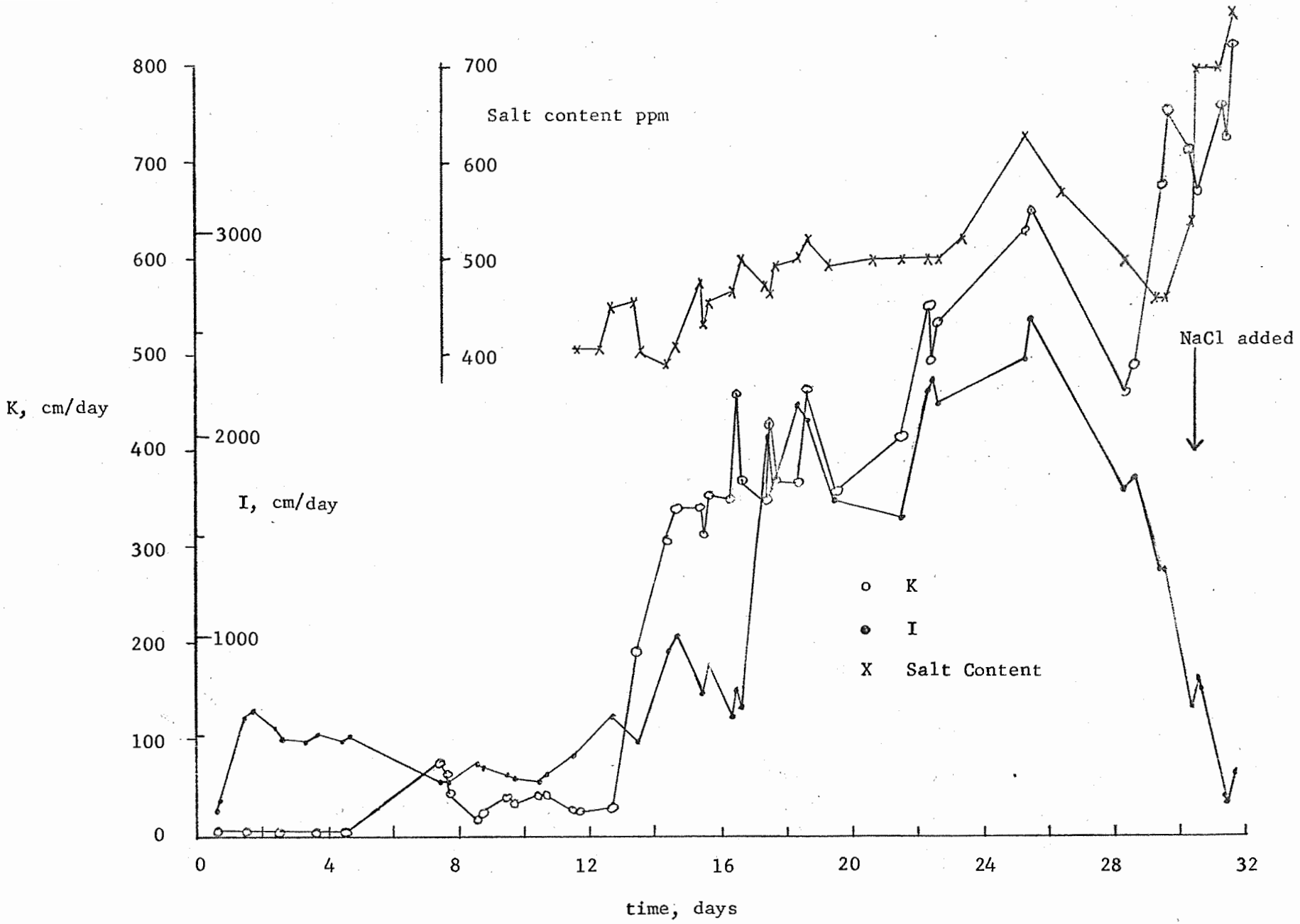

Figure 1. Results of long-term double-tube test.

TITLE: ANALYZING GROUND WATER MOUND FORMATION BY RESISTANCE NETWORK ANALOGS

LINE PROJECT: SWC 4-gG3 CODE NO.: Ariz.-WCL-15

INTRODUCTION:

Although the work originally planned for this project has been completed for some time (Lab. Publ. No. 42, 73, 120), some additional work was performed in 1964. The first part of this work was in preparation for a panel discussion of the Dupuit-Forchheimer assumption at the 1964 ASAE Winter Meeting (Lab. Publ. No. 139). The second part consisted of a study of the use of conformal transformation in representing infinite boundaries of flow systems on the resistance network analog. Application of this technique for electrolytic tank and conductance paper analogs was studied while on an OECD Science Fellowship Program in The Netherlands. With resistance network analogs, infinite boundaries are usually simulated by increased node distances and a termination strip, but they could also be represented by transformation techniques. A comparison between infinity representation on the network analog by increased node distances and by conformal transformation would, therefore, be of interest.

PROCEDURE:

As stated in previous annual reports and publications, the Dupuit-Forchheimer assumption (D-F assumption) loses validity in the analysis of ground water mounds below recharge areas if $D > W$ (see Figure 5 for geometry and symbols). If $D \ll W$, the D-F assumption is valid, but then the neglect of the flow above the original water table, which is another assumption made in the mathematical analysis, loses validity. To illustrate this, a comparison was made between the rate of rise of the center of a two-dimensional mound based on the D-F assumption and neglect of the flow above the original water table, and the rate of rise obtained from resistance network analysis. The latter takes both the vertical flow components and the flow above the original water table into account. The D-F solution was taken from "Theory of Ground Water Movement" by Polubarinova-Kochina.

The representation of infinity on finite analogs or other models through conformal transformation of part of the flow system is described in (1) and (2). The principle of representing infinity conditions through conformal transformation consists of dividing the medium in two parts. The main region of flow is represented in one analog (circle I in Figure 1A). The rest of the medium is inverted and represented in a second analog system (circle II). The real and inverted systems are then electrically connected at a sufficient number of corresponding points, exemplified by A, B, and C in Figure 1A. The criteria for inversion is $rr' = R^2$. Thus, point D outside circle I is represented as D' in circle II and infinity is represented by the center of circle II. The coordinate system in the inverse part consists of circles which intersect each other at right angles. This is shown in Figure 1B, which represents the fourth quadrant of circles I and II. For ease of connecting corresponding points, the inverse is turned 180 degrees so that the corresponding sides of the systems face each other. The fourth quadrant is frequently used for representation of flow systems, because the upper boundary is often a water table and the left boundary is a symmetry line. The hatched sections in Figure 1B show how a square outside the real system is represented in the inverted system. Inversion is a conformal transformation and the real system connected to the inverse behaves as if it were of infinite extent.

The procedure of analyzing flow problems with a real and inverse portion of the medium on the analog was first studied with a system of radial flow to a well in a confined aquifer. The network arrangement is shown as system A in Figure 2. The unit network resistance R_0 was 200 ohms, the unit of length is taken as the unit node distance Δ in the square grid, and R for the real and inverse system was taken as 12Δ. The radius of the well was taken as 0.46Δ, because at this ratio the resistances around the well could be calculated as $(\Delta - 0.46\Delta)\ R_0/\Delta$, according to Vimoke, et al (3). Since the resistors around the well in Figure 2 are symmetry lines, the resistances should be doubled, thus yielding a value of 216 ohms.

Infinite boundaries can not be used in the theory of well flow. Therefore, the outer boundary was selected at a radius of 313Δ, so that the inverse was exactly a replica of the real portion of the flow system (the value of 313Δ is calculated as $144\Delta^2/0.46\Delta$ according to $r' = R^2/r$). Because of the critical importance of the resistances at the well and the inverse of the cylindrical outer boundary, these resistances were adjusted so as to give the theoretically correct potentials of 11.9 percent at $r = \Delta$ in the real system, and of 88.1 percent at $r' = \Delta$ (corresponding to $r = 144\Delta$) in the inverse. The resistors indicated resistance values of 195 ohms instead of the 216 ohms calculated for these resistances according to Vimoke, et al. The final step consisted of measuring flow rates and potentials at the nodes and comparing these values with the calculated values from the theory of radial flow.

Ground water mound studies were performed for the two-dimensional case with a network arrangement as system A in Figure 2, with the cylindrical sink and source replaced by "porous medium" reaching infinity in the inverse system. The top nodes of the systems were connected by conductors representing a horizontal water table. The source conductor representing the top of the flow system under the percolation zone was separated from the sink conductor representing the rest of the original water table by a fictitious vertical solid boundary extending a distance Δ below the water table (see Figure 2B). This method of separating the source and sink conductors is preferable to separation by interruption in the conductor for a distance Δ. A voltage difference of Δh volt was applied to the water table below the percolation zone and the rest of the water table, after which the total current and the downward gradient i at the water table below the center of the percolation zone were measured. The latter was then converted to the dimensionless parameter $iW/\Delta h$, which indicates the disposal capacity of the aquifer below the center of the percolation zone at incipient mound formation. This parameter determines the rate of rise of the mound center for a given recharge rate. Measurements were

made for different values of D, which is the distance between the water table and the impermeable layer, and for different values of W, which is the width of the percolation zone. The parameter $iW/\Delta h$ was then plotted against D/W. Because both D and W were varied in the analyses, overlapping values for the D/W-ratios were obtained for several of the D-values employed. The analyses were carried out for D-values of infinity (as system A in Figure 2), 16△ (system B in Figure 2), 8△ (system C in Figure 3) and 4△ (8△/2, system D in Figure 3). The node density in the inverse part of system C and in both parts of system D was doubled. Systems B, C, and D show how the horizontal impermeable layer appears as part of a circle in the inverted system. After these analyses, the meshes in system D were changed to rectangles with a length of twice their height for the zone indicated by the arrows above system D in Figure 3. This was done to obtain sufficient values in the low D/W range.

RESULTS AND DISCUSSION:

The formation of a two-dimensional mound according to the D-F assumption and according to analog analyses is shown in Figure 4, where the rise H of the center of the mound is plotted against t for a recharge rate of 0.1 K. For dimensionless expression, H is divided by the width W of the percolation zone and t is multiplied by K/fW, where K is the hydraulic conductivity and f the fillable porosity of the medium. The curves appear to coincide initially, which suggests the validity of the D-F assumption for the rather small D-value in this case (D = 0.267 W). Soon after this, however, the mound rises slower for the analog than for the D-F assumption which is probably due to the fact that the analog takes the flow above the original water table into account, while the analysis based on the D-F assumption does not.

The theoretical flow rate Q in a confined aquifer of unit height to a well with a radius of 0.46△ from an equipotential at 313△ is $2\pi KH/\ln(313/0.46) = 0.965$ KH where K is hydraulic conductivity and H is the potential drop from 313△ to 0.46△. The current measured on the analog for the system indicated a flow rate of 0.93KH, or an error of -3.6 percent. The equipotentials as constructed from

potential measurements at the network nodes all plotted essentially as circles. The radii of these circles and the values calculated from radial flow theory are shown in Table 1. In this table, the radii of the equipotentials in the inverse system were converted to the real values. It appears that the greatest errors occur in the vicinity of the well in the real system and the outer boundary in the inverse system. The fact that the errors in these regions are in opposite direction, suggests that the errors are mainly due to insufficient density of the network in the vicinity of the source and the sink of the system. The errors are, however, small and quite acceptable.

The results of the ground water mound analyses are shown in Figure 5, where $iW/\Delta h$ is plotted against D/W. The data agreed closely with the curve which was obtained previously with a resistance network analog using increased nodal distances and a termination surround to simulate infinity (Lab. Publ. No. 42).

SUMMARY AND CONCLUSIONS:

Mathematical treatment of ground water mound behavior is often based on the assumption of horizontal flow and on neglect of the flow above the water table. The latter results in an overestimation of the rise of a mound above a relatively shallow aquifer. This was illustrated by comparing an analytical solution with a solution by resistance network analog. Initially, the solutions showed good agreement indicating the validity of the Dupuit-Forchheimer assumption of horizontal flow. As time progressed, however, neglect of the flow above the original water table resulted in a faster rise of the mound for the analytical solution than for the analog solution.

The condition of infinite extent of a flow medium was represented on the resistance network analog by splitting the medium into a real and an inverse part. With the common surfaces of both parts electrically connected, the real part behaves as if it were of infinite extent. Solutions were obtained for a system with radial flow in a confined aquifer and for a system of incipient ground water mound formation above an unconfined aquifer. The radial-flow system yielded a flow rate that was 3.6 percent below the theoretical value.

The error in the radial distances of the concentric equipotentials varied from 0 percent for the 50-percent equipotential to 6 percent for the 80-percent equipotential. The errors are small and most likely due to insufficient network density near the source and sink of the system and overall instrumental inaccuracies. The results of the ground water mound analyses agreed very closely with data previously obtained with the analog using increased nodal distances and a termination surround for representing infinite media on the analog.

In certain cases, such as homogeneous media of infinite horizontal and vertical extent, inversion gives a simpler network arrangement than increased node distances for infinity representation. However, since horizontal and vertical lines are represented as parts of circles in the inverse, layered or anisotropic media can not be easily represented and infinity in that case can better be simulated by increased node distances and a termination surround. If the lower boundary of a flow system is a horizontal layer of much higher or much lower hydraulic conductivity and if the depth of this layer is to be taken as a variable in the analyses, the choice between inversion and increased nodal distances for infinity representation depends to a large extent on the number of positions of the boundary that should be included in the analyses. The choice between inversion or increased distances for representing infinite flow systems is thus governed by the characteristics of the medium and the boundaries. In some cases, inversion can lead to greatly simplified representation of flow systems with open boundaries on the resistance network analog.

REFERENCES:

(1) Boothroyd, A. R., Cherry, E. C., and Makar, R.
1949. An electrolytic tank for the measurement of steady state response, transient response, and allied properties of networks. Proc. Inst. Electr. Engrs. 96, Pt. I, 163-177.

(2) De Jong, J.
1962. Een eenvoudige methode voor het nabootsen van een

oneindig potentiaalveld. Water 46 (Tijdschrift Drinkwatervoorziening), 185-186.

(3) Vimoke, B. S., Tyra, T. D., Thiel, T. J., and Taylor, G. S. 1962. Improvements in construction and use of resistance networks for studying drainage problems. Soil Sci. Soc. Am. Proc. 26, 203-207.

PERSONNEL: Herman Bouwer

Table 1. Measured and calculated radii of equipotentials.

	Potential in % of total difference	Measured radius of equipotential	Calculated radius of equipotential	Error in %
		Unit network intervals		
inverse system	100	313	313	0
	80	90.0	84.5	+6.5
	70	44.9	44.0	+2.0
	65	32.1	31.8	+2.2
	60	23.2	23.0	+0.9
	55	16.6	16.6	0
	50	12.0	12.0	0
real system	45	8.67	8.63	-0.5
	40	6.21	6.24	-0.5
	35	4.49	4.50	-0.2
	30	3.21	3.25	-1.2
	20	1.60	1.69	-5.6
	0	0.46	0.46	0

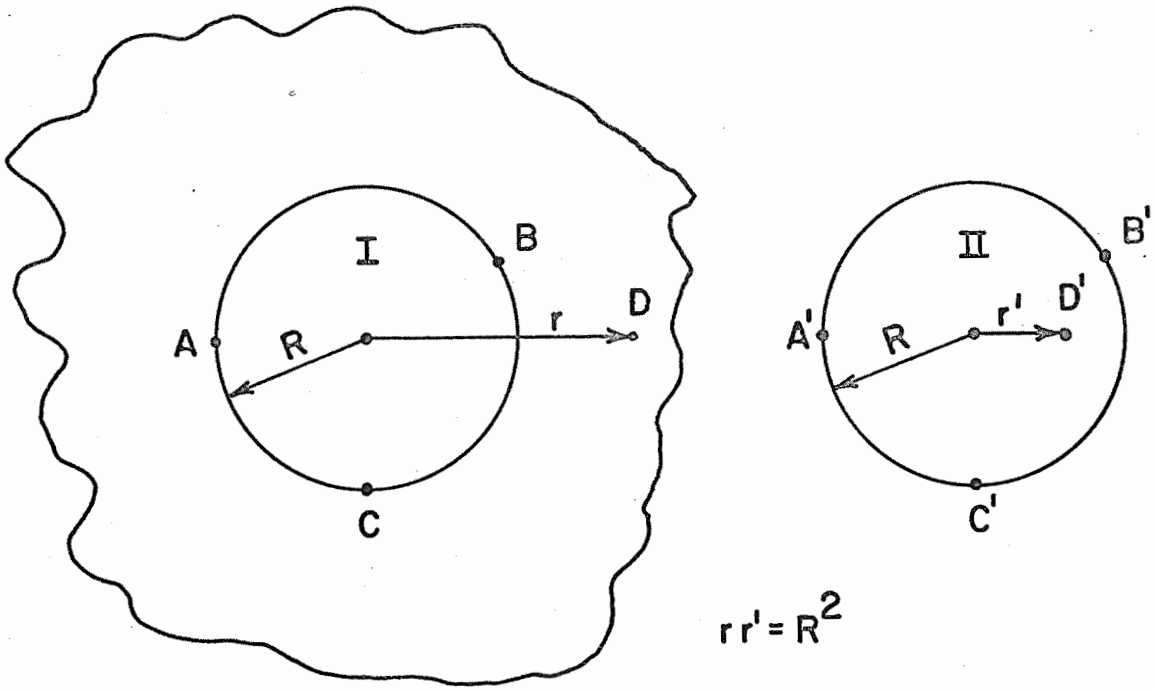

Figure 1A. Principle of inversion.

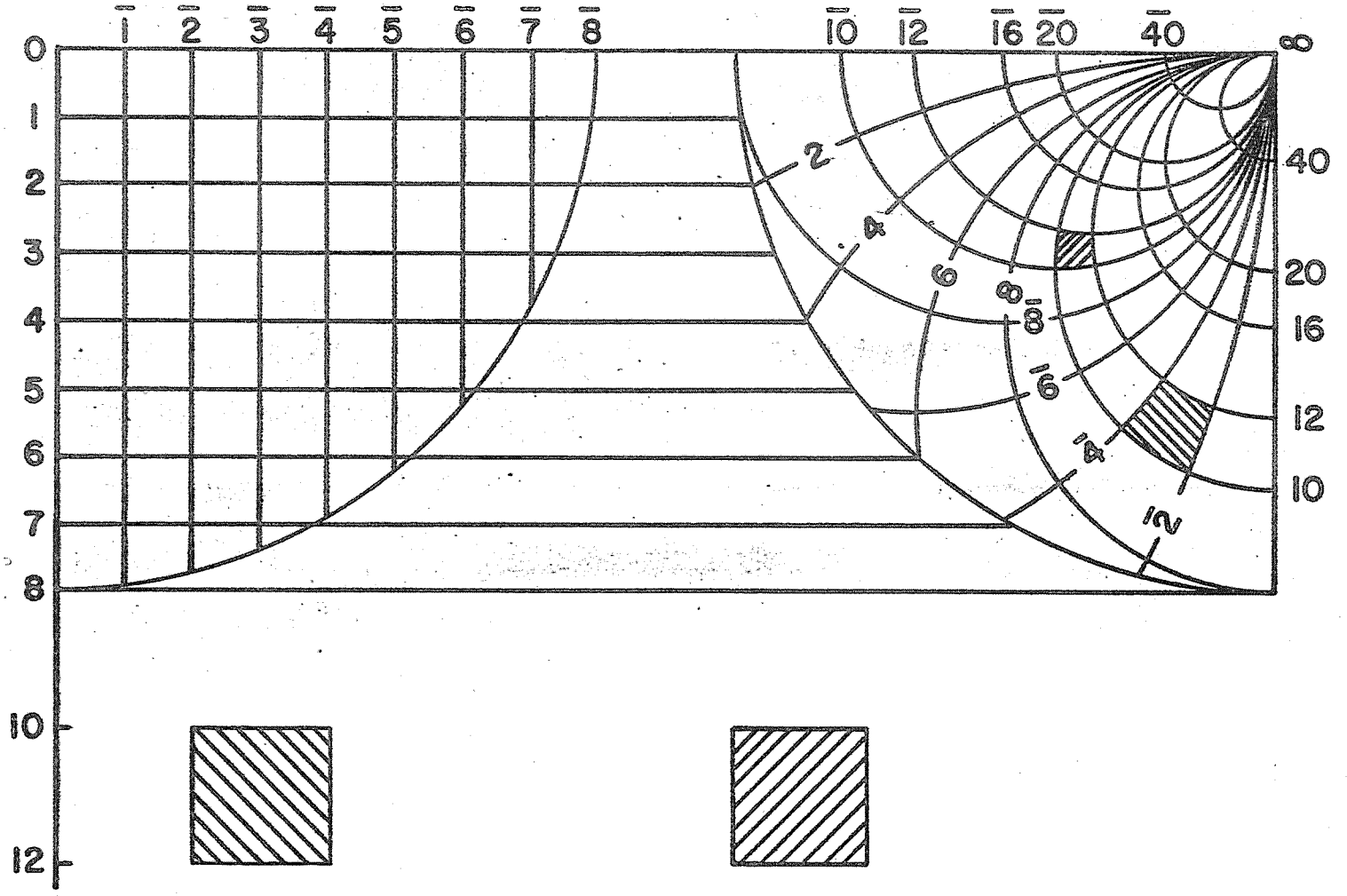

Figure 1B. Coordinates in real and inverse system of fourth quadrant.

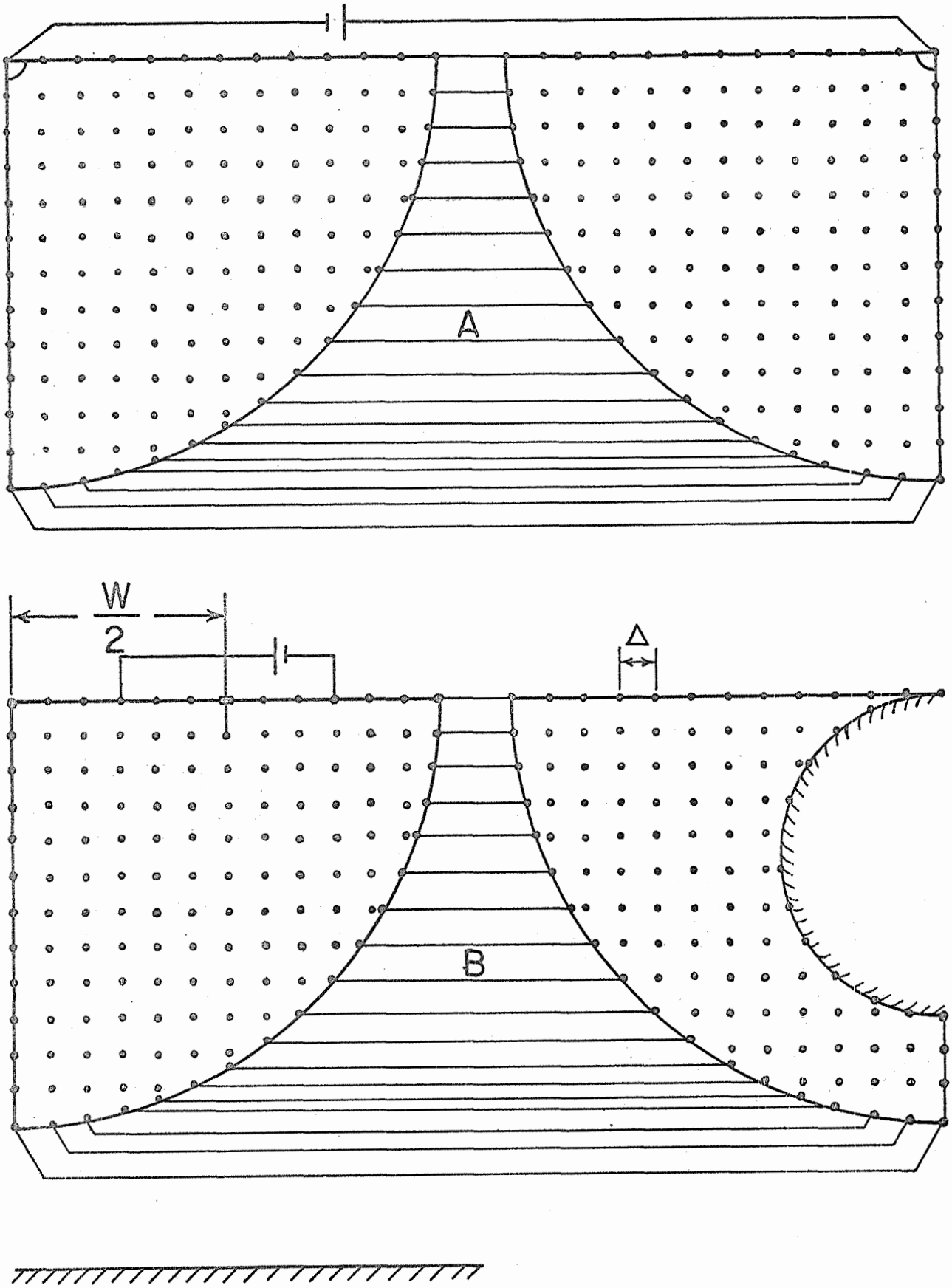

Figure 2. Network arrangement for radial flow (top) and incipient ground water mound formation (bottom).

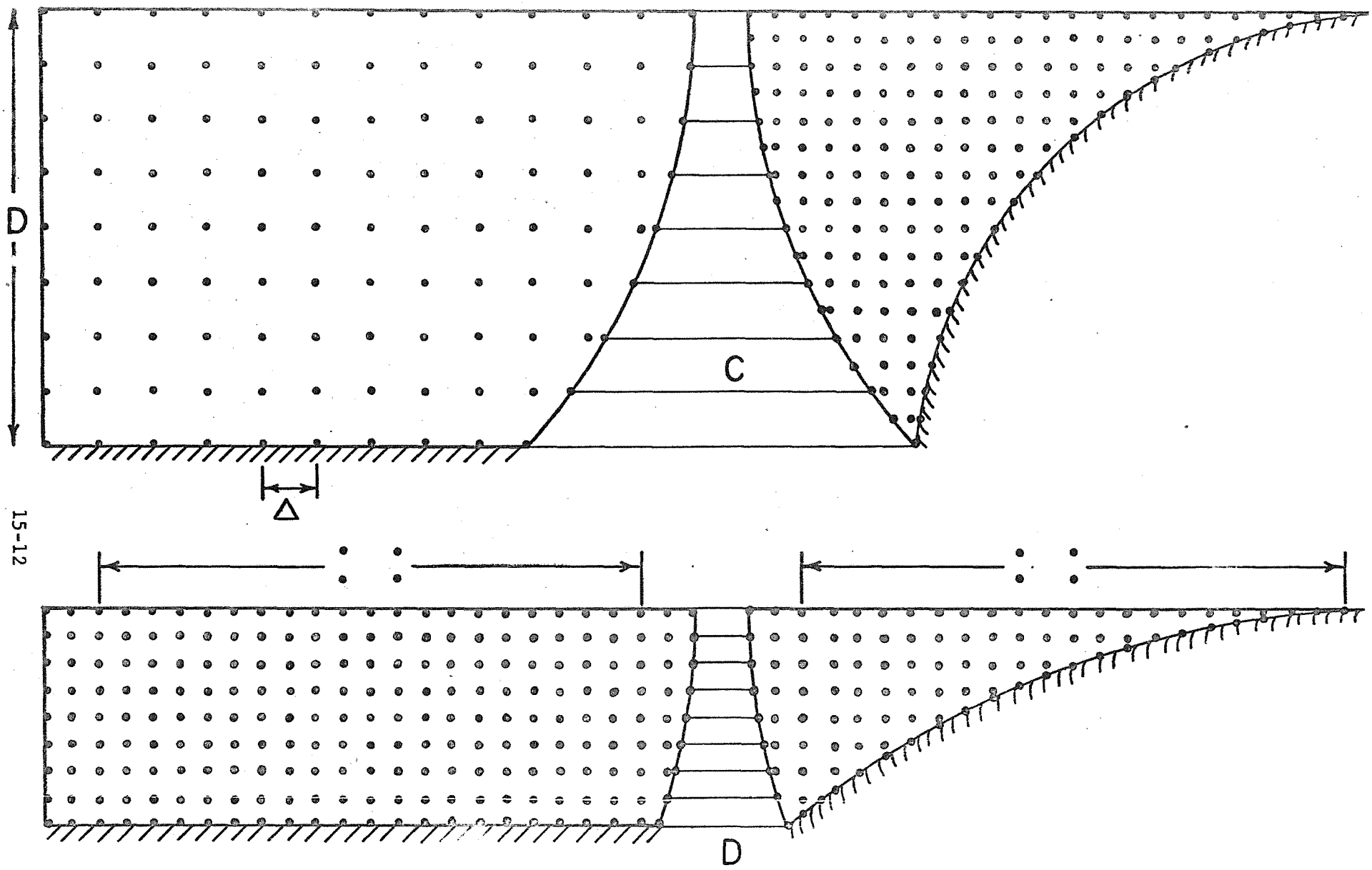

Figure 3. Network arrangement for incipient mound formation for symmetrical D.

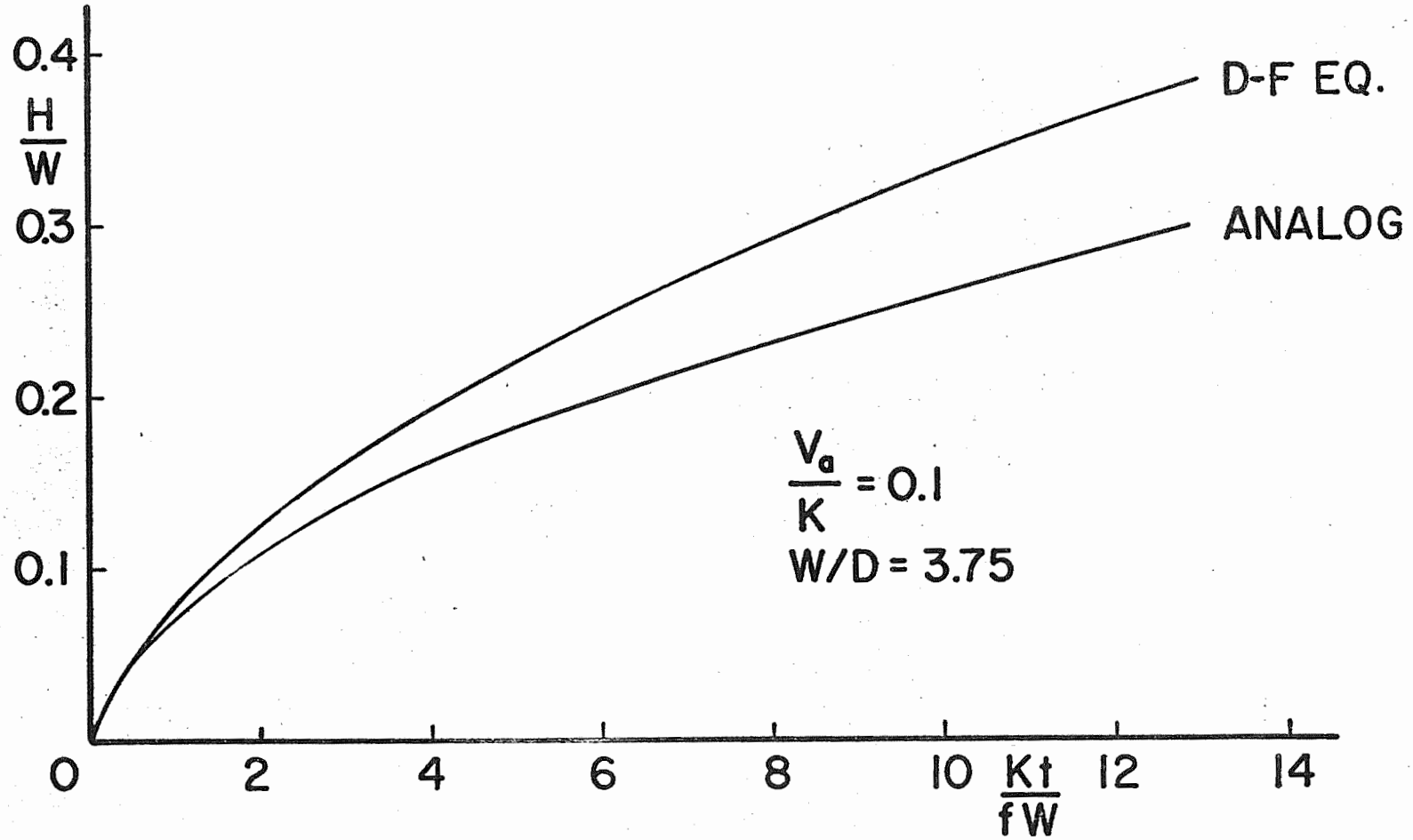

Figure 4. Dimensionless graph of the rise of a two-dimensional mound according to the D-F assumption and to the resistance network analog.

Annual Report of the U.S. Water Conservation Laboratory

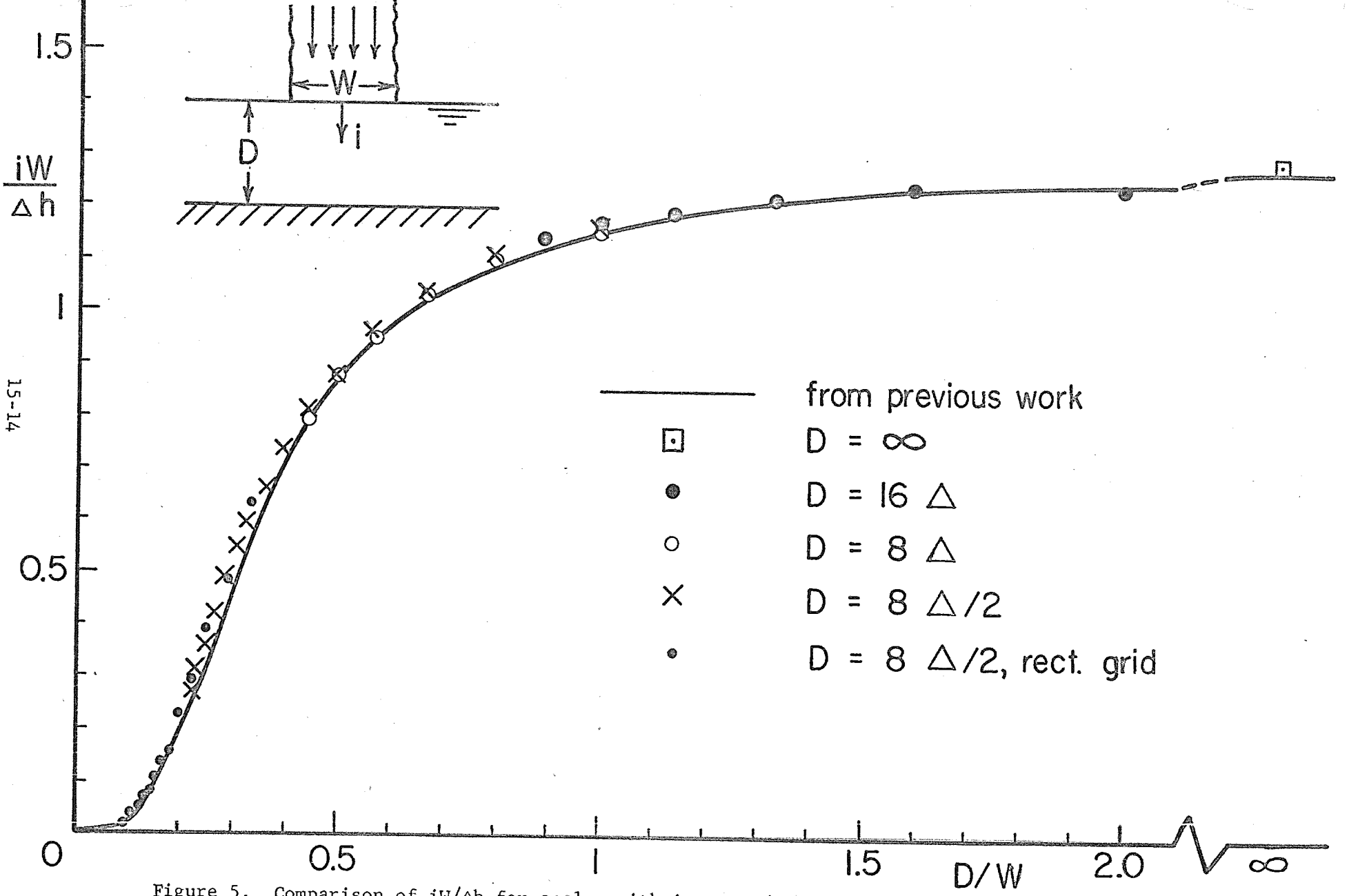

Figure 5. Comparison of iW/Δh for analog with inverse (points) and increased node distance (curve) for representation of infinity.

TITLE: COMPONENTS OF THE RADIATION BALANCE OF FIELD CROPS UNDER IRRIGATED CONDITIONS

LINE PROJECT: SWC 4-gG2 CODE NO.: Ariz.-WCL-18

1. INTRODUCTION:

The evaporative flux from any crop surface — water not limiting — is largely determined by the radiant energy input or net radiation. Measurements of net radiation have been lacking in most field experiments; furthermore, continuous records of net radiation are generally nonexistent. Solar radiation, however, is measured at several locations in this country. Therefore, it would be desirable to estimate net radiation from solar radiation data and to see how the relation would vary with reflected solar radiation. To this end, net radiation and reflected solar radiation were measured over alfalfa, barley, wheat, oats, cotton, and sorghum. These values were then related to solar radiation. The results are presented in this report.

2. EXPERIMENTAL PROCEDURES:

Measurements of incoming and reflected solar radiation, and net radiation were made over alfalfa, barley, wheat, oats, cotton, and sorghum. The measurements were made for one to three day periods biweekly throughout the growing season. They were initiated on 30 January and terminated on 22 September.

Incoming solar radiation was measured with a solarimeter built by Kipp and Zonen of Delft, Holland.

Reflected solar radiation was measured 1 m above the various crop surfaces with the Kipp and Zonen solarimeters. The sensors were removed from the shields and mounted in an inverted position under a single radiation shield, so that the sensing portion of the instrument was in a plane parallel to a 7-inch horizontal disc.

Net radiation was measured 1 m above each of the crops with two compensated net radiometers (1). In the case of row crops, one net radiometer was located over the row, while the other was located over the furrow. The average of the two net radiometers was used for all calculations.

All data were recorded at 15-minute intervals on our data-logging system. Hourly averages were computed from five 15-minute periods.

3. RESULTS AND DISCUSSION:

The data were analyzed in three ways:

(1) Albedos were computed for all crops;

(2) Linear regressions of net radiation on incoming solar radiation were computed; and

(3) Linear regressions of net radiation on net solar radiation were computed.

These data are summarized for crops in Table 1.

3.1 Albedo. The albedos of the various crop surfaces were computed with hourly data. Generally speaking, the ratio was very large during the first hour (about 0.4), then decreased to about 0.2 at solar noon and increased to about 0.4 at the last hour. The large albedos could be attributed to the sensors used. At low sun angles, a small amount of direct radiation would strike the sensing area of either the incoming or inverted sensors; however, energy would be reflected within the hemispherical windshields of both sensors. The amount of energy reflected within the hemispherical windshields would be nearly equal for the incoming and inverted sensors. Thus, ratio of the results would approach one. Since the hourly averages were computed on solar time, it is possible that one or two 15-minute daylight observations would represent the hourly average, causing large albedos in early morning and late evening that would not be representative.

A more realistic way to compute albedo would be to use daily totals. Thus, early morning and late evening values would not affect the albedo as much. The results reported in Table 1 were computed from daily totals.

3.1.1. Alfalfa. Albedo of alfalfa surfaces varied from 0.20 to 0.27, with an average of 0.24. Generally speaking, the larger albedos were obtained from the taller crops. There are a few notable exceptions to this statement, the first occurring on 30 January when the alfalfa was just emerging from dormancy. It was 14 cm tall and had a lot of dry leaves exposed. This would cause a larger albedo. The low albedos on 13 March and 22 September were due to partly cloudy skies.

These data are quite consistent with those reported in last year's annual report. Last year's albedos ranged from 0.20 over recently trimmed alfalfa, 10 cm in height, to 0.23 over 30-cm alfalfa with full leaf development. Dry alfalfa stubble albedos ranged from 0.22 to 0.25, depending on the amount of trash upon the surface.

3.1.2. Barley. Similar to alfalfa, the albedo of barley varied from 0.20 to 0.26. The lowest value, 0.20, was obtained from emerging barley 5 cm tall. At this time the soil surface was moist. Maturity increased the albedo to 0.26. The average albedo of barley was 0.23.

3.1.3. Wheat. The albedos for wheat (Table 3) range from 0.18 to 0.22 with an average of 0.21. The lowest albedo, 0.18, was obtained from an emerging wheat and wet soil surface. It is similar to that reported in last year's annual report for bare soil. They ranged from 0.14 over wet soil to 0.24 over dry soil. Wheat albedos were generally lower than those over alfalfa. They did not reflect an increase at maturity. This may be due to the nature of the crop, being tall and not as leafy.

3.1.4. Oats. The data from oats indicated albedos ranging from 0.16 over an emerging oat and wet soil surface to 0.25. The average was 0.23. Oat albedos were generally higher than those of wheat and barley. This can be attributed to the nature of the crop. The stand was very thick with the leaves orientated at all angles and bending down at the ends, as contrasted to the wheat and barley which had thinner stands and leaves standing more upright. The amount of energy reflected did decrease with the development of inflorescence.

3.1.5. Cotton. The albedo of cotton tended to increase with crop growth, ranging from 0.18 over practically bare soil to 0.27 over 115-cm cotton. The data presented were obtained from three different treatments. The average albedo was 0.22, being slightly lower than the average for alfalfa, barley, and oats.

Since cotton is a row crop, these data reflect the development of the crop; i.e., early in the season a large portion of the soil surface was exposed. This tended to reduce the albedo and thus, reduce the average. After maximum height had been reached, the albedos were very similar to those obtained over alfalfa, averaging about 0.25.

3.1.6. Sorghum. Albedos were measured on four occasions over sorghum, the first when the sorghum was 83 cm and the last after development of the seedheads. The albedos ranged from 0.19 to 0.22, with an average of 0.21.

3.1.7. Summary. These data and those reported in the 1963 Annual Report indicate that normal cultural practices do not alter albedos greatly. The albedos ranged from 14 percent over wet soil to 24 percent over dry soil and up to 27 percent over crop surface. The average albedo over the crop surfaces was 0.24. Row crops tend to have lower albedos until maximum cover is developed. Then the albedos are similar to those of continuous crops, such as alfalfa. Broad leaf plants tended to have greater reflections than grasses. The crops studied are ranked in order of increasing albedos as sorghum, wheat, barley, oats, cotton, and alfalfa.

From the point of view of water conservation, greatest savings would be realized by altering the reflection of soil surfaces, either bare or during early stages of plant development. For example, the difference in albedo of wet and dry bare soil (0.14 to 0.24) on a day of 700 ly amounts to 70 ly. This would be equivalent to 1.2 mm of water if reflection was the only process involved.

3.2. Relations between net, solar, and net solar radiation.

For some purposes it would be desirable to estimate net radiation from solar radiation data. Net and solar radiation relations over different surfaces are not generally available because of the lack of net radiation data. Therefore, these relations were investigated using linear regression techniques.

3.2.1. Net and solar radiation relations. Linear regressions were computed for net radiation on incoming solar radiation. The data used consisted of hourly averages of periods of incoming solar radiation; consequently, included some negative net radiation results at sunrise and sunset. In all cases the net radiation data used consisted of an average of two net radiometers, one being placed over the row and one over the furrow when appropriate.

The regression equations and sample standard deviations from regression, or standard errors of estimate, are listed in Tables 1 through 6. The regression coefficients were all highly insignificant; therefore, are not listed. As can be seen from the tables, the standard deviation from regression was quite small, averaging 0.02 ly min^{-1} for alfalfa, 0.03 ly min^{-1} for barley, 0.03 ly min^{-1} for wheat, 0.02 ly min^{-1} for oats, 0.02 ly min^{-1} for cotton, and 0.02 ly min^{-1} for sorghum. These data indicate that hourly net radiation over different surfaces can be estimated quite satisfactorily from measurements of solar radiation, using individual regression equations. However, the regression equations are a function of crop cover and height, solar radiation, and other meteorological factors affecting net radiation. Therefore, advanced knowledge would be required to know which equation to use. To avoid this problem, individual crop relations were sought.

Data for each crop were pooled and regression equations computed. The results are presented as pooled data at the bottom of Tables 1 through 6. In some cases, the standard errors were 0.02 of a ly min^{-1} greater than the average standard error of individual regression lines. In other cases, they were equal. The results indicate that net radiation can be estimated from solar radiation with standard errors ranging from 0.02 ly min^{-1} to 0.05 ly min^{-1}.

The data for all crops were pooled and a regression equation was computed for net radiation on solar radiation. The resulting standard error was 0.057 ly min^{-1}. Thus, the standard error for all crops was about 3 times as large as that from a single crop for a single day and about 2 times as large as that from a single crop for all days.

3.2.2. Net radiation and net-solar radiation relations. Since reflected solar radiation is one of the terms making up net radiation, net-solar radiation relations should be improved by its addition. Therefore, reflected solar radiation was subtracted from incoming solar radiation. The resulting term is referred to as net solar radiation.

Linear regression was used to compute the regression of net radiation on net solar radiation. The results are listed in Tables 1 through 7. Again, the correlation coefficients were all highly significant. The average standard errors were similar to those of net radiation versus solar radiation, with the exception of wheat and oats. The average standard errors for wheat and oats were 0.02 ly min^{-1}.

Data from each crop were pooled and linear regression computed. The standard errors were similar to those obtained from net radiation versus solar radiation, indicating that the addition of reflected solar radiation did not improve the relation.

The grand regression (all crops and all days) of net radiation on net solar radiation indicated a standard error of 0.057 ly min^{-1}, which is the same as that obtained from net radiation versus solar radiation, again indicating that the correction of incoming solar radiation by subtracting reflected solar radiation does not yield better estimates of net radiation.

3.2.3. Summary. Net radiation measured over transpiring field crops on clear days was found to be very highly correlated with solar radiation. Standard deviations from regression for individual days averaged 0.02 ly min^{-1} for alfalfa, barley, wheat, oats, cotton, and sorghum. However, the regression changed from day to day, thus daily relations are rather useless for estimation purposes.

When seasonal data from individual crops were pooled and used in regression analysis, the standard errors were about twice as large, ranging from 0.02 to 0.05 ly min^{-1}.

A grand regression (all crops and all days) yielded a standard error of 0.06 ly min^{-1}.

Correcting incoming solar radiation by subtracting reflected solar radiation did not reduce the standard errors.

In the absence of net radiation data, either the grand or individual crop regressions may provide sufficiently accurate estimates for some applications.

REFERENCES:

(1) Fritschen, Leo J.
Miniature net radiometer improvements.
(Submitted to the Journal of Applied Meteorology).

PERSONNEL: Leo J. Fritschen

Table 1. Crop height, incoming and reflected solar radiation, ratio of reflected to incoming radiation, net radiation, and intercept, slope, and standard deviation from regression for regression of net radiation on solar radiation and net solar radiation of alfalfa

Date	Crop Height	R_{sd}	R_{su}	$\frac{R_{su}}{R_{sd}}$	R_n	R_n versus R_{sd}			R_n versus $R_{sd} - R_{su}$		
						a	b	$s_{y.x}$	a	b	$s_{y.x}$
1964	cm	ly	ly		ly						
30 Jan	14	361	97	.27	236	−.108	.815	.021	−.076	1.018	.019
5 Mar	15	495	120	.24	281	−.171	.775	.021	−.157	1.000	.028
13 Mar*	2	429	101	.24	227	−.054	.620	.018	−.050	.802	.017
25 Mar	40	620	125	.20	312	−.137	.675	.022	−.123	.824	.018
7 Apr	30	608	143	.24	354	−.196	.795	.021	−.150	.974	.019
16 Apr	26	636	159	.25	356	−.133	.735	.033	−.106	.934	.024
2 May	62	651	177	.27	393	−.097	.720	.017	−.034	.887	.094
3 May	62	674	180	.27	394	−.137	.744	.028	−.109	.968	.020
13 May	71	532	104	.20	292	−.100	.707	.024	−.081	.841	.025
15 May	8	700	143	.20	428	−.152	.769	.013	−.101	.900	.010
27 May	48	659	171	.26	384	−.127	.744	.022	−.109	.974	.020
23 Jun	75	710	164	.23	446	−.196	.807	.014	−.110	.949	.013
24 Jun	75	649	156	.24	423	−.108	.772	.026	−.080	.975	.022
7 Jul	30	607	131	.22	398	−.135	.816	.012	−.091	.974	.014
21 Jul	66	587	143	.24	396	−.072	.771	.026	−.048	.978	.019
28 Jul	49	626	162	.26	418	−.109	.803	.036	−.065	1.013	.033
28 Jul	49	626	150	.24	428	−.041	.735	.031	−.052	.985	.033
29 Jul	49	390	107	.27	237	−.034	.675	.011	−.019	.889	.013
29 Jul	49	390	94	.24	261	−.023	.716	.019	−.025	.949	.018
5 Aug	59	527	126	.24	348	−.086	.788	.027	−.067	.998	.023
7 Aug	20	613	122	.20	405	−.120	.803	.010	−.088	.955	.008
18 Aug	27	604	140	.23	366	−.098	.724	.014	−.086	.924	.011
20 Aug	45	546	119	.22	372	−.065	.768	.012	−.041	.940	.009
1 Sep	45	574	134	.23	371	−.127	.806	.011	−.095	.998	.009
22 Sep*	22	410	99	.24	242	−.061	.678	.012	−.051	.873	.015
				Pooled Data							
		570	138	.24	351	−.110	.751	.048	−.081	.930	.051

* Days not included in pooled values.

Table 2. Crop height, incoming and reflected solar radiation, ratio of reflected to incoming radiation, net radiation, and intercept, slope, and standard deviation from regression for regression of net radiation on solar radiation and net solar radiation of barley

Date	Crop Height	R_{sd}	R_{su}	$\frac{R_{su}}{R_{sd}}$	R_n	R_n versus R_{sd}			R_n versus $R_{sd} - R_{su}$		
						a	b	$s_{y.x}$	a	b	$s_{y.x}$
1964	cm	ly	ly		ly						
13 Mar	5	429	85	.20	231	−.015	.565	.073	−.017	.709	.073
25 Mar	15	620	154	.25	278	−.140	.625	.022	−.123	.802	.021
7 Apr	80	636	135	.21	319	−.147	.696	.029	−.124	.846	.027
2 May	77	651	140	.22	369	−.116	.705	.031	−.069	.828	.037
3 May	77	674	139	.21	374	−.161	.743	.025	−.136	.898	.024
13 May	94	532	128	.24	262	−.120	.681	.026	−.094	.844	.035
27 May	76	659	170	.26	317	−.169	.696	.018	−.140	.890	.010
29 May	76	699	180	.26	331	−.129	.710	.023	−.166	.869	.018
				Pooled Data							
		613	141	.23	310	−.120	.655	.054	−.099	.822	.045

Table 3. Crop height, incoming and reflected solar radiation, ratio of reflected to incoming radiation, net radiation, and intercept, slope, and standard deviation from regression for regression of net radiation on solar radiation and net solar radiation of wheat

Date	Crop Height	R_{sd}	R_{su}	$\frac{R_{su}}{R_{sd}}$	R_n	R_n versus R_{sd}			R_n versus $R_{sd} - R_{su}$		
						a	b	$s_{y.x}$	a	b	$s_{y.x}$
1964	cm	ly	ly		ly						
27 Feb	10	486	90	.18	281	−.178	.797	.023	−.142	.926	.019
10 Apr	80	602	138	.23	365	−.167	.789	.024	−.125	.965	.022
11 Apr	80	595	133	.22	363	−.176	.806	.025	−.136	.982	.023
23 Apr	123	644	144	.22	390	−.186	.814	.027	−.144	.987	.022
6 May	108	661	132	.20	420	−.188	.839	.018	−.132	.974	.009
7 May	130	663	134	.20	415	−.126	.762	.051	−.095	.913	.012
20 May	130	662	142	.22	371	−.116	.795	.026	−.143	.912	.016
				Pooled Data							
		616	138	.22	372	−.174	.808	.032	−.140	.458	.032

Table 4. Crop height, incoming and reflected solar radiation, ratio of reflected to incoming radiation, net radiation, and intercept, slope, and standard deviation from regression for regression of net radiation on solar radiation and net solar radiation of oats

Date	Crop Height	R_{sd}	R_{su}	$\frac{R_{su}}{R_{sd}}$	R_n	R_n versus R_{sd} a	b	$s_{y.x}$	R_n versus $R_{sd} - R_{su}$ a	b	$s_{y.x}$
1964	cm	ly	ly		ly						
27 Feb	10	486	80	.16	278	−.167	.779	.015	−.151	.908	.006
10 Apr	60	602	147	.24	338	−.172	.749	.016	−.144	.951	.016
23 Apr	83	644	162	.25	364	−.175	.761	.019	−.153	.983	.018
6 May	108	661	165	.25	359	−.182	.741	.014	−.139	.926	.009
7 May	108	663	166	.25	364	−.114	.672	.044	−.098	.873	.034
20 May*	168	662	147	.22	408	−.103	.817	.024	−.051	.979	.021
				Pooled Data							
		620	145	.23	352	−.167	.750	.021	−.148	.945	.023

* Day not included in pooled values.

Table 5. Crop height, incoming and reflected solar radiation, ratio of reflected to incoming radiation, net radiation, and intercept, slope, and standard deviation from regression for regression of net radiation on solar radiation and net solar radiation of cotton

Date	Crop Height	R_{sd}	R_{su}	$\frac{R_{su}}{R_{sd}}$	R_n	R_n versus R_{sd} a	b	$s_{y.x}$	R_n versus $R_{sd} - R_{su}$ a	b	$s_{y.x}$
1964	cm	ly	ly		ly						
15 May*	8	700	129	.18	319	−.107	.566	.019	−.107	0.694	.017
29 May*	16	699	127	.18	366	−.149	.677	.031	−.149	.827	.034
16 Jun*	33	710	140	.20	382	−.164	.704	.014	−.153	.864	.019
16 Jun*	33	710	134	.19	364	−.170	.686	.012	−.163	.836	.010
23 Jun*	35	710	128	.18	357	−.137	.642	.018	−.131	.775	.016
24 Jun	35	649	112	.17	351	−.109	.663	.014	−.115	.808	.012
30 Jun	64	668	153	.23	406	−.175	.797	.023	−.143	.989	.017
30 Jun	64	668	138	.21	382	−.196	.783	.014	−.181	.967	.010
1 Jul	64	593	132	.22	368	−.103	.624	.034	−.184	.929	.032
1 Jul	64	593	131	.22	345	−.021	.607	.034	−.062	.843	.027
7 Jul	76	607	114	.19	341	−.158	.748	.012	−.141	.897	.020
14 Jul	72	520	110	.21	360	−.045	.755	.027	−.039	.948	.021
14 Jul	72	520	105	.20	341	−.057	.736	.033	−.063	.931	.037
16 Jul	72	649	146	.23	425	−.144	.815	.008	−.111	1.006	.005
16 Jul	72	649	130	.20	426	−.142	.813	.008	−.120	.988	.006
21 Jul	90	587	144	.24	370	−.078	.734	.022	−.059	.938	.013
7 Aug	115	613	138	.22	385	−.140	.792	.023	−.115	.985	.018
11 Aug	115	568	153	.27	373	−.086	.756	.008	−.061	.997	.010
11 Aug	115	568	146	.26	351	−.097	.731	.014	−.075	.948	.017
20 Aug	117	546	126	.23	346	−.048	.697	.037	−.042	.894	.034
3 Sep	110	581	147	.25	336	−.128	.738	.015	−.099	.944	.015
3 Sep	110	581	140	.24	333	−.120	.723	.023	−.117	.947	.020
25 Sep	90	481	118	.24	260	−.141	.717	.045	−.119	.914	.045
25 Sep	105	481	99	.21	299	−.077	.717	.046	−.155	1.027	.048
				Pooled Data							
		610	131	.21	358	−.100	.738	.046	−.080	.929	.050

* Days not included in pooled value.

Table 6. Crop height, incoming and reflected solar radiation, ratio of reflected to incoming radiation, net radiation, and intercept, slope, and standard deviation from regression for regression of net radiation on solar radiation and net solar radiation of sorghum

Date	Crop Height	R_{sd}	R_{su}	$\frac{R_{su}}{R_{sd}}$	R_n	R_n versus R_{sd} a	b	$s_{y.x}$	R_n versus $R_{sd} - R_{su}$ a	b	$s_{y.x}$
1964	cm	ly	ly		ly						
5 Aug	83	527	99	.19	322	−.106	.767	.032	−.086	0.909	.038
18 Aug	105	604	131	.22	367	−.119	.750	.022	−.097	.923	.015
1 Sep	130	574	130	.23	362	−.142	.809	.015	−.125	1.018	.017
22 Sep	135	410	88	.22	241	−.064	.682	.030	−.052	.847	.028
				Pooled Data							
		529	112	.21	323	−.106	.752	.030	−.092	.930	.032

Table 7. Intercept (a), slope (b), standard deviation from regression $\left(s_{y.x}\right)$, and correlation coefficient (r) for regression of net radiation on solar and net solar radiation for alfalfa, barley, wheat, oats, cotton, and sorghum, 1964

Regression of	a	b	$s_{y.x}$	r
Net radiation on solar radiation	−.118	.734	.057	.991
Net radiation on net solar radiation	−.093	.912	.057	.992

TITLE: THE USE OF SALTY WELL WATER FOR THE PRE-PLANTING IRRIGATION ON SILTY CLAY SOILS

LINE PROJECT: SWC 4-gG3 CODE NO.: Ariz. WCL-22

INTRODUCTION:

For need of study, see Annual Report 1958. The objective of the experiment is to determine the amount of water to apply at the pre-planting irrigation to maintain economic production. The experiment was initiated April 1, 1958.

PROCEDURE: (Barley)

The experiment was located at the University of Arizona Experiment Farm, Safford Branch, Safford, Arizona. The experiment was conducted on Field "I" borders 1-18.

Plots were plowed November 30, then harrowed and planted to Arivat barley. On December 2, 1963, the following amounts of planting-date-leaching water (3150 ppm) were applied.

1. 8 inches of well water - plots 4, 6, 12, 17.
2. 12 inches of well water - plots 3, 8, 10, 16.
3. 15 inches of well water - plots 2, 7, 11, 14.
4. 16 inches of well water - plots 5, 9, 13, 15.

Before planting, 320 pounds of 25-25-0 per acre was applied. Fifty pounds of nitrogen per acre was applied previous to the first spring irrigation. Four irrigations were given March 3, April 9, April 28, and May 26.

Soil salt measurements were made on all plots previous to and after the leaching irrigation. A final soil-salt measurement was made prior to harvest.

Five one-yard-square areas randomly selected were used to determine yields for each plot. Forty heads were randomly selected within each plot and harvested to determine the number of seeds per head.

RESULTS AND DISCUSSION:

A very poor stand of barley was obtained due to the late planting date and the cool weather in December and January.

Yield of Barley at Safford, Arizona

Pounds per Acre

Leaching Treatments	Replications 1	2	3	4	Mean
8	1631	1416	1840	1778	1666
12	1757	1718	1791	1998	1816
15	1883	2113	2089	2019	2026
16	2008	1961	2164	2264	2099

Sig. 1%

Treatments	Mean
16	2099 a
15	2026 a b
12	1816 b c
8	1666 c

Barley Seeds per Head at Safford, Arizona

Leaching Treatments	Replications 1	2	3	4	Mean
8	31.2	27.9	38.4	33.8	32.8
12	33.6	29.4	36.3	40.8	35.0
15	29.8	30.2	35.9	38.2	33.5
16	33.3	34.2	34.6	37.2	35.0

No. sig.

Weight of Barley in Grams Per One Hundred Seeds at Safford, Arizona

Leaching Treatments	Replications 1	2	3	4	Mean
8	4.16	4.23	4.18	4.39	4.24
12	4.25	4.36	4.33	4.38	4.33
15	4.36	4.22	4.46	4.41	4.36
16	4.38	4.38	4.53	4.33	4.40

No. sig.

SUMMARY AND CONCLUSIONS:

There was a statistically significant difference in barley yield for the various leaching treatments. The variance was at the one percent level. The yield on the 8-inch leaching treatment was lower than for the other treatments. Differences were not significant for seeds per head or weight per seed.

Soil-salts were reduced with the leaching irrigation by all leaching treatments in the top foot. Salts were increased in the second foot when only 8 inches of leaching water was added. Salts increased in the third foot in all leaching treatments by the leaching irrigation. Salt content was increased at all depths with the irrigations subsequent to the leaching irrigation. Soil-moisture content on the planting date was higher than desired and intake rates were slow. Practically speaking, because of slow intake rates the desired amounts of leaching water were not attained in the eighteen- and twenty-four-inch leaching treatments. High initial moisture content probably resulted in the lack of salt removal in the second and third foot soil profiles.

PROCEDURE: (Sorghum)

The leaching study was continued after the barley was harvested. The plots were immediately plowed, then harrowed and planted to Georgia 615 sorghum at 38-inch row widths.

On July 8, 1964, the following amounts of pre-planting-leaching water (3136 ppm) were applied.

1. 8 inches of well water - plots 4, 6, 12, 17.
2. 12 inches of well water - plots 3, 8, 10, 16.
3. 18 inches of well water - plots 2, 7, 11, 14.
4. 22 inches of well water - plots 5, 9, 13, 15.

Soil salt measurements were made before and after the leaching irrigation and a final soil-salt measurement was made at harvest. Four hundred pounds of 25-25-0 was applied to barley stubble previous to plowing.

The sorghum plots were irrigated on August 6 and September 4 in addition to the leaching irrigation. During August and September, ten rains occurred, amounting to 2.46 and 2.31 inches, respectively.

Two rains in August and one in September amounted to 3.05 inches of the total for the two months.

RESULTS AND DISCUSSION:

A good stand of sorghum was obtained. Practically no bird damage was noted on this variety. Visual differences in heads, weight of heads and plant height were observed, especially between the 8-inch leaching treatments and others.

Yield Sorghum at Safford, Arizona

Pounds per Acre

Leaching Treatments	Replications 1	2	3	4	Mean
8	3186	3622	3530	3348	3422
12	3760	4218	3828	3508	3828
18	3852	4264	4264	4058	4110
22	4264	4310	4288	3990	4213

Sig. 1%

Treatments	Mean		
22	4213	a	
18	4110	a	b
12	3828		b
8	3422		c

SUMMARY AND CONCLUSIONS:

There was a statistically significant difference in sorghum yield for the various treatments. The variance was at the one percent level. Yields were increased with increases in leaching water. The yield on the 8-inch leaching treatment was significantly less than all other treatments.

The two highest amounts of leaching water reduced soil-salts at all depths.

PERSONNEL: Leonard J. Erie and Orrin F. French.

TITLE: CONSUMPTIVE USE OF WATER BY CROPS IN ARIZONA

LINE PROJECT: SWC 11-gG1 CODE NO.: Ariz.-WCL-23

INTRODUCTION:

See Annual Report for 1963.

PROCEDURE:

Consumptive use measurements were made at the following locations in 1964.

1. Safflower - Mesa Experiment Farm.
2. Sugar Beets - Mesa Experiment Farm.
3. Grapes - Mesa Experiment Farm.
4. Dry Onions - Mesa Experiment Farm.
5. Bermuda Lawn - U. S. Water Conservation Laboratory.

PERSONNEL:

Leonard J. Erie and Orrin F. French.

Table 1. Semi-monthly use and "K" values for various crops in Arizona 1964

	BERMUDA		GRAPES		DRY ONIONS		SUGAR BEETS	
	CU	K	CU	K	CU	K	CU	K
Jan 1-15					.33	.21	1.44	.91
Jan 16-31					.50	.28	1.46	.82
Feb 1-14					.53	.31	1.22	.71
Feb 15-29					.69	.41	1.43	.85
Mar 1-15					.90	.43	1.77	.86
Mar 16-31					1.52	.58	2.13	.81
Apr 1-15			.39	.22	3.93	1.39	2.55	.90
Apr 16-30	2.13	.73	1.37	.47	4.71	1.61	3.65	1.25
May 1-15	2.57	.83	2.63	.83	5.75	1.81	4.85	1.52
May 16-31	3.36	.85	4.56	1.16	.99	.36	5.87	1.46
Jun 1-15	4.05	1.09	2.72	.71			5.01	1.31
Jun 16-30	5.55	1.34	4.31	1.05			4.25	1.04
Jul 1-15	5.85	1.38	3.82	.89			3.41	.79
Jul 16-31	5.73	1.26	1.60	.69			2.34	.51
Aug 1-15	4.85	1.26						
Aug 16-31	4.51	1.10						
Sep 1-15	3.50	1.00						
Sep 16-30	2.81	.88						
Oct 1-15	1.89	.64					.65	.21
Oct 16-31							1.25	.43
Nov 1-15					.05	.02	1.47	.63
Nov 16-30					.11	.05	1.94	.97
Dec 1-15					.18	.10	1.88	1.02
Dec 16-31					.27	.15	1.74	.94
Total	46.80		21.40		20.46		50.31	
Seasonal "F"	44.22		26.47		31.23		55.24	
Seasonal "K"	1.06		.81		.66		.91	

Table 2. Semi-monthly use and "K" values for various crops in Arizona 1964

	SAFFLOWER	
	CU	K
Jan 1-15	.12	.08
Jan 16-31	.32	.18
Feb 1-14	.46	.27
Feb 15-29	.75	.44
Mar 1-15	1.14	.55
Mar 16-31	2.10	.80
Apr 1-15	5.10	1.80
Apr 16-30	6.63	2.26
May 1-15	5.33	1.67
May 16-31	5.97	1.49
Jun 1-15	6.08	1.60
Jun 16-30	6.38	1.56
Jul 1-15	1.58	.37
Jul 16-31		
Aug 1-15		
Aug 16-31		
Sep 1-15		
Sep 16-30		
Oct 1-15		
Oct 16-31		
Nov 1-15		
Nov 16-30		
Dec 1-15		
Dec 16-31	.02	.03
Total	42.0	
Seasonal "F"	37.29	
Seasonal "K"	1.13	

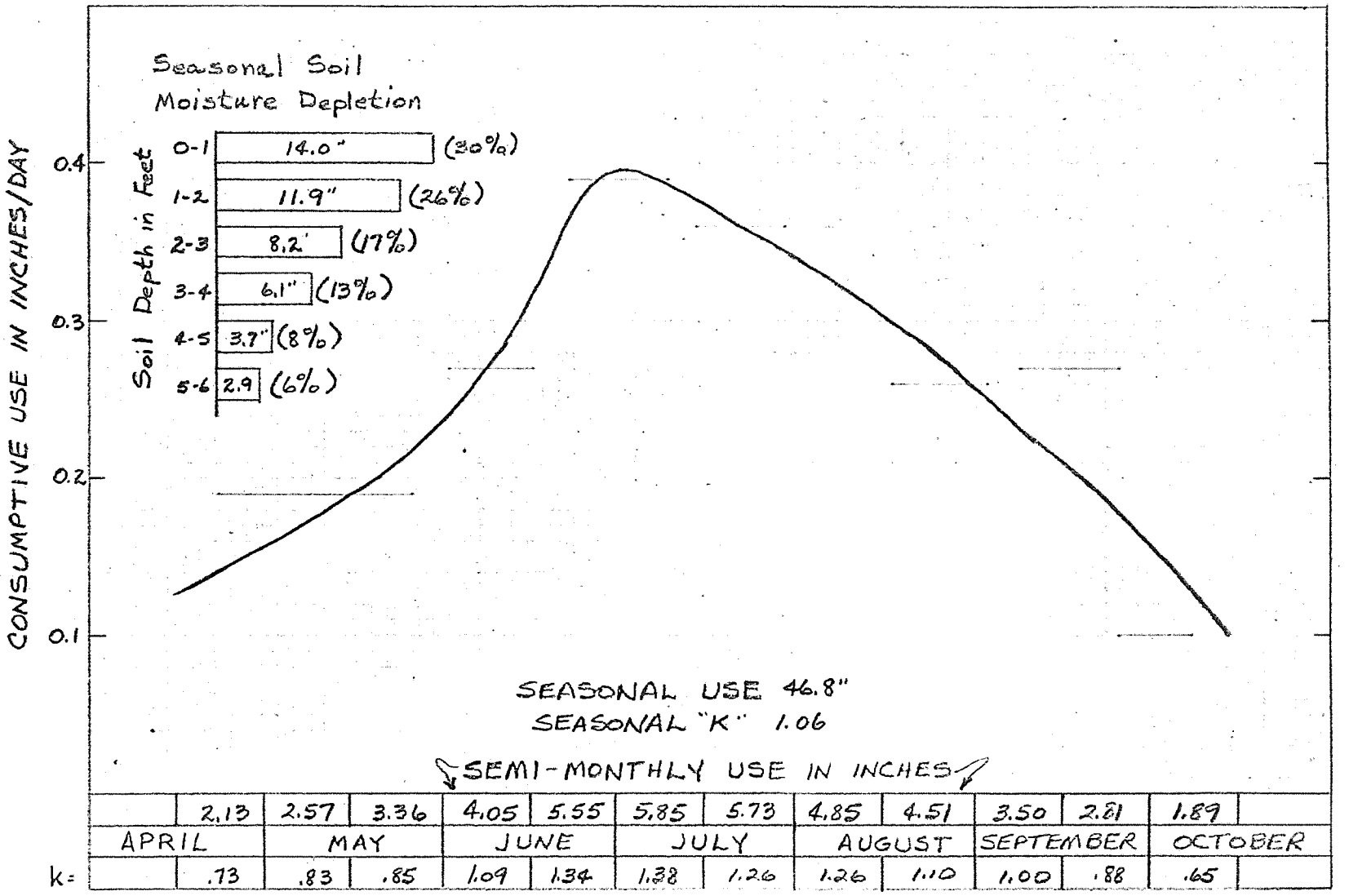

Figure 1. Consumptive use for lawn Bermuda at Tempe, Arizona in 1964, with bar graph showing soil moisture depletion per foot of depth.

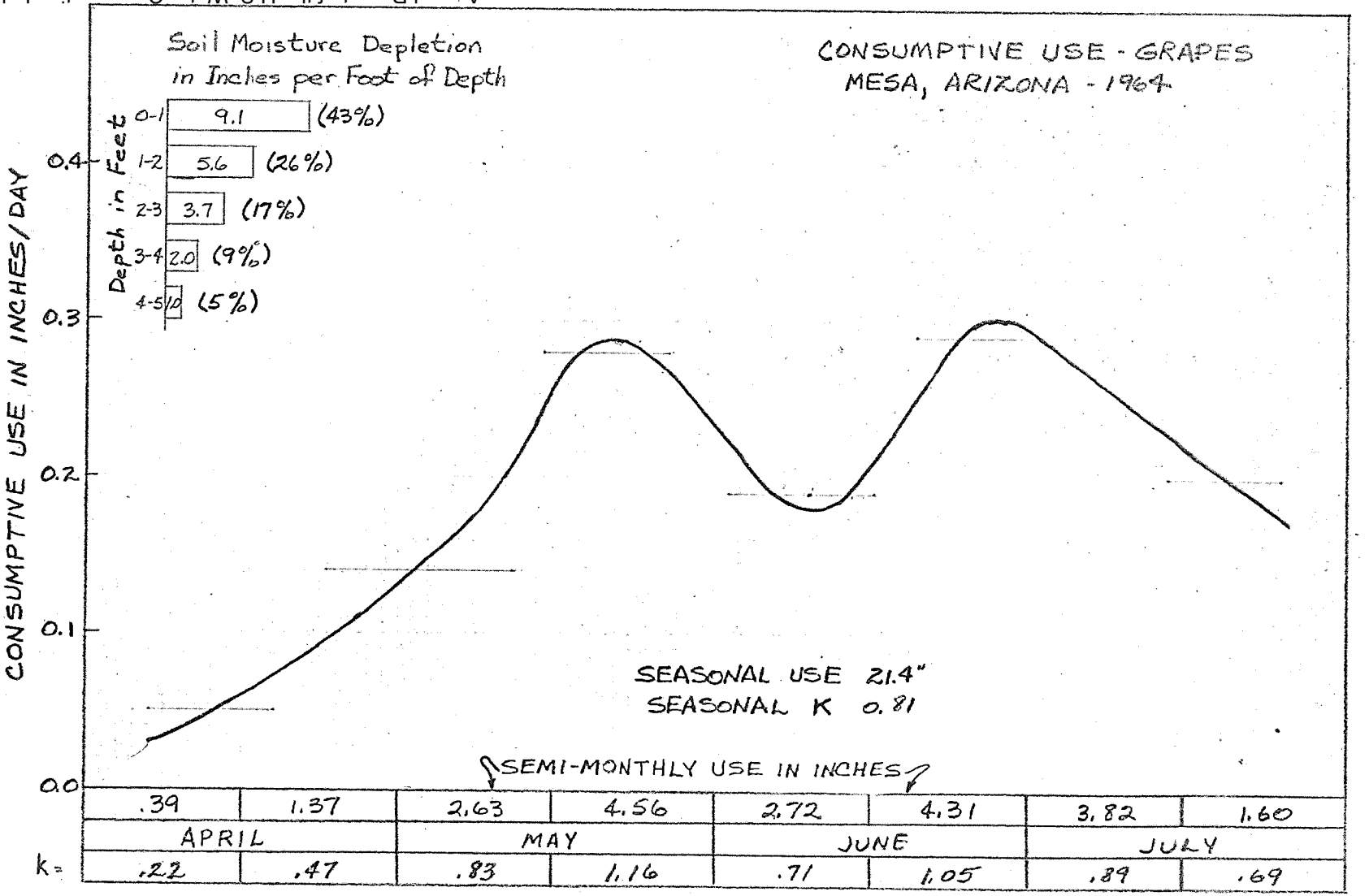

Figure 2. Consumptive use for grapes at Mesa, Arizona, 1964, with bar graph showing soil moisture depletion per foot of depth.

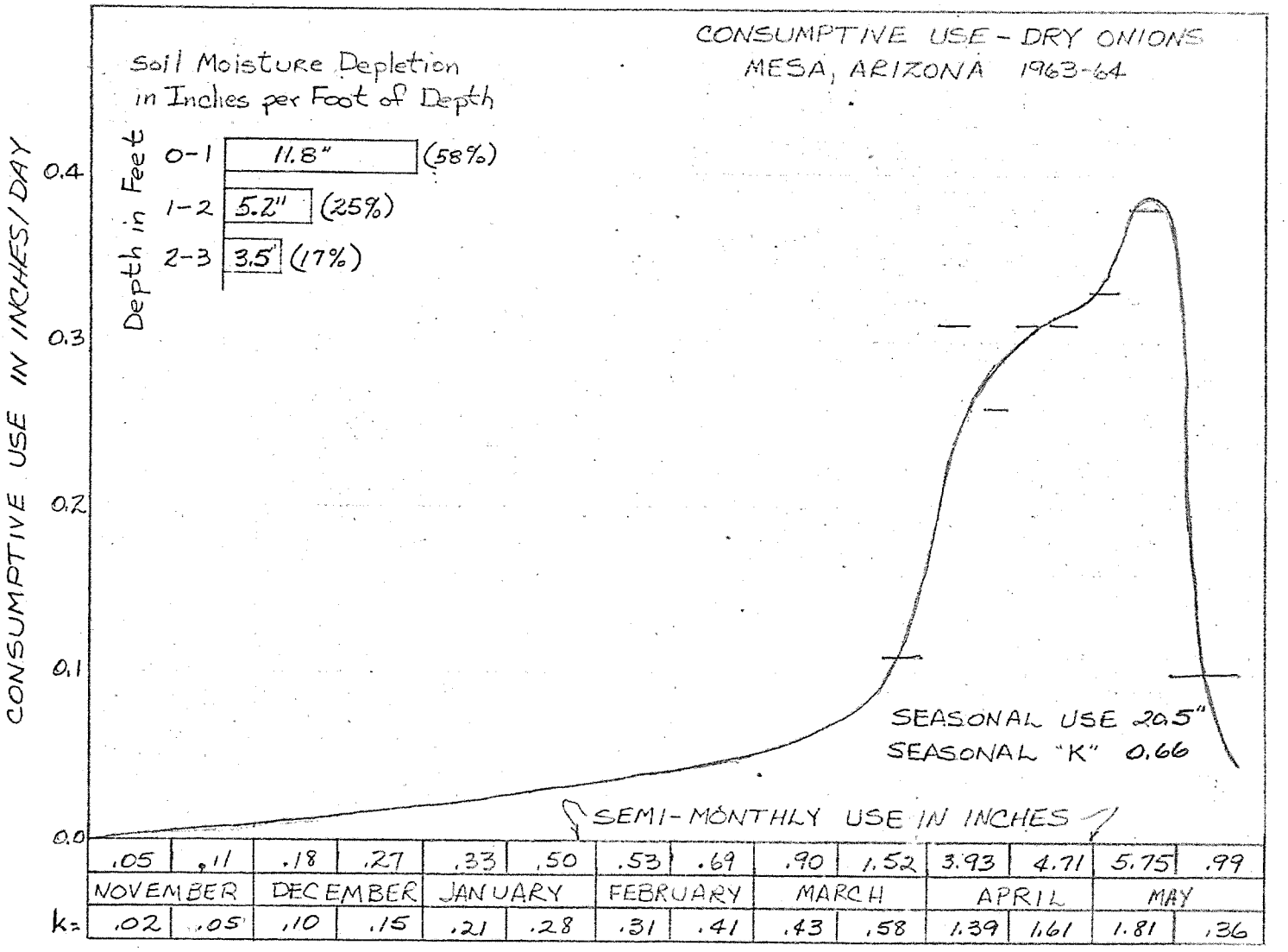

Figure 3. Consumptive use for dry onions at Mesa, Arizona, 1963-1964, with bar graph showing soil moisture depletion per foot of depth.

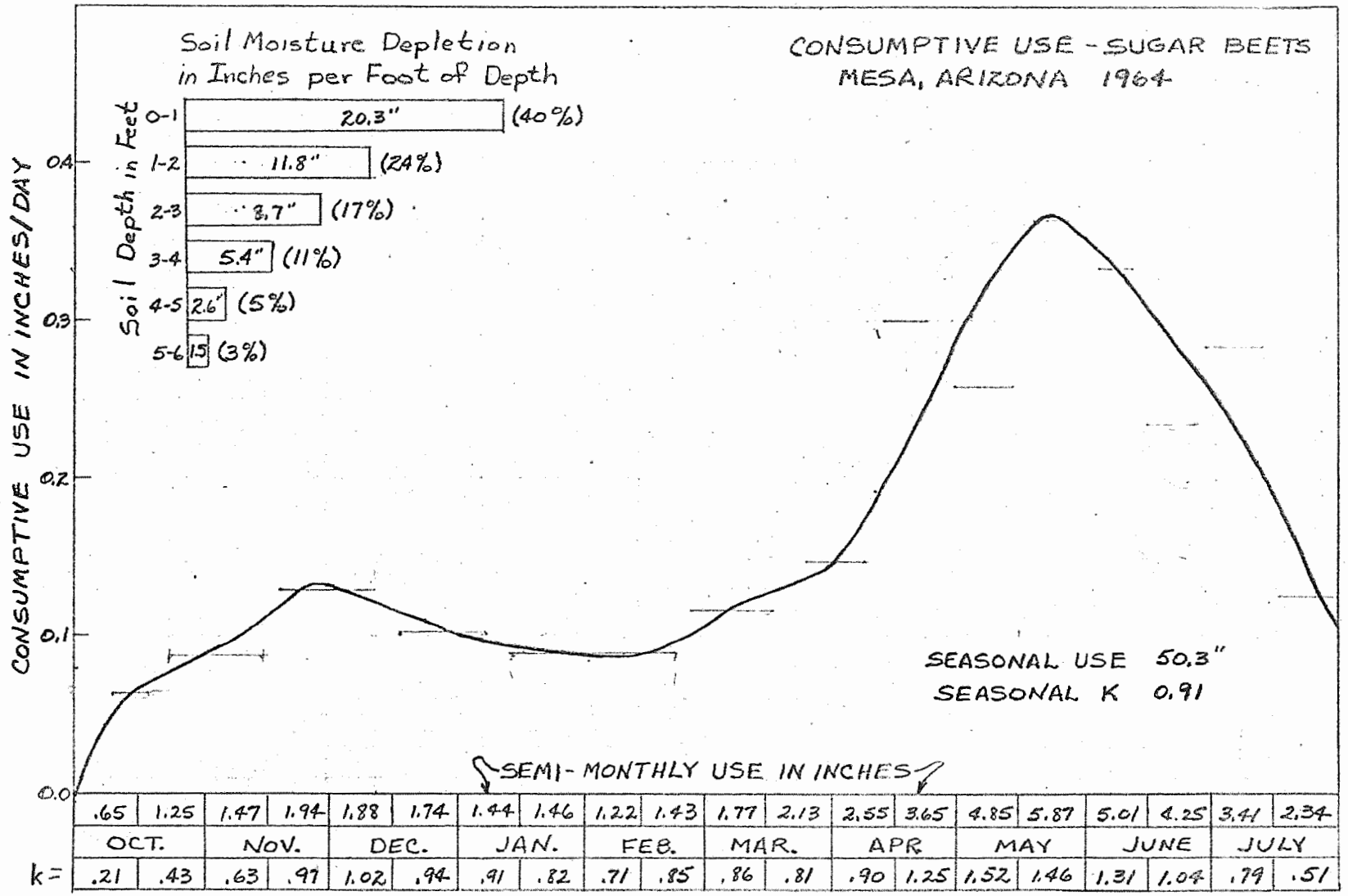

Figure 4. Consumptive use for sugar beets at Mesa, Arizona, 1964, with bar graph showing soil moisture depletion per foot of depth.

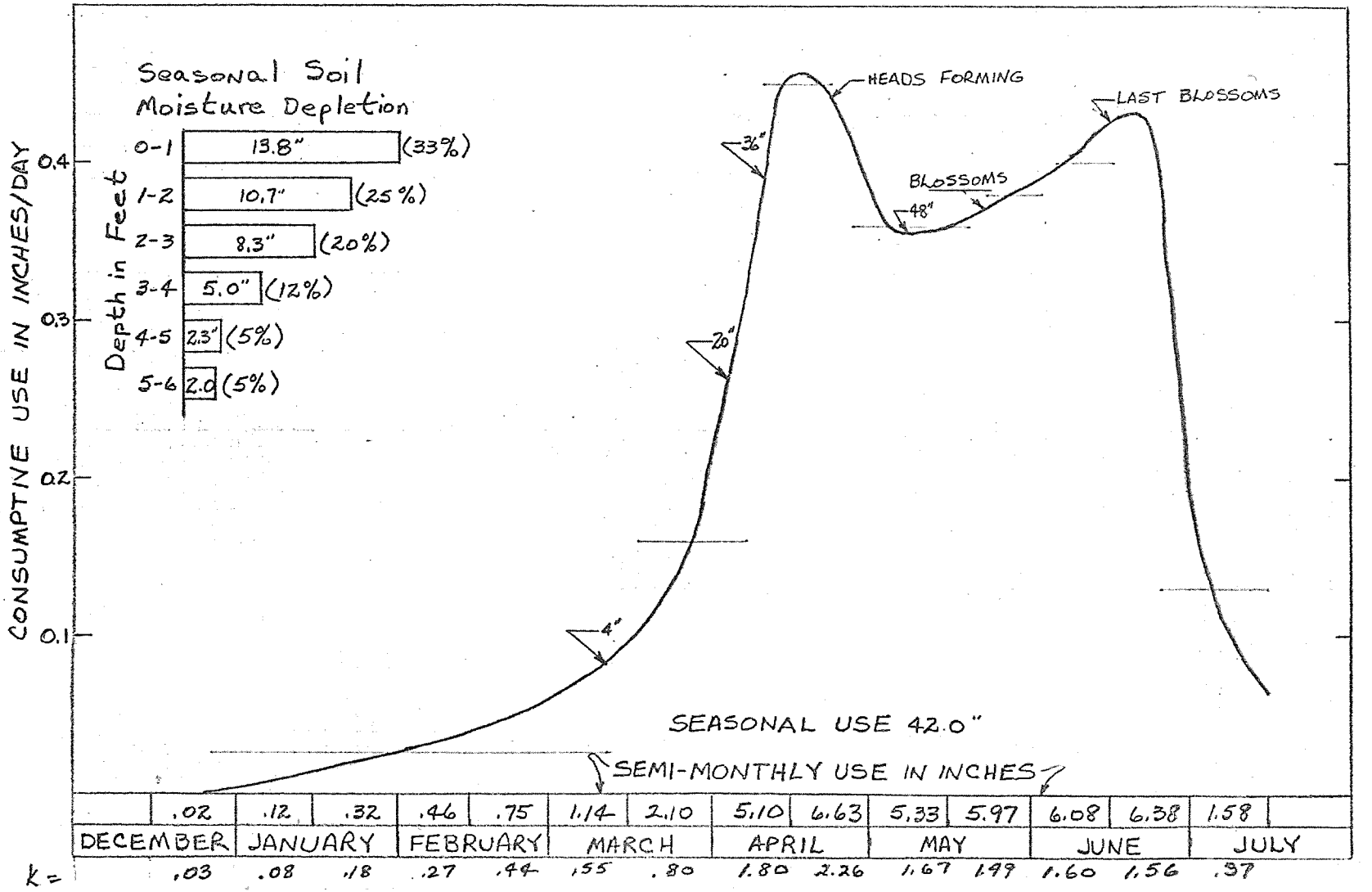

Figure 5. Consumptive use for safflower at Mesa, Arizona in 1964, with bar graph showing soil moisture depletion.

TITLE: THEORETICAL EFFECT OF SOIL, WATER TABLE, AND CANAL CONDITIONS ON SEEPAGE FROM CANALS

LINE PROJECT: SWC 4-gG1 CODE NO.: Ariz.-WCL-24

INTRODUCTION:

The work originally planned under this project has been completed and a manuscript has been prepared and accepted for publication (Lab. Publ. No. 131). The inclusion of unsaturated flow in these analyses led to a generalized approach for taking into account the effects of unsaturated flow in the solution of certain underground systems of water movement. The principle of this approach is the replacement of the generally S-shaped unsaturated hydraulic conductivity curve by a step-function and the use of resulting "critical pressure head" as boundary condition where the flow system is in contact with atmospheric air. A paper on this subject was published (Lab. Publ. No. 127). Because of the usefulness of critical pressure head in theoretical analysis of steady or quasi-steady flow systems, the possibility for direct measurement or estimation of critical pressure head in the field was investigated with preliminary tests in the laboratory. The remaining activity under this project was an analysis of the validity of the Dupuit-Forchheimer assumption (D-F assumption) for the calculation of seepage from open channels in relatively shallow, uniform soils. This work was done in partial preparation of a panel discussion on the D-F assumption at the 1964 Winter Meeting of the American Society of Agricultural Engineers (Lab. Publ. No. 139).

PROCEDURE:

The principle of direct estimation of critical pressure head in the field would consist of measuring the air entry value of the soil at a wet front that has advanced a small distance below a cylinder installed in the soil. The principle was tested in the laboratory on vertical columns of air-dry, 76 μ glass beads in two-inch plexiglass cylinders (Figure 1). The columns were hand packed to a density of approximately 1.64. Distilled deaired water was applied to the top of the columns at a certain pressure head H cm with respect to the surface of the beads. After the column was wetted

for a pre-selected distance L, the supply of water at the top of the column was cut off and the pressure in the closed body of water above the glass beads was measured with a 1 mm mercury manometer. Manometer readings in relation to time were obtained photographically. Tests were carried out for H-values of 10, 40, and 100 cm and L-values of 10, 30, and 50 cm, with 3 to 6 replications per test (six columns were used per test, but air leaks caused occasional failures). The values of the pressure head at the wet front, P, were evaluated by referring the water pressure above the column as indicated by the manometers to the position of the wetting front. The P-values thus obtained were negative and showed a minimum value after some time. This minimum value was taken as the air entry value or as P_c. These values were then compared with the bubbling pressure measured on five samples in conventional pressure cells. In addition to glass beads, P_c was determined for an air-dry sample of a 50 to 500 μ fraction of a sand. The measured values of P_c in this case were compared with P_c calculated from the unsaturated hydraulic conductivity characteristic of this material, which had been determined previously by Dr. R. D. Jackson.

The D-F assumption yields an exact solution for the case of flow through a body of soil with vertical walls above an impermeable base. The resulting equation was applied to the case of seepage from a trapezoidal channel in uniform soil underlain by an impermeable layer. Using the same terminology as in previous annual reports, the resulting expression was

$$\frac{I_s}{K} = \frac{D_w}{22.8\ W_b} \left(1.5 + \frac{2\ D_i}{W_b} - \frac{D_w}{W_b}\right).$$

This equation applies to a canal with 1:1 side slopes and a water depth of 0.75 W_b. The vertical distance D_w between the water level in the canal and the water table in the soil is measured at a horizontal distance of 10 W_b from the center of the canal bottom. Based on this equation, a graph was constructed showing I_s/K as a function

of D_i/W_b for different values of D_w/W_b. The resulting curves were then compared with curves obtained from analyses with the resistance network analog.

RESULTS AND DISCUSSION:

A typical example of the behavior of the pressure head P at the position of the wetting front, as evaluated from the manometers connected to the top of the columns, is shown in Figure 2. The graph applies to five columns of 76 μ glass beads, to which water was applied at a pressure head of 100 cm above the top of the column. When the wet front had advanced 30 cm, the water supply was turned off. At this time (time 0 in the Figure), the pressure head P showed a rapid reduction and then a more gradual reduction to a certain minimum value, after which a slow increase followed by a more rapid increase took place. The minimum value of P was interpreted as the air entry value at the wet front which in turn was used as an estimate of P_c. The subsequent gradual increase in P was attributed to upward movement of air in the column, and the rapid increase at the end of the test to a breakthrough of air at the top of the column. The elapsed time at this breakthrough showed wide variation among replications, and its relation to L and H was not clear. Until the time of breakthrough, the position of the wet front remained essentially constant. The P_c-values obtained with the glass bead studies are summarized in Table 1. For the tests with H = 40 cm and H = 100 cm, P_c showed a slight increase (less negative) with increasing L. This is probably due to the fact that the wet front loses "sharpness" as L increases, so that in reality the manometer readings should have been referred to a level somewhat above the wetting front if L is large. This effect was not noticed for the tests with H = 10 cm, however. The air entry values as estimates of P_c in Table 1 compared favorably with the bubbling pressure of the glass beads as measured in a pressure cell. The average bubbling pressure of five samples of the beads was -61.6 cm. The results of the P_c-estimates on the columns of 50 to 500 μ sand were as follows:

L	H	P_c
cm	cm	cm water
10	100	- 60.6
10	100	- 61.6
15	100	- 62.8
15	100	- 57.5
15	100	- 54.3

These P_c-values of which the average is -59.4 cm, compared favorably with the P_c-value of -64 cm as calculated from the unsaturated hydraulic conductivity characteristic of the sand for desorption.

Figure 3 shows that the equation based on the D-F assumption yields a linear relationship between I_s/K and D_i/W_b up to infinity. The analog data, which take the vertical flow component into account, yield a curvilinear relationship where I_s/K increases with D_i/W_b at decreasing rate to approach a finite value when D_i approaches infinity. Thus, the D-F assumption leads to increasingly large errors in the predicted seepage as D_i/W_b increases, and to the absurdity of infinite seepage in uniform soil of infinite vertical extent. However, the D-F assumption yields a reasonable estimate of I_s/K if $D_i/W_b < 4$ and fairly accurate estimates if $D_i/W_b < 2$. To apply these criteria to channels with shapes other than trapezoidal and 1:1 side slopes, an equivalent W_b must be determined from the actual water surface width and depth of the channel as if the channel were trapezoidal with 1:1 side slopes.

SUMMARY AND CONCLUSIONS:

In a number of cases, the contribution of unsaturated flow to the underground movement of water can be taken into account by simplifying the unsaturated hydraulic conductivity curve of the soil to a step-function and taking the resulting "critical pressure head" as the boundary condition where the flow system is in contact with atmospheric air in the soil. Direct estimation of the critical pressure head in the field may be possible through measurement of the minimum pressure at the depth of a wetting front below a covered infiltration

cylinder. This pressure is determined from pressure measurements on the water in the cylinder above ground surface after cessation of the water supply to the cylinder. Laboratory tests on columns with air-dry glass beads showed good agreement between the minimum pressure head thus measured and the bubbling pressure, i. e., -63.0 and -61.6 cm of water, respectively. Similar tests with a 50 to 500 μ sand fraction showed good agreement between the minimum pressure head (-59.4 cm) and the critical pressure head (-64 cm) calculated from the unsaturated hydraulic conductivity characteristic for desorption. The study will be continued with columns of initially moist glass beads, after which equipment and procedures for field measurement will be explored.

Solutions of seepage from open channels in uniform soil underlain by an impermeable layer based on the Dupuit-Forchheimer assumption were compared with solutions obtained by a resistance network analog to investigate the validity of the Dupuit-Forchheimer assumption for seepage prediction in this case. The Dupuit-Forchheimer assumption yielded acceptable solutions for the seepage rates if the distance of the impermeable layer below the channel bottom was less than four times the width of the bottom. This width is calculated from the water surface width and the water depth of the canal as if the canal cross-section were trapezoidal with 1:1 side slopes.

PERSONNEL: Herman Bouwer

Table 1. Results of P_c-measurements on glass-bead columns.

L cm	H cm	Replications	P_c cm water
10	10	3	- 64.4 ± 3.4
30	10	3	- 63.3 ± 1.2
50	10	3	- 65.8 ± 2.7
10	40	6	- 64.0 ± 2.0
30	40	4	- 63.1 ± 2.2
50	40	5	- 58.0 ± 3.4
10	100	4	- 69.1 ± 5.4
30	100	5	- 63.4 ± 2.6
50	100	5	- 58.6 ± 4.8
	Average	38	- 63.0 ± 4.4

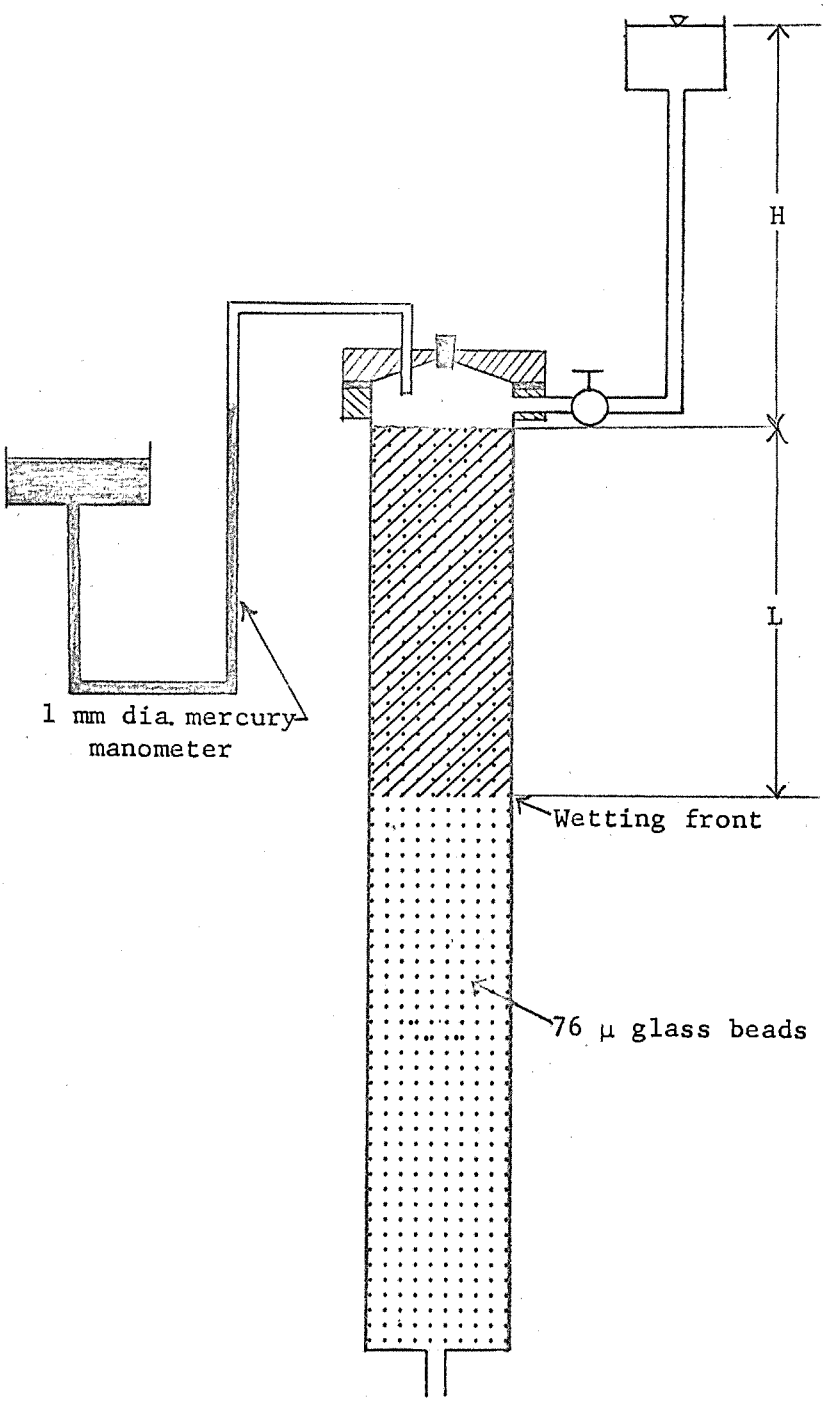

Figure 1. Sketch of column with water supply and manometer for measuring air entry value of soil.

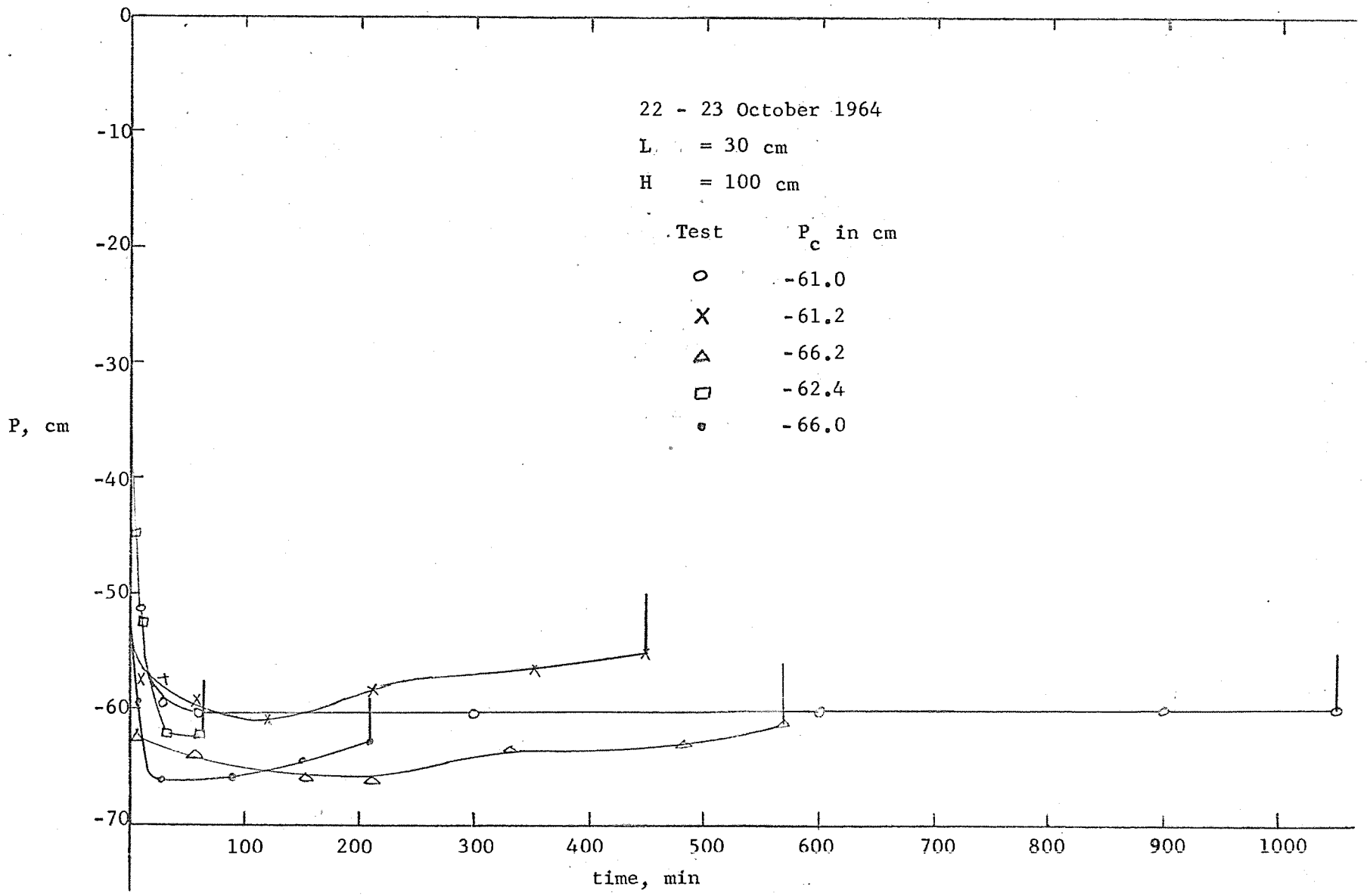

Figure 2. Typical example of pressure head at wetting-front elevation in relation to time for 76 μ glass beads.

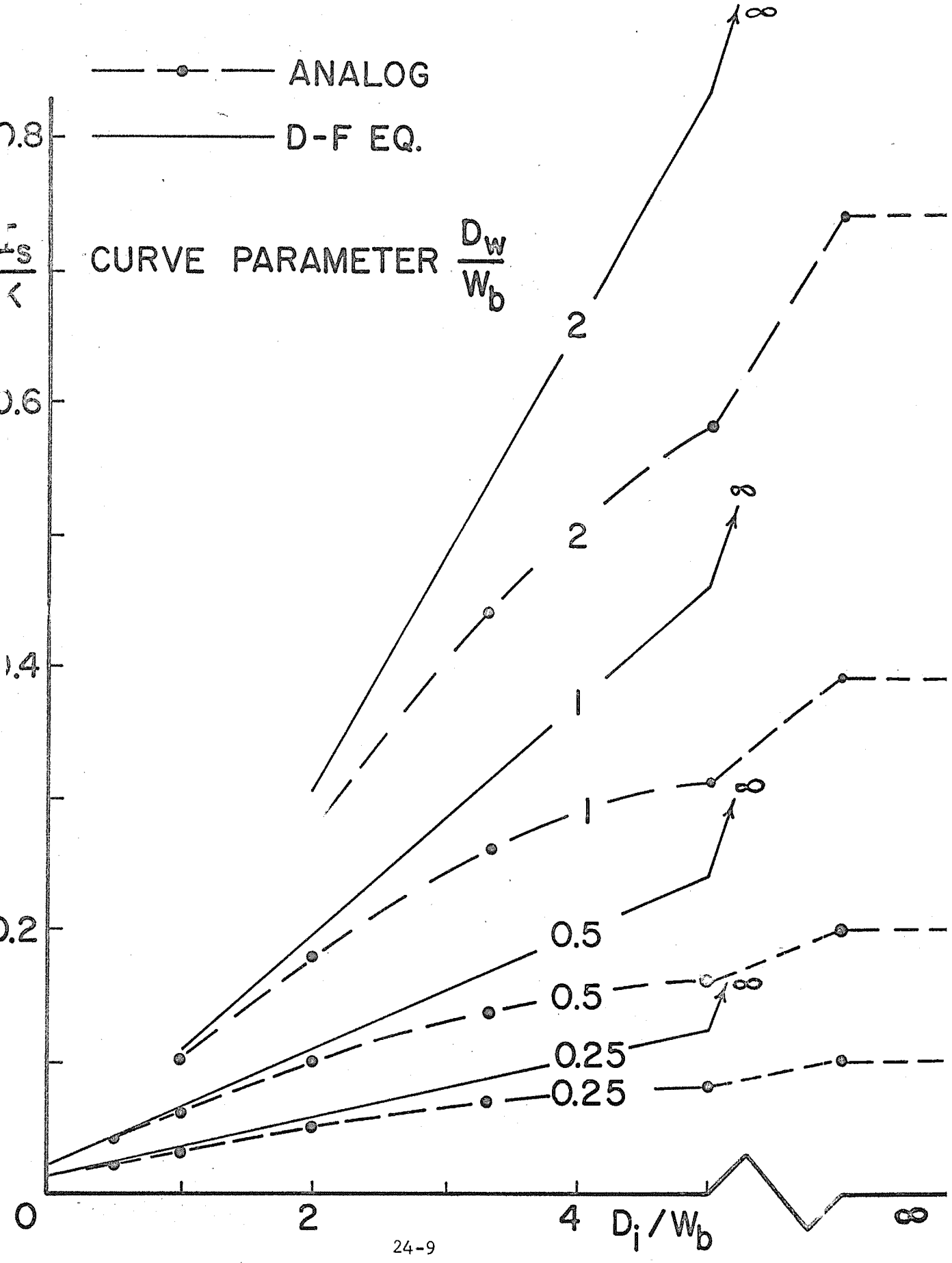

Figure 3. Comparison of seepage from trapezoidal channel according to the D-F assumption and to the resistance network analog.

TITLE: MEASURING HORIZONTAL AND VERTICAL CONDUCTIVITY OF SOIL WITH THE DOUBLE-TUBE METHOD

LINE PROJECT: SWC 4-gG1 CODE NO.: Ariz.-WCL-25

INTRODUCTION:

The work on this project was continued with the development of fast-reacting piezometers for measurement of the vertical gradient below the auger hole. Such a development was prerequisite to measuring directional hydraulic conductivity with the double-tube method on soils other than sands. After unsuccessful attempts to develop a minimum-displacement diaphragm pressure cell for this purpose, a commercial transducer and indicator were obtained. Two anisotropy tests were conducted in Adelanto loam south of the laboratory in which the piezometers, transducer, and indicator performed satisfactorily and permitted the measurement of the vertical gradient below the auger hole.

PROCEDURE:

Attempts were made to develop a recording device for the piezometric pressures using the diaphragm-type minimum flow pressure cell (see Annual Report 1963). This was done by connecting a source of compressed air and of vacuum via a three-way solenoid valve to the pressure cell. When the diaphragm in the pressure cell made contact with the electrode in the cell (pressure in cell chamber less than pressure in piezometer), a relay was energized which opened the solenoid valve to the compressed air side. The resultant pressure increase in the cell chamber forced the diaphragm up, which broke the contact with the electrode. This in turn caused the solenoid valve to switch to the vacuum side, which moved the diaphragm down to reestablish contact with the electrode, etc. If the sequence of contact-pressure-loss of contact-vacuum was repeated fast enough, the average "back" pressure fluctuated very little and thus indicated the piezometric pressure to be measured. The back pressure was recorded by connecting the pressure chamber in the cell to one leg of a three-inch U-tube manometer filled with water. The pressure was then recorded by a water stage recorder in the other leg of the manometer.

The system was tested against known pressure heads. Arcing between the diaphragm and the electrode was suppressed by a capacitor in parallel with the contact points. The system appeared to give troublesome performance, however, so that a commercial linear voltage differential transformer type pressure transducer (Sanborn 267B) and a battery-operated amplifier-indicator (Sanborn 312) were obtained. This equipment was used with a Sargent recorder in two anisotropy tests in three-foot deep auger holes in the Bermuda lawn south of the hydraulics laboratory. The two test locations were approximately six feet apart. Of the three piezometers that were inserted below the inner tube, two were of the shielded, open hole type, the third one had a wrapping of 200-mesh brass screen. The measurement of the double-tube conductivity K_{dt} and the vertical conductivity K_v, and the calculation of K_h were performed according to the procedures outlined in previous annual reports.

RESULTS AND DISCUSSION:

The attempt to make a recording pressure gauge with the diaphragm pressure cell was not successful. Diaphragm failure occurred within several hours of operation, probably resulting from metal fatigue due to the rapid movement of the diaphragm under the alternating application of pressure and vacuum. The use of the pressure cell with manual operation was also discarded because of the displacement of water. Although this displacement is small (1.1 mm^3), it occurs at each measurement and because of the number of measurements required to detect stable piezometric readings, erroneous results may be obtained. The Sanborn 267B transducer has a displacement of 0.022 mm^3 per pressure change of 100 cm water and a continuous read-out.

The results of the two anisotropy tests are summarized in Table 1. The plots of piezometric head, h, against piezometer penetration Z for determination of dh/dZ are shown in Figure 1. The points yield a reasonable straight line which almost pierces the origin. This indicates absence of surface sealing or clogging at the hole bottom. In general, the time required for the piezometer

readings to become stable varied from 10 to 20 minutes after each increase in Z. In test 1, only two piezometers responded, the third one probably became plugged. The difference between K_v and K_{dt} may be due to two reasons. One possibility is that the soil below the wall of the inner tube became compacted upon insertion of the inner tube, thus yielding a K_{dt}-value that is lower than K_v. Another possibility is anisotropy with $K_h \ll K_v$, as may be caused by the presence of vertical root holes and other macropores with little or no horizontal interconnection. If the difference between K_v and K_{dt} is solely attributed to anisotropy, K_h can be estimated. Accurate evaluation of K_h, however, was not possible because the flow factors, F_f, were only evaluated for R_c/d-values that are considerably less than the $R_c/\bar{d}$-values in the equivalent isotropic system for this case (R_c and d are the radius and depth of penetration of the inner tube, respectively). Thus, F_f was extrapolated on log paper from the R_c/d range of 1 to 10 to R_c/d-values up to 2000! As shown in Table 1, the resulting K_h-values are only a small fraction of K_v. Such a pronounced difference between K_h and K_v in both tests may be due to the presence of vertical root holes with little or no horizontal interconnection. Whether this is a natural condition, or an artificial condition caused by soil compaction and resulting closure of horizontal channels below the wall of the inner tube due to insertion of this tube in the auger hole bottom, is a question that requires further investigation.

SUMMARY AND CONCLUSIONS:

Repeated volume displacement and failure of the diaphragm of a minimum flow pressure cell for reading piezometric heads led to discontinuing the use of this cell. A commercial linear voltage differential transformer pressure transducer with portable indicator was obtained. This equipment performed satisfactorily in two anisotropy tests with the double-tube method in Adelanto loam south of the laboratory. The tests yielded a double-tube conductivity that was 0.091 and 0.053 the vertical hydraulic conductivity, respectively. This difference may be due to disturbance of the soil below the wall of the inner tube, or to soil anisotropy with the vertical conductivity

exceeding the horizontal conductivity as may be caused by vertical root holes or other macropores with little or no horizontal connection. If the difference is solely attributed to anisotropy, the resulting horizontal conductivity is only a very small fraction of the vertical conductivity. This may be a natural condition, or it may reflect disturbance caused by compression of the soil below the wall of the inner tube.

PERSONNEL: Herman Bouwer and R. C. Rice.

Table 1. Results of anisotropy tests with double-tube method.

Test	$\frac{d}{R_c}$	K_{dt} cm/min	$\frac{dh}{dZ}$	I cm/min	K_v cm/min	$\frac{K_{dt}}{K_v}$	$\frac{K_h}{K_v}$	K_h cm/min
1	0.35	0.01	33	3.6	0.11	0.091	7×10^{-4}	7.7×10^{-5}
2	0.22	0.003	34.5	2.2	0.062	0.053	3×10^{-4}	1.9×10^{-5}

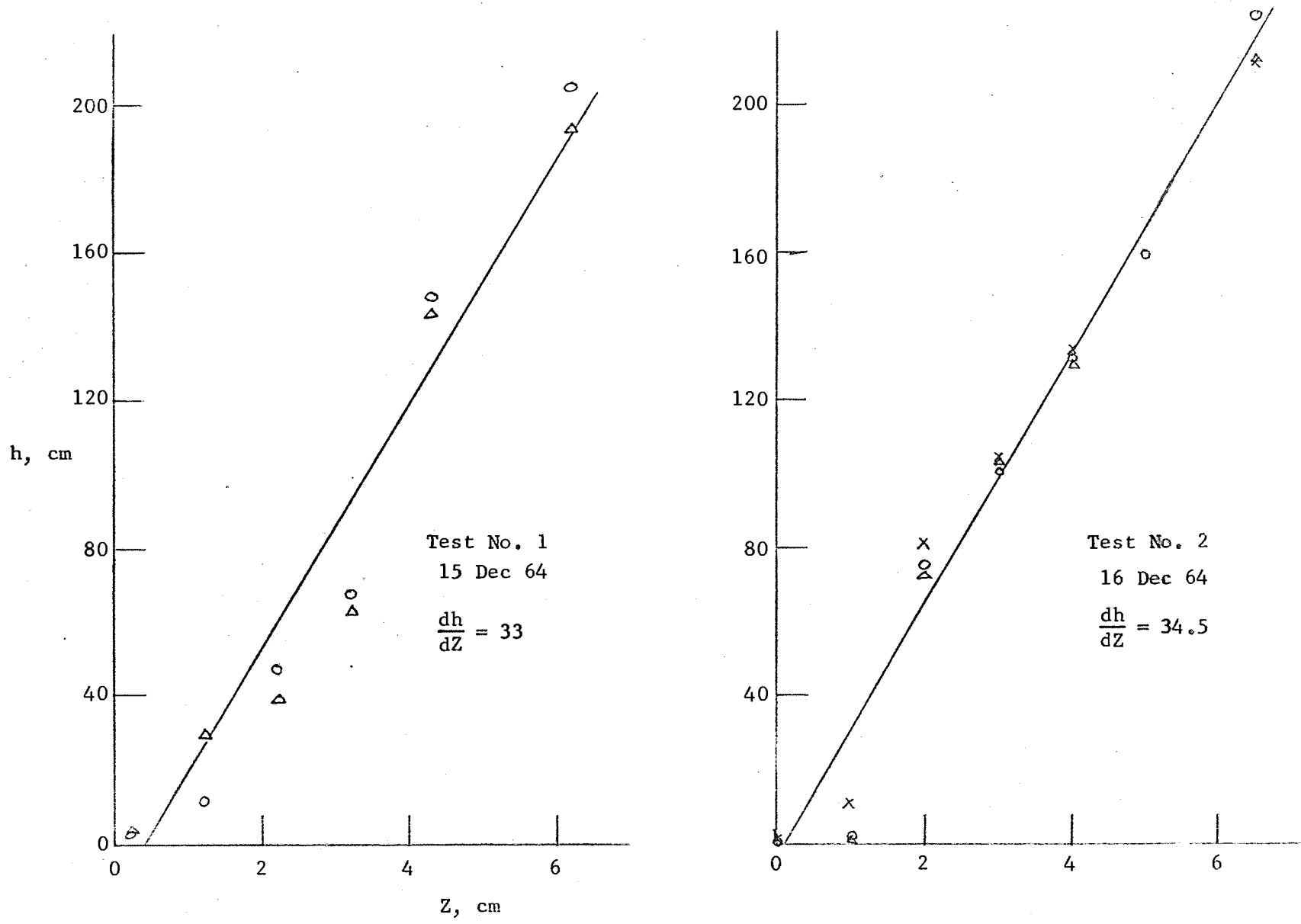

Figure 1. Piezometric measurements for evaluating downward gradient dh/dZ below auger hole.

TITLE: NONDESTRUCTIVE BETA RAY TRANSMISSION METHOD FOR MEASURING WATER CONTENT IN PLANTS

LINE PROJECT: SWC 11-gG1 CODE NO.: Ariz.-WCL-26

INTRODUCTION:

The objectives of the project have been discussed in the Annual Reports of 1962 and 1963. To further check the performance of the equipment, a test of the gauge was conducted in the field. In addition to following the leaf water content changes of field cotton plants, the study gave us an opportunity to determine whether the short-term cyclic water changes occurred in the field plants in a similar manner as those observed previously when the plants were grown in the environmentally controlled growth chamber (Ariz.-WCL-29).

PROCEDURE:

Laboratory Study. The equipment and methods are described in the 1962 and 1963 Annual Reports.

Field and Greenhouse Studies. A 2 μc, Pm-147 beta ray source similar to the one described in the 1963 Report was used. To provide for accurate counting and convenience, the Nuclear-Chicago Model 2800 portable scaler was modified so that the preset timing system was controlled by an electromechanical device instead of the mechanical timer supplied with the original equipment. Counts were taken continuously over 3-minute periods, starting about sunrise and ending after sunset. The gauge was calibrated with standard aluminum absorbers and the count rates, which were measured on the leaves, were then converted to absorber thicknesses using the appropriate conversion factors.

The gauge was placed on the upper, first-fully mature Deltapine cotton leaf which was exposed directly to solar radiation. It was taped securely to the leaf, and precautions taken to minimize excessive movement of the plant caused by wind, by supporting it with stakes. Because of plant growth and consequent shading of the test leaf, the gauge was relocated to an upper leaf during successive weekly and biweekly measurements.

In addition to the leaf gauging, leaf temperatures on adjacent plants which were similarly exposed as the gauge test plant were taken. (See WCL-26A for specific details of leaf temperature measurements.) Air temperature was also measured 40 cm above the crop canopy. The air thermocouple sensor was placed in a 2-inch diameter by 12-inch aluminum-lined plastic cylinder. Air was drawn past the sensor by a 30 cfm squirrel-cage blower.

Because it was not practicable to follow leaf water content in field plants during and immediately following an irrigation, part of this study was conducted in the greenhouse. Cotton plants were grown in soil until the total soil-water suction approached -15 bars. The plant was then irrigated and the leaf water content followed at the same time.

RESULTS AND DISCUSSION:

Laboratory Study. The beta ray gauge was used in conjunction with other studies (see: Water absorption, transpiration, and internal water balance of cotton plants as affected by changes in evaporative demands, Ariz.-WCL-29) as a routine measuring instrument. By following the leaf water content of cotton leaves continuously, it was noted that a cyclic change in leaf water content occurred when the plants are exposed to sudden illumination in an otherwise constant environment of temperature, water vapor pressure deficit and carbon dioxide concentration.

Field and Greenhouse Studies. The leaf thickness equipment worked satisfactorily in the field without any electronic or mechanical failure at ambient air temperatures ranging from 15 to 43 degrees C. Leaf thickness values for the various dates are plotted in Figures 1 (7 July 1964), 2 (14 July 1964), 3 (28 July 1964), 4 (11 August 1964), 5A (1 September 1964) and 5B (18 September 1964).

The maximum change in leaf thickness observed in the dawn to dusk readings was in the order of 1.5 mg cm^{-2}. With the exception of days 14 July and 11 August, the leaves decreased continuously in thickness following the increase in light intensity. However, starting at approximately 1400 there was a gradual increase in leaf thickness.

The observed increase in leaf water content starting at this period of the day is in contradiction with the popularly held belief that water recovery starts to occur after sunset. Furthermore, the observed increase in water content cannot be explained on the basis of a slowing down in the rate of water loss. Indications are that transpiration had not decreased significantly during this period, as shown by the data of stomatal resistance (see Project Ariz.-WCL-29) obtained at the same time on an adjacent plant, i.e., the leaf stomatal resistance at 1400 to 1600 was the same as the earlier 1000 to 1500 period. Thus, the recovery of water in the leaf must be caused either by a decrease in the net root resistance to water flow or increase in the water potential gradient between the leaf and soil water, or a combination of both.

Short-term, cyclic changes in leaf water content, similar to the ones reported in Ariz.-WCL-29, were not observed with the field plants. The standard deviations for the 3-minute counts are shown in each of the graphs. This is in the order of $\pm$ 0.04 mg cm^{-2}. Although it is impractical to test every one of the variations in leaf water content, the deflections observed seem to be real changes in the leaf water contents. These can be caused by changes in wind velocity, causing changes in the resistance of the air around the leaf and also due to changes in cloud cover.

The seemingly anomalous behavior of an increase in leaf thickness during the morning for 14 July (Figure 2) and 11 August (Figure 4) cannot be explained adequately at present. The possibility of a shift in position of the gauge in respect to the leaf which would then arise in a possible different leaf thickness reading was considered, but, if this had occurred, the changes observed would have been much more abrupt than that shown by the data.

Temperature data for the field experiments are presented in Figure 6. These are presented in terms of the temperature difference between the leaf and air. Negative values indicate that the leaf is cooler than the air. Only the results for 28 July 1964 are presented since the other data are similar. The leaf temperature ranged from

2 degrees C warmer to 7 degrees C cooler than the air. Air temperature ranged from 15 to 43 degrees C during the experiment. The leaf was cooler than the air to a greater extent in the afternoon period than the morning. Cyclic changes in temperature were not measured with the field plants.

The preliminary greenhouse study on the extent of recovery of plant immediately following an irrigation is presented in Figure 7. Within a period of approximately 1 hour after irrigation (suction change from 15 bars to <0.1 bar), the leaf had regained water close to its maximum thickness. It does not appear that root or stem impedance was of a significant factor in affecting the recovery in this situation.

SUMMARY AND CONCLUSIONS:

Continued use of the beta ray gauging equipment showed that it was a reliable instrument for measuring leaf thickness changes in a routine manner in the laboratory. Tests also showed its suitability in the field under a temperature range of 15 to 43 degrees C. Field measurements indicated that cotton leaves were recovering a large portion of the water in midafternoon, contrary to popular belief that this occurred in the evening and nighttime hours. It was also possible to observe with the gauge the rapid uptake and distribution of water in the leaf following irrigation of the cotton plant which was originally under a moisture stress.

PERSONNEL: F. S. Nakayama and W. L. Ehrler.

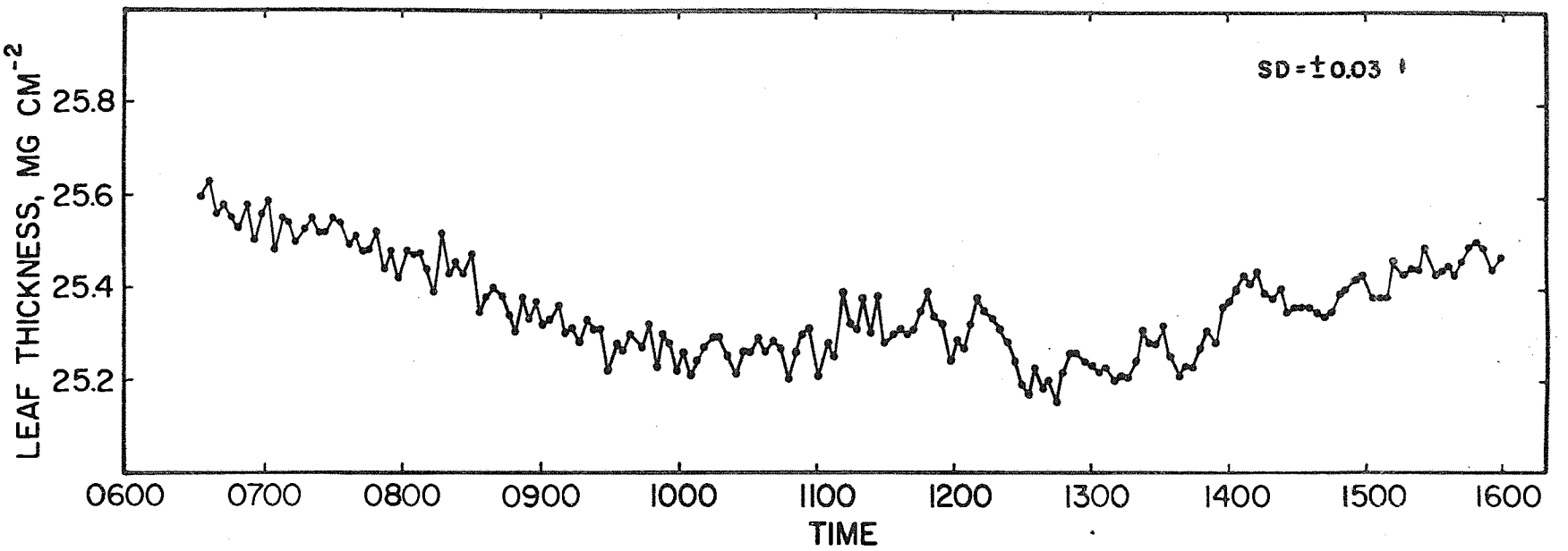

Figure 1. Leaf thickness of field cotton plant, 7 July 1964.

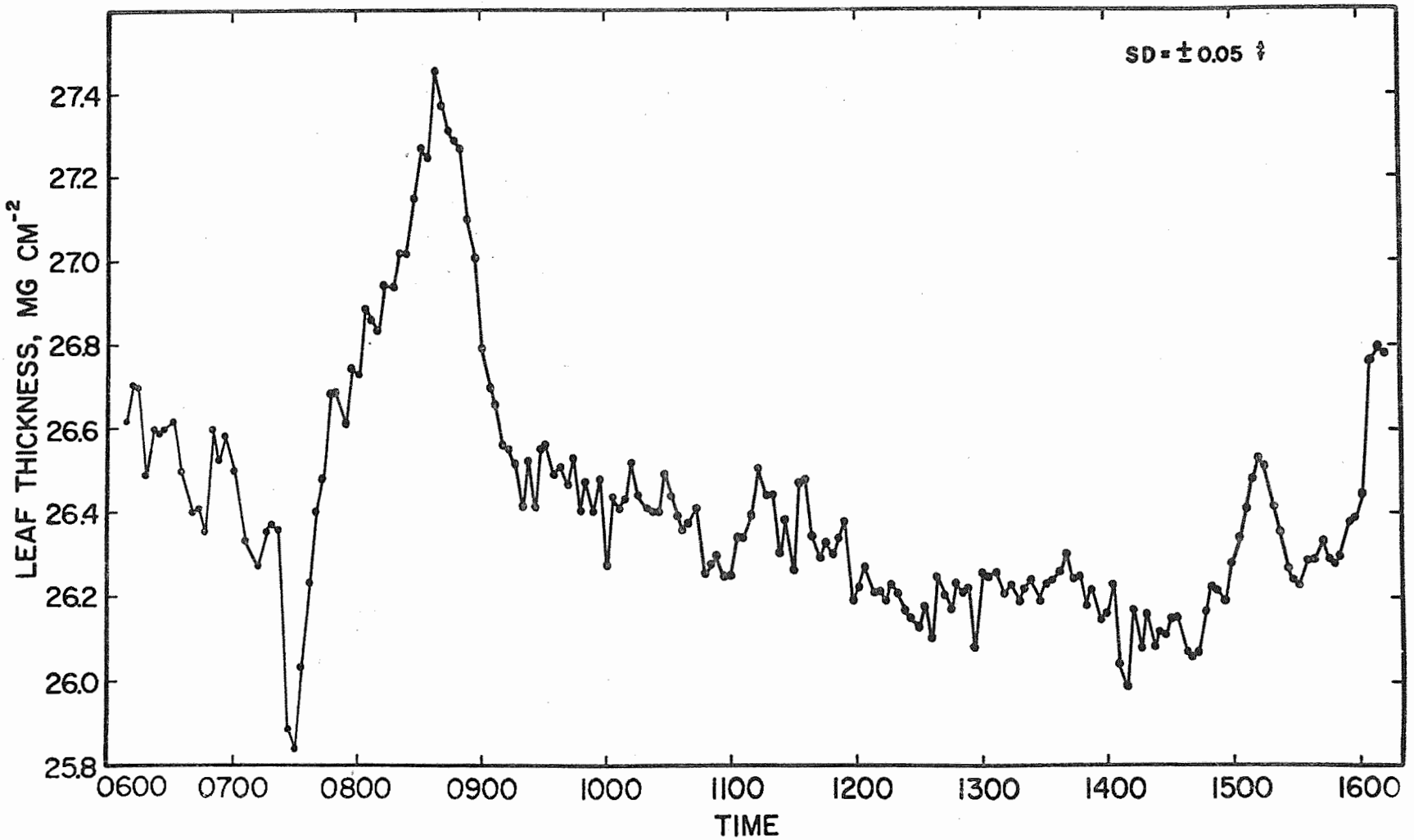

Figure 2. Leaf thickness of field cotton plant, 14 July 1964.

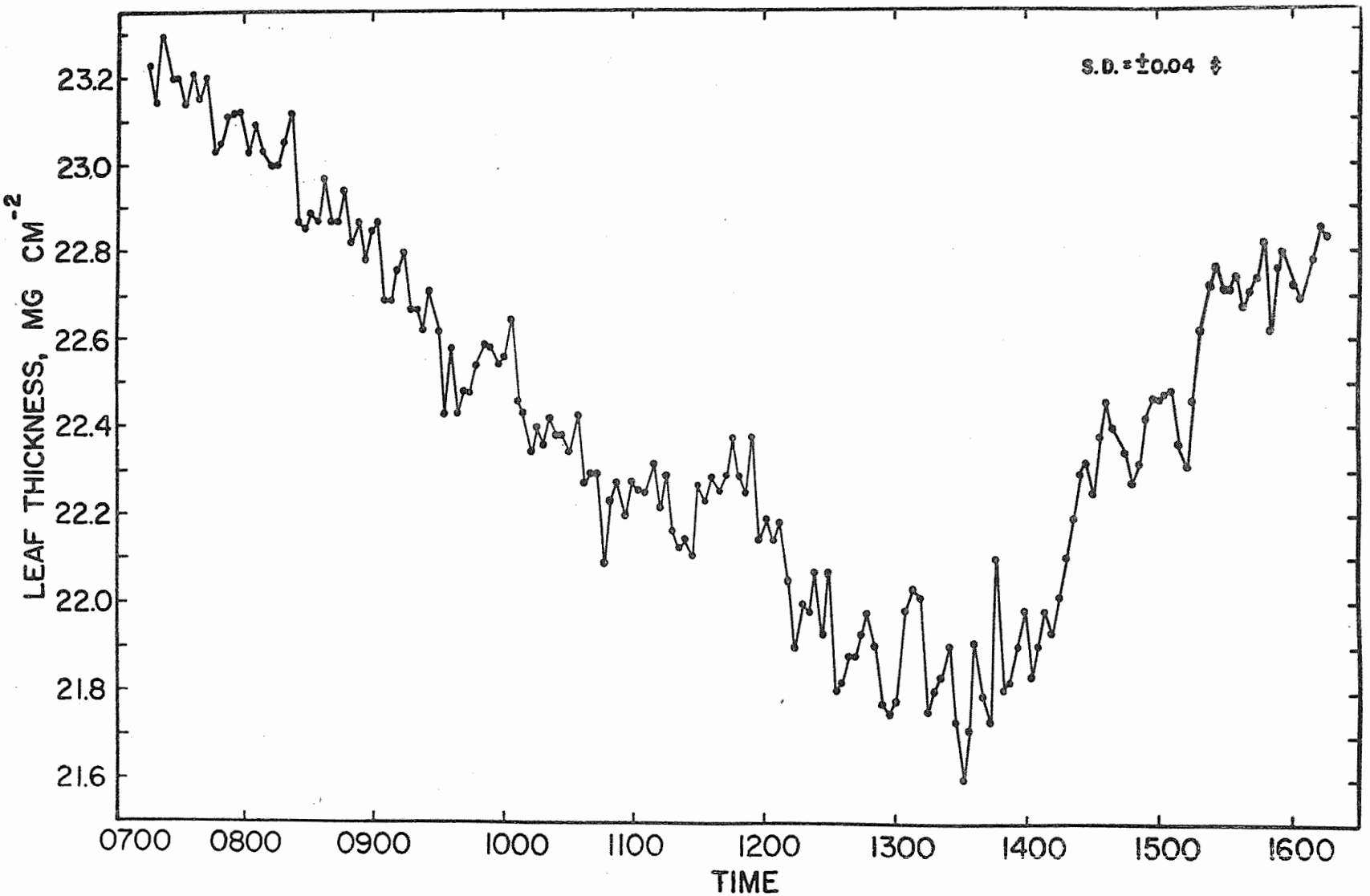

Figure 3. Leaf thickness of field cotton plant, 28 July 1964.

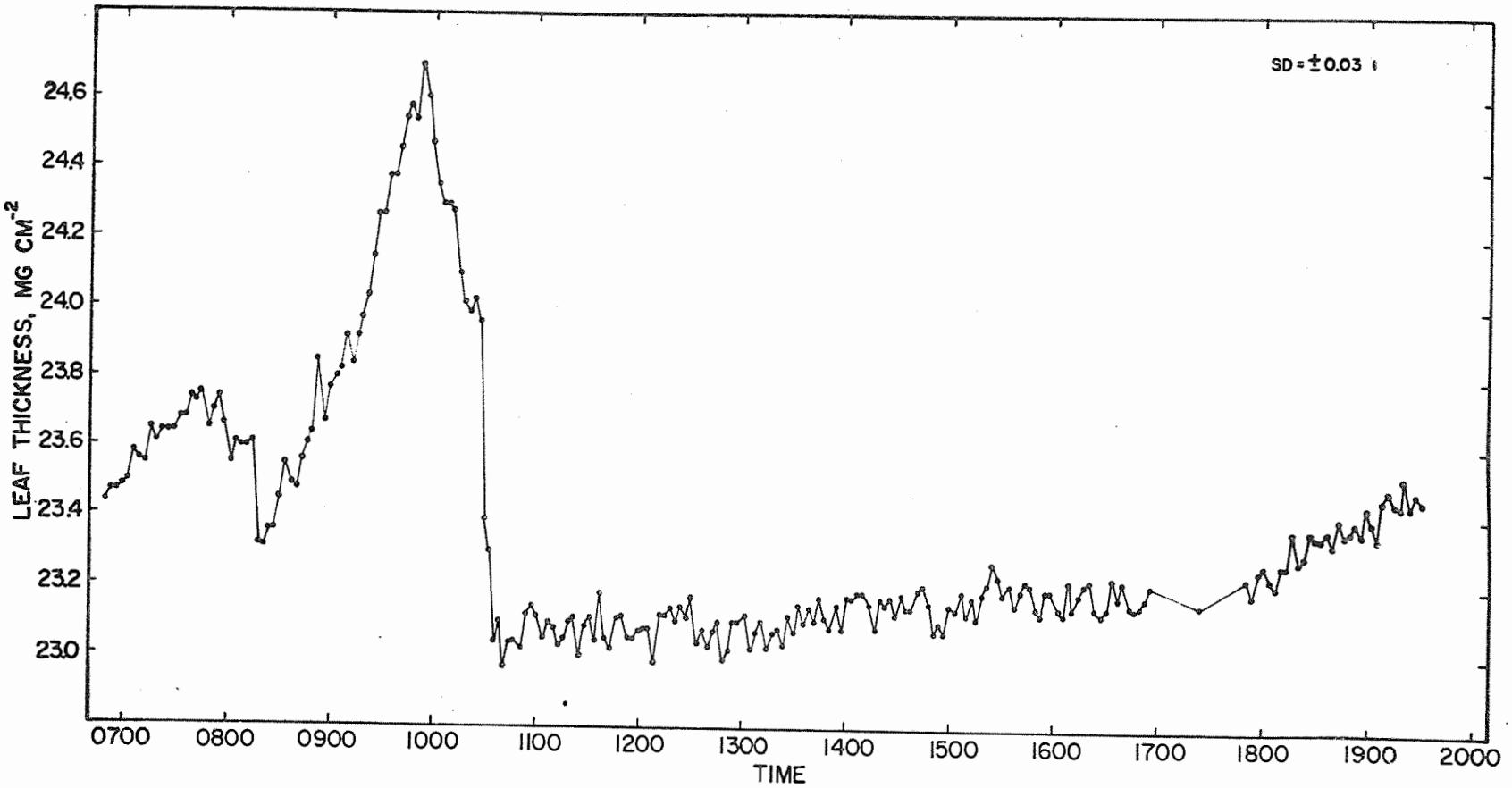

Figure 4. Leaf thickness of field cotton plant, 11 August 1964.

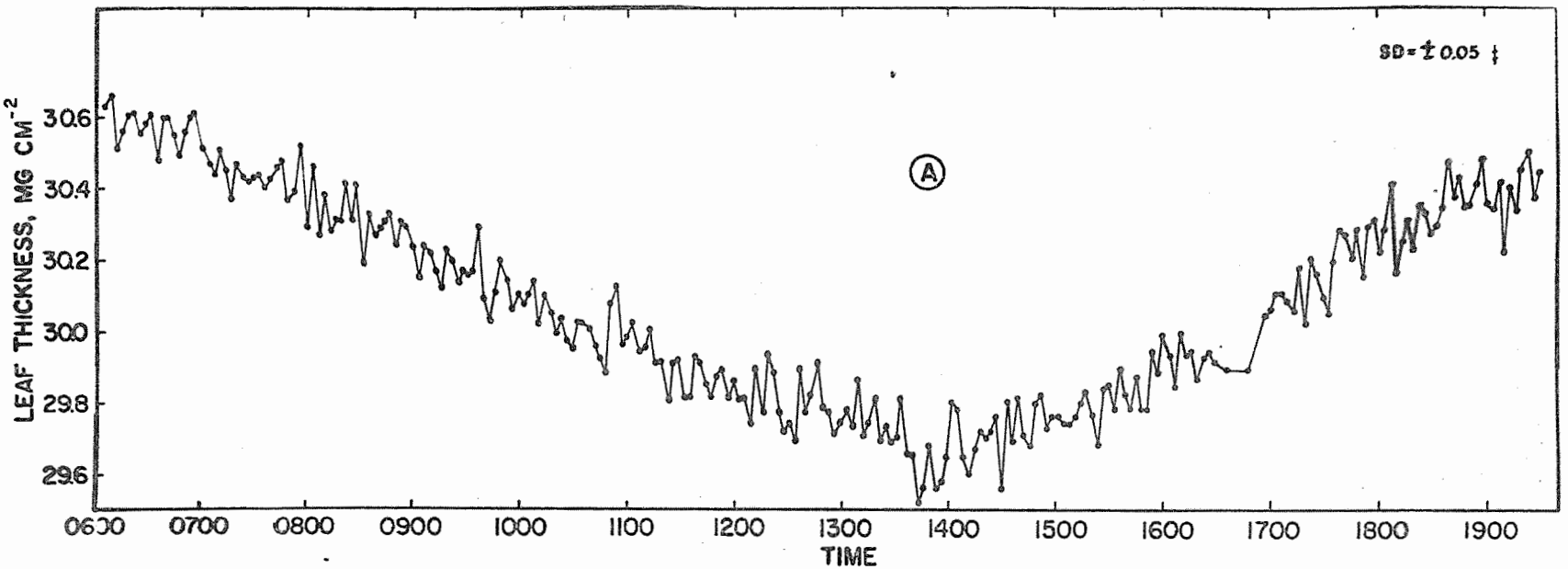

Figure 5A. Leaf thickness of field cotton plant, 1 September 1964.

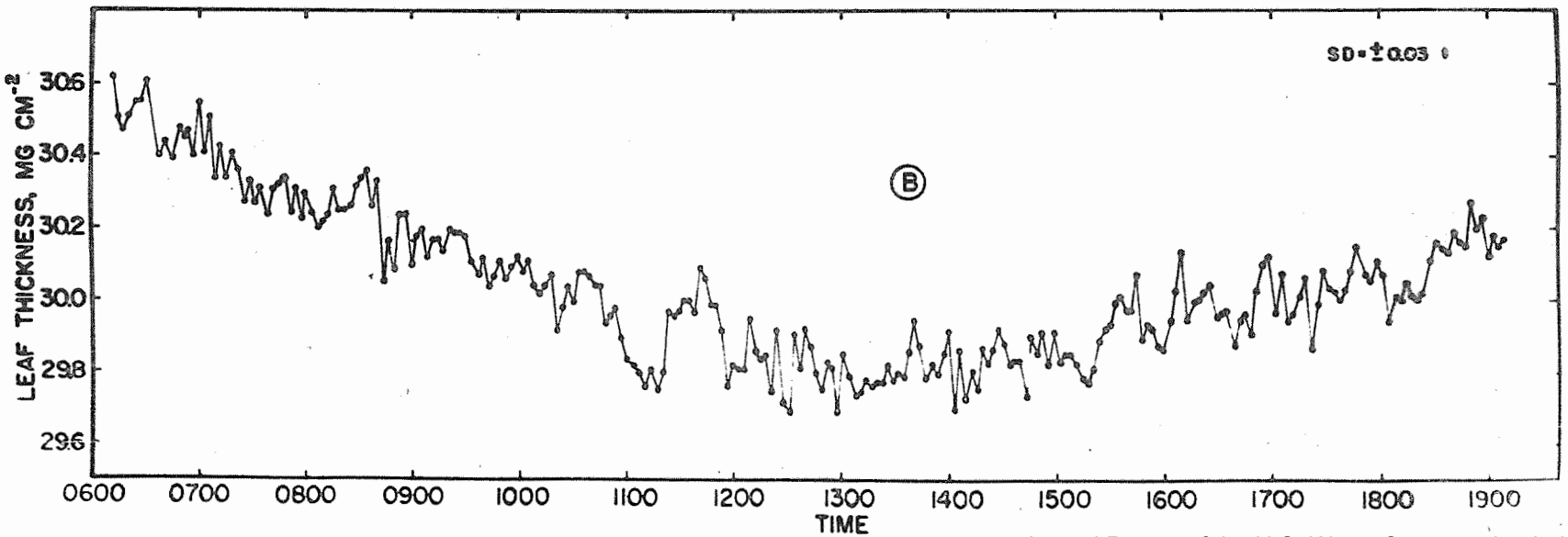

Figure 5B. Leaf thickness of field cotton plant, 18 September 1964.

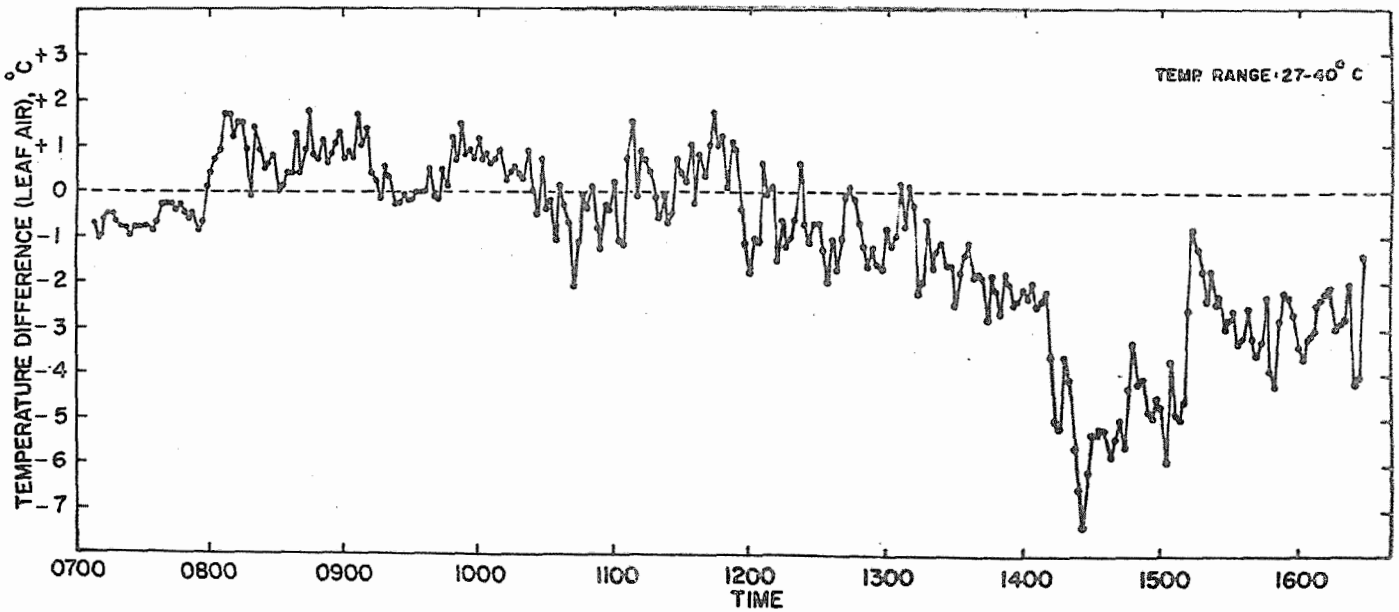

Figure 6. Leaf temperature (leaf-air) of field cotton plant.

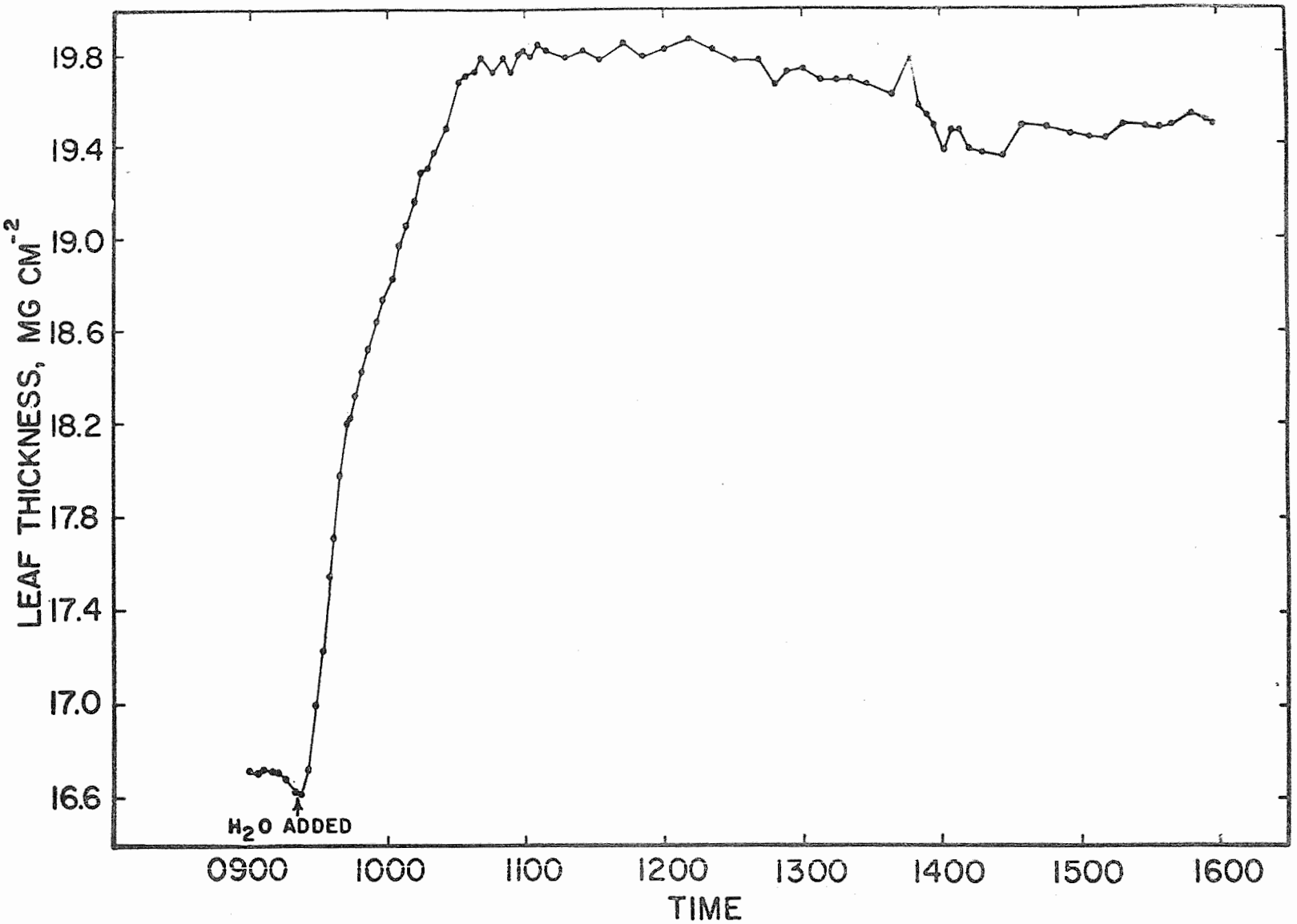

Figure 7. Leaf thickness behavior of cotton plant following irrigation.

TITLE: LEAF TEMPERATURE MEASUREMENTS

LINE PROJECT: SWC 11-gG1 CODE NO.: Ariz.-WCL-26A

INTRODUCTION:

In the pursuit of research projects in the area of water relations of plants (WCL-26, WCL-29 and WCL-34), it became increasingly evident that a need existed for characterizing the temperature of leaves and moist blotter paper to get a more quantitative measurement of the water-loss process.

The purpose of this study is to construct and test miniature thermocouples for measuring leaf temperature.

PROCEDURE:

Thermocouples were made from 4 mil (0.10 mm) bare, copper and constantan wires. Fine capillaries were made from 2 mm Pyrex glass tubing. The diameter of the capillary was slightly larger than the 4 mil wire. A thin lead bead was soldered on the end of the 6-inch copper and constantan wires. The beaded end of the 2 wires was slipped into a 15 mm section of the fine capillary from the opposite openings and the wires butted against each other at the middle of the tube section. Heat was applied to the joint with a soldering iron and the solder allowed to flow and re-form over the wires. After cooling, the thermocouple was removed by either slipping it through the capillary or breaking the capillary, depending upon the condition of the joint. The burrs and thickness of the solder-joint were smoothed down with sandpaper. Microscopic examinations of the butt joints showed joints which were in the order of 0.02 mm thicker than the original wire.

For leaf temperature measurements, the constantan end of the thermocouple wire was inserted into a leaf vein slightly larger than the thermocouple. With careful threading procedure, 3 to 5 mm segments can be embedded within the vein. It was possible to insert such thermocouples on cotton, sunflower, alfalfa, corn, soybean and fava bean plants.

Two methods for expressing leaf temperature were used. In one case, the absolute temperature was measured and in another the

temperature difference between the leaf and air was recorded. In the latter case, the reference air thermojunction was placed within a 5 × 25 cm aluminum-shielded plastic tube, with air drawn past the junction with a 30 cfm squirrel-cage blower.

Two, 12-week old Pima S-2 cotton plants grown in 1/2 Hoagland nutrient solution were brought into the Controlled Environment Room 1 day prior to the experiment for pre-conditioning. Room temperature was 30 degrees C and vapor deficit at 27 mb. Thermocouples were placed in leaves number 12 and 14 of both plants. Continuous readings were taken on leaves 12 and 14 in alternate fashion over 1 minute periods.

RESULTS AND DISCUSSION:

Results for one of the different sets of leaf temperature measurements are presented in Figure 1. A more complete picture of the role of leaf temperature is discussed in Project Ariz.-WCL-29.

The leaf temperature was about 1 degree C less than air temperature in the dark. As soon as the lights were turned on, the temperature increased due to radiation, and then decreased due to opening of the stomates and consequent transpiration. Temperature difference ranged from +2.5 to -3 degrees in a cyclic manner. The periodic cycle, however, was not the same for both plants in the same environment. The observed periodicity in temperature is in agreement with the results obtained with the beta ray gauging equipment reported in the Annual Report for 1963 (Ariz.-WCL-29).

SUMMARY AND CONCLUSIONS:

Leaf temperatures of cotton plants were measured using specially constructed, thin-wire (0.10 mm) thermocouple sensors in a controlled environment of 30 degrees C and 27 mb vapor deficit. The leaf temperature was 1 degree C lower than air in the dark. When the plant was exposed to light, the temperature varied in a periodic 30 minute cycle, ranging from 3 degrees C higher to 3 degrees C lower than the air. The measurement of leaf temperature is a sensitive method for following the changes in transpiration occurring in the cotton plant in the

growth chamber. The measurement can also be automated and thus, serves as a precise method for the continuous monitoring of the plant during an experiment.

PERSONNEL: F. S. Nakayama and W. L. Ehrler

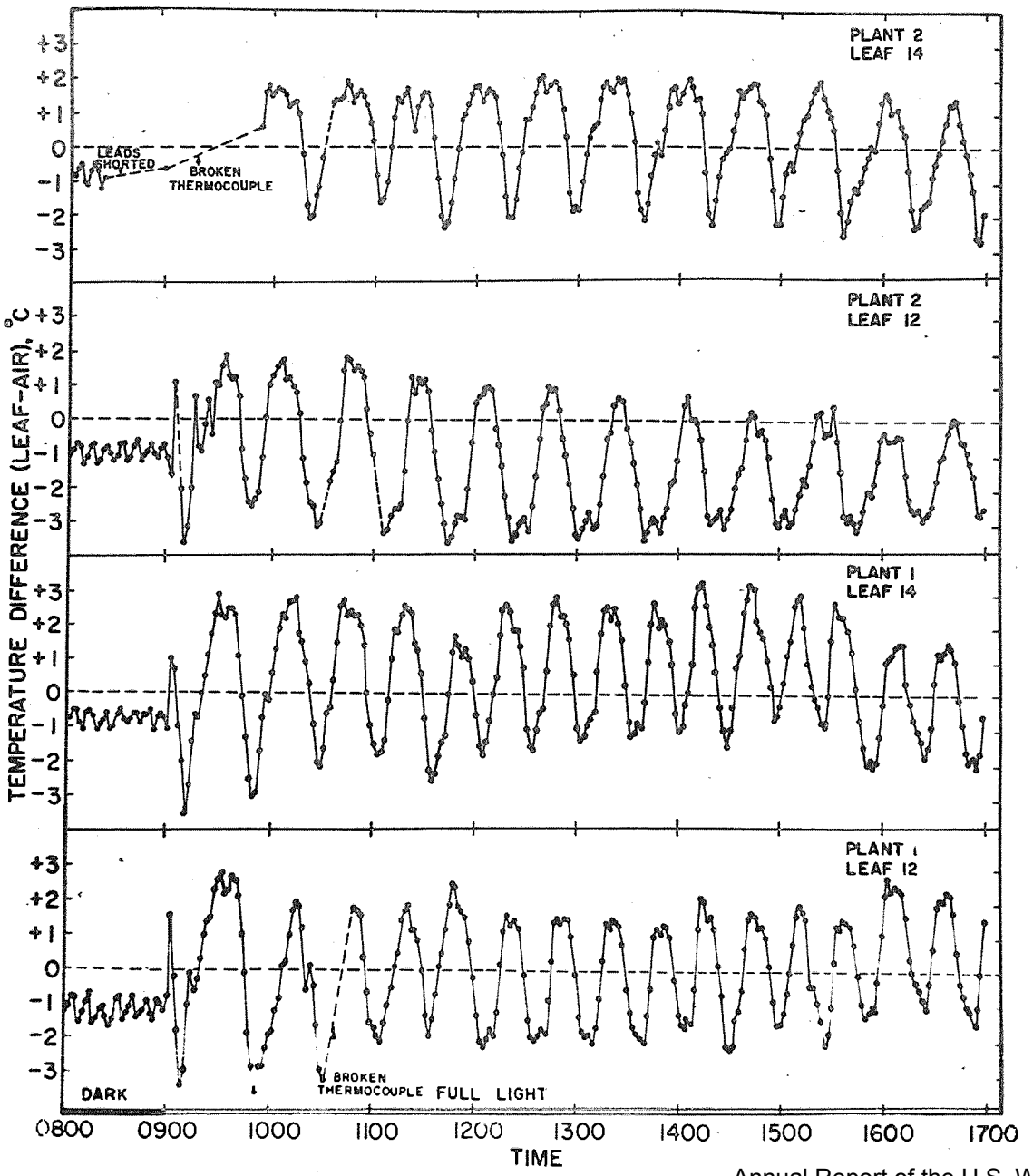

Figure 1. Temperature (leaf-air) of cotton leaf under dark and light and constant environment of 30° C and 27 mb vapor pressure deficit.

TITLE: WATER ABSORPTION, TRANSPIRATION, AND INTERNAL WATER BALANCE OF COTTON PLANTS AS AFFECTED BY CHANGES IN EVAPORATIVE DEMANDS

LINE PROJECT: SWC 11-gG1 CODE NO.: Ariz.-WCL-29

This report consists of five independent units, followed by a Summary and Conclusions section pertaining to all of the work done.

PART 1. CYCLIC VARIATIONS IN LEAF WATER CONTENT AND TRANSPIRATION OF COTTON

INTRODUCTION:

Beta ray gauge records of leaf thickness indicated a prolonged response by cotton plants to a suddenly induced acceleration of transpiration (Annual Report 1963). Oscillations in leaf water content continued long after the initial environmental changes had been completed, and thus appeared to represent changes brought about primarly by corresponding variations of stomatal aperture. Better instrumentation was needed to confirm this hypothesis, however. Accordingly, comprehensive experiments were undertaken to study this phenomenon.

PROCEDURE:

A standard procedure has been developed to obtain uniform experimental material. The controlled environment studies are carried out with nonbranched plants of long-staple cotton, 8 to 10 weeks old, grown in greenhouse water cultures and then preconditioned. Preconditioning takes place in the controlled environment room, where air temperature, vapor pressure, and carbon dioxide content of the air are held steady during 12 hours of high-intensity fluorescent light followed by 12 hours of darkness. During this period the plants are in aerated nutrient solution.

Since the rate of rise in transpiration seemed to be implicated in setting off cyclic responses of cotton, only treatments known to cause a large upset in water balance were employed. Air temperature was kept constant at 30.0 $\pm$ 0.2C. Figure 1-1 illustrates the results of the first method of generating an internal water deficit. The vapor-pressure deficit (saturation deficit, sd) was increased from 10 to 30 mb from 0930 to 1000 by lowering the vapor pressure. In

addition, full illumination (2000 ft-c) occurred instantaneously at 0930. The other method of dehydrating a plant gave results shown in Figure 1-2. In this experiment sudden illumination (2000 ft-c) was given to plants preconditioned at a sd of 27.3 mb (air temperature 30.0 ± 0.2C). In both instances the objective was to attain rapid, light-induced stomatal opening and thus a more rapid rate of increase in transpiration than water absorption. This would upset the balance between transpiration and water absorption that occurs in the dark, resulting in the temporary decrease in leaf water content which constitutes the first phase of cyclic behavior.

RESULTS AND DISCUSSION:

The leaf-temperature data, Figure 1-1, indicate a cooling of the leaf below ambient temperature in the dark, which is interpreted as due to a moderate loss of water from the leaf, and consequent evaporative cooling. The minor fluctuations represent room-temperature variations, with a variation of three per 10-minute period. Upon sudden illumination the leaf rapidly heats up above air temperature, but only momentarily. The subsequent cooling of the leaf to a −4C minimum differential indicates rapid stomatal opening in the light and a large increase in evaporative cooling. Later the leaf becomes increasingly less cool than air until it finally is equal to air temperature, and later, considerably above ambient temperature. This is interpreted as due to progressive stomatal closure, whereupon less evaporative cooling creates a condition of insufficient dissipation of the radiant heat input to the leaf. After the leaf becomes about 1 degree warmer than air temperature, the process is reversed, leading to repetitions of the cycle. The important point is that these oscillations continue beyond the time at which the lowering of vapor pressure was concluded — under conditions of steady light intensity and evaporative demand. The cycle length is about 30 minutes.

The other graph in Figure 1-1, demonstrating leaf-thickness changes, confirms the cyclic behavior shown by leaf temperature. A beta ray gauge on the same leaf having the thermocouple shows a steady level of leaf water content in the dark, followed by a cyclic pattern of loss and gain of water after the sharp change in evaporative demand and sudden illumination. The peaks and troughs coincide with those of leaf temperature. The data of Figure 1-1 are from only the lower leaf of a pair of leaves instrumented on the same plant. The upper leaf, several nodes up the nonbranched stem, showed virtually identical results, thus demonstrating both cyclic behavior and the unity of water within the plant.

In Figure 1-2 the interpretation of the leaf-temperature data is the same as before, clearly indicating a cyclic behavior beyond 0900, i.e., in an environment that was steady in regard to temperature, vapor pressure, light intensity, and carbon dioxide content of the air.

In this experiment direct determination of transpiration by weight loss also demonstrates a cyclic behavior under the steady environmental conditions existing from 0900 to beyond 1100. A third, independent measurement which indicates cyclic behavior of transpiration is the leaf diffusion resistance (Figure 1-2), measured by a leaf resistance meter (Part 2, WCL-29). Illumination quickly lowered leaf diffusion resistance; however, in continued full-intensity illumination, under very steady air temperature, vapor pressure, and CO_2, leaf resistance alternately rose to a high level and returned to a low level, synchronously with the changes already noted in leaf temperature and transpiration rate. The conclusion is that the stomates are opening and closing rhythmically, even under a steady environment. Again the cycle length is about 30 minutes, but this has been observed to range from 25 to 40 minutes with different plants.

In summary, the two types of experiments illustrated lead to the conclusion that cyclic behavior of cotton persists in a steady environment, after being induced by a rapid environmental change. Measurements of leaf diffusion resistance, leaf temperature, leaf water content, and transpiration all show oscillations under steady conditions of temperature, vapor pressure, light, and carbon dioxide content of the air. The cycle length tends to be 30 minutes.

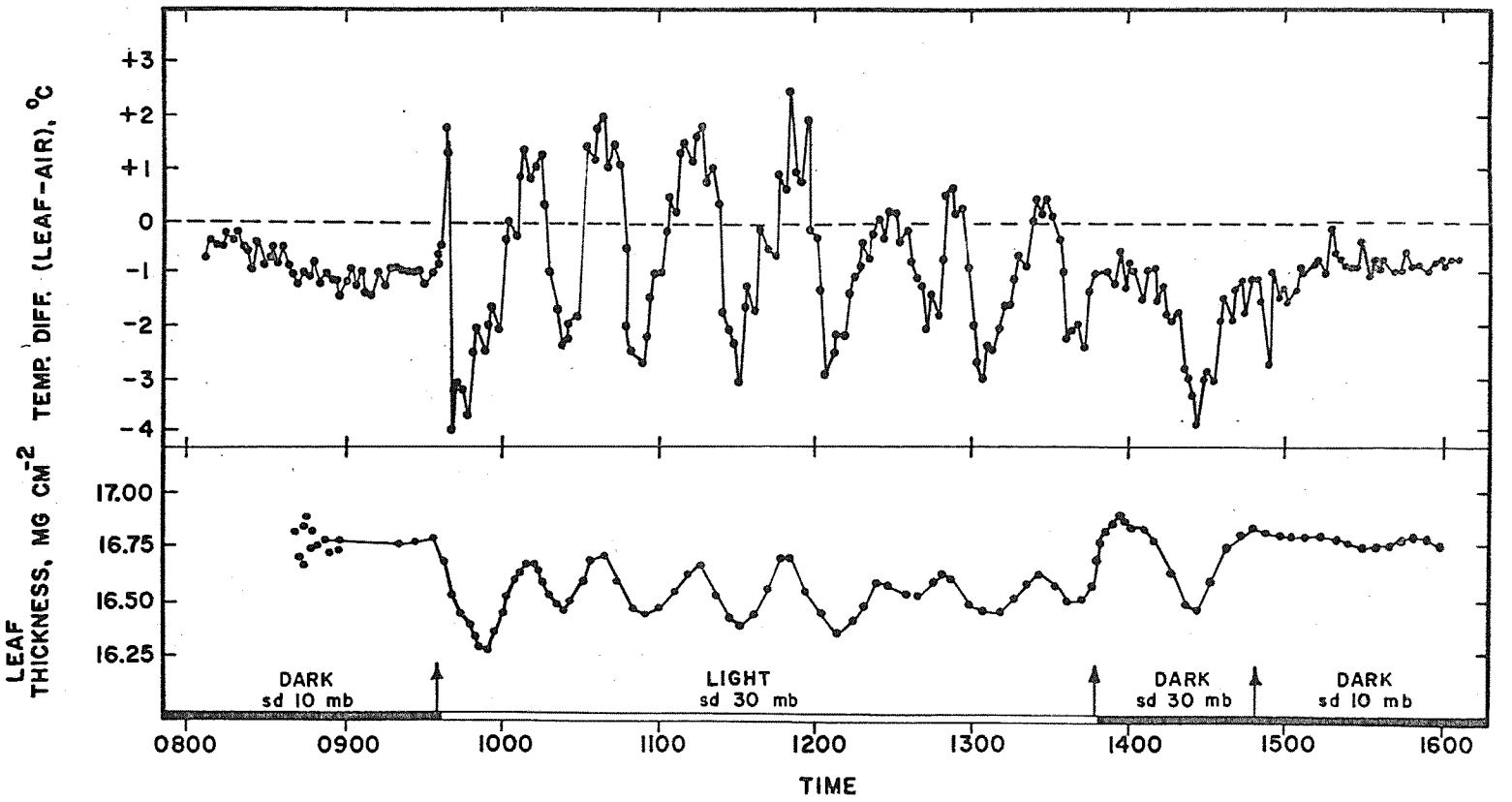

Figure 1–1. Comparison of simultaneous measurement of periodic changes in leaf thickness and leaf temperature.

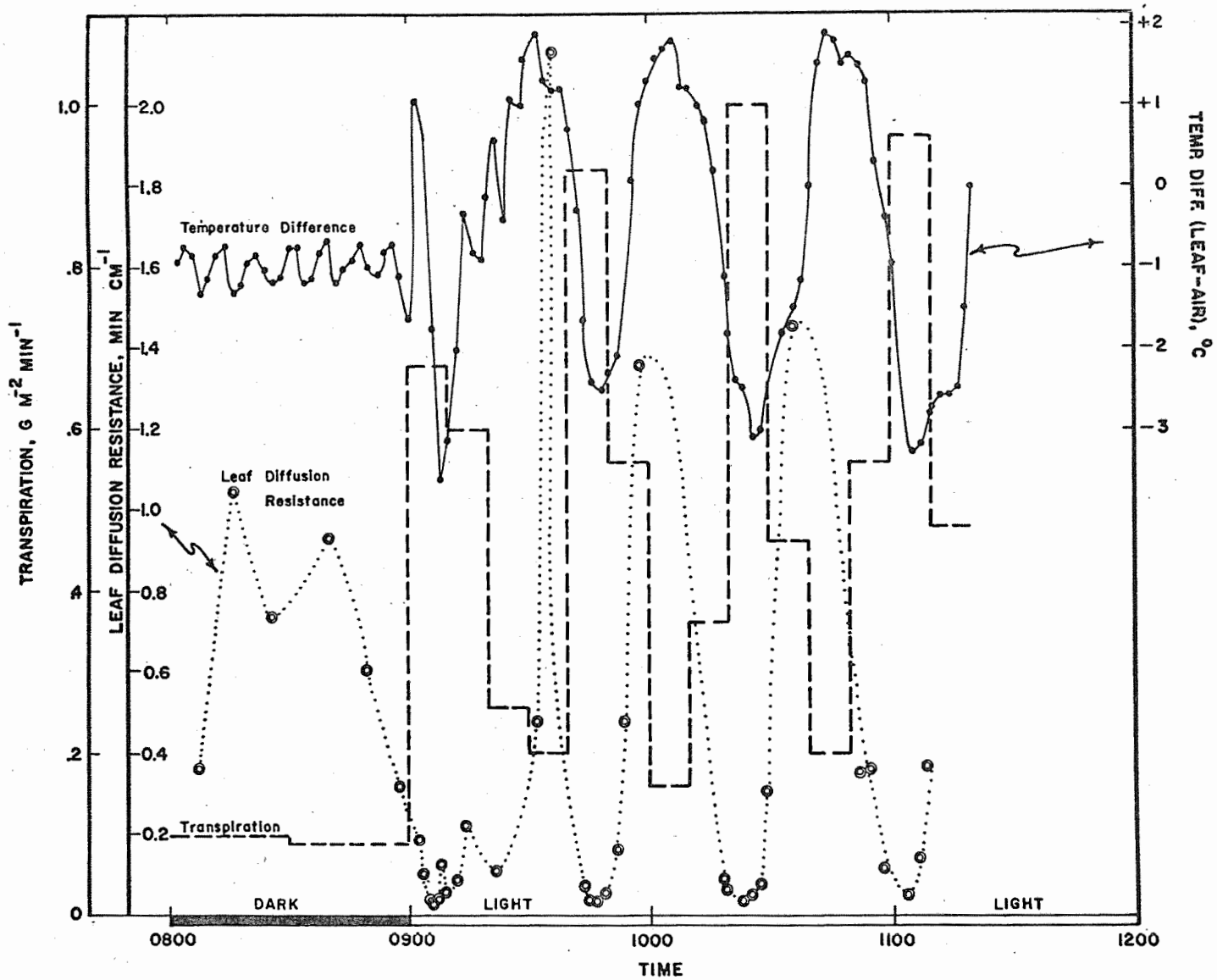

Figure 1–2. Comparison of simultaneous measurements of periodic changes in transpiration (dashed line), leaf temperature (solid line), and leaf diffusion resistance (dotted line).

PART 2. A DIRECT METHOD FOR MEASURING TRANSPIRATION RESISTANCE OF PLANT LEAVES

INTRODUCTION:

It is generally recognized that the leaf structure — in particular the stomates — can play a significant role in determining the transpiration from leaves, whole plants, and canopies. Nevertheless, a generally useful field method for the purpose of characterizing this factor has not been available. We here have tried to use direct observation, silicone impressions, and pressure porometers, all with poor results in spite of much work. In 1964 we finally found a straightforward answer to the problem. The results of this effort are documented in WCL Report No. 2 and in an article to appear in Plant Physiology (MS 135). For greater detail these reports should be consulted.

PROCEDURE:

The principle of the measurement is to expose a small area of leaf surface for a short period of time to a quantitatively known evaporative demand and, further, to measure the evaporation under these conditions. This is accomplished by clamping a small cup onto the leaf, the cup containing a lithium-chloride resistance "humistor," which serves as a sink for water vapor as well as a sensor.

By calibrating the instrument with water vapor sources of known diffusion resistance, the rate of change in "humistor" resistance can be interpreted in terms of the diffusion resistance of the evaporating surface. The resistance is conveniently expressed in min cm^{-1} or sec cm^{-1}. It is necessary to know the temperature of the evaporating surface to the nearest degree Celsius for data reduction.

To facilitate the measurement, a light-weight AC resistance bridge was designed and built, using transistors and mercury batteries.

Figure 2-1 schematically illustrates the apparatus.

RESULTS AND DISCUSSION:

The method has proved to be very practical and useful for all manner of studies. It can be and has been used by us in the climate room, greenhouse, and field. It enables one to quickly find effects of darkness and light, drought, carbon dioxide, and the difference between upper and lower epidermis, old and young leaves, and different species, all in regard to stomatal and cuticular diffusion resistance and changes therein.

The method has been applied by us on cotton, beans, corn, citrus, various ornamentals, sunflower, and alfalfa. So far the method has not been adapted for use with blade- or needle-type leaves, although this should be possible. Also, at resistances below 0.01 min cm^{-1}, the method is no longer sensitive. This can probably be overcome also.

As a part of transpiration and water balance studies, the method has proved to be useful in predicting plant transpiration (See Part 4), in studying cyclic phenomena in the plant water balance (See Part 1), and in assessing the effect of light intensity in the transpiration process (See Part 3).

In connection with field studies of water management and energy disposition, the method offers great promise. It can document effects of imbalance between demand and supply of water upon plants, the effects of light intensity and shading in the canopy, and the efficacy of antitranspirants. In a sense, the method can supplant certain measurements that can now only be found from precision lysimeters or tedious micrometeorological measurements. In the near future we hope to systematically explore these various possibilities.

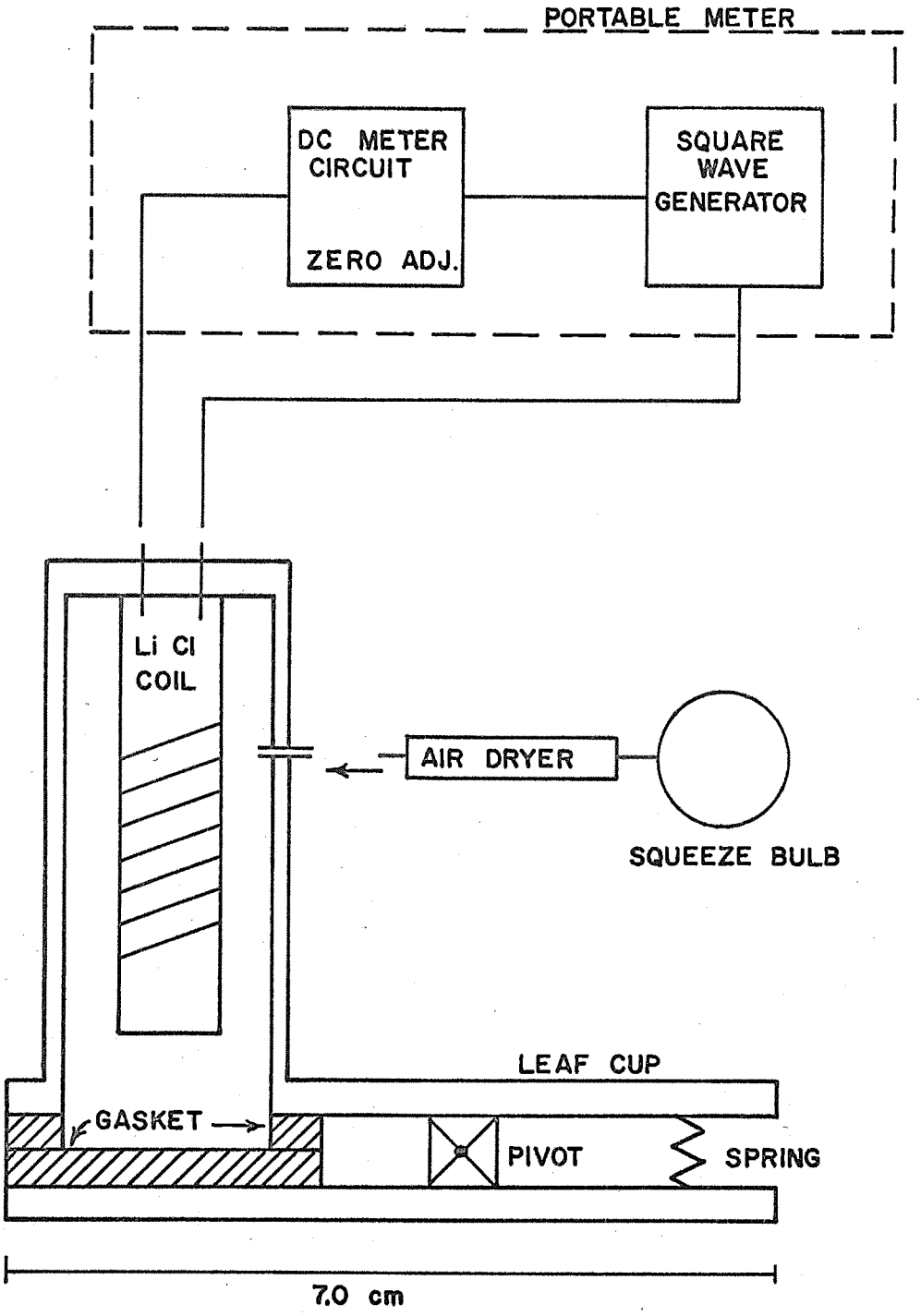

Figure 2-1. Schematic drawing of apparatus to measure leaf diffusion resistance.

PART 3. EFFECT OF STEPWISE INCREASES IN LIGHT INTENSITY ON LEAF DIFFUSION RESISTANCE OF FIVE CROPS

INTRODUCTION:

Although leaf diffusion resistance (R_ℓ) depends on several environmental factors, light is of such importance that in nature stomates generally are closed in the dark (high R_ℓ) and open in the light (low R_ℓ). Direct measurements of R_ℓ of the cotton leaf indicated differences in the lowest attainable R_ℓ in the field as compared to the laboratory. Controlled-environment room studies showed a minimum R_ℓ of 0.02 min cm^{-1} at the light intensity normally used, 2500 ft-c. In contrast, in July for example, field cotton in soil with available water commonly showed R_ℓ values of 0.00 cm min^{-1} from 0830 to 1530 (Part 5, WCL-29). The extremely high light intensities prevailing in the field during most of a clear summer day in Tempe, Arizona, from 10,000 to 12,000 ft-c, may be the primary reason for the lower R_ℓ values outside than in the controlled environment room. Determining the effect of stepwise increases in light intensity on R_ℓ would clarify the situation provided interacting factors, such as leaf hydration and carbon dioxide content of the air were kept constant.

Another difference between field and laboratory results was that upper and lower epidermes reached equal values of R_ℓ outdoors about 3 hours after dawn, but not in the lower light intensity of the laboratory. This presumably was due to not attaining the threshold light intensity in the laboratory, which seems to be greater for the upper than for the lower epidermis, regardless of experimental site. Experiments were conducted to determine the effect of light intensity on R_ℓ under controlled conditions of all environmental factors thought to have a bearing on stomatal aperture.

PROCEDURE:

Standard technique was to grow a plant in water culture until it was tall enough for two leaves several nodes apart to be measured simultaneously, both leaves being fully expanded and nonsenescent. Three similar plants were preconditioned before an experiment. The preconditioning environment was as follows: air temperature, 30.0 ± 0.2C; vapor pressure, 15.0 ± 0.2 mb; carbon dioxide content of the air, 375 ± 10 ppm; and 12 hours of high-intensity light (up to 4000 ft-c at the specific upper leaf that was to be measured for R_ℓ), followed by 12 hours of darkness.

Plant 1 had a 0.1-mm diameter thermocouple inserted in a veinlet in each of two leaves. Leaf resistance measurements were made on plant 2; plant 3 was reserved for silicone rubber impressions for direct determination of stomatal width. Analogous pairs of leaves were chosen on the three plants. Measurements of leaf temperature differences by means of thermocouples were started on the preconditioning day and lasted until the end of the experiment (on plant 1). However, no measurements were made on plants 2 and 3 until the end of the 12-hour dark period of preconditioning. These later measurements were begun in the dark and made at frequent intervals throughout successive 1.5-hour periods, in which light intensity generally was increased from 0 to 1000, 3000, and 4000 ft-c. For the last three experiments, R_ℓ was measured in the dark again, following the highest light intensity. Sites for placement of the leaf resistance meter cup were chosen to be suitable to a particular kind of leaf, and provision was made for rotation of sites, with avoidance of excessively large veins. Attainment of the highest light intensity necessitated support of some species at a level higher than the main bench normally used (for a closer approach to the light source). For the first two species, cotton and snap bean, a hypodermic thermistor probe was used, instead of a thermocouple inserted in a vein, to register leaf temperature. Leaf temperature was needed to calculate R_ℓ from the water vapor transit time obtained with the leaf resistance meter. Light intensity was

measured with a Weston light meter, with the sensor placed horizontally and as near to the specific leaf as possible, so that a "canopy" value is represented. Generally, a silicone rubber leaf impression was taken in both dark periods, and very near the end of the light periods, except for the 3000 ft-c period. A leaf resistance reading was taken just before a leaf impression to correlate microscopically measured stomatal widths with R_ℓ.

RESULTS AND DISCUSSION:

Data for five crops are presented for only the upper leaf of the pair of leaves measured, since the results were quite similar for both leaves. Leaf diffusion resistance on a logarithmic scale is plotted against light intensity. In cotton, Figure 3-1, R_ℓ for the lower epidermis was high in the dark, but reached a minimum value of 0.02 min cm^{-1} at the highest light intensity, 3800 ft-c. The effect of intermediate light intensities was not so straightforward, but the overall result of increasing light was the expected lowering of R_ℓ (interpreted as stomatal opening). At all points the upper epidermis had a higher R_ℓ than the lower. Monitoring of the leaf temperature indicated absence of cycling (See Part 1).

Snap bean, Figure 3-2, showed the same type of response to light intensity as cotton, but the disparity between upper and lower epidermis was much greater. Even at 4175 ft-c the final R_ℓ of the upper epidermis in snap bean was as high as 0.25 min cm^{-1}, thus indicating a low contribution to total water loss from the leaf. In contrast to the previous results, R_ℓ values for the upper and lower epidermis of fava bean, Figure 3-3, were not far apart at all light intensities. Again, the general effect of increasing light intensity was to lower R_ℓ. Sunflower, Figure 3-4, was like fava bean in not showing much difference in R_ℓ of the upper and lower epidermis. Moreover, R_ℓ was not much higher in the dark than in the light, confirming literature reports of open stomates at night. The R_ℓ value of 0.01 min cm^{-1} for the lower epidermis at the highest light intensity (4050 ft-c) represents the lowest value achieved by any species in the controlled environment room.

In corn, Figure 3-5, the upper epidermis again shows a higher R_ℓ than the lower epidermis at all points. The effect of increasing light intensity is the same as was found in the other crops, namely, a steady lowering of R_ℓ with each added increment of light.

In general, all five species responded to increasing light intensity in the same manner, showing a decrease in R_ℓ of both upper and lower epidermis. However, there are definite species differences in regard to disparity between the upper and lower epidermis R_ℓ values. In the three species for which the highest light intensity tested was substantially the same (about 4000 ft-c), R_ℓ was 0.02 min cm^{-1} or less. For corn and fava bean, however, the maximum intensity attained was about 1000 ft-c lower, which may have been a sufficient reduction to account for the higher minimum values of R_ℓ (0.03 min cm^{-1}) than in the three other crops. Sunflower with a R_ℓ of 0.01 min cm^{-1} is notably low in comparison with cotton and snap bean. This may be an indication of species differences in stomatal responsiveness.

It is apparent from the data for all five species that the highest intensities utilized in the controlled environment room were not sufficient for minimal R_ℓ values, since the curves for R_ℓ did not become level with increasing light supply. Therefore, it is concluded that saturation light intensity for stomatal opening is higher than 4000 ft-c, when leaf hydration is high and the carbon dioxide concentration of the air is about 375 ppm. Data for cotton in the field in moist soil (Part 5, WCL-29) show R_ℓ values of 0.01 min cm^{-1} or less, but not until solar radiation has reached an intensity equivalent to several thousand ft-c. Thus, the laboratory experimental results in general are in harmony with field data. It is likely that failure to obtain R_ℓ values for cotton in the controlled environment room as low as those in the field is due to insufficient light intensity in the room. This does not exclude the possibility, however, that field carbon dioxide levels were lower during the day than those of the controlled environment room, which also would tend to promote stomatal opening (low R_ℓ).

Microscopic observations and measurement of stomatal width by means of the silicone rubber impression technique showed a good correlation with the R_ℓ data. In general, stomatal aperture was low in the dark, and successively greater with each increment of light intensity. Even after making allowance for the limitations on accuracy of measurement at low stomatal widths, it was obvious that the stomates of all five species were not tightly shut in darkness. This suggests that what usually is called "cuticular" loss of water actually is due partly – or even mainly – to a stomatal contribution. It is doubtful that stomates ever are hermetically sealed.

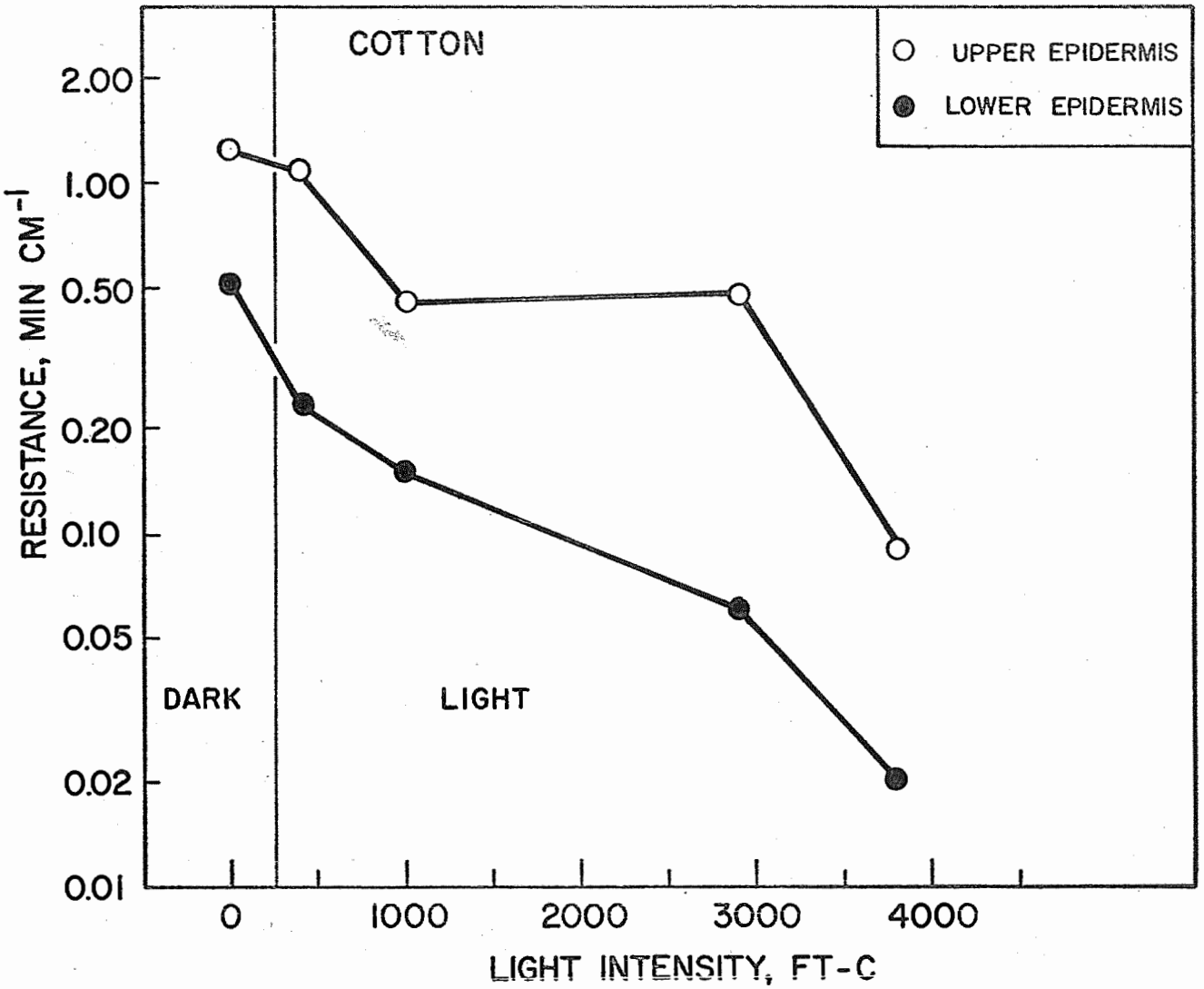

Figure 3-1. Effect of light intensity on leaf diffusion resistance of cotton.

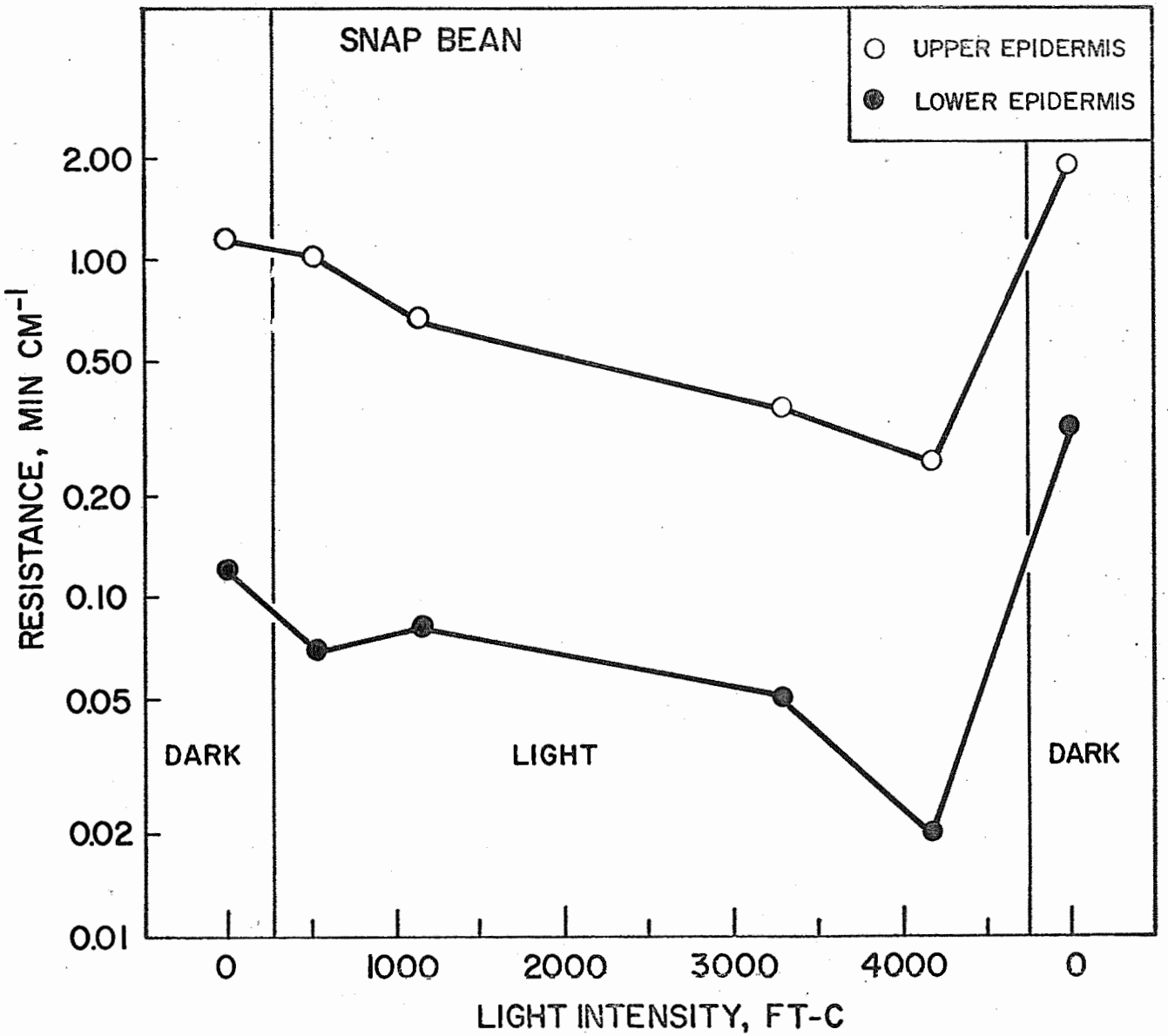

Figure 3–2. Effect of light intensity on leaf diffusion resistance of snap bean.

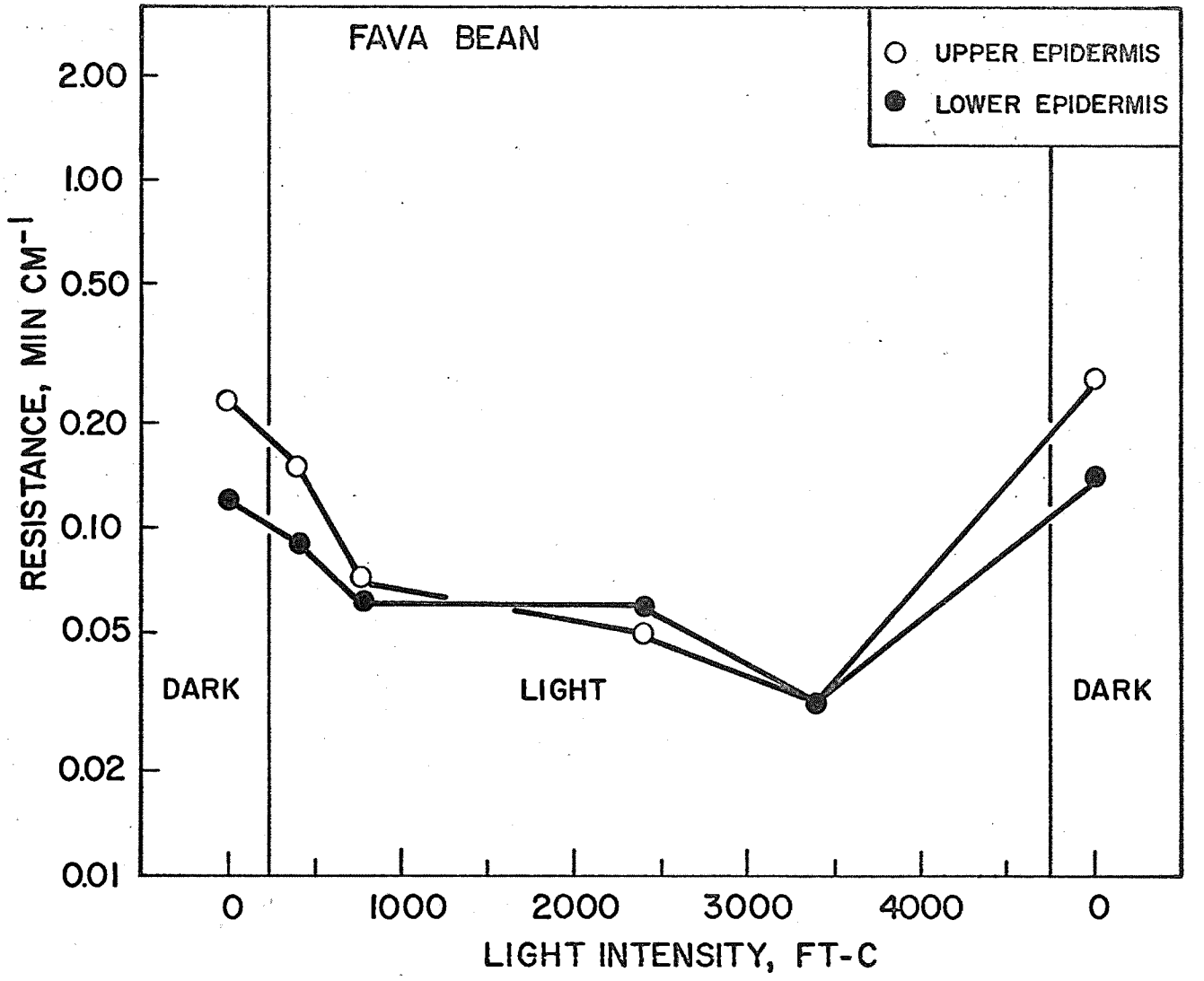

Figure 3–3. Effect of light intensity on leaf diffusion resistance of fava bean.

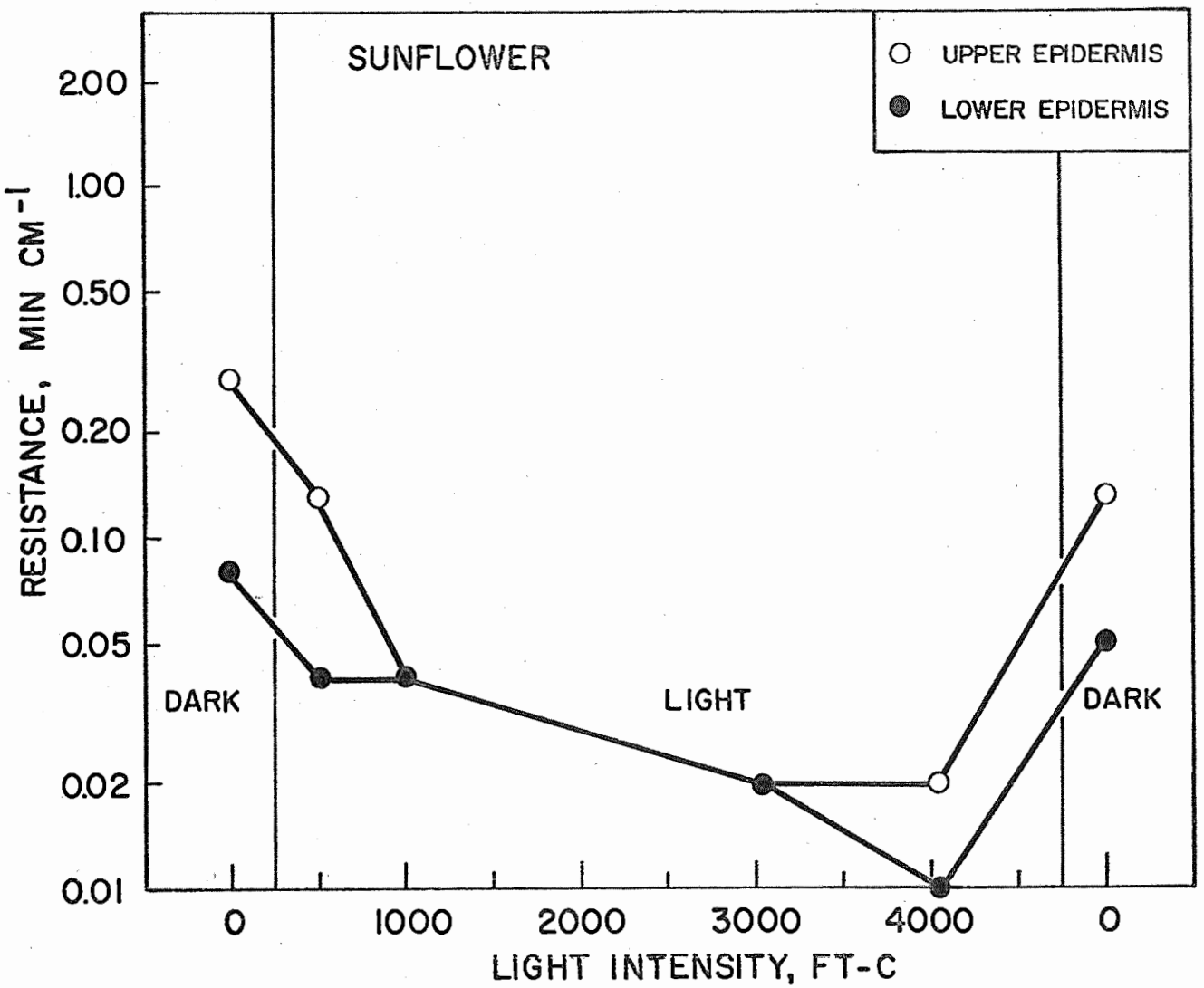

Figure 3-4. Effect of light intensity on leaf diffusion resistance of sunflower.

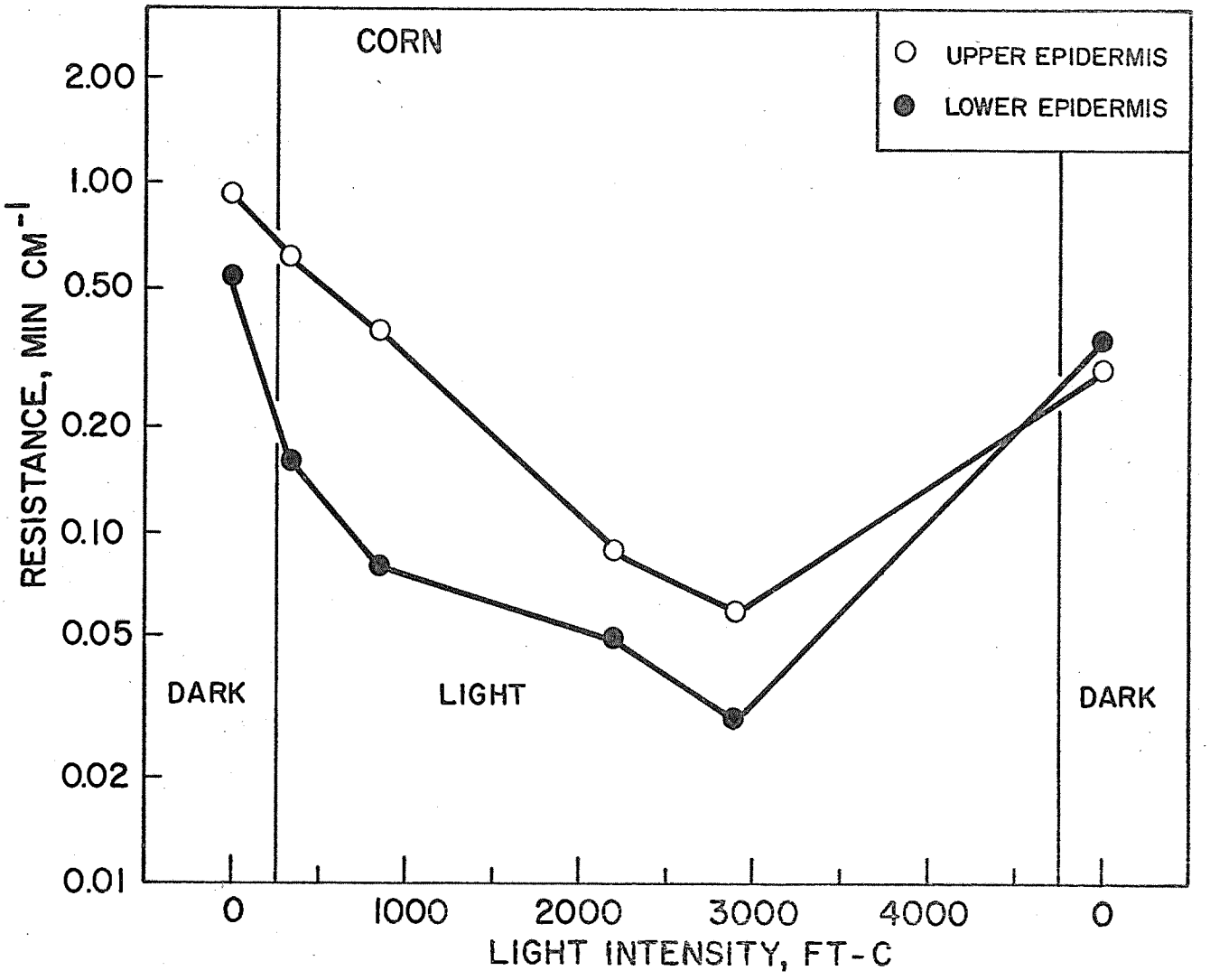

Figure 3–5. Effect of light intensity on leaf diffusion resistance of corn.

PART 4. TRANSPIRATION AND LEAF DIFFUSION RESISTANCE

INTRODUCTION:

Characterization of leaf diffusion resistance (R_ℓ) is only a partial answer to the problem of predicting the transpiration rate. However, when supplemented with information on leaf boundary layer resistance (R_a), R_ℓ is a powerful tool in calculating transpiration, since at a given gradient of water vapor concentration, water loss from a leaf is inversely proportional to the sum of these two resistances. The remaining problem is to standardize the water vapor gradient from leaf to external surroundings, which can be accomplished in a controlled environment room.

PROCEDURE:

Controlled environment studies were carried out with cotton. During these experiments precise measurements were made of each item used as a term on the right side of the equation:

$$E = \frac{\Delta d}{R_a + R_\ell} ,$$

in which E is evaporation (or transpiration) in g cm^{-2} min^{-1}; Δd, the gradient in density of water vapor from leaf to air in g cm^{-3}; R_a, the resistance of the air; and R_ℓ, the resistance of the leaf, both in min cm^{-1}. From these measurements E was calculated and compared with the value obtained from direct weighing of the live plant, the same plant on which the R_ℓ measurements were made. The controlled value of vapor density in the room was used in conjunction with the handbook value for the vapor density of water at a given leaf temperature to calculate Δd. Leaf temperatures were measured by means of 0.1-mm thermocouples and used both for looking up the tabular value of saturation vapor density and calculation of R_ℓ from the water vapor transit time.

During measurements the controlled environment room was maintained at an air temperature of 30.0 $\pm$ 0.5C with vapor pressure at 15.0 $\pm$ 0.2 mb. Temperature was determined from the dry-bulb controller thermohm, and in a later experiment, additionally by means of a 30-gauge copper-constantan thermocouple in a radiation-shielded blower near the plant. The vapor pressure was measured by the dew probe used in the controller and confirmed in a later experiment by several sets of readings with an Assmann psychrometer. Previous experiments with 5- by 10-cm rectangles of wet blotter paper had established an R_a value of 0.023 min cm^{-1} for the controlled environment room. In a later experiment, green blotter paper replicas of cotton leaves oriented realistically on a lucite stem were used. This synthetic plant was placed adjacent to the live plant. To establish a value for R_a, a formula similar to the previous one was used:

$$E = \frac{\Delta d}{R_a} \quad .$$

Direct weighing determined E, which was expressed on a unit area basis by knowing the total area of evaporating surface. The humidity gradient was determined in the same way as for the live plant. Again thermocouples embedded in the leaf (blotter paper) gave the temperature of the evaporating surface. Solving for the unknown quantity in the above equation gave R_a. The value, 0.029 min cm^{-1}, the mean of the values at high- and low-light intensities, was slightly higher than that from rectangular blotter paper.

The R_ℓ values determined during the cyclic behavior of cotton in a steady environment (Part 1, WCL-29) were used in conjunction with the R_a value from the rectangular blotting paper. The transpiration so calculated then was compared with the values measured directly over 10-minute periods on a Mettler balance. A later experiment was carried out under conditions of steady transpiration, regulated at two different rates by means of different light intensity. In this instance the R_a determined from the synthetic plant was used.

RESULTS AND DISCUSSION:

Cyclic conditions. In Figure 4-1 the calculated transpiration is seen to be less than the directly measured amount, but the wide changes in measured weight loss are accurately reflected by the calculated values throughout the whole set of cycles. The bar graph values of measured transpiration have had a correction applied to compensate for the lack of R_ℓ determinations on the upper epidermis during cycling. The correction was based on the relative contribution to water loss of upper and lower epidermis on the previous day when conditions were steady.

Steady conditions. On the day previous to that in which cyclic behavior occurred, transpiration was steady. From the average R_ℓ value for the lower epidermis of 0.020 min cm^{-1}, transpiration was calculated as 3.74×10^{-4} g cm^{-2} min^{-1}. For the upper epidermis, with an R_ℓ of 0.148 min cm^{-1}, transpiration was 0.94×10^{-4} g cm^{-2} min^{-1}. For the leaf as a whole (two sides) the transpiration rate was the sum, 4.68×10^{-4} g cm^{-2} min^{-1}, whereas the average measured value from water loss determination of the entire plant was 3.75×10^{-4}g $cm^{-2}min^{-1}$. Thus, the calculated rate was 1.25 times as great as the measured.

Table 4-1 gives the results of a separate experiment in which two levels of light intensity produced different average values of stomatal aperture (R_ℓ) and hence, different steady transpiration rates. Transpiration was not cyclic because the light intensity was increased very gradually.

Table 4-1. Steady-state transpiration of a cotton plant in the controlled environment room

Light intensity	Transpiration, g cm^{-2} min^{-1} Measured	Calculated	Calculated/Measured
3800 ft-c	1.34×10^{-4}	1.72×10^{-4}	1.28
87 ft-c	0.63×10^{-4}	0.79×10^{-4}	1.25

While the discrepancy between measured and calculated transpiration is rather large, it is extremely consistent, being virtually identical in the three separate measurements under steady conditions. Present thinking is that no further refinement is necessary in the determination of R_a. The most likely source of error in the calculated values is in R_ℓ. It is possible that recalibration of the leaf resistance meter cup will be necessary. Nevertheless, it is believed that the data presented above provide a most promising approach to an accurate definition of the transpiration process. Further studies are envisioned with sunflower and citrus.

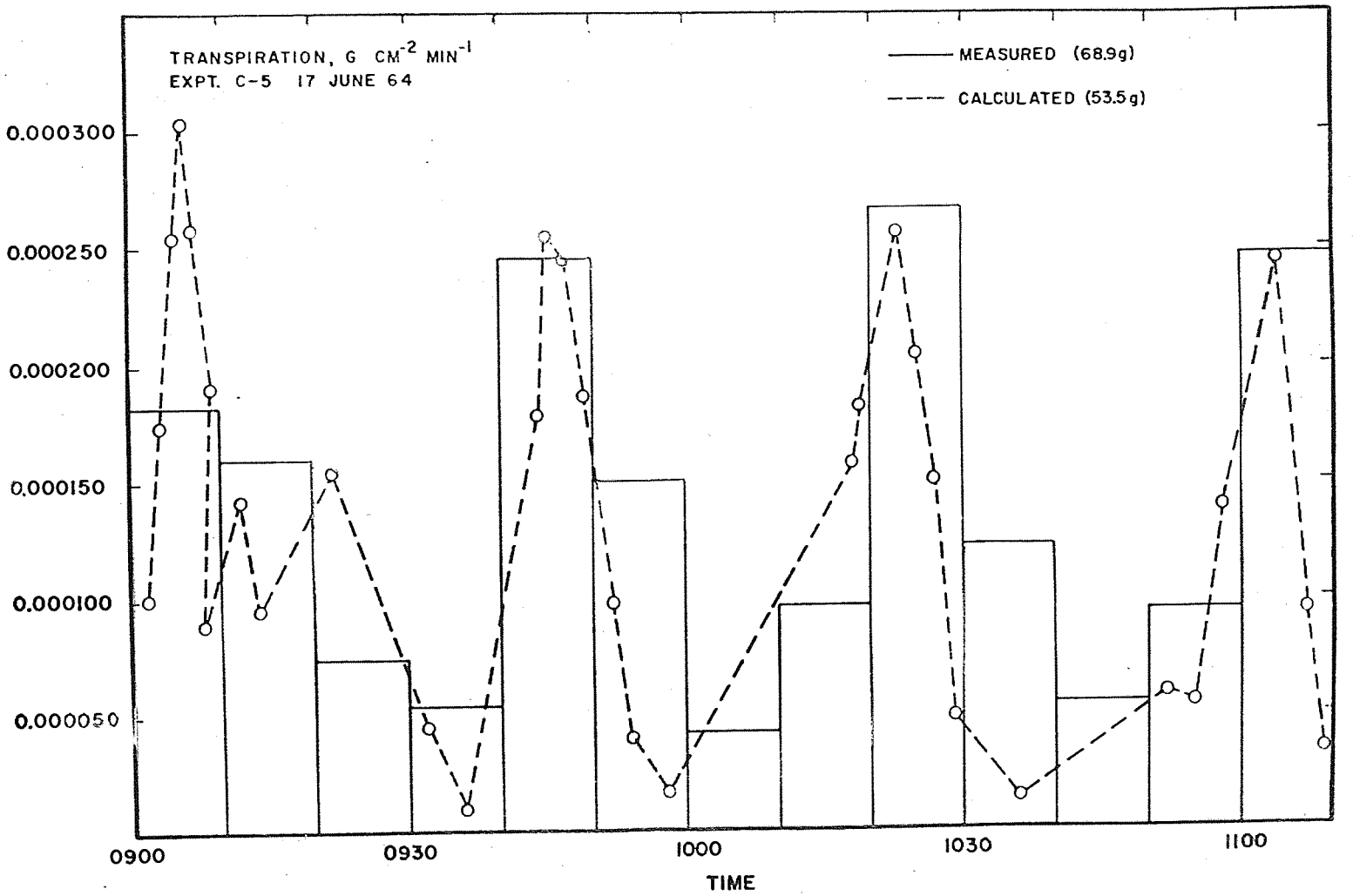

Figure 4–1. Comparison of measured with calculated transpiration of cotton during cyclic behavior.

PART 5. LEAF DIFFUSION RESISTANCE OF COTTON UNDER FIELD CONDITIONS

INTRODUCTION:

Since leaf diffusion resistance was shown to be an important element in the transpiration process (See Parts 1 and 4 and also WCL-33, Part 1), a number of measurements were made on cotton leaves in the field. The plants were grown in the plots used for the evapotranspiration studies (WCL-33, Part 3) and for measurement of leaf temperature and thickness (WCL-26 and 26A).

Thus the findings could be correlated with other plant and environment properties, the latter including evaporative demand, actual evaporation, and soil moisture. The study was intended as an exploratory one, with three objectives:

(a) To test the feasibility of the leaf diffusion resistance measurement under outside conditions;

(b) To see the influence of daylight intensity upon resistance;

(c) To study the effect of declining soil-moisture reserves during the progress of an irrigation cycle.

PROCEDURE:

The method for measuring leaf resistance is described elsewhere (Part 2). Well-developed sunlit leaves were chosen and repetitive measurements made on both upper and lower epidermes. Leaf temperature was obtained from contemporaneous thermocouple measurements when available or from air temperature in the immediate vicinity of the shady side of the leaf. Two schedules were followed: one in which leaf resistance was measured three times daily at around 1000, 1300, and 1600 and another in which an essentially continuous record was obtained from before dawn until dusk. Twelve records of the first kind were obtained and eight of the second during July, August, and September 1964.

RESULTS AND DISCUSSION:

Clear-cut and important information was obtained from the diurnal studies, exemplified in Figures 5-1 and 5-2. In these diagrams, the logarithm of the leaf diffusion resistance in min cm^{-1} is plotted versus time of day. Also shown is a record of short-wave incoming radiation in ly min^{-1} measured about 0.5 km from the site and an interpretative scale of light intensity in kilolux.

Both Figures 5-1 and 5-2 demonstrate that cotton stomates are closed in the dark (maximum resistance about 0.8 cm min^{-1}), and that opening proceeds gradually as light intensity increases. At light intensities of about 50 kilolux, the minimum resistance is found. This finding is tentative, since meaningful measurements below 0.01 min cm^{-1} cannot be obtained with present equipment.

Also, we find consistently that the upper epidermis has a higher resistance than the lower one, until values of 0.01 min cm^{-1} are reached where differences cannot be further demonstrated, presumably due to lack of sensitivity.

The data of 14 July were obtained shortly after an irrigation (9 July), whereas those of 1 September typify the advanced stage of a drying cycle (last irrigation 31 July). It is obvious that the broad daylight values of leaf diffusion resistance were higher on 1 September than they were on 14 July.

Less clear indications were obtained by relating leaf resistance to progressive drying of the soil. Values of lower epidermis leaf resistance obtained at 1000 and at 1600 are shown in Figure 5-3, which covers an entire irrigation cycle during August and part of September. Also shown is the evaporation from the cotton as determined daily with single loadcell lysimeters (solid circles) and twice weekly with the neutron method (horizontal bars). Potential evaporation (open circles) is shown as calculated from hourly weather data with the combination method.

Obviously, the evaporation continued at about the potential rate until around 24 August, whereafter it declined sharply. The record of leaf resistance is less clear-cut, indicating a generally rising trend from values around 0.01 min cm^{-1} to around 0.05 min cm^{-1}.

From these exploratory data it appears that cotton is a plant not given to extreme reaction to increases in diurnal evaporative demand or to progressive decreases in soil-moisture availability. Thus, it can be described as adapted to an arid and extreme environment, but not in the sense of using water conservatively.

Correlation with leaf-thickness data (WCL-26) does not indicate that the diurnal changes in water content that were invariably found are related to synchronous changes in leaf diffusion resistance. The limited data obtained with the beta gauge technique suggest a marked difference in water balance character in the first few days after irrigation, as contrasted to the remainder of the irrigation cycle. However, this is not reflected in leaf diffusion resistance or — by implication — in transpiration.

Detailed studies under controlled conditions are definitely indicated to describe the reaction of the cotton plant to declining soil-moisture availability.

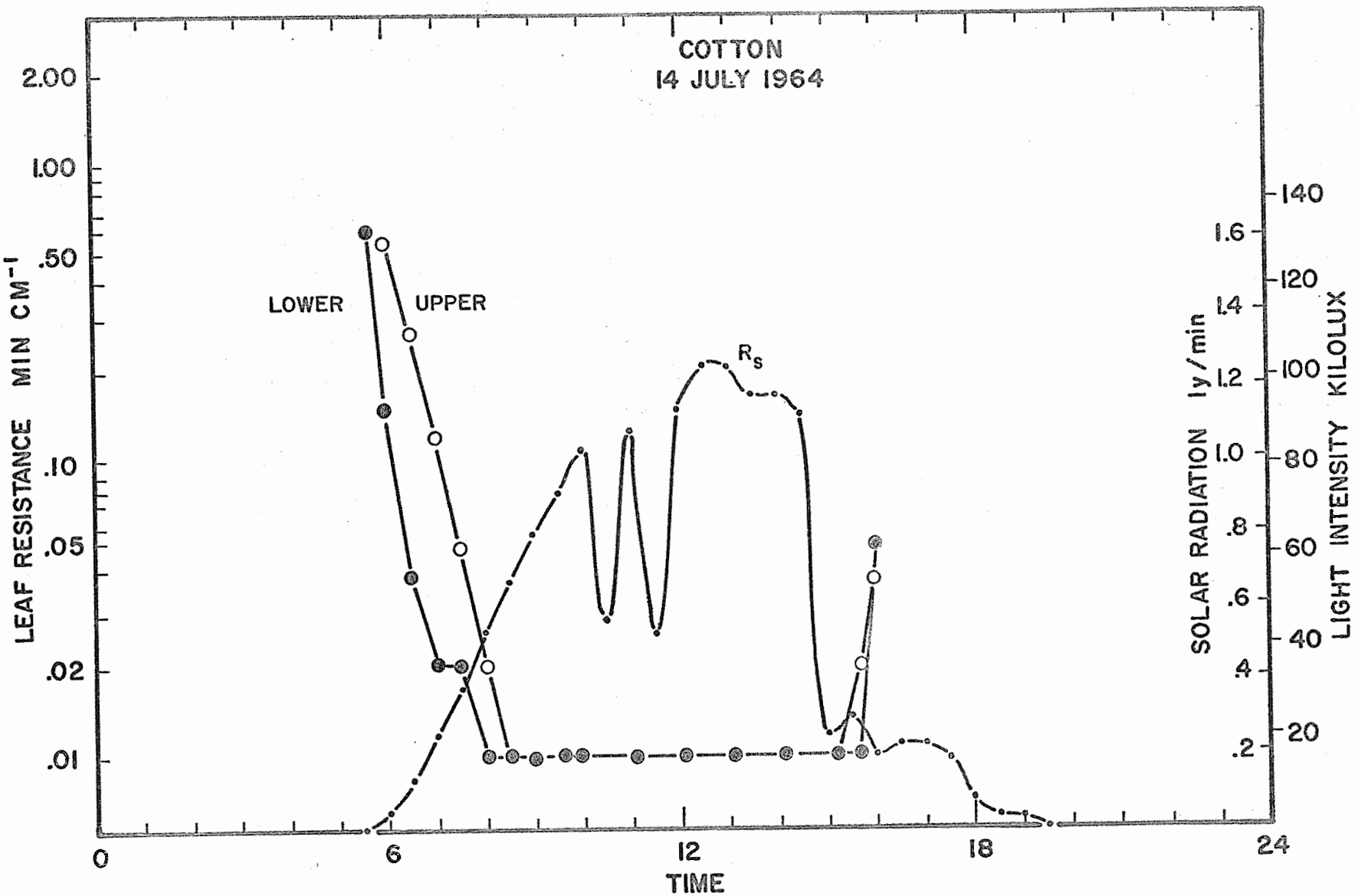

Figure 5-1. Leaf diffusion resistance of Deltapine cotton in the field for upper and lower epidermes, 15 July 1964; also, solar radiation and derived light intensity.

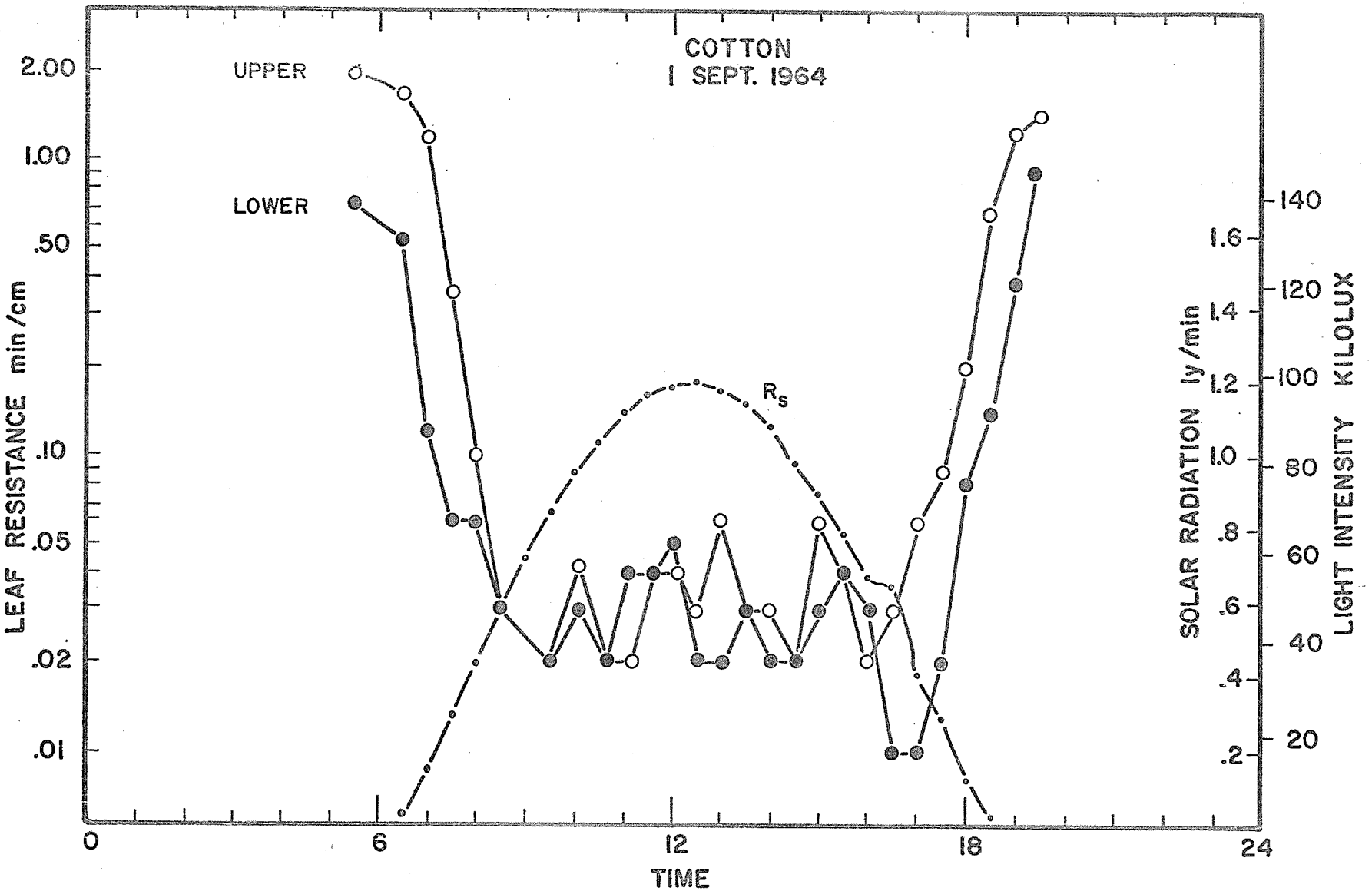

Figure 5–2. Leaf diffusion resistance of Deltapine cotton in the field for upper and lower epidermes, 1 September 1964; also, solar radiation and derived light intensity.

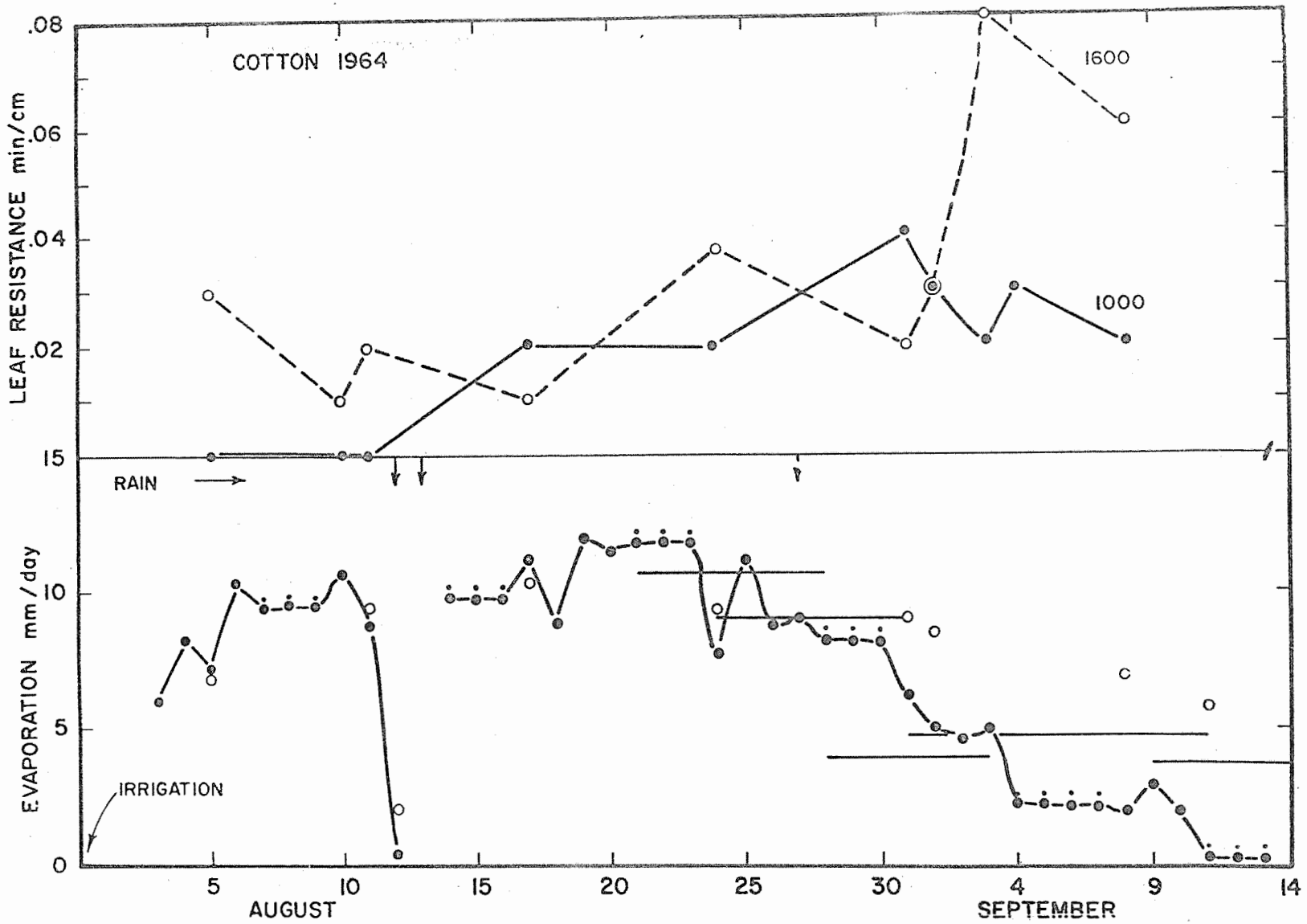

Figure 5–3. Leaf diffusion resistance of lower epidermis at 1000 and 1600 of Deltapine cotton in the field; also, evaporation as found from lysimeters (solid circles), and from neutron moisture data (horizontal bars). Open circles are potential evaporation values. A small dot over a solid circle indicates an average of more than one day.

Annual Report of the U.S. Water Conservation Laboratory

SUMMARY AND CONCLUSIONS:

Cyclic changes in stomatal aperture in the cotton plant were found under steady conditions of the major environmental factors known to influence stomates, i.e., light, temperature, vapor pressure, and carbon dioxide content of the air. Evidence for a 30-minute cycle was provided by independent measurements of changes in (1) transpiration, (2) leaf temperature, (3) leaf diffusion resistance, and (4) leaf water content. The data indicate that the oscillations were due to internal changes in the plant -- not to environmental periodicity. The cycles may be due to the interplay between a stomatal-opening factor, light, and a stomatal-closing factor, leaf dehydration with its consequent loss of turgor potential by guard cells. This, in turn, implies that a major causal factor in the initial triggering of the cycle is a slower rate of water absorption than transpiration when stomates open rapidly, owing to the resistance to water flow inherent in living cells.

A portable meter for measuring leaf diffusion resistance has been perfected. It overcomes many objections to previous porometers by rapidly and quantitatively measuring leaf resistance to the outward diffusion of water vapor. This measurement is made by recording the time for water vapor to move from a leaf surface to a lithium-chloride element serving both as a sensor and sink for water vapor. A small cup containing the "humistor" is clamped momentarily on either surface of a leaf, exposing it to a standard evaporative demand. Proper calibration enables the rate of change of "humistor" resistance to be interpreted in terms of diffusion resistance of the evaporating surface, expressed in min cm^{-1}. Necessary circuitry includes a light-weight AC resistance bridge incorporating transistors and mercury batteries. The instrument has been used successfully with many plant species to ascertain leaf diffusion resistance (stomatal aperture) of plants exposed to various environmental conditions in the laboratory, greenhouse, and field. It is particularly useful in differentiating between upper and lower epidermis. Typical readings range from 0.01 min cm^{-1} or less in full light to

1.00 min cm^{-1} in the dark. It should be possible to adapt the instrument for use with blade- or needle-type leaves.

Light is one of the two most important factors influencing stomatal aperture and, hence, leaf diffusion resistance, R_ℓ. With the leaf resistance meter, precise measurements of light effects on R_ℓ in several species were made. The experiments were conducted under constant conditions of air temperature, vapor pressure, and carbon dioxide content of the air, with an optimum root environment provided by a nutrient solution. After a 24-hour conditioning period, an experiment began in the dark, progressed through stepwise increases in light intensity, and ended in darkness again. Measurements of R_ℓ varied from 1 min cm^{-1} in darkness to 0.02 min cm^{-1} at 4000 ft-c (0.01 for sunflower). Duplicate leaves gave similar responses. Regardless of species (cotton, snap bean, fava bean, sunflower, and corn), increasing light lowered R_ℓ for both the upper and lower epidermis. The upper epidermis consistently showed a higher R_ℓ than the lower at most light intensities, even in species found to have equal stomatal frequency on both leaf surfaces. Despite the similarities in general response, definite species differences exist.

Significant progress has been made toward explaining transpiration by plants in terms of pertinent physical properties of environment and plant. Calculated transpiration values for entire cotton plants, grown under three different sets of conditions, were compared with direct measurements of weight loss. The calculated value follows from a measurement of the ambient vapor pressure, the temperature, and the diffusion resistance of representative leaf areas, the external or aerodynamic vapor transfer coefficient, and the total leaf area. The external transfer coefficient follows from evaporation data obtained with blotter paper, cut in either rectangular or leaf shape. During steady-state experiments the calculated values were 25 percent too high, but reflected accurately the twofold difference in transpiration at 3800 ft-c versus that at 87 ft-c. During cyclic behavior the calculated values faithfully portrayed the variations

in the measured transpiration, but were still 25 percent too high. Improvements in technique promise to increase the accuracy of the calculation. The work will be extended to other species.

Leaf diffusion resistance measurements on cotton in the field showed a pronounced diurnal change in response to light and a less well-defined rise in R_ℓ as soil moisture was depleted. Cotton stomates were apparently closed in the dark (maximum R_ℓ 0.8 min cm^{-1}) and fully open when the light intensity exceeded about 5000 ft-c (R_ℓ below 0.01 min cm^{-1}) in recently irrigated soil. At low light intensities R_ℓ for the upper epidermis was higher than for the lower one. Soil-moisture depletion eventually caused R_ℓ to rise to about 0.05 min cm^{-1} in the light, this rise coinciding with a fall in transpiration below the potential rate. However, this did not occur until far into the drying period. Thus, cotton stomates seem not very sensitive to leaf dehydration under field conditions. Leaf resistance measurements made along with beta ray gauging showed no rise in resistance as the leaf water content decreased in the middle of the day. The subsequent recovery in leaf hydration thus could not be attributed to significantly lessened transpiration due to stomatal closure. Studies under controlled conditions are planned to clarify the effect of declining soil moisture on the reactions of the cotton plant.

PERSONNEL: W. Ehrler, C. H. M. van Bavel, F. S. Nakayama.

TITLE: QUANTITATIVE MEASUREMENT OF WATER FLOW WITH CHEMICAL TRACERS

LINE PROJECT: SWC 4-gG5 CODE NO.: Ariz.-WCL-30

INTRODUCTION:

Field equipment and techniques for quantitative measurements of dilute fluorescent tracer concentrations have been previously developed so that concentrations in the range 10 to 100 parts per billion can be measured with less than 1 percent error (see Annual Reports for 1962 and 1963). Equipment and techniques developed for measuring the flow rates with fluorescent dyes were tested on two different Salt River Project canals during March 1963. The system and methods worked very well under actual field conditions. Accurate measurements of dye concentrations of 16 to 26 parts per billion in the canal water samples were made without difficulty. Problems were encountered in verifying the tracer flow measurements with other concurrent flow measurements. In general the other flow measurements were made under conditions of questionable reliability.

Adequate lateral mixing of dye with the canal flow did not occur in a straight reach of about 1 mile, in one of the canals which had a mean velocity of approximately 1.3 feet per second. However, a similar distance of 1.2 miles in the second canal, with a mean velocity of 2.5 feet per second, was adequate. The second canal contained more curves and was visibly more turbulent than the first canal. The adequacy of mixing could be verified from paired samples, one taken near the bank, and one taken near the center line of the canal, and could also be observed visually. Verification of the tracer measurement accuracy still remains a problem under study, because absolute discharges on large canals are difficult to obtain by other methods. In the spring of 1964 a laboratory flume study was initiated to determine the accuracy of the entire system as developed.

PROCEDURE:

A laboratory study was designed to model typical field conditions encountered with the tracer measurement technique to check the accuracy and precision of tracer-determined discharge measurements. The flow rate in the laboratory could, of course, be more accurately

controlled and more accurately measured. The scale of measurement was much smaller than that usually encountered in field measurements. This should not be a problem since the method, from all evidence and analysis, is not scale sensitive. Two similar laboratory set-ups were eventually used in the study. A straight, rectangular flume, one foot wide and 36 feet long, was the basic test channel. Flow was supplied directly from a centrifugal pump to a head box and stilling basin of about 6 cubic feet fitted with a sluice gate. The flow was measured with a 3-inch elbow meter that had been volumetrically calibrated. Maximum flow was about 0.75 cfs. Later a gravimetric flow measuring system was installed in the laboratory. New space limitations reduced the channel length by 8 feet, but the maximum pumping capacity through the channel was subsequently increased to about 1 cfs, and the accuracy of checking the actual rate of flow improved to better than $\pm$ 0.5 percent. The flow measuring procedure included placing sampling pumps in the stream cross section at a distance down stream from the tracer drop position to assure adequate lateral mixing. This lateral mixing is difficult to achieve or to predict accurately. In the field, more than one sample pump was used for this reason. By placing one pump near each bank, and one or two near the center of the stream, the adequacy of mixing could be verified by the degree of agreement between the two pumps.

Four sampling pumps were used in the laboratory studies. With four sample pumps located in the cross section, a flow measurement with accuracies acceptable to most applications can be obtained even if adequate mixing has not occurred. For convenience and improved time accuracy, a noncontaminating switching valve was fashioned to switch the flow from the pumps into the sample containers, or to waste. It was simply two clamping bars, operating alternately to "gang-clamp" all the tygon sampling tubes attached to one leg of "Tee" connections and simultaneously release those attached to the other leg. Thus the samples could be quickly started or stopped to facilitate accurate time measurement.

In the laboratory channel, the four sampling pumps could not be placed in the same cross section because of their size. Instead,

they were randomly scattered in the last 6 to 8 feet of the channel. Three ranges of discharges were chosen and three tracer drops made for each range. The absolute discharge for each tracer drop of each of the three series could not be exactly repeated because of power fluctuations to the supply pump. One of the sampling pumps, usually the one with the shortest length of tygon plastic tubing and, thus, the maximum pumping capacity under field conditions or, in the case of the laboratory set-up, the farthest upstream pump, was directed through the fluorometer for detecting the start and end of the tracer wave.

Sufficient water from the flowing channel was collected to construct the calibration standards. The fluorescent tracer, 50 ml taken from an initial 8 liter supply that was diluted to 2 g per liter of Pontacyl Pink B, was first introduced into the channel near the upstream end. Visual observation of the poor lateral mixing was confirmed by the wide variation in the discharge calculated from the four samples. It became quickly apparent that the physical limitations on the length of the laboratory channel prevented direct modeling of the flow conditions in the field. In order to test the precision and accuracy of the equipment, artificial lateral mixing would have to be induced to replace the loss of sufficient channel length. The tracer was then introduced into the channel head box with some, but not sufficient, improvement. Finally, injection was made on the suction side of the pump. The tracer passed through the pump rotor, then through about 25 feet of 3-inch pipe with five elbows, and finally through a diffuser outlet into the head box. Table 1, tests 1-7, lists the pertinent information about these tests. The improved mixing resulted in discharge determinations which differed from the true discharge as determined from the elbow meter by a maximum of 1.8 percent. The maximum standard deviation calculated on the basis of four sampling pumps in each test was $\pm$ 2 percent. Tests 8 and 10 illustrate the magnitude of error that can occur if the sampling time is reduced so that the end part of the sampling wave is lost. Some of the apparent error in discharge (maximum 1.8 percent, Table 1,

column 10) between the tracer determined discharge and the elbow meter discharge is undoubtedly due to fluctuations in the readout of the elbow flow meter. The standard deviations (column 7) indicate that barely adequate mixing has been achieved.

After the laboratory gravimetric flow measuring equipment was installed, the channel was supplied with the same pump, but with only about 15 feet of 6-inch pipe, instead of 25 feet of 3-inch pipe. The dye was injected as before through the pump rotor, but this time it was visibly evident that mixing was not adequate. This was confirmed by the high differences between the four collected samples. Finally, inducing a strong hydraulic jump with the sluice gate on the head box, and then running the flow through a slatted baffle produced good visual lateral mixing and satisfactory discharge measurements. Table 2 lists the pertinent data. The standard deviation was reduced to a maximum of 1.4 percent on run 1, and the discharge computed from the four samples agreed within 1.4 percent of the actual discharge (determined gravimetrically to better than $\pm$ 0.5 percent). As can be noted in Table 2, runs 3 and 4 agree with the weight discharge to three significant figures.

Before the tracer was introduced into the channel, the sampling system was flushed for a short time with water obtained from the channel. The dilution water that would be used later for constructing the standards was then collected. In general, about 150 pounds of water was needed for each set of standards constructed, regardless of stream size. A measured quantity of the tracer was then introduced into the stream as described. In the laboratory procedure the tracer was introduced through the supply pump rotor. The approximate quantity needed can be estimated from the relation

$$S = Q \bar{c} \Delta t$$

where S is the sample size, $\bar{c}$ is the average concentration in the integrated sample, and Δt is the sampling interval which must be equal to, or greater than, the tracer-wave time of passage. Greater time lengths than necessary do not change the value of Q, the stream

discharge, but do lower the value of $\bar{c}$, and thus the detection accuracy may be slightly reduced. For example, assume a desirable value of $\bar{c}$ to be 10 to 20 parts per billion and a Q, in the stream to be measured, estimated to be near 1000 cfs. An estimate of Δt can be obtained from rough time of travel estimates for the wave front to reach the drop station. A fraction of this, say one-half, can be used as a conservative estimate of the passage time for the entire wave. Thus, in a 10,000 foot reach of channel, with mean velocity of 5 fps, Δt can be estimated to be about 1000 seconds. Therefore,

$$S = \left(\frac{1000\ ft^3}{sec} \times \frac{62.4\ lbs}{ft^3} \times \frac{20\ parts}{10^9\ parts}\right) \times 1000\ sec = 1.25\ lbs\ of\ tracer$$

This estimate will usually keep the tracer concentration, $\bar{c}$, within acceptable measurement limits. It is desirable to keep the readout dial on the fluorometer, which is marked into 100 divisions, in the range of 50 to 100 for optimum accuracy. Neutral density filters and a range of exciting light intensities allow considerable latitude in obtaining this reading range. Of course, all filters and light intensities used on the sample, must likewise be used with the standards to eliminate transfer errors between filter and light intensity ranges. As previously described, one of the sampling pumps, usually a center pump in the open channel of field measurements or the farthest upstream pump in the laboratory measurements, was connected through the fluorometer. When the instrument first sensed the arrival of the tracer wave front, the time interval was begun and the pump switched from waste into the sample containers. The samples were continuously collected until the fluorometer indicated the end of the tracer wave. Sampling was continued for about 10 to 20 percent more time to insure that the very dilute end of the wave was sampled. The sampling valve was then switched to waste and the sampling time recorded. Each of the samples was then thoroughly stirred and circulated with a small tubing pump through the continuous flow cuvette of the fluorometer. Enough of each sample was usually available to allow the sample to be discharged to waste, and thus avoid sample-to-sample contamination,

and the possibility of diluting the sample with water trapped in the cuvette circuit. The fluorescence readings and the sample temperature were recorded for each sample. If the temperatures of the samples and the constructed standards were different, then a temperature correction was applied, since a 1 degree Centigrade change in temperature can make 2 to 3 percent change in fluorescence readings. Usually the temperatures can be kept within a degree or two so that a typical temperature correction curve made with distilled water (see Figure 1) as the dilutent can be used with negligible error. Differences in temperature of 5 degrees Centigrade or more should be corrected with a temperature response curve, constructed with the background water of the particular stream.

The comparison standards were constructed for a range of fluorescence readings covering those of the samples. Since the fluorometer responds very linearly for concentrations below 100 parts per billion of Pontacyl Pink B, only 3 points were needed to establish and check the fluorescence response curve. For the 1 percent accuracy range, it is desirable practice to develop the least squares linear regression equation using five or more points.

Two dilutions were used to obtain the few parts per billion range needed. For example, the first dilution using part of the same mother solution that was used in the test injection might be designed to produce a first dilution of 1 g of dry powdered Pontacyl Pink B per liter of solution. The second dilution to achieve 4 parts per billion could then be obtained with 0.250 ml of the first dilution mixed in 62,500 ml of water (approximately 137 lbs of water). The fluorescence reading for this could be recorded and another 0.250 ml of the first dilution added to obtain the 8 parts per billion reading, etc. In this procedure, the standard must be recirculated through the fluorometer and back into the container. Small amounts of distilled water used to wash the cuvette before starting the construction of the standard caused negligible error because of the relatively large volume of the standard involved at this stage.

The corrections that were made for reduction of fluorescence with increasing temperature were based on measurements made on the

Pontacyl Pink B using distilled water as a dilutent and 16, 32, and 48 parts per billion tracer concentration. This plotted as a straight line on semi-logarithmic paper and had the equational form

$$F = F_o e^{nt}$$

where F is the fluorescence of the sample at temperature t degrees C, F_o is the fluorescence at the reference temperature, and n is the temperature coefficient having units of C^{-1}. The resulting temperature coefficient ($-0.024\ C^{-1}$) is somewhat less than that given in the literature ($-0.029\ C^{-1}$) for Pontacyl Pink B. The calculated values for n varied from -0.0234 to -0.0248 for the three concentrations. The trend was not consistent and is not considered significant. Figure 1 shows a temperature correction curve for Pontacyl Pink B, based on the relation

$$F_r = F_s e^{n(t_r - t_s)}$$

where subscripts r and s refer to the reference temperature and the sample temperature, respectively. The temperature coefficient is sufficiently large to require correction for temperature differences as small as 0.5 C if an accuracy in determining the tracer concentrations is to be within 1 percent.

DISCUSSION AND RESULTS:

From the laboratory measurements it was concluded that accurate stream flow measurements could be obtained if the effects of tracer losses through absorption on the banks and stream bottoms, etc., and inadequate lateral mixing were reduced to negligible amounts. Although the effects of absorption and adsorption on suspended particles is compensated by constructing the standards from the stream water, the tracer lost to the boundaries cannot be readily evaluated. If there is much suspended matter, the total surface area of the suspended material is very large compared to the surface area of the stream boundaries. Since the process of constructing the standards compensates for this suspended material, the adsorption and absorption loss is reduced essentially to that lost to the stream boundaries. No loss was detectable in the laboratory discharge measurements for any of

the tracers studied, Pontacyl Pink B and Rhodamine B. As mentioned before, the loss of tracer on soil columns for Pontacyl Pink B was about 1/10 that of Rhodamine B and is expected to be negligible in natural channels. Another tracer, Rhodamine WT, also from the DuPont Chemicals Company, is under investigation. It appears to be much less absorbed on sand than even the Pontacyl Pink B, while its other characteristics are similar to those of the Rhodamine B, including the lower cost.

Only limited data is available to indicate the magnitude of the problem of absorption on channel boundaries. Table 3 indicates the pertinent data for four measurements made on the South Canal in 1963. Three of these measurements were made using a drop station of 1.2 miles above the sampling station, and the fourth used a drop station of 2.9 miles. If dye were being significantly absorbed on the stream boundaries, the longer travel length of the last run should indicate a dye loss and, because of the structure of the equation, would cause an increase in the average discharge for the channel. As can be seen in Table 3, the last run agrees within 1 percent of at least two of the other three runs. If absorption were present, it was on the order of 1 percent or less for the difference in reach between the 1.2 mile and 2.9 mile stations. This is, then, approximately one-third percent loss per mile. Of course, this is only one measurement and will require further verification since this difference could be caused by seepage losses between the upstream station and the downstream station or by lack of adequate mixing.

The problem of inadequate lateral mixing deserves some review. In open channels the thread of maximum velocity usually occurs near the center of the channel and is somewhat depressed depending on the strength of the secondary currents which, in turn, appear to be a function of the channel geometry and channel roughness. If it were possible to insert a vertical sheet of uniform dye mixture into the stream cross section that extended from bank to bank and top to bottom, it would at first appear that uniform lateral mixing were guaranteed. In effect, it acts as if it were laterally mixed, but this is not necessarily the actual behavior.

Consider the situation with no dispersion. The sheet would quickly cease to be a plane surface and would become a type of paraboloid becoming more and more extended as it progressed downstream. Under these assumptions the sheet would retain its original thickness as measured parallel with the flow direction. Sampling at several points on the down stream cross section would account for the same quantity of dye passing each point, but those samples near the banks would encounter a time lag.

Now assuming, in addition, only longitudinal dispersion, the sheet would now simply take a longer time to completely pass the sampling station. The sheet would no longer have a sharply defined front and sharply defined tail. The wave at a given cross section would arrive first near the center of the channel, but it would also pass first, resulting in the same total quantity of dye being collected from the center as from near the banks, the only difference being a simple time lag. There would be a pronounced lateral gradient of the tracer near the front and near the tail of the wave at a given cross section. Finally, consider the usual case with lateral and vertical dispersion, the longitudinal sheet of dye would behave similarly to that described for one-dimensional dispersion, but the lateral and vertical dispersion would tend to decrease the concentration gradients in the transverse direction. There would always be a transverse gradient near the front of the tracer wave which ideally is exactly compensated by the reverse situation at the tail of the tracer wave. As the wave progresses downstream, it becomes increasingly dispersed. At some station at distance x, the rate of change of the tracer concentration passing the sampling station becomes so small that the corresponding lateral gradient, assumed to be similar, results in negligible instantaneous differences between the center line tracer concentration and that at a point near the stream banks.

It is this behavior of the dispersed tracer wave that allowed the tracer to be injected at a point, over an arbitrary period of time instead of instantaneously. It also eliminated the requirement of uniform injection as a transverse sheet. Thus, it was only necessary

that distance x be chosen large enough. The use of several sampling pumps in the cross section serve to clarify this particular situation. If the samples at the center line and the bank agreed, adequate lateral mixing was achieved.

While measurements on the samples collected can now be made without difficulty, two problems connected with the use of the method in the field still remain to be verified. Currently under study are methods to determine the magnitude of channel absorption on various dyes, primarily Rhodamine B, Pontacyl Pink B, and the most recently obtained dye, Rhodamine WT. Means of obtaining an absolute discharge comparison on a large channel in the field is still being investigated.

SUMMARY AND CONCLUSIONS:

Equipment and techniques have been developed to quantitatively detect dilute fluorescent tracer concentrations of 10 to 100 parts per billion with less than 1 percent error in natural stream waters. This permits stream gauging with a potential accuracy of this same order by special application of chemical dilution techniques. A carefully measured quantity of fluorescent tracer is dumped into the stream to be gauged. A sample is continuously collected at a uniform rate as this tracer wave passes a downstream station. The station must be located at a distance from the drop station great enough to permit adequate lateral mixing of the tracer with the stream waters. A single analysis of the tracer concentration in the continuously collected sample permits the stream flow to be calculated from

$$Q = \frac{S}{\bar{c}\Delta t}$$

where Q is the discharge, S is the quantity of tracer used, $\bar{c}$ is the concentration of the sample collected continuously for time Δt.

Limited field data were collected in 1963. Field-scale comparisons are difficult because few field methods are capable of the potential accuracy of $\pm$ 1 percent.

Laboratory studies were designed to model typical field conditions to carefully evaluate the accuracy and precision of tracer determined discharges. Tracer determined discharges compared within 1.4 percent

with gravimetrically determined discharges which were accurate to ± 0.5 percent. Adequate lateral mixing was achieved in the laboratory channel, which was 1 foot wide and 30 feet long, with a series of baffles. A distance equal to at least 100 stream top widths appears to be necessary in natural streams for adequate lateral mixing. This depends on the number of curves and other mixing devices located in the reach to be gauged.

The laboratory studies showed that stream discharge measurements, accurate to ± 1 or 2 percent, can be obtained if the effects of lateral mixing and tracer losses to the channel boundaries are reduced to negligible amounts. The quantitative detection equipment and techniques have been improved to the point that the accuracy limitations on discharge measurements are those imposed by these effects.

Reliable criteria for guaranteeing adequate lateral mixing are under study. Additional samples collected at various locations in the stream cross section indicate by their agreement if adequate lateral mixing were accomplished, but this is "after the fact" and deserves improvement. Limited field data indicate that the effects of tracer losses to stream boundaries are negligible for Rhodamine B, the dye expected to be most sensitive to absorption losses. Loss effects of Pontacyl Pink B and Rhodamine WT remain to be verified.

PERSONNEL: J. A. Replogle, K. J. Brust, and L. E. Myers

Table 1. Laboratory discharge measurements using Pontacyl Pink B as the tracer with a calibrated elbow flow meter discharge comparison.

Series	y 1/	$\bar{V}$ 2/	$\mathbb{R}_R$ 3/	S 4/	Δt 5/	$\bar{c}$ 6/	σ_c 7/	Q_T 8/	Q_E 9/	ΔQ 10/
	ft	ft/sec		gm	min	μg/L	%	cfs	cfs	%
1	0.83	0.49	140,000	0.100	3.500	40.9	± 0.3	0.411	0.407	+ 0.9
2	0.83	0.49	140,000	0.100	5.000	29.4	± 1.7	0.401	0.408	- 1.7
3	0.83	0.49	140,000	0.100	3.500	40.9	± 1.2	0.411	0.410	+ 0.2
4	0.83	0.49	140,000	0.100	3.500	41.0	± 1.2	0.410	0.410	0
5	0.89	0.74	220,000	0.100	3.000	29.4	± 0.6	0.666	0.655	+ 1.8
6	0.89	0.77	230,000	0.100	3.000	28.3	± 2.0	0.693	0.685	+ 1.2
7	0.89	0.76	225,000	0.100	3.000	29.6	± 1.9	0.665	0.673	- 1.1
8*	1.07	0.70	210,000	0.100	2.000	37.2	± 0.6	0.792	0.747	+ 6.0
9*	1.07	0.70	210,000	0.100	2.000	38.1	± 0.9	0.772	0.748	+ 3.1
10*	1.07	0.70	210,000	0.100	2.000	37.7	± 1.2	0.780	0.747	+ 4.3

1/ Flow depth in laboratory channel near sampling stations.
2/ Average velocity in flume near sampling stations.
3/ Reynolds number based on hydraulic radius = $\frac{VR}{\nu}$
4/ Amount of dry weight tracer used.
5/ Sampling time length.
6/ Average tracer concentration derived from four collected samples, μg/L ≈ ppb.
7/ Standard deviation computed for four samples from each series.
8/ Discharge determined from tracer samples ($Q_T = 58.85 \frac{S}{\bar{c}\Delta t}$), 58.85 is conversion factor for units as given.
9/ Discharge determined with elbow flow meter.
10/ $100(Q_T - Q_E)/Q_E$.
* Sampling time too short, part of sample lost.

Table 2. Laboratory discharge measurements using Pontacyl Pink B as the tracer with weighed discharge comparisons.

Series	y 1/	$\bar{V}$ 2/	$\mathbb{R}_R$ 3/	S 4/	Δt 5/	$\bar{c}$ 6/	σ_c 7/	Q_T 8/	Q_W 9/	ΔQ 10/
	ft	ft/sec		gm	min	μg/L	%	cfs	cfs	%
1	0.84	1.16	305,000	0.100	3.00	20.37	± 1.4	0.963	0.974	- 1.1
2	0.84	1.16	305,000	0.100	3.00	20.37	± 0.5	0.963	0.977	- 1.4
3	0.67	0.68	162,000	0.100	3.00	43.11	± 0.6	0.455	0.455	0.0
4	0.67	0.68	162,000	0.100	3.00	43.35	± 0.4	0.453	0.453	0.0

1/ Flow depth in laboratory channel near sampling stations.
2/ Average velocity in flume near sampling stations.
3/ Reynolds number based on hydraulic radius = $\frac{VR}{\nu}$.
4/ Amount of dry weight tracer used.
5/ Sampling time length.
6/ Average concentration derived from four collected samples; μg/L ≈ ppb.
7/ Standard deviation computed for four samples from each series.
8/ Discharge determined from tracer samples, $Q_T = 58.85 \frac{S}{\bar{c}\Delta t}$, 58.85 is conversion factor for units as given.
9/ Discharge determined gravimetrically by weight-time relation.
10/ $100(Q_T - Q_W)/Q_W$.

Table 3. Field discharge measurements with Rhodamine B.

Canal	Drop No.	Mixing length	Tracer added	Integrated sample 1/	Sampling time	Travel time Front	Travel time Peak	Calculated discharge
		miles	grams	ppb	min	min	min	cfs
Ariz.	1	1.0	940.8	24.8 26.4	35.00	33.0	39.0	630 599
South	2	1.2	470.4	15.9 15.7	17.07	18.0	22.0	1020 1033
South	3	1.2	470.4	15.8 15.8	17.15	19.0	22.5	1022 1022
South	4	1.2	470.4	16.0 16.3	17.30	19.5	23.5	1001 982
South	5	2.9	1411.2	26.4 26.1	30.65	62.5	65.0	1026 1038

1/ First value is from canal center and the second 5 feet from canal bank.

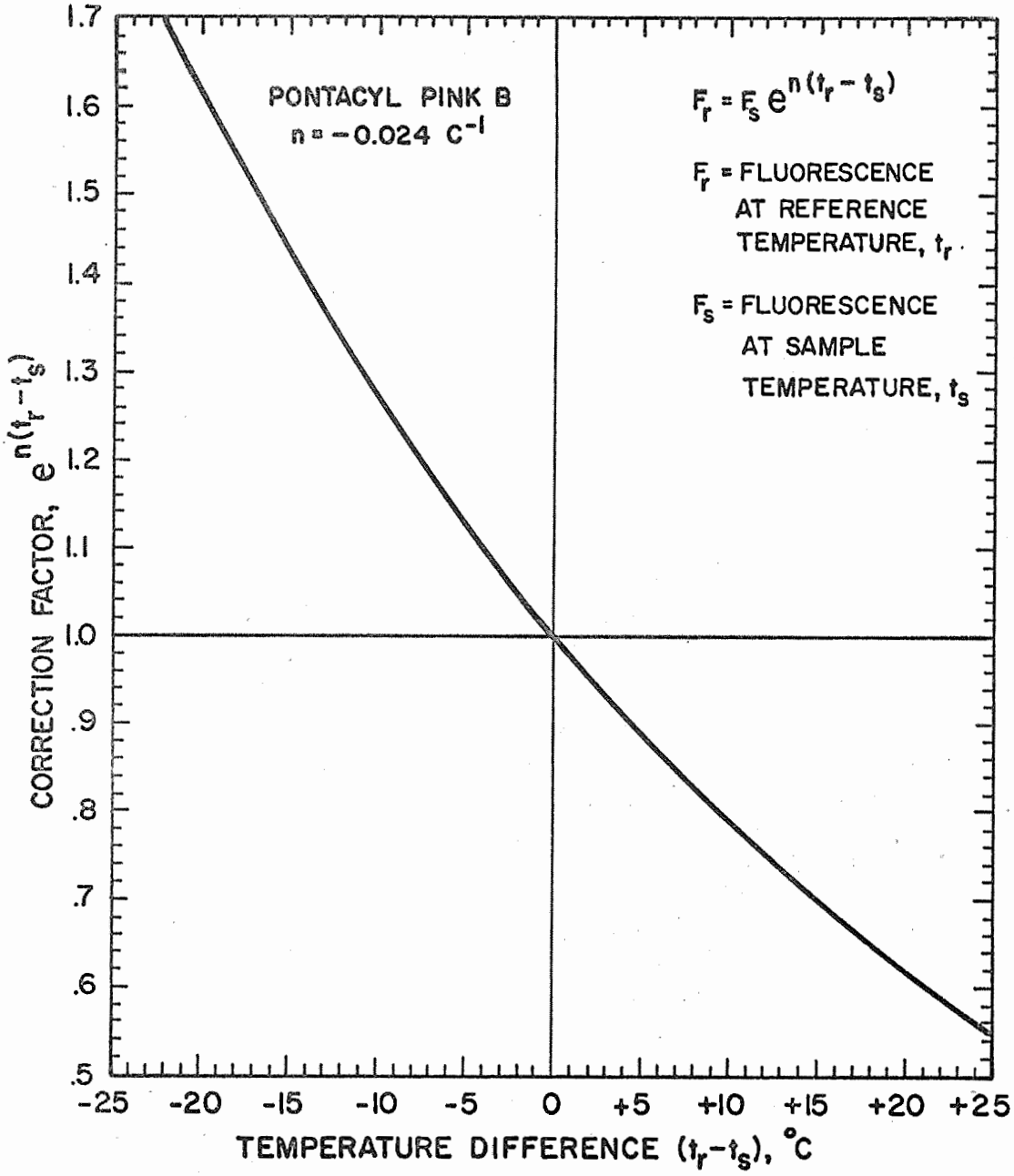

Figure 1. Temperature correction curve for Pontacyl Pink B.

TITLE: WATER VAPOR DIFFUSION IN SOILS

LINE PROJECT: SWC 4-gG4 CODE NO.: Ariz.-WCL-31

The objectives and need for study for this project were reported in the 1963 Annual Report of the U. S. Water Conservation Laboratory. In that report results were presented for transient and steady-state measurements of water vapor diffusion in relatively dry soil. These results have been published.

This report is in two parts. Part I covers further work on vapor diffusion, specifically the temperature and pressure effects on sorption diffusion coefficients and the separation of the total diffusion coefficients into liquid and vapor components. Part II covers work done while the project leader was an O.E.C. D. Fellow at the Rothamsted Experimental Station, Harpenden, England June-August 1964. This part concerns water movement in both liquid and vapor phases under a temperature gradient.

PART I. TEMPERATURE AND PRESSURE EFFECTS ON WATER VAPOR DIFFUSION COEFFICIENTS.

INTRODUCTION:

Water transfer in relatively dry soil occurs by vapor diffusion through the air-filled pores and by movement through thin water films or, at very low water contents, along the surfaces of the soil particles. This "non-vapor" movement has been called surface diffusion, film diffusion, and liquid diffusion. In this discussion the term "liquid diffusion" will be used to denote all forms of "non-vapor" flow. The vapor and liquid phases are coupled by evaporation and condensation processes which essentially control vapor diffusion and may exert some influence on liquid diffusion. By assuming that liquid diffusion is affected only slightly by the evaporation-condensation reaction, we can consider the two transfer mechanisms as occurring in parallel. The expression relating the total to the liquid and vapor diffusion coefficients is

$$D_{\theta v} = D_{\theta} + D_{v}\, \partial\rho/\partial\theta \qquad [1]$$

where $D_{\theta v}$ is the total diffusion coefficient, D_θ the liquid (or non-vapor) diffusion coefficient, D_v the diffusion coefficient for water vapor in air modified by the tortuosity and porosity, ρ the vapor density, and θ the water content.

At the pressures used here, water can be considered incompressible whether in thin films or as water molecules adsorbed on particle surfaces. Assuming, as we did in the development of equation [1], that liquid diffusion is affected only slightly by the evaporation-condensation reaction, we can take the liquid diffusion coefficient as independent of pressure. The pressure dependence of the vapor diffusion coefficient can be evaluated by expanding the right-hand term in [1], i. e.

$$D_v \frac{\partial \rho}{\partial \theta} = \beta D_a \rho_o \frac{\partial(\rho/\rho_o)}{\partial \theta} \qquad [2]$$

where β is a geometry factor which includes the porosity and tortuosity, D_a is the water vapor diffusion coefficient in air, and ρ_o is the saturated vapor density. Of the terms on the right-hand side of [2], only D_a depends upon pressure. D_a is proportional to $P_o/(P - P_v)$, where P_o is a reference pressure, P the ambient pressure, and P_v the partial pressure of water vapor. When $P \gg P_v$, P_v can be neglected. Therefore, the total diffusion coefficient $D_{\theta v}$ decreases as the ambient pressure increases. We can now write

$$D_{\theta v} = D_\theta + D_{vap} P_o/P \quad , \qquad [3]$$

where, for brevity and convenience, D_{vap} has been written $D_v \, \partial\rho/\partial\theta$. The liquid and vapor diffusion coefficients D_θ and D_{vap} can be evaluated by measuring the total diffusion coefficient $D_{\theta v}$ at several pressures at a constant temperature. Plotting $D_{\theta v}$ versus P_o/P should yield a straight line with a slope of D_{vap} and an intercept of D_θ.

Both D_θ and D_{vap} are temperature dependent. An estimate of the temperature dependence can be obtained by employing the concept of an activation energy for diffusion, as defined by the equation

$$D = D^{o} \exp[-E(1/T - 1/T_{o})/R] \ , \qquad [4]$$

where D^{o} is a diffusion coefficient at the reference temperature T_{o}, T is the absolute temperature, E is an activation energy, and R is the ideal gas constant. The term "activation energy" is used here as an index of the temperature dependence of diffusion coefficients and does not necessarily have other connotations frequently associated with the term.

By defining E_{θ} as the activation energy for liquid (or "non-vapor") diffusion and E_{v} as the activation energy for vapor diffusion and using [3], we can write

$$D_{\theta v} = D^{o}_{\theta} \exp[-E_{\theta}(\frac{1}{T} - \frac{1}{T_{o}})/R] + D^{o}_{vap} (\frac{P_{o}}{P}) \exp[-E_{v}(\frac{1}{T} - \frac{1}{T_{o}})/R] \qquad [5]$$

to describe the temperature and pressure dependence of the total diffusion coefficient for water in relatively dry soil. The superscript ^{o} now signifies the value of the diffusion coefficients at the reference temperature T_{o} and pressure P_{o}.

A value for E_{v}, the activation energy for vapor diffusion, can be calculated from the temperature dependence of the terms in equation [2]. The geometry factor β does not change with temperature and, in the first approximation, the relative vapor pressure (ρ/ρ_{o}) can be taken independent of temperature. Values of the remaining factors D_{a} and ρ_{o}, at several temperatures, are tabulated in the literature. An activation energy of 11 kcal mole^{-1} was calculated from a linear plot of $\ln(D_{a}\rho_{o})$ versus 1/T.

The saturated vapor density ρ_{o} refers to water vapor over pure liquid water. The water contents of interest here varies from essentially zero to those corresponding to about 0.95 relative vapor pressure. Studies on the adsorption of water vapor by soils (3, 5) indicate that about 1.5 kcal mole^{-1} more energy is required to evaporate a water molecule from a particle surface than from a free water surface. We will assume, <u>a priori</u>, that the activation energy E_{v} is increased by approximately 1.5 kcal mole^{-1} at water contents

below a monomolecular layer, and take E_v to be 12.5 kcal mole^{-1} at zero water content, decreasing to 11 kcal mole^{-1} at a monolayer, and remaining at 11 at the higher water contents.

The activation energy for liquid diffusion E_θ in relatively dry soil is difficult to estimate because water in thin films around soil particles probably has a different structure than has pure water (4). Low (4) and Anderson et al. (1) have demonstrated that the activation energy for water flow near clay surfaces is higher than in bulk water, with values up to 6.1 kcal mole^{-1} reported. A lower limit may be set by considering the temperature dependence of flow at higher water contents. Jackson (2) has shown that the temperature dependence for transient viscous flow of bulk water in soil can be explained by the temperature dependence of the viscosity of water. An E value for this process is about 3.9 kcal mole^{-1}.

EXPERIMENTAL:

The soil materials used were Adelanto loam and Pachappa loam, taken from the same supply as used in experiments reported in the 1963 Annual Report. Some physical properties of these soil materials, the procedure for preparing columns and the details of the diffusion experiments are given in previous annual reports. The bulk densities were 1.42 and 1.38 g cm^{-3} for Adelanto and Pachappa, respectively.

The experimental procedure for the pressure experiments was slightly different from that of the experiments reported last year. For pressures above ambient, acrylic plastic columns containing soil were put into 2-inch-diameter steel cylinders which were capped at both ends. The cylinders were positioned vertically and water was placed at the bottom. The soil column was held several millimeters above the water surface. The cylinders were maintained at the desired constant pressure.

For pressures less than ambient, acrylic plastic cylinders were used. A water reservoir at the bottom supplied vapor for diffusion as in the above ambient pressure cylinders. The cylinders were connected to a vacuum source. The vacuum was controlled by a solenoid valve activated by a capacitance relay. Changes in the

height of a mercury column in an absolute manometer were detected by the capacitance relay, which caused the valve in the vacuum line to be opened or closed as needed. This system controlled the pressure to $\pm$ 2 mm Hg.

For the pressure experiments diffusion measurements were made at 1505, 1105, 508, 320, and 295 mm Hg total pressure. Both soil materials were used at the three higher pressures. Pachappa was used at 320 mm Hg and Adelanto was used at 295 mm Hg. All pressure experiments were conducted at 25 C. At the completion of pressure runs other than at atmospheric ambient pressures, air had to be introduced into or released from the column prior to sectioning and measuring the water content distribution. To ascertain the influence of this mass flow of air on the water content distribution, air was allowed to enter opposite ends of two columns otherwise treated in a similar manner. No detectable difference in water content distributions was observed.

The temperature experiments were carried out at 6.5, 21.0, 27.0, 35.5, and 42.5 C. Ambient temperature control within the diffusion apparatus was $\pm$ 0.4 C. Average ambient pressure was 730 mm Hg. Measurements of $D_{\theta v}$ were made on three columns at each pressure and each temperature. Data for the three columns were averaged.

RESULTS AND DISCUSSION:

Pressure Effects. Total diffusion coefficients measured at four pressures were used to calculate vapor and liquid diffusion coefficients. D^o_{vap} and D^o_{θ}, the slope and the intercept of the $D_{\theta v}$ — P_o/P plots, were calculated using regression analysis for water content intervals of 0.0025 over the range 0.0050 to 0.0475 gravimetric water content for Adelanto and intervals of 0.001 over the range 0.002 to 0.022 for Pachappa. Figures 1a and 1b show $D_{\theta v}$ versus P_o/P at four water contents for Adelanto and Pachappa, respectively. The relationship depicted here is typical for all water contents. The water contents shown in the figure were selected to indicate the range of slopes and intercepts and also to indicate how well the data fit equation [3].

Total, vapor, and liquid diffusion coefficients for Adelanto loam at 25 C and 730 mm Hg pressure are shown in Figure 2. The liquid diffusion coefficients are essentially constant at 0.60×10^{-5} cm^2 sec^{-1} from 0.0475 to 0.0200 gravimetric water content. Below 0.0200, D_θ decreases linearly toward zero. These values of D_θ indicate that water adsorbed on soil particles and in the first few molecular water layers is mobile. The values of D_θ reported here have, as a frame of reference, the entire porous medium. The value of D_θ probably depends upon the surface area available for diffusion. One can speculate that D_θ would be larger for clays than for sands because of the greater surface area of clays. On the other hand, D_{vap} should be larger for sands than for clays because, in general, the individual pores are larger in sands. The larger pores provide longer paths for vapor to travel before encountering particle surfaces. The ethylene glycol surface areas for Adelanto loam and Pachappa loam were 110 and 45 m^2 g^{-1}, respectively.

Figure 3 shows diffusion coefficients for Pachappa loam. The data points at the lower part of the graph indicate the calculated values of D_θ. The open circles were calculated using data for four pressures. Most of these values are negative - a physical impossibility. Examination of the $D_{\theta v}$ versus P_o/P plots (Figure 1b - Pachappa) indicated that values for P = 320 may have been high. Other information indicated some variability in the P = 320 data. Therefore, D_θ's were calculated using data for the three higher pressures. These values are shown as solid circles in Figure 3. These data are generally positive but still quite variable. We conclude that the values for D_θ for Pachappa are small in comparison to D_{vap} and not precisely measurable with the present technique. If the D_θ's are proportional to surface areas, then the D_θ's for Pachappa should be about 40 percent of those for Adelanto. We will, therefore, assume that D_θ's for Pachappa are negligible in comparison to D_{vap}, and that D^o_{vap} equals $D^o_{\theta v}$. Values of $D^o_{\theta v}$ are shown by the circles connected with the solid line in Figure 3. These data are averages of the data for four pressures reduced to P = 730 at 25 C.

Temperature Effects. As discussed in the introduction, the activation energy for vapor flow is about 12.5 kcal $mole^{-1}$ at zero water content, and decreases to about 11.0 kcal $mole^{-1}$ at a monolayer. The water content at which a monolayer is formed is open to question. Puri and Murari (6) present data which supports the view that a monolayer of water occurs when one layer of water exists between each pair of platelets and one layer is formed on the edges and external surfaces. The ethylene glycol method of measuring surface areas assumes that two layers of molecules exist between each pair of platelets and one layer on the external surfaces. Ethylene glycol surface areas for Adelanto and Pachappa, 110 and 45 m^2 g^{-1}, respectively, were used to estimate the water area by taking one-half the internal glycol area and adding the external glycol area. The resulting areas were 79 and 35 m^2 g^{-1} for Adelanto and Pachappa, respectively. Assuming the area of a water molecule to be 10.8 square angstroms, the water contents at which the first complete monolayer is formed are 0.0220 for Adelanto and 0.0097 for Pachappa. These values correspond very nearly to the water contents at which the maximum value of the diffusion coefficient occurs.

With the preceding monolayer information, values of the activation energy (E_v) for vapor diffusion in Adelanto loam were assumed as shown in Figure 4. These values of E_v, the values of D^o_θ and D^o_{vap} obtained from the pressure experiments (Figure 2), and the measured $D_{\theta v}$'s were used to obtain estimates of E_θ. Rearrangement of equation [5] allowed the calculation of E_θ by least squares from the data obtained at five temperatures. The results are represented by the circular symbols in Figure 4. The solid line was arbitrarily drawn to fit the calculated points. The broken lines are extrapolations.

These data indicate that the temperature dependence of water movement in thin films (water contents above a monolayer) is only slightly greater than the temperature dependence of bulk flow of water in soils. The approximate value of the activation energy for liquid diffusion above a monolayer is about 4.2 kcal $mole^{-1}$,

quite close to the value of 3.9 for viscous flow of bulk water. As the water content decreases to a monolayer and below, E_θ increases sharply. At a water monolayer, E_θ is about 6.7 kcal mole^{-1} and is almost twice as large (11 kcal mole^{-1}) at about one-half the total monolayer coverage.

Values of E_v and E_θ shown in Figure 4 and values of D_θ^o and D_{vap}^o shown in Figure 2 were used to predict $D_{\theta v}$'s at five temperatures for Adelanto loam. The predicted values are shown as lines in Figure 5. The circles are the measured data. The agreement between measured and calculated values is good.

Because D_θ^o for Pachappa was small and not measurable with this technique, values of E_θ could not be calculated. Data for $D_{\theta v} = D_{vap}^o$ from Figure 3 were used to calculate $D_{\theta v}$ at five temperatures, as shown in Figure 6. Values of E_v were assumed to be 12.5 kcal mole^{-1} at zero, decreasing linearly to 11.0 at $\theta = 0.010$ (water monolayer) and remaining at 11.0 for all water contents above 0.010. The predicted values are shown as solid lines and measured values as circles. The agreement between calculated and measured values indicates that the assumed values for the activation energy for vapor diffusion are reasonable.

At the higher temperatures the predicted values at the maximum ($\theta = 0.010$) are slightly higher than the measured. This is especially true for the 27 C data, which are taken from an earlier report. They were the first data taken in this series of experiments and are from two soil columns. All subsequent measurements have shown that the maximum occurs at $\theta = 0.010$, not $\theta = 0.009$ as indicated by the earlier data.

CONCLUSIONS:

Water transfer in relatively dry soils occurs in both liquid and vapor phases. The liquid and vapor components can be separated out by measuring the total diffusion coefficient at several different ambient pressures. The separation of liquid and vapor components is necessary to account for the temperature dependence of the total diffusion coefficient. In coarse-textured soils vapor diffusion with

the associated evaporation-condensation process is the predominant mechanism, while liquid diffusion is negligible. In fine-textured soils, or soils with large surface areas, diffusion in thin water films and along particle surfaces is appreciable. The total diffusion coefficients change 8- to 10-fold over the temperature interval of 36 C.

REFERENCES:

(1) Anderson, D. M., Linville, A., and Sposito, G.
1963. Temperature fluctuations at a wetting front: III. Apparent activation energies for water movement in the liquid and vapor phases. Soil Sci. Soc. Amer. Proc. 27: 610-613.

(2) Jackson, R. D.
1963. Temperature and soil-water diffusivity relations. Soil Sci. Soc. Amer. Proc. 27: 363-366.

(3) Kutelik, M.
1962. The influence of inorganic soil colloid surface on soil water properties. Joint Meeting Com. IV and V Trans., Internatl. Soc. Soil Sci. New Zealand. pp. 88-93.

(4) Low, P. F.
1959. Viscosity of water in clay systems. Clay & Clay Minerals 8: 170-182.

(5) Orchiston, H. D.
1953. Adsorption of water vapor: I. Soils at 25° C. Soil Sci. 76: 453-465.

(6) Puri, B. R., and Murari, K.
1963. Studies in surface area measurements of soils: 1. Comparison of different methods. Soil Sci. 96: 331-336.

PERSONNEL: R. D. Jackson

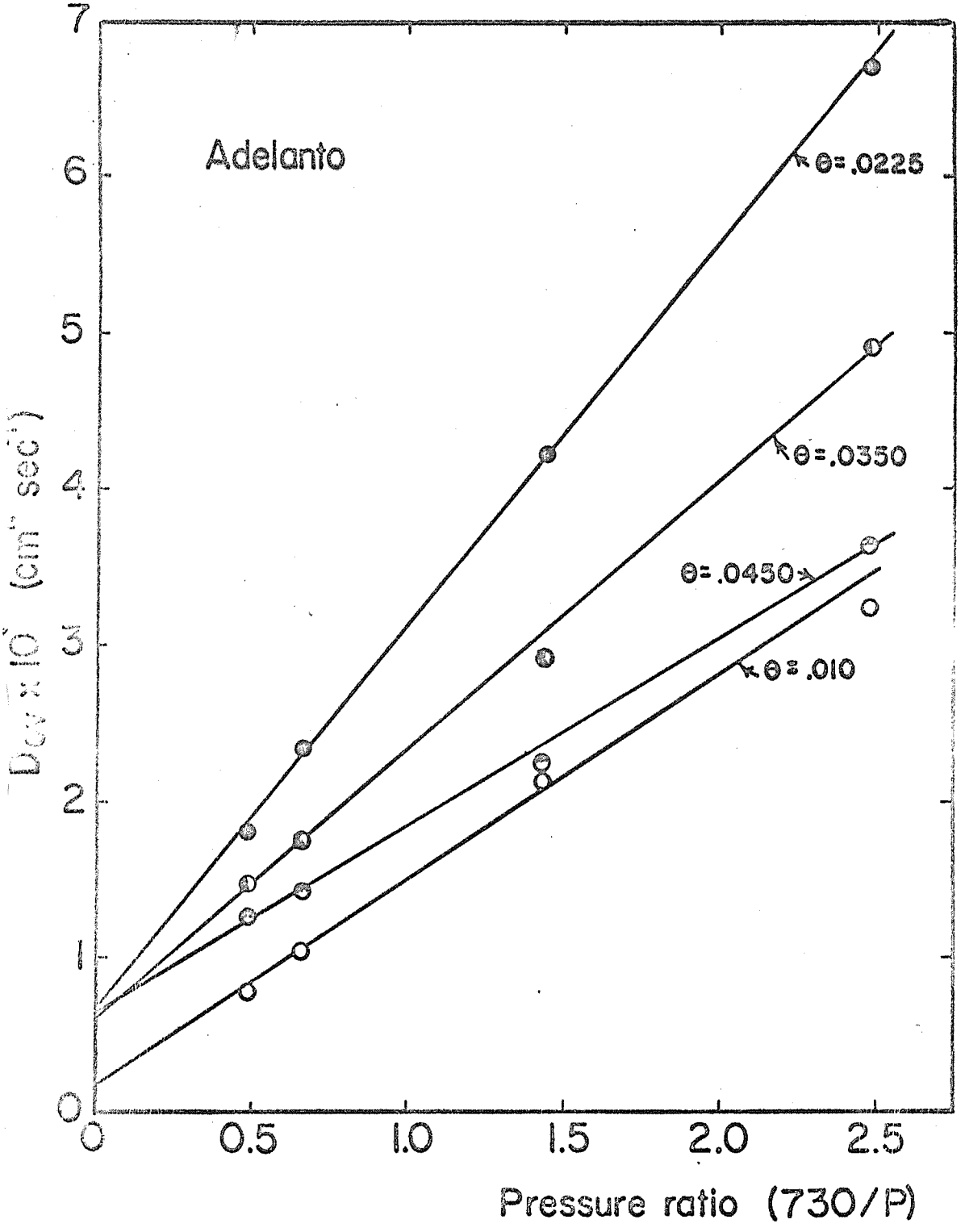

Figure 1a. Diffusion coefficients for water transfer as a function of the pressure ratio P_o/P at several water contents.

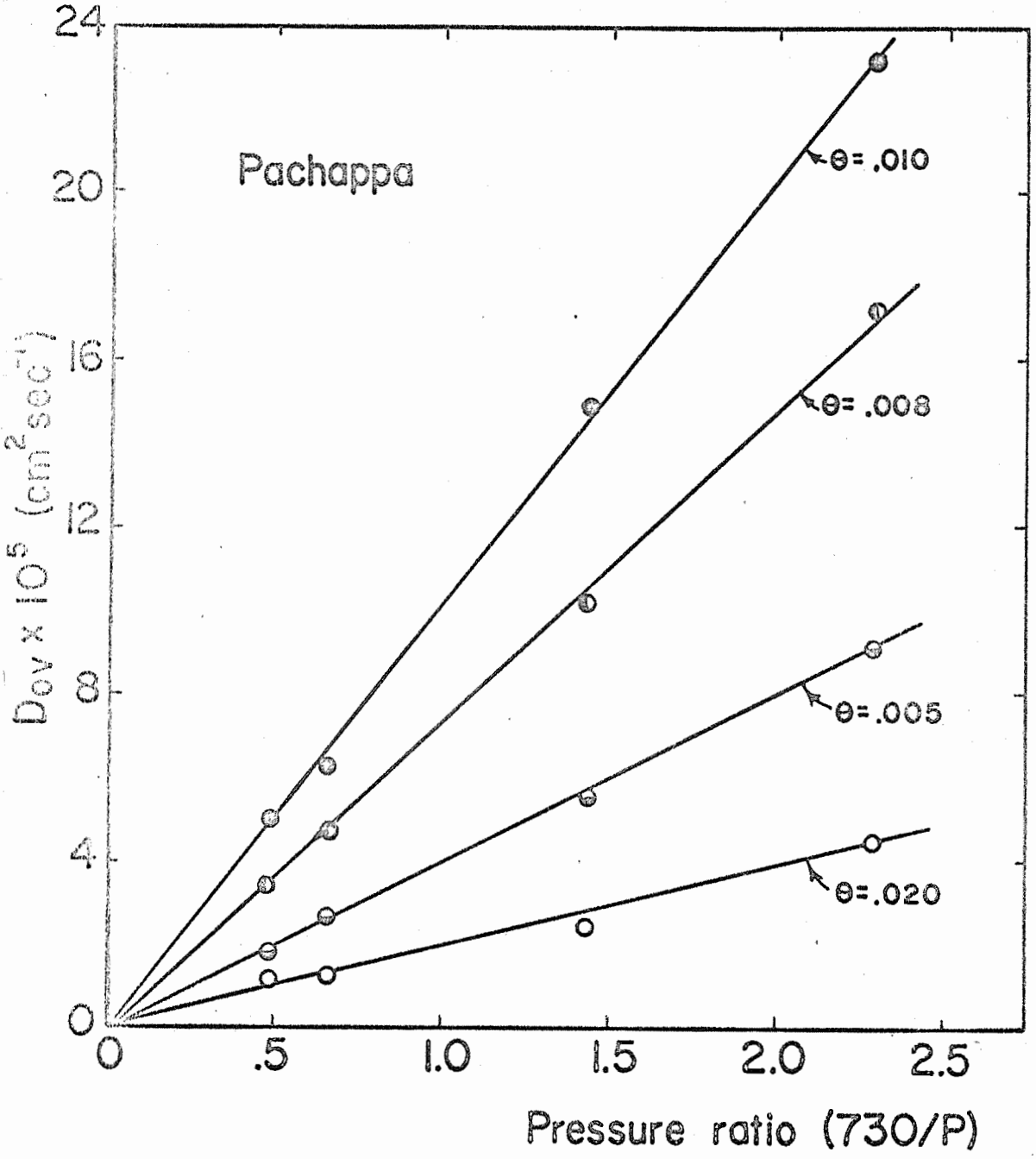

Figure 1b. Diffusion coefficients for water transfer as a function of the pressure ratio P_o/P at several water contents.

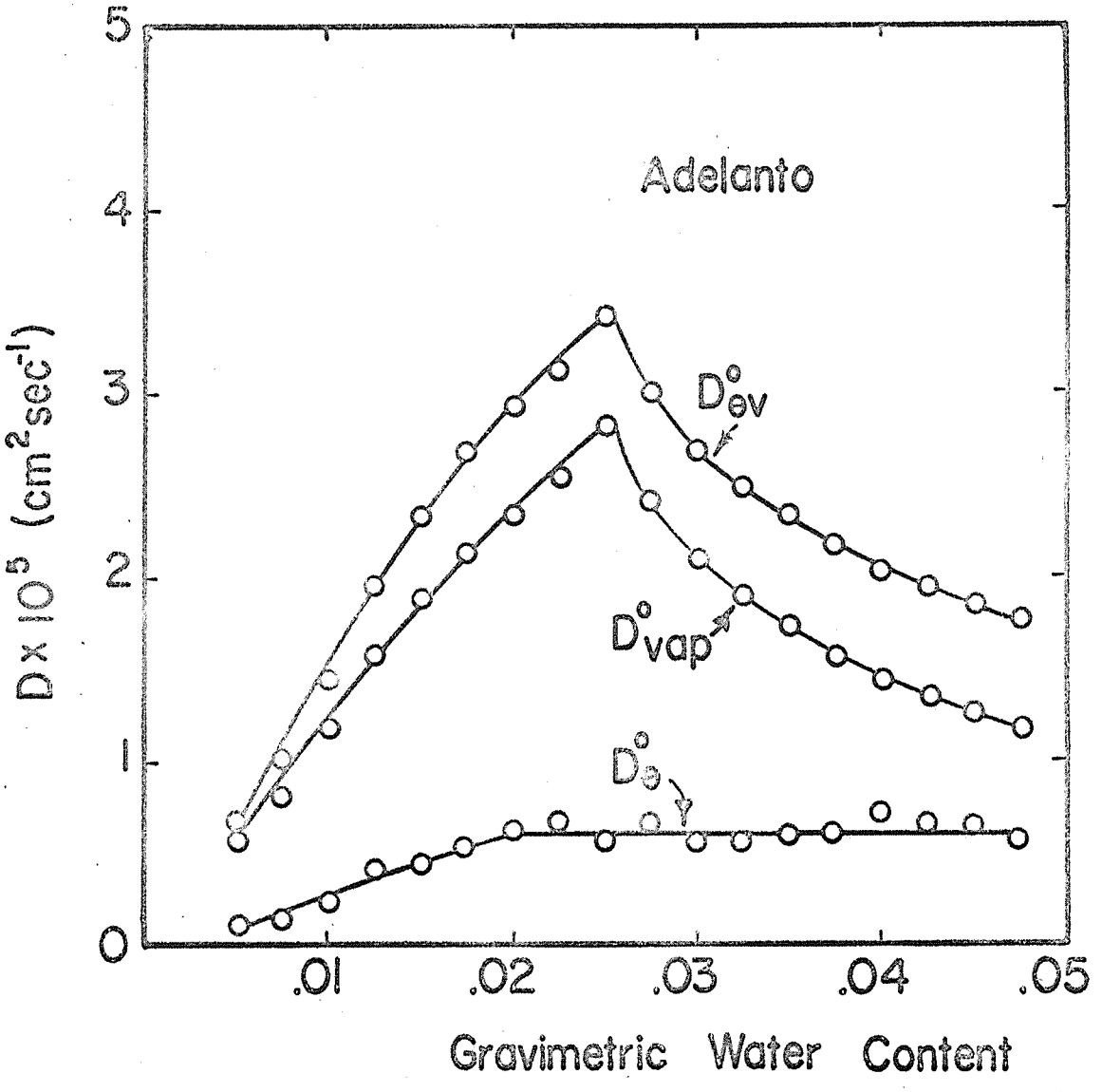

Figure 2. Total, vapor, and liquid diffusion coefficients for Adelanto loam at P = 730 mm Hg and T = 25° C.

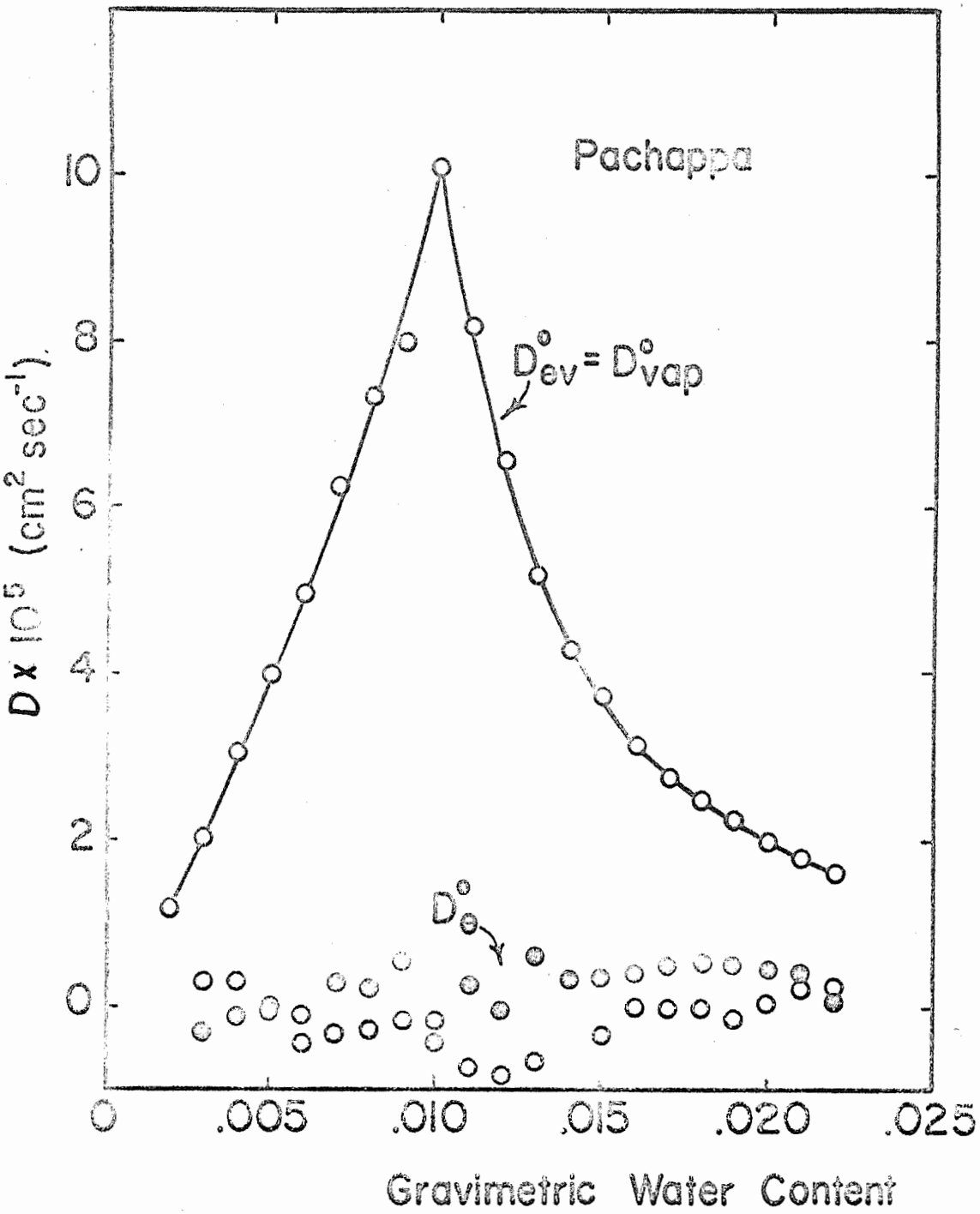

Figure 3. Diffusion coefficients for Pachappa loam at P = 730 mm Hg and T = 25° C.

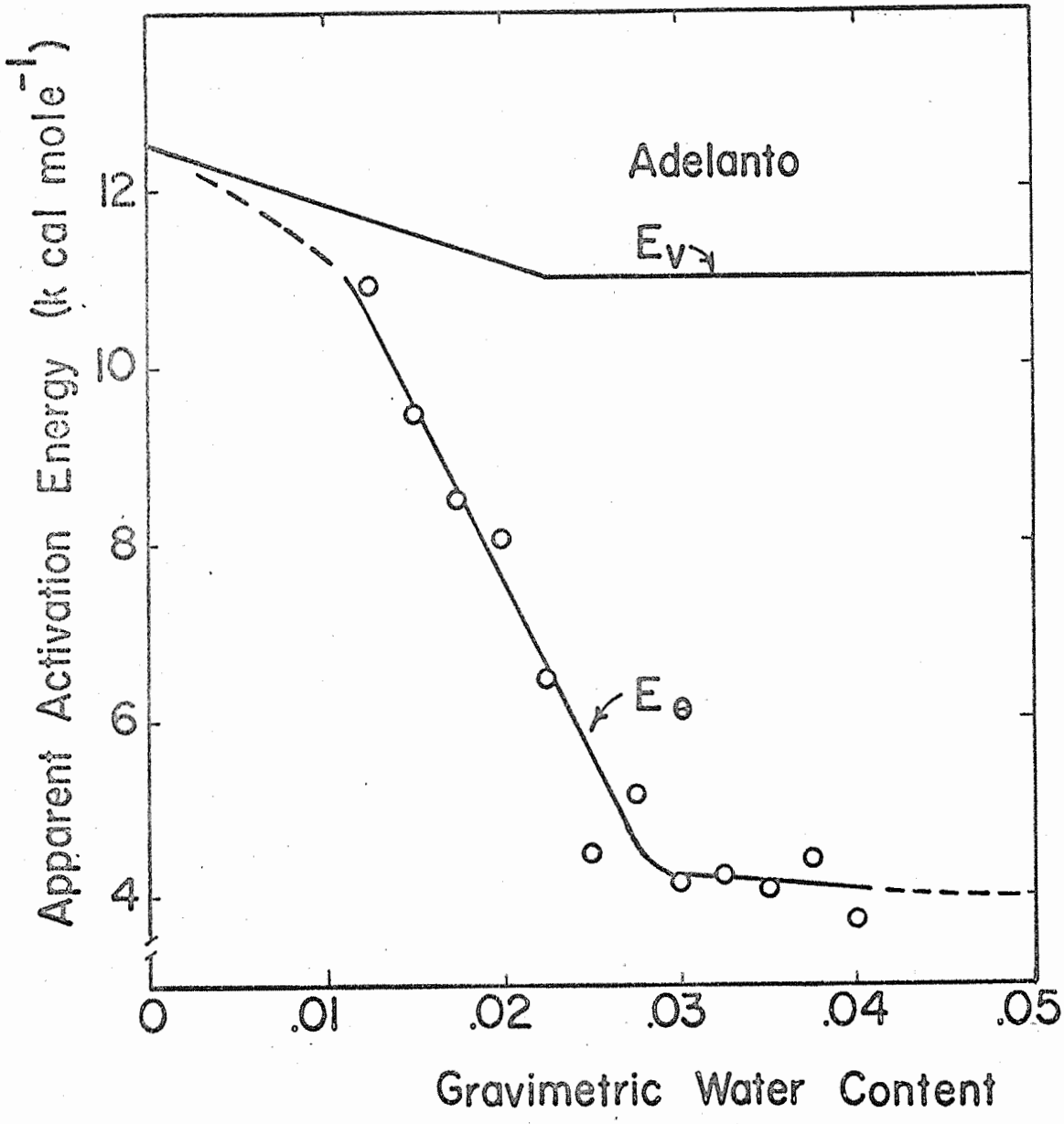

Figure 4. Theoretical and calculated apparent activation energies for vapor and liquid diffusion, respectively, for Adelanto loam.

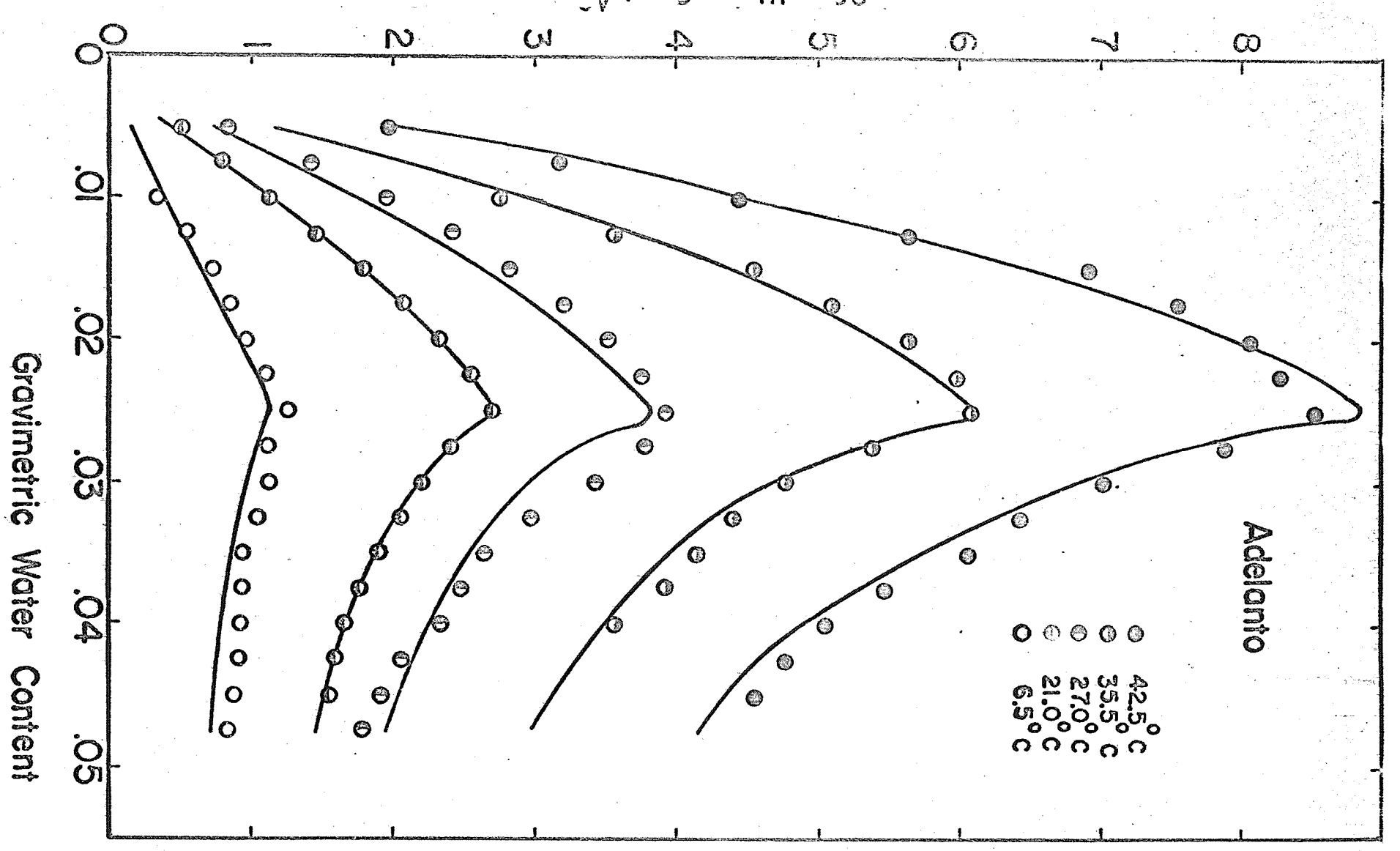

Figure 5. Temperature dependence of diffusion coefficients for Adelanto loam, the solid lines are predicted and the symbols are measured data.

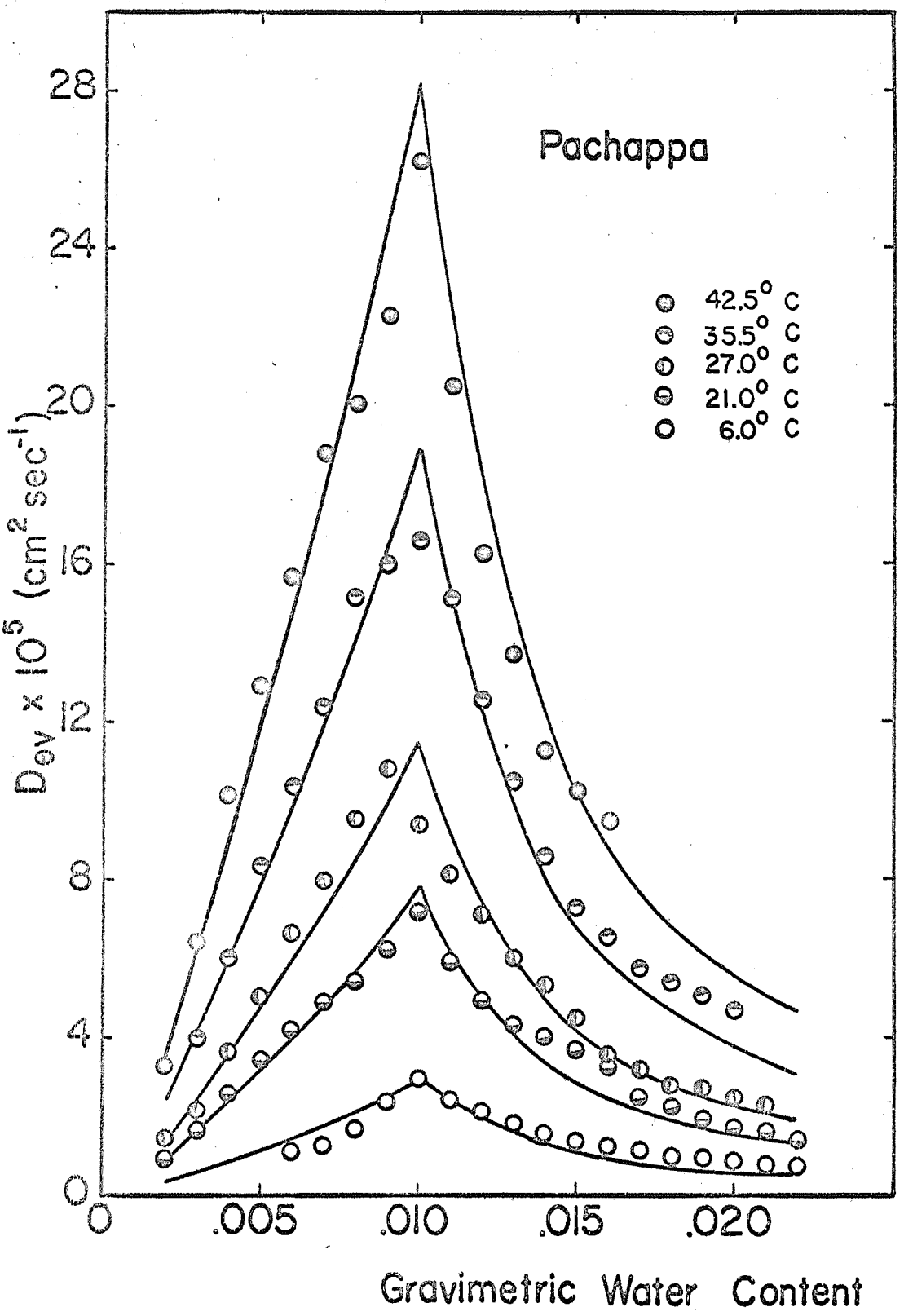

Figure 6. Temperature dependence of diffusion coefficients for Pachappa loam, the solid lines are predicted and the symbols are measured data.

PART II. THE CIRCULATION OF WATER IN SOIL UNDER A TEMPERATURE GRADIENT.

INTRODUCTION:

Several workers (1, 2) have suggested that, when a temperature gradient is applied to a uniform closed soil column, a circulatory system is set up, and that any eventual steady moisture distribution is actually a dynamic balance of opposing fluxes, predominantly vapor from hot to cold, and predominantly liquid from cold to hot. In this part we show that, at equilibrium, a static system cannot exist, and confirm experimentally the existence of a circulatory system.

In a porous material

$$\ln h = g\psi/RT = g(\psi + \pi)/RT \qquad [1]$$

where h = relative humidity, g = acceleration due to gravity (cm/sec^2), R = gas constant for water vapor (erg/g deg), T = temperature (deg K), and ψ is the total water potential (cm water) comprising matric (ψ) and osmotic (π) components.

Also, for water vapor, over a small temperature range,

$$\ln \rho_s = \alpha + \beta T \qquad [2]$$

where ρ_s (g/cm^3) is the saturated vapor density at T^o K, and α and β are positive constants.

At any point, the vapor density $\rho = h\rho_s$, so differentiating and using [1] and [2], the vapor density change along a column subjected to a temperature gradient must satisfy

$$\frac{1}{\rho}\,\delta\rho = \frac{g}{RT}\left[\delta\psi - \frac{\psi}{T}\,\delta T\right] + \frac{g}{RT}\left[\delta\pi - \frac{\pi}{T}\,\delta T\right] + \beta\,\delta T \qquad [3]$$

For static equilibrium, the fluxes of liquid, vapor and solute must all be zero simultaneously, i.e. $\delta\psi$, $\delta\rho$, and $\delta\pi$ must all be zero, and therefore

$$0 = \delta T(\beta - g\psi/RT^2)$$

which is impossible because ψ is always negative or zero. Thus, simultaneous static equilibrium of temperature, vapor, liquid, and solute cannot be achieved.

EXPERIMENTAL:

Columns, 10 cm length and 3.8 cm diameter, built from one-centimeter sections of Perspex tube, were uniformly packed with soil, saturated, drained at $\psi = -100$ cm, and sealed with a vacuum sealing compound. The columns, well-insulated, were screwed to thick brass plates in intimate contact with constant temperature baths at 17.6 and 27.8 C.

Two inert porous media were used: (1) a fine white sand, of density 2.65 g/cm^3 and porosity 0.39; (2) ignited 1/2-1 mm aggregates of local topsoil, of density 2.54 g/cm^3 and porosity 0.66. In each experiment there were four replicate columns, two each with water and strong sodium chloride solution. Temperatures were measured with copper-constantan thermocouples inserted at one-centimeter intervals.

After 12 days the columns were sectioned, the liquid distribution found by oven drying, and the salt distribution estimated conductometrically. The initial uniformity of salt and liquid distributions within the columns was tested in the same way on other replicates not subjected to a temperature gradient.

RESULTS:

Figure 1 shows the final liquid distributions, and Figure 2 the final salt distributions; Figure 2(a) shows the ratio mmole NaCl/g water, and 2(b) the ratio mmole NaCl/100 g soil. Each point is the mean of duplicates, and the mean value and initial deviation for the column is indicated by each line. Temperature distributions in the saline and non-saline columns differed (Figure 3); the results for sand are consistent with thermal conductivity differences caused by liquid content differences.

For both materials there was, as expected, net water movement from hot to cold, the movement being greater in the absence of salt, possibly because the salt acted as a sink for water vapor at the hot end. In the sand there was little net transfer of water in the presence of salt.

Figure 2 is of more interest. When a temperature gradient is applied along a column in which water and salt are initially uniformly

distributed, two kinds of transfer are possible. If water moves only as vapor, the ratio mmole salt/g soil will remain constant, but the ratio mmole salt/g water will increase in regions where evaporation occurs and decrease in regions of condensation. Conversely, if water moves only as liquid, the ratio mmole salt/g water will remain constant, but that of mmole salt/g soil will increase in the regions to which the liquid flows and decrease in those from which it flows. The results of Figure 2 are thus consistent with a vapor flux moving from hot to cold, and return liquid flux from cold to hot - a circulatory system.

REFERENCES:

(1) Curr, C. G., Marshall, T. J., and Hutton, J. T.
1952. Movement of water in soil due to a temperature gradient. Soil Sci. 74: 335-345.

(2) Hutcheon, W. L.
1958. Moisture flow induced by thermal gradients within unsaturated soils. Highway Res. Bd. Spec. Rpt. 40: 113-133.

PERSONNEL: R. D. Jackson, U. S. Water Conservation Laboratory; D. A. Rose and H. L. Penman, Rothamsted Experimental Station.

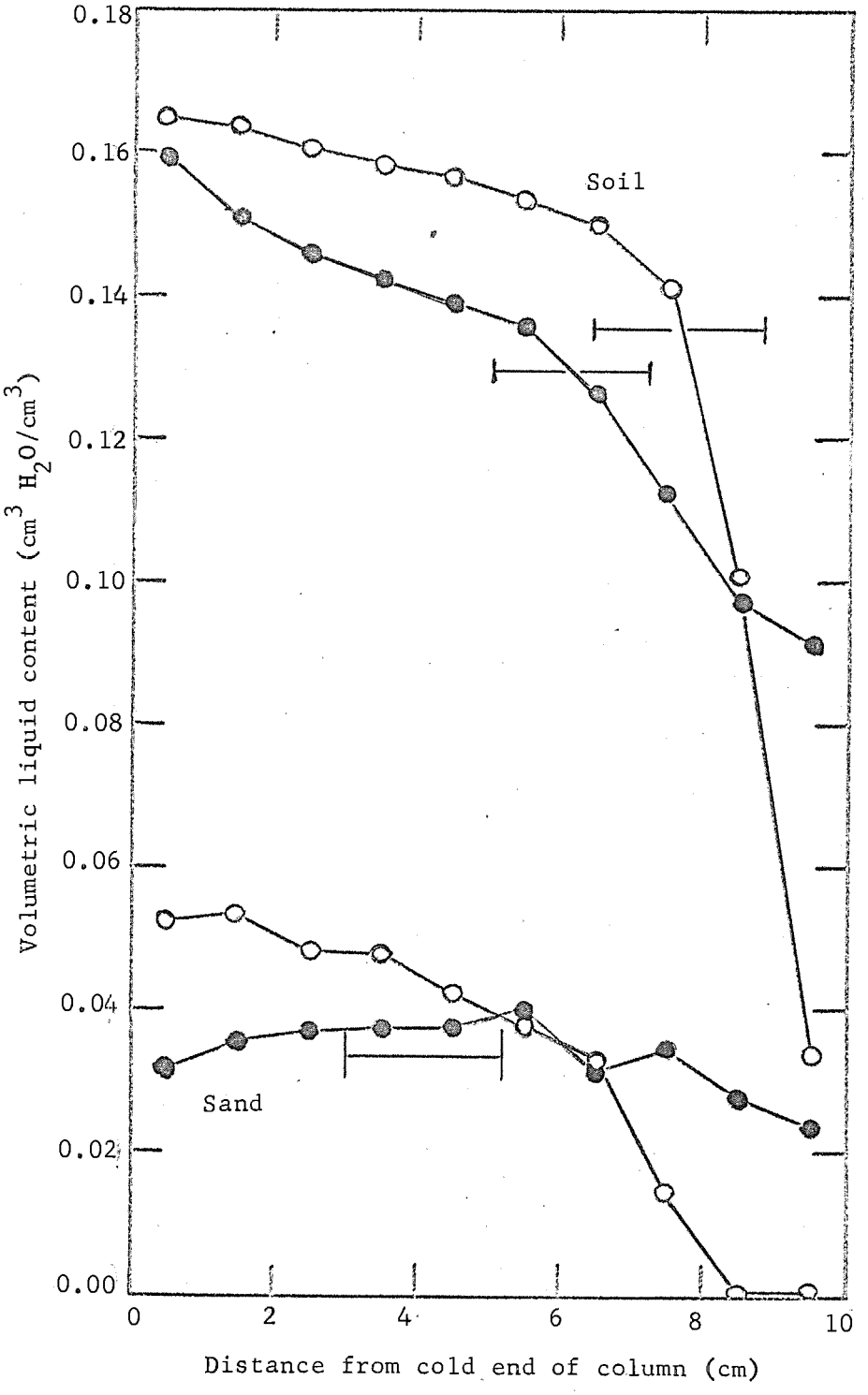

Figure 1. Final liquid distributions. Volumetric liquid content plotted against distance from the cold end of the soil columns. ○, non-saline; ●, saline; ├──┤, initial mean value (horizontal line) and standard deviation (vertical bur).

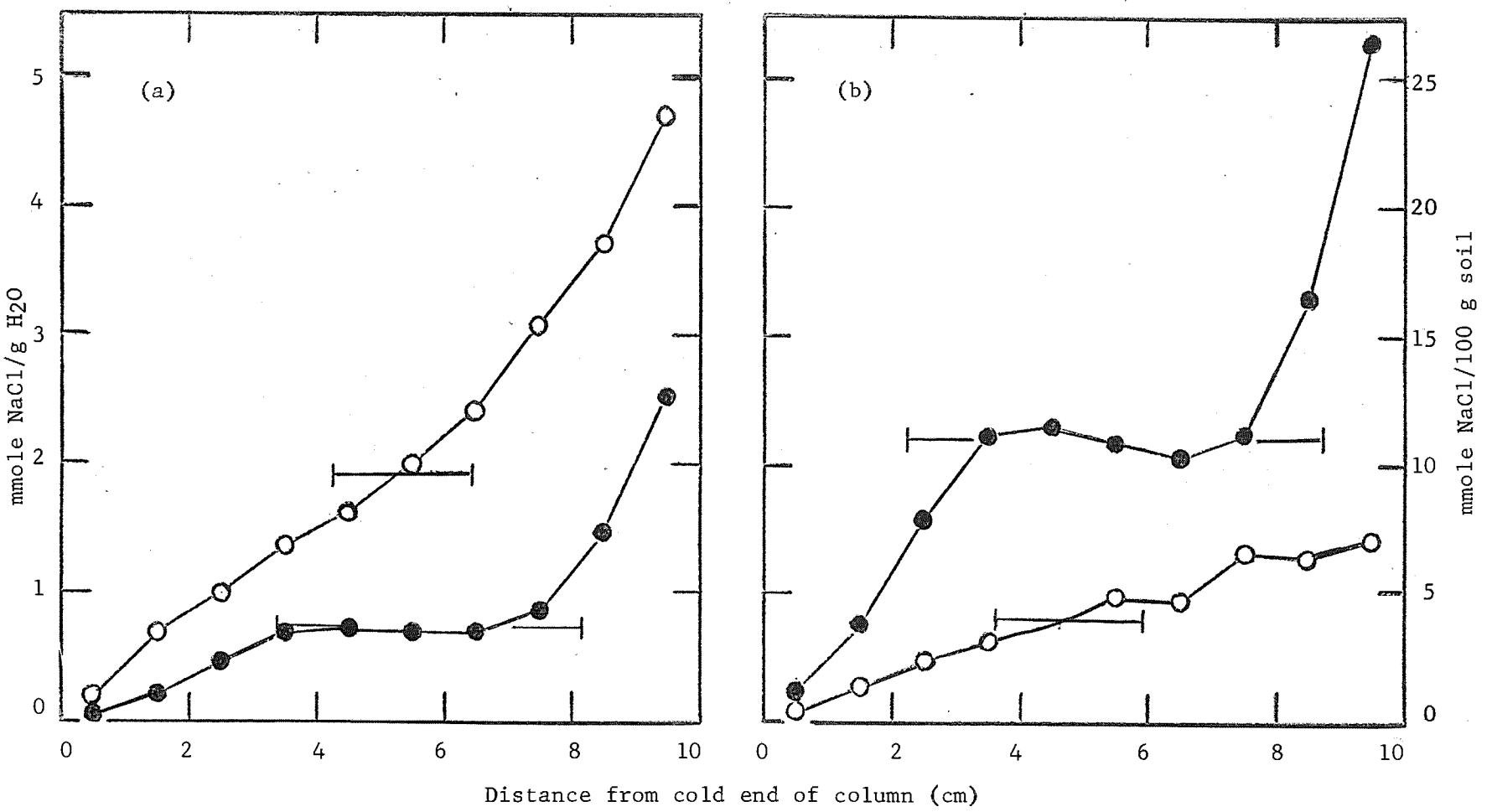

Figure 2. Final salt distributions: (a) ratio mmole NaCl/g H_2O, and (b) ratio mmole NaCl/100 g soil as functions of distance from cold end of columns. ○, sand; ●, soil.

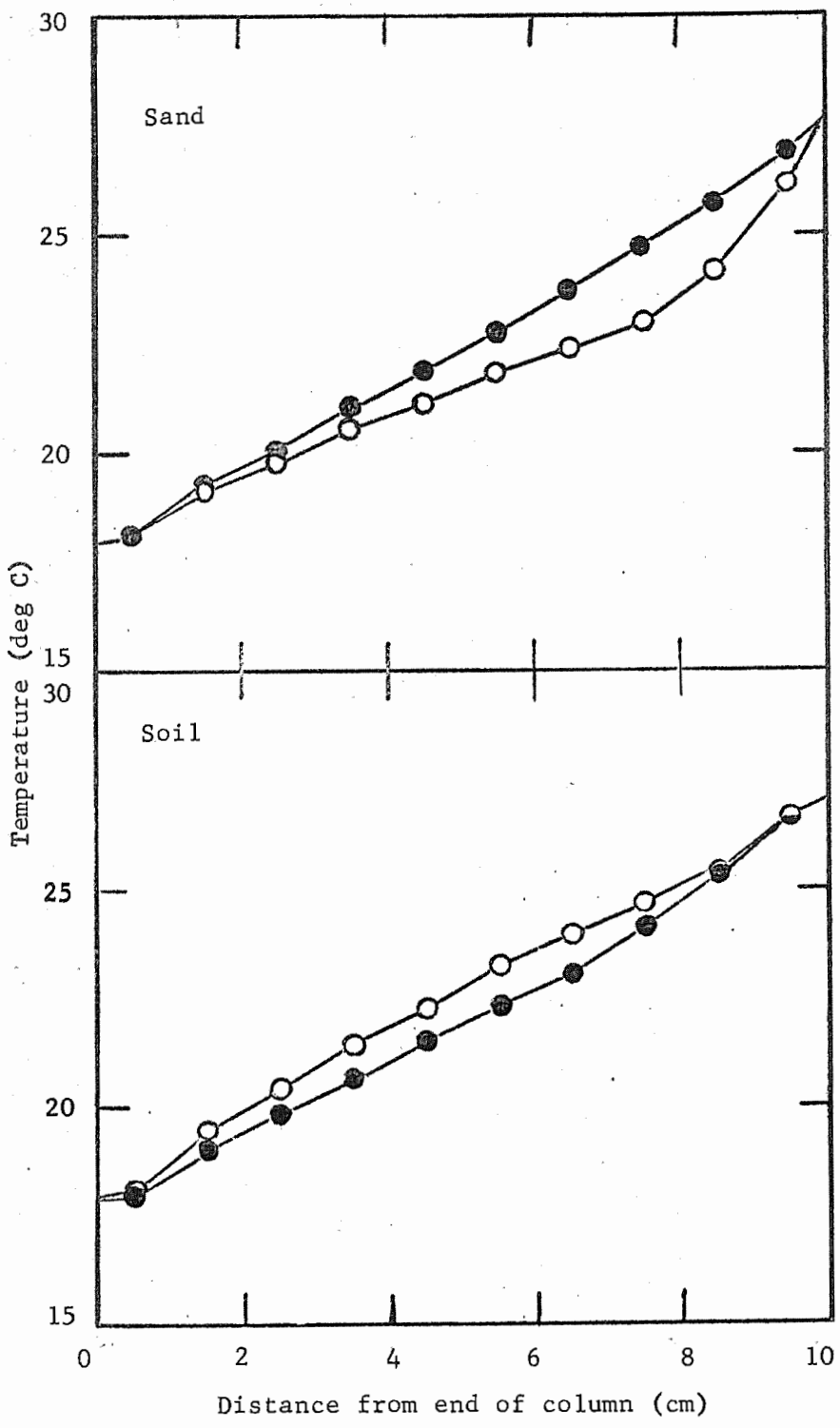

Figure 3. Final temperature distributions: O , non-saline; ● , saline.

TITLE: MICROMETEOROLOGICAL DETERMINATIONS OF WATER LOSS FROM VARIOUS SURFACES

LINE PROJECT: SWC 4-gG2 CODE NO.: Ariz.-WCL-32

1. INTRODUCTION

Evaporation from the earth's surface accounts for the greatest loss of potentially available water, the evaporative process being controlled primarily by meteorological processes that supply energy and transport water vapor. In order to control or reduce the evaporative loss, a more complete understanding of the energy-exchange and turbulent-transport mechanisms and their complex interrelationship with the soil-plant continuum is required. This can be accomplished only by precise and intensive measurements of the micrometeorological elements and evaporative flux. Consequently, instrumentation for determining the evaporative flux by a micrometeorological model, known as the Bowen ratio, was tested. Duplicate instrumentation was later used for simultaneous determination of the evaporative flux from different field crops. The crops under investigation were alfalfa, barley, cotton, oats, grain sorghum, and wheat. The results of these studies and associated micrometeorological parameters are reported.

2. THEORY

The Bowen ratio is one of many micrometeorological models used to determine evaporative and sensible heat fluxes. Since it is based on a statement of energy conservation, it is one of the more reliable models. I. S. Bowen (1) originally proposed that the equation used to calculate evaporation from open water surfaces,

$$R_n + LE + W = 0 \quad , \qquad [1]$$

be modified by the addition of a sensible heat term (see Appendix 1 for definition of terms). He discussed the ratio of sensible to latent heat from different conditions. This ratio was later called the Bowen ratio.

C. B. Tanner (4) proposed that the Bowen ratio, measured above the surface, be used to determine evaporation from cropped surfaces. The Bowen ratio for this purpose can be defined from vertical gradients of temperature and vapor pressure, and is referred to as the Gradient Bowen Ratio. The vertical gradient equations for sensible and latent heat flux are

$$A = C_p \rho (K_h) \overline{\Delta T}/\Delta Z \qquad [2]$$

$$LE = \frac{L \epsilon \rho}{P} (K_w) \overline{\Delta e}/\Delta Z \quad . \qquad [3]$$

Thus, the Gradient Bowen Ratio takes the form

$$\beta_g = \frac{A}{LE} = \frac{C_p P}{L\epsilon} \frac{K_h}{K_w} \frac{\overline{\Delta T}}{\overline{\Delta e}} \qquad [4]$$

when the gradients are measured over the same height interval. Evaporation from any surface may be determined when the Gradient Bowen Ratio is combined with the energy balance equation by assuming that $K_h = K_w$, that the horizontal divergence of sensible and latent heat is zero, and ignoring the change in energy stored in the crop canopy and the energy used in photosynthesis. The resulting equation is

$$\widehat{LE} = \frac{-(R_n + S)}{1 + \frac{C_p P}{L\epsilon} \frac{\overline{\Delta T}}{\overline{\Delta e}}} \qquad [5]$$

Since the diurnal and seasonal ambient pressure in the Tempe area varies by less than 1 percent (973 $\pm$ 5 mb), $\frac{C_p P}{L\epsilon}$ may be taken as 0.642. Equation [5] becomes indeterminate when $0.642\ \overline{\Delta T}/\overline{\Delta e} \rightarrow -1$. This occurs during the relatively uninteresting times when the energy exchanges are low, such as at sunrise and sunset.

3. INSTRUMENTATION

The success of any micrometeorological model is contingent upon the ability of the instrumentation to accurately translate the required parameter into analog form suitable for recording. Since most of the instrumentation required is not commercially available, considerable effort was expended in designing, constructing, calibrating, and field testing. The instrumentation used during 1964 is then described:

3.1. Net radiation, R_n. Net radiation is the most important parameter in determining the evaporative flux by the Gradient Bowen Ratio. Consequently, measurements must be representative and accurate. In all studies, R_n was measured 1 meter above the crop surface with two net radiometers. Where row crops were investigated, one net radiometer was located over the row, while the other was located over the furrow. The average was used in evaporation calculations.

The net radiometers used are described elsewhere (2). It suffices here to state that an improved net radiometer was designed with increased sensitivity to match a $\pm$ 5-mv potentiometer used in our multichannel recording system. Its sensitivity is sufficient to give a full-scale range of $\pm$ 1.4 ly min^{-1}, with a recording sensitivity and accuracy of 0.003 ly min^{-1}. The radiometer sensor consists of a 22-junction manganin-constantan thermopile with compensating thermistor embedded in epoxy resin. Effects of ambient temperature from 11 to 54C are virtually eliminated by means of a circuit comprised of a shunt thermistor and rheostat. The blackened surfaces of the transducer are shielded against the effects of wind by thin polyethylene hemispheres. The improvements also include uniform sensitivity among sensors, better spectral response, and relative ease of construction.

3.2. Soil heat flux, S + S'. Soil heat flux at the surface was obtained by adding the soil heat flux at 5 cm, S, to the change in energy storage in the top 5 cm of soil, S'. The soil heat flux at 5 cm was measured with two National Instruments Laboratory heat-flow

discs, Model No. HF-2, one being located in the row and the other in the furrow when appropriate.

The change in energy storage in the top 5 cm of soil, S', was calculated from

$$S' = \frac{cd(\overline{T}_b - \overline{T}_e)}{t}$$

where 0.5 was taken for the heat capacity. The average soil temperature was measured with 12 parallel thermocouples at 4 depths (from 3 mm to 5 cm) and 3 locations.

3.3. Vapor pressure. The vapor pressure was obtained by two methods. Early in the year, the differential psychrometer described in the 1963 Annual Report was employed. Later in the year, Minneapolis-Honeywell dewprobes (SSP129Z005) were used to measure the vapor pressure. The switchover was made to reduce the power requirement for ventilation and to avoid the problems of supplying water to the wicks. Exposure and operation of the dewprobes are described in 3.8.

3.4. Air temperature.

3.4.1. Air-temperature gradients used in Bowen ratio calculations were measured with 2-junction copper-constantan thermopiles. A single junction was used to measure the absolute temperature. The thermocouple and thermopile were housed with the dewprobe, as described in 3.8.

3.4.2. Air temperatures for profiles were obtained at 5, 20, 40, and 80 cm above the cropped surface. The absolute temperature was determined at 80 cm with a copper-constantan thermocouple, while the temperature difference between 80 cm and the other heights was determined with single-junction thermopiles. All junctions were mounted in the center of 1-inch horizontal copper tubes, which were connected to a manifold for common ventilation. Approximately three-eights inch of foam plastic covered with aluminized mylar was used to insulate the copper tube.

3.5. Solar radiation.

3.5.1. Incoming solar radiation (the sum of direct plus diffuse) was measured with a Kipp pyranometer.

3.5.2. Reflected solar radiation (the sum of direct plus diffuse) was measured with inverted Kipp pyranometers. The metal bases supplied with the instruments were removed and the sensing element mounted in an inverted position in a radiation shield. The Kipp pyranometers have a nominal output of 8 mv ly^{-1} min.

3.6. Wind speed. During most of the studies wind speed was measured at 4 elevations (5, 20, 40, and 80 cm) over 2 different surfaces with Casella sensitive-type anemometers. The anemometers have light-weight electrical contacts that close 2 times for every 3 revolutions of the cups. The instruments were pressurized with dry air to prevent dust from entering the housing.

Since the anemometer is too large to obtain profiles by stacking the instruments, they were mounted on uprights spaced horizontally. The uprights were welded on a horizontal bar with 1-m spacing between the 5, 20, and 40 cm heights and 50 cm between the 40 and 80 cm heights. The horizontal bar was orientated north and south with the lowest anemometer to the south. Since the prevailing winds were easterly in the morning and southwesterly in the afternoon, the winds were either perpendicular or at an angle of 45 degrees from the anemometer array.

3.7. Wind direction. Wind direction was obtained by measuring the voltage drop across a 1 K ohm, single-turn, continuous Helipot, Model T.P., which had a Beckman & Whitley vane mounted on the shaft.

3.8. Spatial sampling tower. Spatial sampling of micrometeorological elements is deemed necessary for two main reasons:

(1) To obtain representative values when instruments are mounted close to a cropped surface. This is especially necessary for row crops.

(2) During periods of light winds, convection cells may exist that would bias data obtained with fixed sensors. With moving sensors, spatial average can be obtained, thus reducing errors due to location within convection cells.

It would be desirable to sample spatially with all micrometeorological sensors. However, since leveling is critical on all radiation measuring devices, radiation (net and reflected) was not sampled with moving sensors.

The portable towers described in the 1963 Annual Report were used to move the air-temperature and vapor-pressure sensors through space. The tower swept out a 180° arc of 10-foot radius every 10 minutes. The only modification consisted of using two right-angle braces set at 90° to support the upright, instead of guy wires. This reduced the setup time considerably.

During the period January through April, the differential psychrometers described in the 1963 Annual Report were used with the towers to obtain air-temperature and vapor-pressure gradients. After April these were replaced with differential air-temperature sensors and differential dewprobes. The latter units were housed similarly to the first; that is, the air siphoned in fixed intakes (35 cm apart) passed through a 4-way switching valve to the sensors. A shaded pole blower was used to siphon the air. After the data-logging system had recorded the data, an electrical pulse caused the 4-way valve to reverse the intakes with respect to the sensors, thus canceling out any sensor bias. The polarity of the differential signal was also reversed by the same electrical pulse.

3.9. Recording. All data were recorded with the data-handling system (3) located in the mobile micrometeorological laboratory. Only one small modification was made on the data-handling system. Since the power supplied to the data-handling system was from an a-c generator with inadequate cycle control, the system timing was not reliable enough. Therefore, an electrically wound spring-driven clock providing 1-minute contact closures was added to actuate the system digital clock.

The data-handling system worked very well during the season. A total of 48 days (700,000 data points) of usable data were collected.

All data recorded were analyzed with General Electric computers using the generalized linear program described in the 1963 Annual Report. Equation [5] was solved with the basic 15-minute data.

3.10. Accuracy of measurements. The accuracy of measurements of the micrometeorological elements is given in Table 1. Accuracy of measurement of net radiation is more important in terms of evaporative flux in that it is, for the most part, directly proportional to net radiation. Errors in the measurement of $\overline{\Delta T}$ or $\overline{\Delta e}$ are relatively insignificant, for example, when LE is 1.138 ly min^{-1}, net radiation is 0.782, $\gamma P\overline{\Delta T}$ is 0.3262, and $\overline{\Delta e}$ is −1.0197. If Δe was measured with a 20 percent error (−0.8158), then the resulting LE would be 1.267, which amounts to an error of 11 percent. Measurements of $\overline{\Delta T}$ and $\overline{\Delta e}$ became increasingly more demanding as $\gamma P\overline{\Delta T}/\overline{\Delta e}$ approached −1 (see section 2). Therefore, greatest concern should be given to measurement of net radiation. Net radiometers should be calibrated frequently, located properly, and replicated.

4. FIELD TESTING OF EQUIPMENT

Continued field testing of sensors was necessary to establish and to improve the accuracy of evapotranspiration determinations with the Gradient Bowen Ratio. To this end, five runs were made in the experimental field at the Laboratory, where the evapotranspiration determinations could be compared with results obtained from the weighing lysimeters. The data obtained are summarized in Table 2.

4.1. A4–1. At the time of the first experiment, the alfalfa was recovering from frost damage. It was 14 cm tall, with some taller dry stems that had been frozen. Two hours' data were omitted from the totals because of equipment adjustment. The agreement between the two methods is amazing. There was only a 2-ly difference in the daily and daylight totals. A 0.02 ly min^{-1} bias in any of the instruments would result in a daily error of 29 ly.

4.2. A4–2. During A4–2, a differential dew probe was also tested. In this run the alfalfa was 15 cm tall. The evaporative flux was double that of A4–1, and the agreement between the results obtained with the lysimeters and the differential psychrometers, not as good. A −24-ly difference occurred in the daily totals and +24-ly difference in the daylight totals. Both values are within a 0.02 ly min^{-1} bias and could easily be due to sampling.

The results obtained with the differential dewprobes were considerably better. An hourly comparison of the evaporative flux from the lysimeter and that calculated from dewprobe data is shown in Figure 1. The agreement is very good when one considers all of the possible errors. The greatest hourly discrepancy was less than 0.05 ly min^{-1}. This close agreement, plus the ease of operation of dewprobes compared to psychrometers, prompted the rapid conversion from differential psychrometers to differential dewprobes. Therefore, all the remaining results contain dewprobe data.

4.3. A4–3. On 7 April, run A4–3 was made. Valid data for the Gradient Bowen Ratio were not obtained because of a faulty diode in the $\pm$ 0.5-mv range of the data-logging system. Therefore, only energy balance data are presented. At this time the alfalfa was 26 cm tall.

4.4. A4–4. The run A4–4 was conducted on 23 and 24 May. The alfalfa, 20 cm tall, was recovering from a complete cutting and was not very uniform. Photographs indicated that the lysimeters had less growth than the areas over which the vapor-pressure and temperature gradients were measured. (Notice the difference in R_n between lysimeters in Table 2.) Therefore, direct comparisons of the lysimeter data and micrometeorological calculations are not valid. However, a very important fact was obtained from the micrometeorological calculations.

Run A4–4 was conducted to test the effect of different distances (ΔZ) over which the gradients of vapor pressure and temperature were measured [see Equation 4, page 32-2]. On 23 May, both air-sampling towers were set for a ΔZ of 35 cm. Air sampler 1 was changed to a 75-cm ΔZ on 24 May. The results obtained on 23 May are shown in Figure 2. Average R_n and S + S' were used in the calculations. Except for the hour 1100 to 1200, the agreement is quite good.

Different results were obtained on 24 May when air sampler 1 was changed to a 75-cm ΔZ (Figure 3). The results from the two samplers diverged when the wind speed exceeded 1 m sec^{-1}. This cannot be attributed to the location of the air samplers with respect to the edge of the experimental field. During the morning hours with easterly

winds, sampler 2 was upwind, while sampler 1 was upwind during the afternoon hours. The difference appears to be due to the relation between the distance (ΔZ) over which the gradients were measured and the boundary layer of the experimental field; that is, with a wind speed of less than 1 m sec^{-1} (0600 to 0700, 0900 to 1300, 1500 to 1800), both air samplers appeared to be within the boundary layer. As the wind speed increased, the field boundary layer became shallower; thus, the 80-cm intake of sampler 1 became less representative of the field. These data indicate that, for small fields, temperature and vapor-pressure gradients should be measured as close to the surface as possible to obtain representative results.

4.5. A4–5. The alfalfa was 49 cm tall when A4–5 was conducted. Data were collected for two days, a clear day and a cloudy day. Evapotranspiration calculated by the Gradient Bowen Ratio agreed quite well with the results from the lysimeter on both days (Table 2).

Hourly comparison of the methods of 29 July is shown in Figure 4. The 29th of July was selected to illustrate the effectiveness of the micrometeorological method on cloudy days. During the daylight hours, comparable results were obtained. Discrepancies occurring between 0800 and 1000 may be due to the relation between the time constant of the instruments and the intermittent cloudiness; that is, the vapor-pressure and temperature sensors had time constants of 5 minutes, while the time constant of the net radiometers was 12 seconds. A 5-minute time constant was desired to smooth out the variability in the temperature and vapor-pressure gradient signals. A long time constant was not required for net radiation, since it is relatively conservative. However, during periods of intermittent cloudiness, the signals from the various sensors may not represent the same period. Under such conditions more frequent sampling would also be desirable; four samples per hour hardly seem adequate.

The increased evaporation rate from 0100 to 0500 and from 2100 to 2400 was associated with advected energy and wind speeds up to 5.5 m sec^{-1}. This is a very rare case in this area. It appears that the Gradient Bowen Ratio failed to properly assess the advected

energy during these periods. Radiation divergence may also account for part of the error. This point needs to be investigated further. In any case, the error in nocturnal values is hardly significant when daily totals are concerned.

4.6 Summary of field testing. The results of field tests indicate that the Gradient Bowen Ratio can be used successfully to determine the evaporative flux for short periods (1 hour or less). When differential psychrometers were used to sense vapor-pressure and temperature gradients, error of estimate appeared to be 0.02 ly min^{-1} or less. However, when differential dew probes were used, the error of estimate appeared to be an order of magnitude less, or less than 5 percent of daily totals. Some of the error could be real and associated with site variability.

The Gradient Bowen Ratio method yields meaningful results on cloudy days, as well as clear days. However, more frequent sampling appears to be necessary on cloudy days.

When the Gradient Bowen Ratio is used on small fields (2 acres), the gradients should be measured as close to the surface as possible. Gradients from 5 to 40 cm above the crop surface yielded satisfactory results, while gradients from 5 to 80 cm above the surface did not when the wind speed exceeded 1 m sec^{-1}.

The Gradient Bowen Ratio may be used over any surface. No assumptions are made concerning the state of the surface. The only assumption used was that the ratio of the transfer coefficients, K_h/K_w, is one. This assumption appears to be valid. When the method is used over a water surface, difficulty may be encountered in properly assessing the energy storage in the water. This is strictly an instrumental problem.

Commercial dew probes were found to be very reliable and relatively easy to use to obtain vapor-pressure gradients. Furthermore, less equipment was required with dew probes than with psychrometers.

5. EVAPORATIVE FLUX DETERMINATIONS FROM DIFFERENT CROP SURFACES

The mobile micrometeorological laboratory was equipped with duplicate sensors (see section 3) to simultaneously determine the evaporative flux from two different crop surfaces. The original plans included biweekly measurements over alfalfa–barley, alfalfa–cotton, and alfalfa–sorghum combinations at the University of Arizona Experimental Farms in Mesa. The plans were later augmented to include biweekly measurements over wheat–oats and cotton at the Cotton Research Center in Tempe. A total of 20 runs were made in Mesa, and 15 runs were made in Tempe.

The recording schedule really tested the ruggedness and mobility of the equipment. By the end of the season, only 6 man-hours were required to spot the mobile laboratory in the field, unwind 1.5 miles of cable, wire the data-handling system, calibrate all cables and channels, and install all sensors. A total of 38 sensors were installed for each run.

5.1. University of Arizona Experimental Farm runs. At Mesa data were collected over alfalfa–barley, alfalfa–cotton, and alfalfa–sorghum combinations. The plot location is shown in Figure 5. The areas were divided into 33- by 100-feet irrigation borders, running north and south from the pipelines.

Soil moisture was measured in one irrigation border of each crop with a neutron soil-moisture meter. Three tubes were installed in each plot to a depth of 150 cm. Moisture loss from the top 3 inches was determined by drying soil samples. Soil moisture was determined twice weekly, and the soil-moisture depletion was computed whenever possible.

Micrometeorological sensors were located near the center soil-moisture tube; thus the minimum fetch was at least 30 meters. A 50:1 fetch-to-height relation would permit sensors to be installed up to 60 cm above the surface in the direction of the minimum fetch.

All cultural operations on the plots were performed by the Mesa Farm personnel. No special operations were requested. Care was taken to minimize damage to the plots when installing sensors.

Daylight totals of the components of the energy balance equation and solar radiation are presented in Table 3. These basic data are discussed in the following sections.

5.1.1. Alfalfa. More data were obtained from alfalfa than from the other crops, since they were to be compared with alfalfa. Presented in Figure 6 in graphical form are the soil-moisture depletion, evaporative flux, crop height, time of irrigation of alfalfa, and time and amount of rainfall. Plot 1 was located adjacent to barley and cotton; consequently, most of the data were obtained on plot 1. However, plot 1 was plowed under in late August; therefore, the alfalfa-cotton comparison was terminated. Data were collected from plot 2 after the sorghum had germinated, so that a comparison could be obtained between sorghum and alfalfa. The horizontal lines with vertical bars on either end represent the average soil-moisture depletion between readings. Dashed horizontal lines indicate the results obtained on plot 2. The x's connected by lines and the ●'s connected by dashed lines represent the evaporative-flux determinations using micrometeorological data. The downward-orientated arrows indicate the time of irrigation of plots 1 and 2. During most of the season alfalfa was irrigated every 2 weeks.

During March and April, fair agreement existed between the soil-moisture depletion and evaporative-flux determinations. There does not appear to be any correlation between these two methods throughout the rest of the growing season. The soil-moisture depletion values appear to be consistently lower than the evaporative-flux determinations and lower than would be expected. Throughout the season the evaporative-flux determinations appear to be consistent, being well correlated with crop growth and time of year, or evaporative demand. The only inconsistencies for crop height appear on 21 and 23 July. This is because the alfalfa had been knocked down by a windstorm.

The yield of alfalfa from plot 1 was 84.5 tons per acre for 6 cuttings, while 118.7 tons per acre were obtained from 7 cuttings on plot 2.

5.1.2. Barley. The results obtained from barley are shown in Figure 7. Notation used in Figure 7 is similar to that used in Figure 6, with the exception that rainfall amounts are omitted. They may be obtained from Figure 6. The barley, grown for seed, was planted at 10-inch row spacing. The stand was rather thin; consequently, the evaporative-flux determinations reflect to a greater degree the evaporation from soil surface. Although the stand was rather thin, yield of 49 bushels per acre was obtained.

Considerable scatter was noted in the soil-moisture depletion data early in the season, making comparisons between soil-moisture depletion and evaporative flux very difficult. Soil-moisture depletion indicated greater consumptive use during latter May than did evaporative-flux determinations. However, the crop was maturing at this time; therefore, part of the difference after the early May irrigation may be explained by deep percolation.

5.1.3 Sorghum. Data obtained from the sorghum are also presented in Figure 7. In this case the plots were split with single- and double-row plantings. Two soil-moisture tubes were placed in each type of planting. Net radiation and soil heat flow were measured over and in each type. However, the air-temperature and vapor-pressure sensors were set to sample over both types of planting; therefore, the resulting evaporative-flux determination would be representative of both types. Again, considerable scatter is noted in the soil-moisture depletion values, making it difficult to construct any sort of trend. Evaporative-flux determinations are more consistent and illustrate an increase in evapotranspiration with crop height and a decrease upon maturity.

5.1.4. Cotton. The results from the cotton plots, presented in Figure 8, indicate a better correlation between soil-moisture depletion and evaporative-flux determinations during May, June, and July than obtained on the other crops. The evaporative-flux determinations appear to be consistently higher than the soil-moisture depletion data. In late July and early August, the soil-moisture depletion values appear to be considerably larger than the evaporative-flux determinations. During the first part of August a windstorm

partially knocked down the cotton; therefore, evaporative-flux determinations at that time may reflect this. Toward the middle of August, partial regrowth of the cotton occurred, resulting in a slightly larger evaporative flux. Because the alfalfa immediately south of the cotton plots was plowed under in late August and the cotton was wind damaged, the cotton experiments were terminated at the same time.

5.1.5. Crop comparisons. One of the primary objectives of the Mesa studies was to obtain comparative evaporative-flux data from two different crops. The data were obtained with duplicate instrumentation on the same day; thus, both crops would be exposed to the same meteorological conditions. The results would then reflect true differences in crop nature or cultural practices. Since the evaporative demand changes from day to day and throughout the season, the evaporative flux was normalized by dividing by net radiation. The results are presented in Figure 9. A comparison between alfalfa and barley would suggest that alfalfa consistently uses more water than does barley, under the conditions of this experiment. However, the barley was planted on 10-inch spacings; therefore, these results may not be typical.

The ratio of evapotranspiration to net radiation from cotton reflected crop growth from May through June. During this period the evapotranspiration was very much lower than that of alfalfa, as would be expected. After maximum height was reached, the ratio of evapotranspiration to net radiation appeared to be comparable to that of alfalfa, or slightly less, although insufficient data were collected to substantiate this fact.

Sorghum, like barley, appeared to have a lower evapotranspiration to net radiation ratio than did alfalfa. This ratio appeared to be consistently lower, even after maximum crop height was reached.

5.1.6. Evapotranspiration and pan evaporation. At the University of Arizona Experimental Farm in Mesa a meteorological station is maintained from which max-min temperatures, total wind movement, and pan evaporation are obtained. At the present time, this station is poorly located with respect to buildings, drives, bushes, trees, etc.; therefore, the use of this data can be severely criticized. The pan evaporation, although not representative of field conditions, should be consistent throughout the season. Therefore, the evapotranspiration, determined by meteorological data, was divided by the evaporation from the pan. This ratio was plotted as a function of plant height (Figure 10). The small w adjacent to six points indicates conditions when the soil surface was extremely wet or when water was ponded in the irrigation border. These points also represent times when a large percentage of bare soil was exposed. Although there is considerable scatter and far too few data points, the results do suggest a relation between the ratio of evapotranspiration to pan evaporation and plant height. For example, previous studies indicated that for similar meteorological conditions, more evaporation resulted from bare soil than from a free-water surface. This condition would be represented by the points marked with w — that is, large amount of wet bare soil exposed. There appears to be another relation between the ratio and crop height for alfalfa, although some five points lie well below the line. Two of the five points represent extremely cloudy days, and the third represents a windy day. All would have a tendency to reduce the evapotranspiration in relation to pan evaporation, since the evapotranspiration was only computed for the daylight hours and the pan was computed for a 24-hour basis. There appears to be another relation between the ratio and crop height for barley, cotton, and sorghum. These data suggest a relation between evapotranspiration and pan evaporation as a function of crop height for a solid-covered crop, such as alfalfa, and a different relation for row crops, such as barley, cotton, and sorghum. To the author's knowledge, these relations have not been investigated previously because of the lack of daily evapotranspiration data. This interesting graph suggests the possibility of future research.

5.1.7. Summary of the Mesa Farm data. The following conclusions can be drawn from the data presented thus far. Under the conditions of the experiments – that is, frequent irrigation – evapotranspiration inferred from soil-moisture depletion data appears to be very erratic and does not give a consistent trend. This could be due to deep percolation, which would tend to explain the high results, and to experimental error. However, these data were carefully obtained. On the other hand, the evaporative flux determined from micrometeorological data does yield a consistent trend reflecting crop growth, maturity, and seasons of the year. Although too few data were collected to compute seasonal water use, the point should be made that the Gradient Bowen Ratio approach is a very practical method to determine evapotranspiration. It is not an empirical method requiring experimentally derived constants, does not make any assumptions about the surface in question, and does not reflect deep percolation losses. The sensors and recording devices could be designed so that it would be just as practical to determine evapotranspiration by the Gradient Bowen Ratio as by the neutron soil-moisture method, when labor and initial investment are considered.

Under the conditions of the experiments and the cultural practices encountered, it appears that the evapotranspiration of alfalfa is consistently larger than that of barley, cotton, and sorghum. The evapotranspiration of cotton approaches that of alfalfa after a full cover has been developed.

Different relations appear to exist between the ratio of evapotranspiration to pan evaporation and crop height for a continuous crop and row crops.

5.2 Cotton Research Center runs. Micrometeorological data were collected over a wheat and oats combination and cotton at the Cotton Research Center in Tempe, Arizona. The experimental fields were divided into irrigation borders similar to those at Mesa. The micrometeorological sensors were located so that the minimum fetch would again be 30 m.

Daylight totals of the components of the energy balance equation and solar radiation are presented in Table 4. These basic data are discussed in the following sections.

5.2.1. Wheat and oats. The evapotranspiration data calculated for wheat and oats were normalized with respect to net radiation. The results are presented in Figure 11. The ratios of evapotranspiration to net radiation were greater than one for oats throughout most of the season, while the ratios for wheat were less than those of oats. The wheat crop appeared to be more advanced than the oats, maturing in early May, while the oats matured in early June. Comparing these data with results in Figure 9, it appears that the ratios for oats are similar to those for alfalfa, while the ratios for wheat are similar to those of barley, being less than those of alfalfa. The stand of wheat was much more dense and was about 50 cm taller than that of barley.

5.2.2. Cotton. The ratio of evapotranspiration to net radiation for cotton (Figure 11) was generally above one and was similar to that of alfalfa obtained at Mesa (Figure 9). The drop in the ratio between late June and middle July was associated with the general increase in the average vapor pressure of the air. On 30 June and 1 July the average air temperatures were 31C, vapor pressures were 10 mb, and the wind movements were 161 and 136 cm sec^{-1}, respectively, while on 14 and 16 July the average air temperatures were 30C, and the average vapor pressures were 20 mb. The average wind movement was 198 and 152 cm sec^{-1}, respectively. The general increase in atmospheric water vapor decreased the vapor-pressure gradient from the plant to atmosphere, thus reducing the evapotranspiration to a point where it was approximately equal to net radiation. The differences between 30 June and 1 July, and 14 July and 16 July, are associated with the difference in the average wind speed, the temperature and vapor pressure being similar for each pair of days.

During August a portion of the cotton field was not irrigated. This portion of the field did show the effects of lack of irrigation, even though it did receive a substantial amount of rain. The data collected over the two different treatments are indicated as wet and dry plots. The ratio of evapotranspiration to net radiation for the wet plot was greater than that for the dry plot, both being greater than one.

On 24 September the actual difference in evapotranspiration between the two plots was relatively small (18 ly). The difference in ratios was largely due to the difference in net radiation (40 ly). The dry plot appeared to be more brownish and to have a more open canopy than the wetter portion of the field, even though the field was uniform before the dry treatment was imposed.

5.2.3. Summary of the Cotton Research Center data. Although the crops were sampled too infrequently for definite conclusions to be drawn, the following trends were observed:

The ratio of evapotranspiration to net radiation of oats was generally greater than one and similar to that of alfalfa obtained at the Mesa Experimental Farm. The ratio of evapotranspiration to net radiation for wheat was generally one and similar to that obtained on barley at the Mesa Farm, even though the wheat was much denser and approximately 50 cm taller than barley.

The results obtained on the cotton plots indicated a ratio of evapotranspiration to net radiation greater than one throughout most of the season. These ratios were very comparable to the ratios obtained from alfalfa at the Mesa Experimental Farm. The dry treatment imposed upon part of the field decreased the evapotranspiration somewhat, but appeared to influence net radiation more by affecting the color and the density of the crop.

APPENDIX 1

Symbol	Units	Definition of Terms
A	$cal\ cm^{-2}\ min^{-1}$	Sensible heat flux
C_p	$cal\ g^{-1}\ {}^{o}C^{-1}$	Specific capacity of dry air at constant pressure
E	$cm\ cm^{-2}\ min^{-1}$	Evaporation rate
K_h	$cm^2\ min^{-1}$	Eddy diffusivity for heat
K_w	$cm^2\ min^{-1}$	Eddy diffusivity for water vapor
L	$cal\ g^{-1}$	Latent heat of vaporization
LE	$cal\ cm^{-2}\ min^{-1}$	Evaporative flux obtained from weighing lysimeters
$\widehat{LE}$	$cal\ cm^{-2}\ min^{-1}$	Evaporative flux determined with the Bowen ratio
P	mb	Absolute pressure
R_n	$cal\ cm^{-2}\ min^{-1}$	Net radiation
R_{sd}	$cal\ cm^{-2}\ min^{-1}$	Solar radiation down
R_{su}	$cal\ cm^{-2}\ min^{-1}$	Solar radiation up
S	$cal\ cm^{-2}\ min^{-1}$	Soil heat flux
S'	$cal\ cm^{-2}\ min^{-1}$	Change in energy storage in the layer of soil above the heat-flow transducer
T	${}^{o}C$	Temperature
$\overline{U}$	$m\ sec^{-1}$	Average wind speed
W	$cal\ cm^{-2}\ min^{-1}$	Change in energy storage in water
Z	cm	Height
c	$cal\ cm^{-3}\ {}^{o}C^{-1}$	Heat capacity of soil
d	cm	Depth
e	mb	Vapor pressure of air
t	minute	time

APPENDIX 1—Continued.

Symbol	Units	Definition of Terms
β_g		Gradient Bowen Ratio
ϵ		Ratio of mole weight of dry air to water vapor
γ	mb $^oC^{-1}$	$C_p P/L\epsilon$
ρ	g cm^{-3}	Density

Subscripts

b	Beginning of period
e	End of period

REFERENCES:

(1) I. S. Bowen.
1926. The ratio of heat losses by conduction and by evaporation from any water surface. Phys. Rev. 27:779-787.

(2) L. J. Fritschen.
Miniature net radiometer improvements.
Submitted to the J. App. Meteor.

(3) L. J. Fritschen and C. H. M. van Bavel.
1963. Micrometeorological data handling system.
J. App. Meteor. 2:151-155.

(4) C. B. Tanner.
1960. Energy balance approach to evapotranspiration from crops.
Soil Sci. Soc. Proc. 24:1-9.

PERSONNEL: Leo J. Fritschen

Table 1. Recording and sensor accuracy of micrometeorological elements

Element	Accuracy	
	Recording	Sensor
Net radiation	± 0.003 ly min^{-1}	± 0.02 ly min^{-1}
Solar radiation	± 0.003 ly min^{-1}	± 0.02 ly min^{-1}
Soil heat flux	± 0.003 ly min^{-1}	± 0.02 ly min^{-1}
Temperature absolute	± 0.25C	± 0.41C
1-Junction differential	± 0.125C	± 0.125C
2-Junction differential	± 0.062C	± 0.062C
Vapor pressure	0.4 mb at 30 mb	1 mb at 30 mb
Wind speed	0 m sec^{-1}	± 0.15 m sec^{-1}

Table 2. Summary of evapotranspiration of alfalfa obtained from weighing lysimeters and determined by the Bowen ratio

Date	Run	Lys	R_{sd}	R_n	S+S'	LE	A	$\widehat{LE}$	LE	$\widehat{LE}$
1964			ly day^{-1}						ly period^{-1} [a]	
30 Jan	A4-1	1	362	156	8	−108	−56			
		2		105	6	−115	4			
		2 [b]				−95		[c] −97	−87	[c] −85
5 Mar	A4-2	1	504	206	2	−208	0	[c] −192	−198	[c] −234
		2		192	9	−217	16	[c] −182	−206	[c] −224
		3		193	8	−211	10	[c] −188	−196	[c] −217
		2		192	9	−217	16	[d] −194	−206	[d] −197
7 Apr	A4-3	1	618	295	−5	−318	28			
		2		282	2	−324	40			
23 May	A4-4	1	594	327	−6	−452	131			
		3		308	−12	−401	105			
24 May	A4-4	1	656	377	−11	−512	146			
		3		365	−12	−467	114			
28 Jul	A4-5	3	627	389	2	−505	114	−502	−480	−500
29 Jul	A4-5	3	390	239	2	−506	265	−445	−449	−446

[a] Period consisted of hours of positive net radiation.

[b] The 16th and 17th hours omitted from totals because of equipment adjustment.

[c] Differential psychrometers used for vapor-pressure gradient.

[d] Differential dew probes used for vapor-pressure gradient.

Table 3. Daylight totals of solar and net radiation, soil heat flow, evapotranspiration, and sensible heat measured over alfalfa, barley, cotton, and sorghum at the Mesa Experimental Farm

Date	Run	Crop	Height	R_{sd}	R_n	S+S'	$\widehat{LE}$	A
1964			cm	<———	ly	———>		
13 Mar	AB4-1	alfalfa	2	429	247	–51	–250	54
		barley	5		236	–70	–215	49
25 Mar	AB4-2	alfalfa	40	620	318	–49	–282	13
		barley	15		288	–78	–207	–3
7 Apr	AB4-3	alfalfa	30	636	366	–31	–461	126
		barley	80		330	–71	–341	82
2 May	AB4-4	alfalfa	62	651	396	–18	–677	299
		barley	77		373	–58	–415	100
3 May	AB4-4	alfalfa	62	677	397	–21	–658	282
		barley	77		368	–55	–468	145
13 May	AB4-5	alfalfa	71	532	297	–39	–329	71
		barley	94		269	–49	–314	94
15 May	AC4-1	alfalfa	18	709	428	–45	–554	171
		cotton	8		318	–86	–108	–124
27 May	AB4-6	alfalfa	48	660	390	–22	–726	358
		barley	76		323	–63	–73	–188
29 May	BC4-1	barley	76	712	331	–39	–27	–265
		cotton	16		366	–57	–228	–81
23 Jun	AC4-3	alfalfa	75	724	446	–24	–620	198
		cotton	35		360	–10	...	...
24 Jun	AC4-3	alfalfa	75	644	424	–17	–601	194
		cotton	35		351	–2	–367	18

Table 3. Continued.

Date	Run	Crop	Height	R_{sd}	R_n	S+S'	$\widehat{LE}$	A
1964			cm	<———		ly		———>
7 Jul	AC4-4	alfalfa	30	618	398	−35	−386	22
		cotton	76		341	−56	−404	119
21 Jul	AC4-5	alfalfa	66	588	396	−5	−389	−2
		cotton	90		368	−25	−553	209
23 Jul	AS4-1	alfalfa	60	565	391	−24	−375	8
		sorghum	38		322	−40	−357	75
5 Aug	AS4-2	alfalfa	59	529	344	−7	−617	280
		sorghum	83		322	−24	−397	99
7 Aug	AC4-6	alfalfa	20	619	405	−40	−649	284
		cotton	115		385	−28	−387	30
18 Aug	AS4-3	alfalfa	27	608	366	−20	−482	136
		sorghum	105		362	−23	−431	92
20 Aug	AC4-7	alfalfa	45	548	372	−13	−607	248
		cotton	117		330	−16	−480	166
1 Sep	AS4-4	alfalfa	45	575	371	+32	−602	199
		sorghum	130		341	−24	−495	178
22 Sep	AS4-5	alfalfa	22	414	241	−40	−447	246
		sorghum	135		241	−4	−282	45

Table 4. Daylight totals of solar and net radiation, soil heat flow, evapotranspiration, and sensible heat measured over wheat, oats, and cotton at the Cotton Research Center, Tempe

Date	Run	Crop		Height	R_{sd}	R_n	S+S'	$\widehat{LE}$	A
1964				cm	<———		ly		———>
27 Feb	W04-1	wheat		10	478	277	–78	–216	17
		oats		10		275	–96	–260	18
10 Apr	W04-2	wheat		80	615	365	–42	–347	24
		oats		60		338	–39	–565	266
11 Apr	W04-2	wheat		80	608	363	–40	–331	8
		oats		60		331	–40	–541	251
23 Apr	W04-3	wheat		123	645	390	–35	–496	141
		oats		83		361	–27	–472	138
6 May	W04-4	oats		108	667	359	–13	–435	89
7 May	W04-4	wheat		130	669	415	–36	–412	33
20 May	W04-5	wheat		130	672	371	–58	–24	–289
		oats		168		408	–42	–618	252
6 Jun	C4-1	cotton		33	724	382	–63	–311	–8
30 Jun	C4-2	cotton		64	681	382	30	–610	197
1 Jul	C4-2	cotton		64	605	345	29	–542	168
14 Jul	C4-3	cotton		72	527	360	7	–363	–4
16 Jul	C4-3	cotton		72	661	425	–24	–344	–57
3 Sep	C4-5	cotton	dry	110	582	336	–30	–478	171
			wet	110		333	–31	–525	223
24 Sep	C4-6	cotton	dry	90	489	301	–23	–457	90
			wet	105		260	–30	–475	105

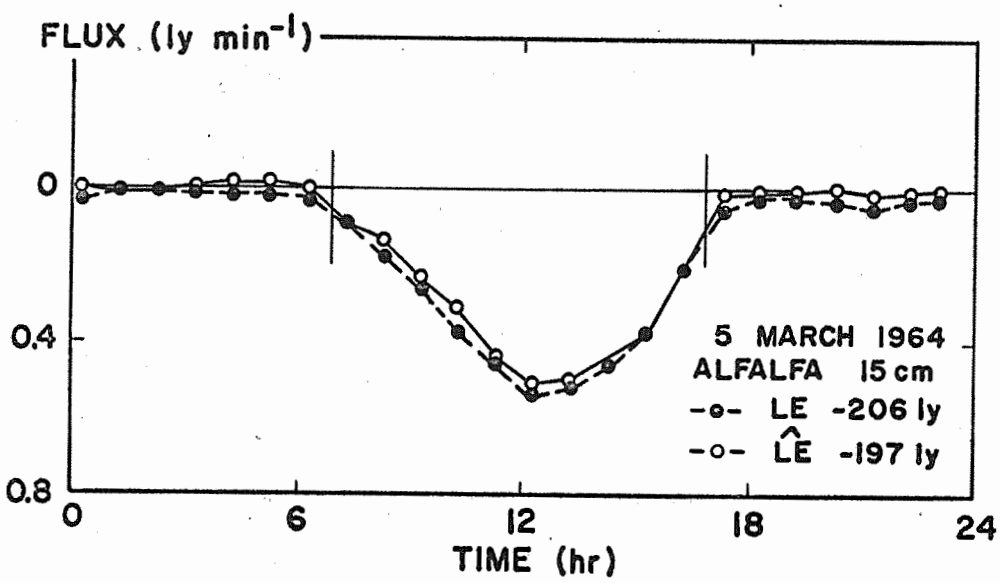

Figure 1. Comparison of hourly evaporative flux from 15-cm alfalfa obtained from a weighing lysimeter, LE, and calculated with the Gradient Bowen Ratio, $\widehat{LE}$, on 5 March 1964.

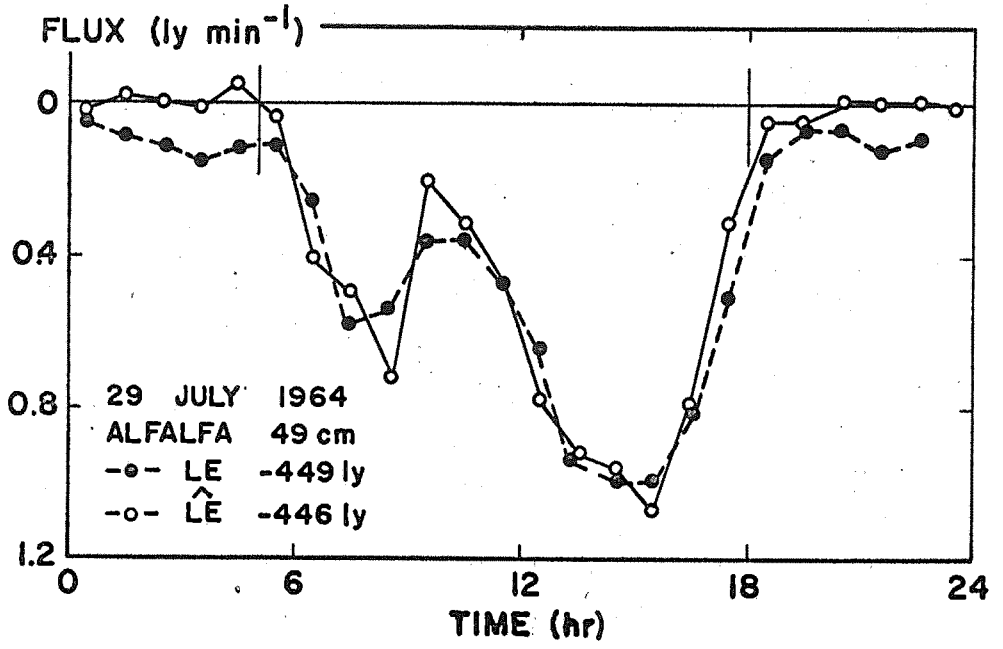

Figure 2. Evaporative flux determined by the Gradient Bowen Ratio with air samplers set for 35-cm gradients and located 80 feet apart.

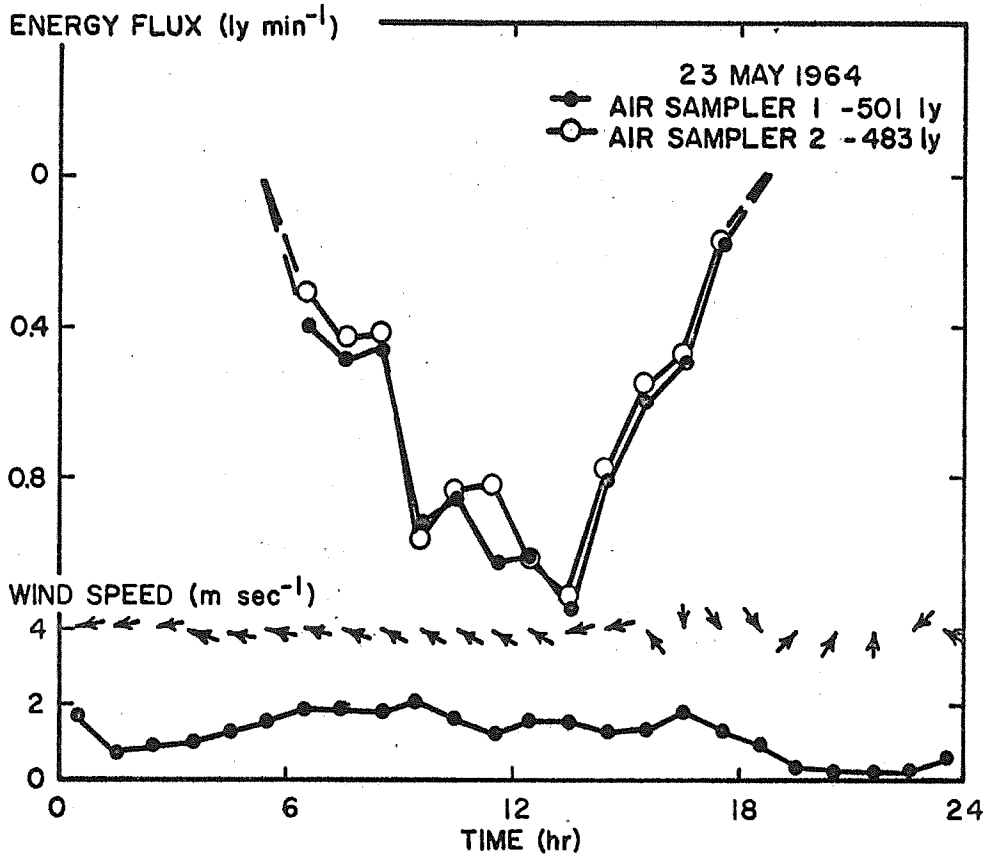

Figure 3. Evaporative flux determined by the Gradient Bowen Ratio with air sampler 1 set for 75-cm gradient and air sampler 2 set for 35-cm gradient.

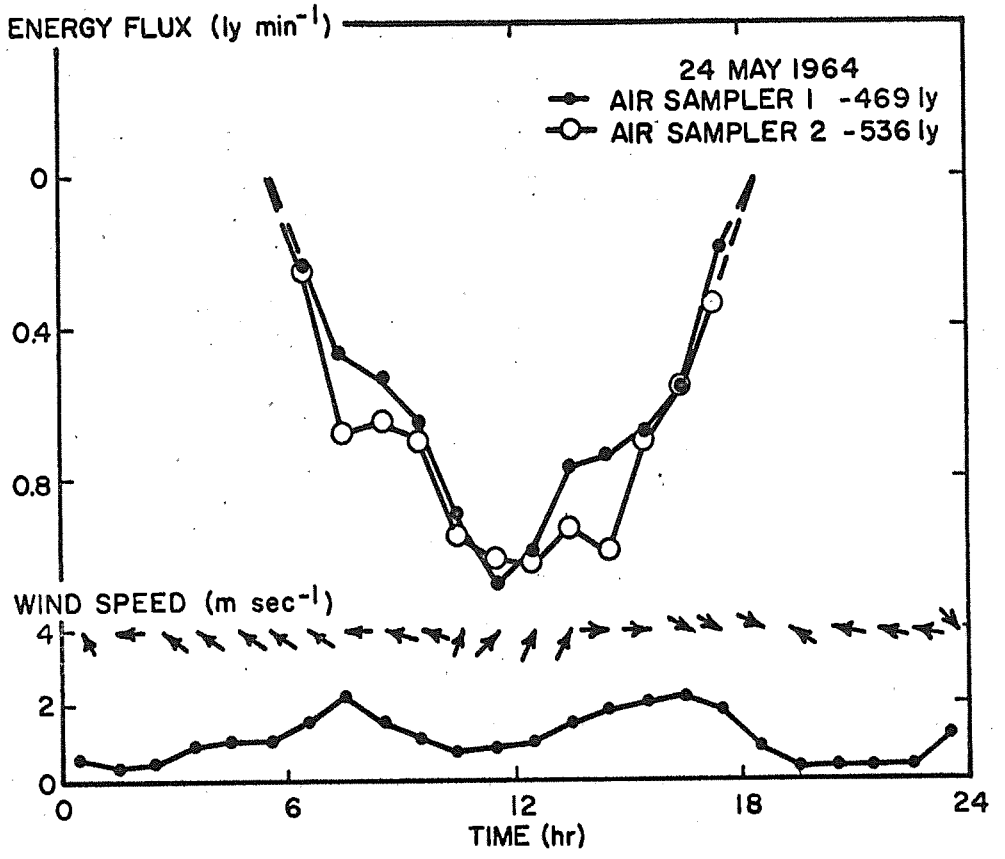

Figure 4. Comparison of hourly evaporative flux from a weighing lysimeter, LE, and calculated with the Gradient Bowen Ratio, $\widehat{LE}$, on 29 July 1964.

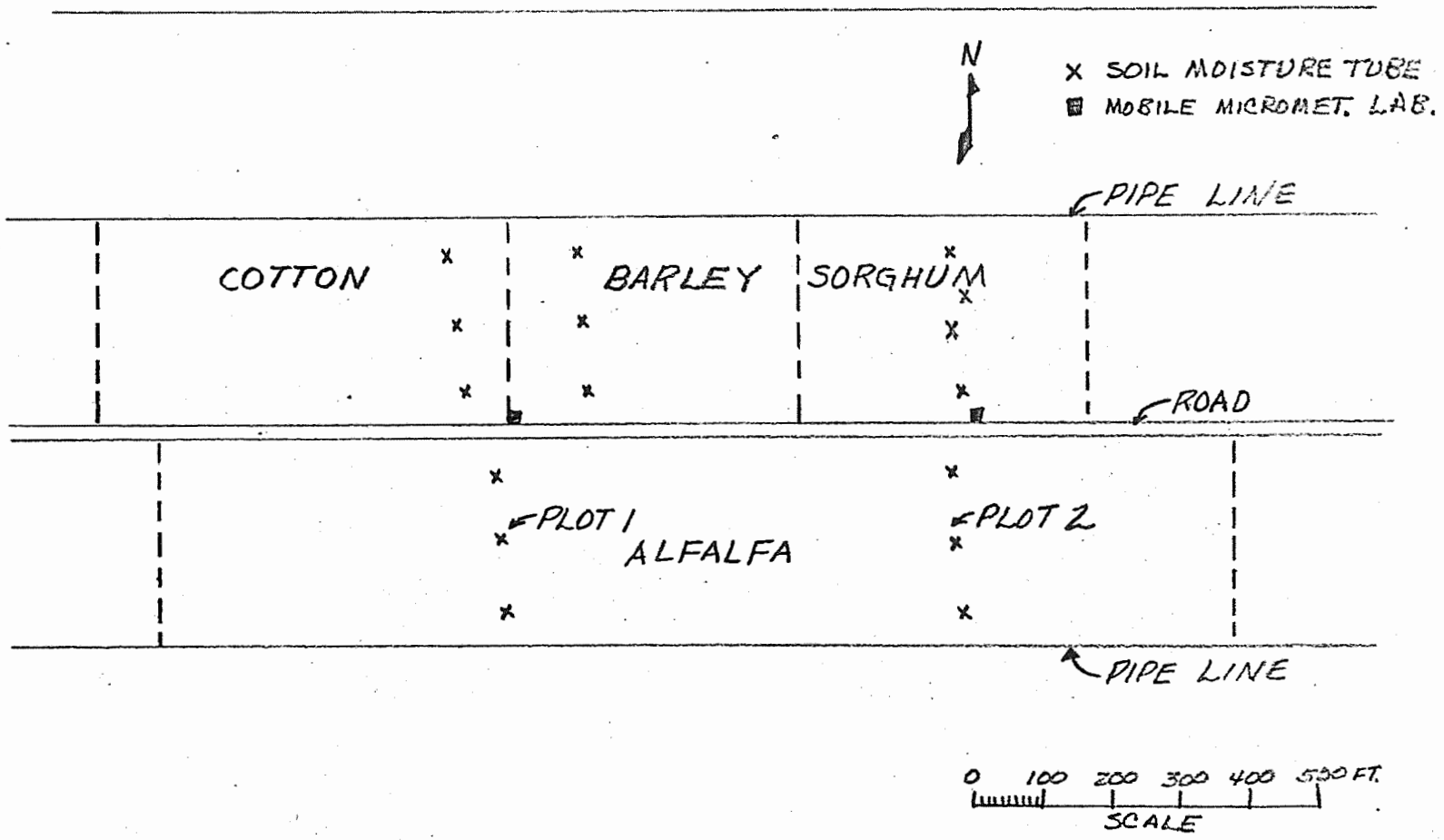

Figure 5. A portion of the east half of University of Arizona Experimental Farm in Mesa.

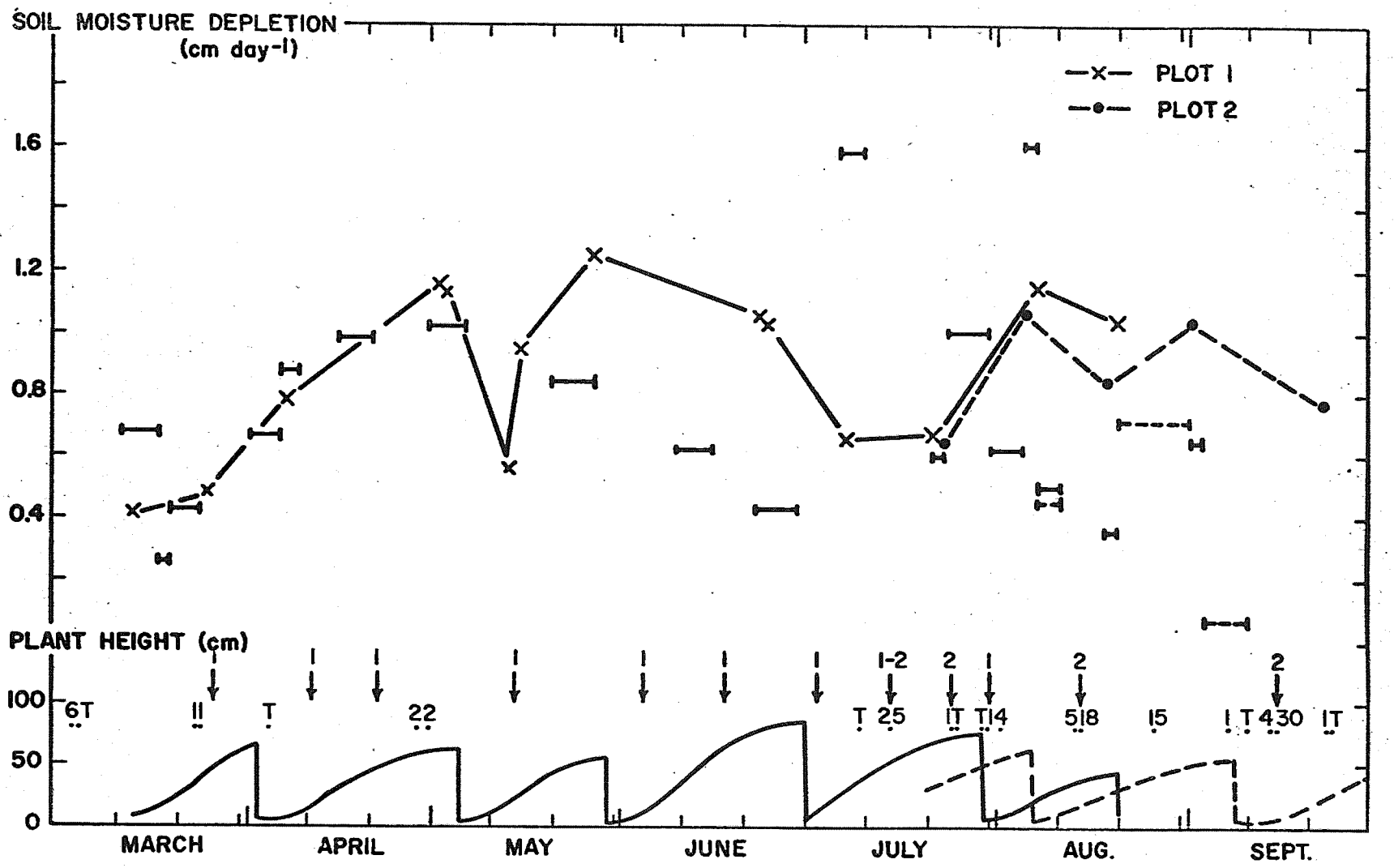

Figure 6. Soil-moisture depletion, evaporative flux, crop height, time of irrigation (↓) of alfalfa, and rainfall (mm) at the Mesa Experimental Farm, 1964.

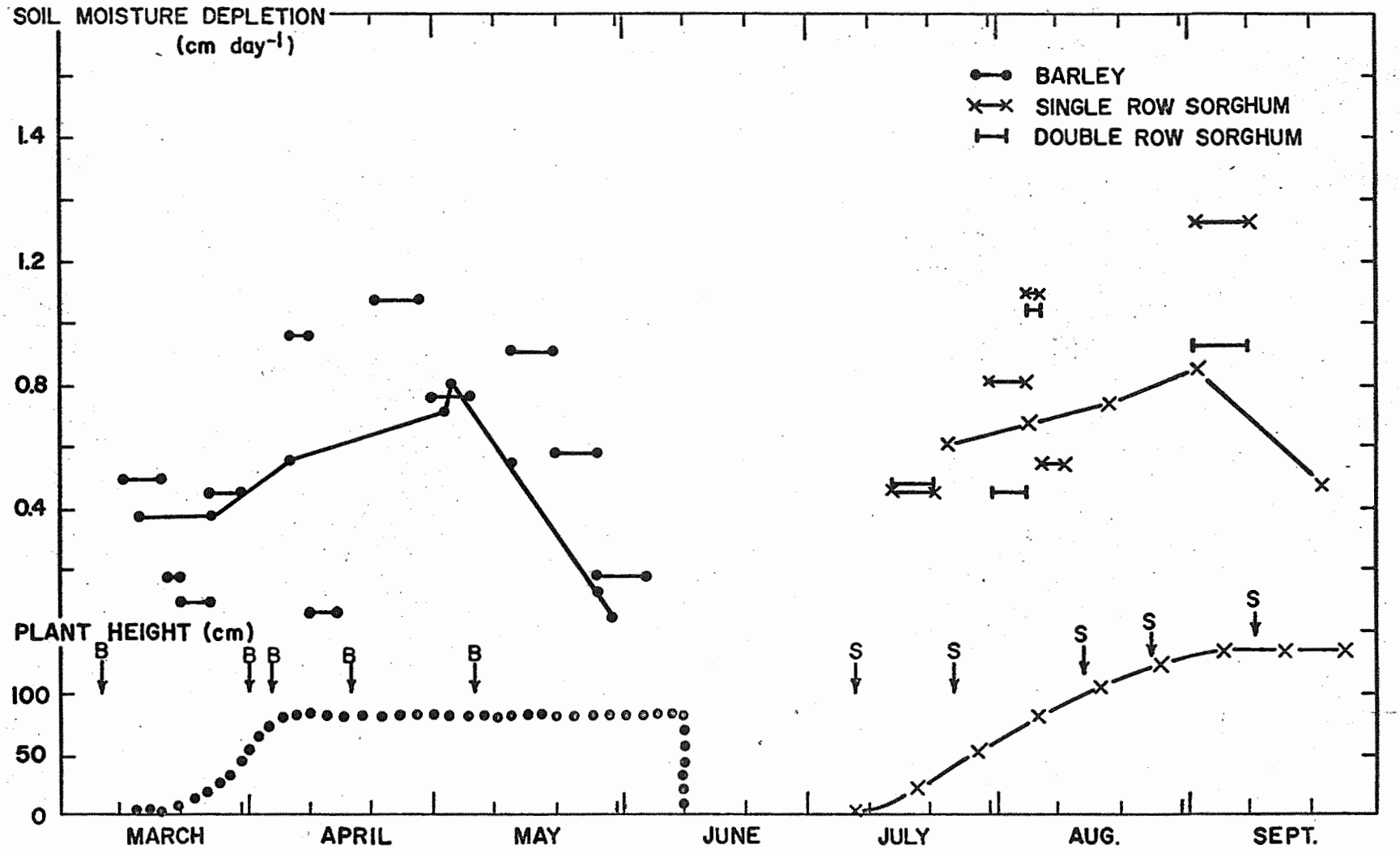

Figure 7. Soil-moisture depletion, evaporative flux, crop height, and time of irrigation (↓) of barley and single and double rows of sorghum at the University of Arizona Experimental Farm in Mesa, 1964.

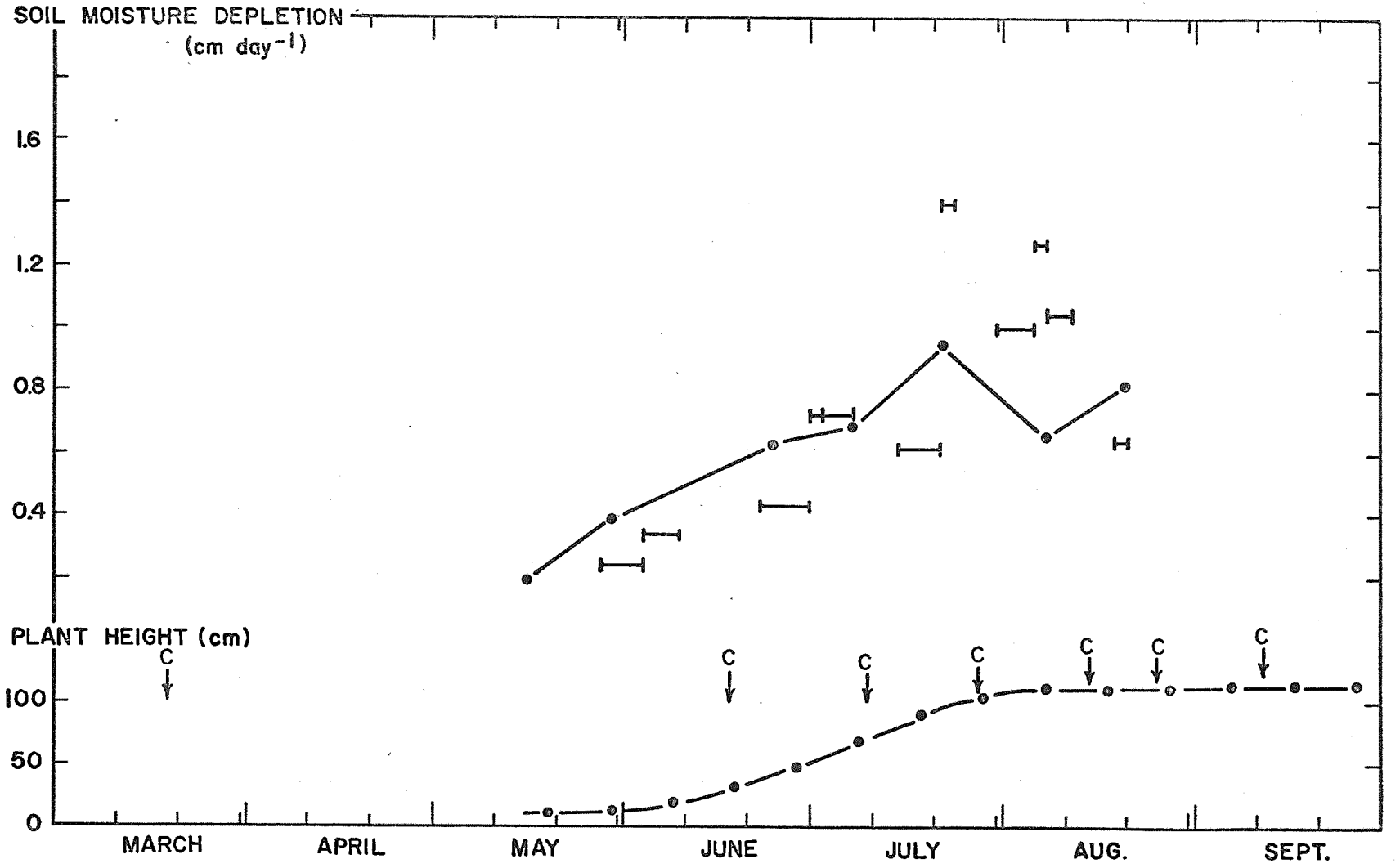

Figure 8. Soil-moisture depletion, evaporative flux, crop height, and time of irrigation (↓) of cotton at the University of Arizona Experimental Farm in Mesa, 1964.

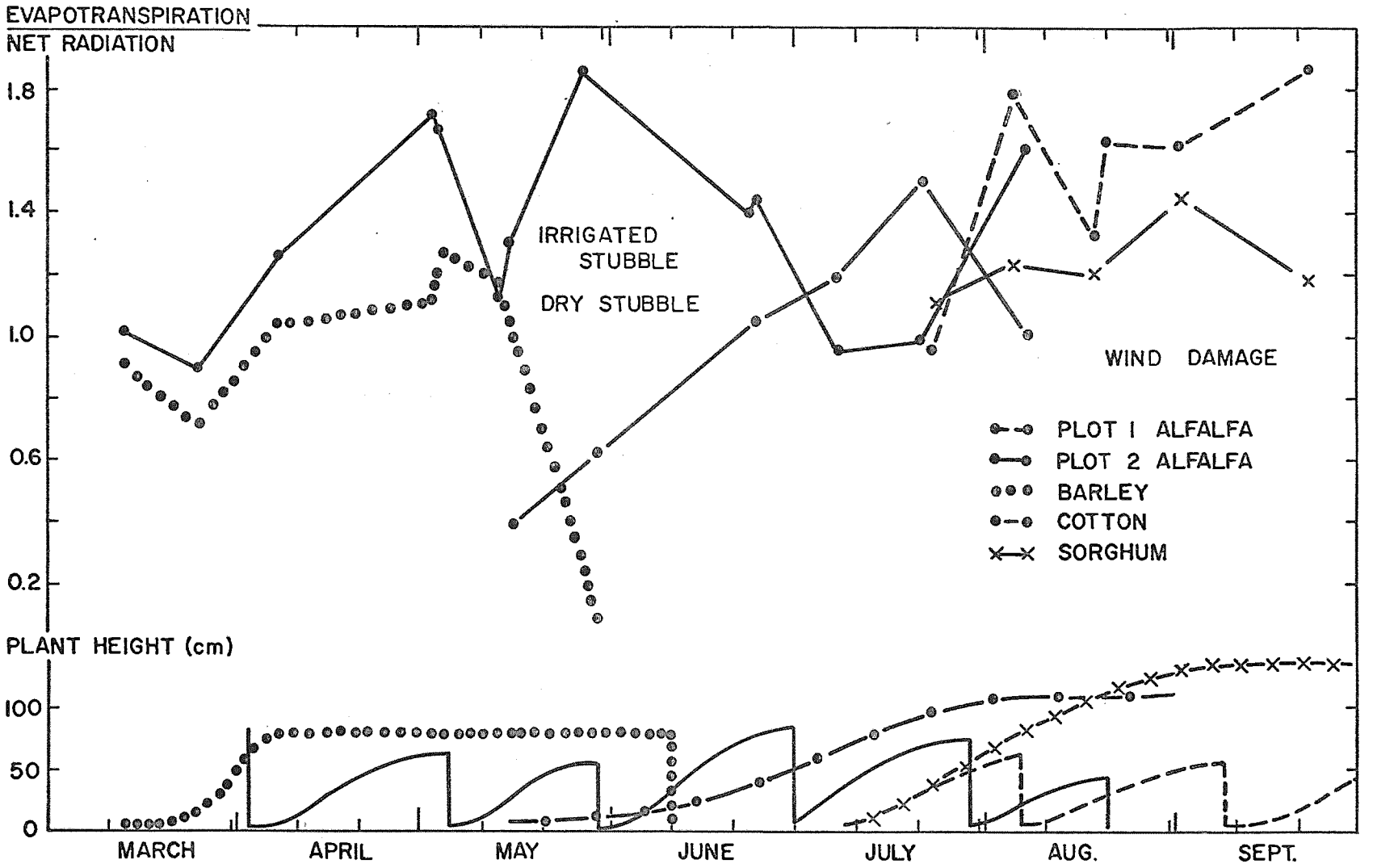

Figure 9. The ratio of evapotranspiration to net radiation and crop height of alfalfa, barley, cotton, and sorghum at the University of Arizona Experimental Farm in Mesa, 1964.

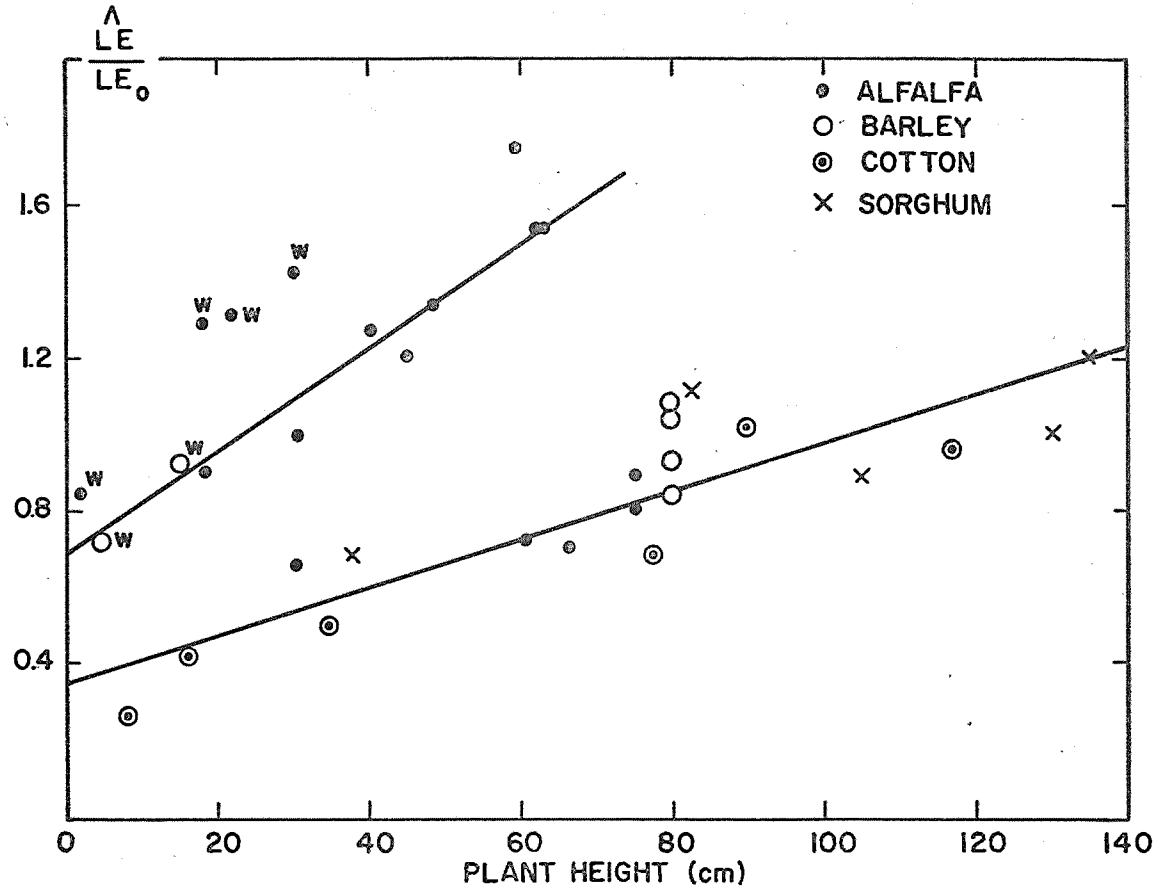

Figure 10. The ratio of evapotranspiration to pan evaporation as a function of crop height of alfalfa, barley, cotton, and sorghum.

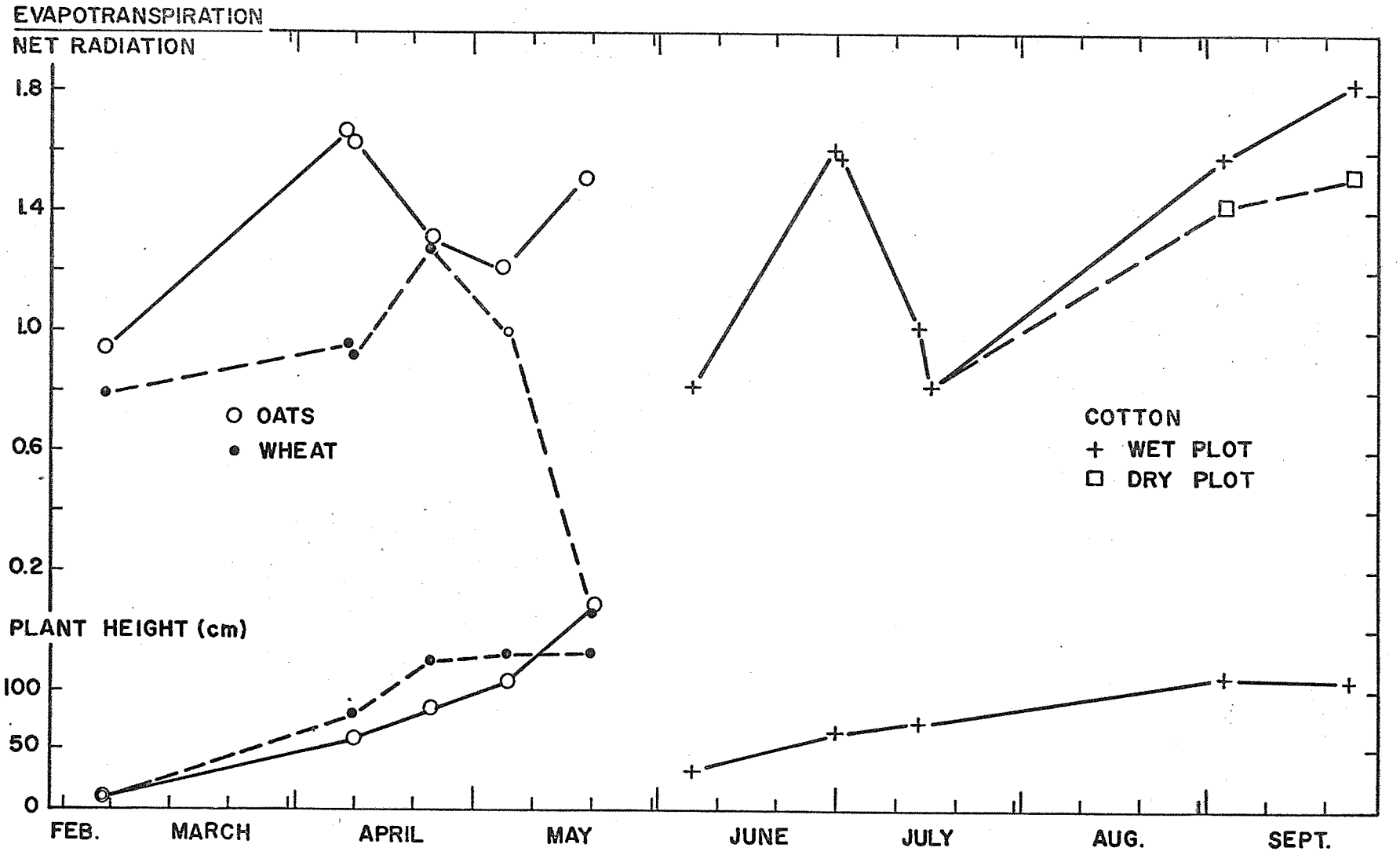

Figure 11. The ratio of evapotranspiration to net radiation and crop height of wheat, oats, and cotton at the Cotton Research Center in Tempe, 1964.

TITLE: DIRECT MEASUREMENT OF EVAPOTRANSPIRATION AND THE ENERGY BALANCE OF IRRIGATED CROPS

LINE PROJECT: SWC 4-gG2 CODE NO.: Ariz-WCL-33

INTRODUCTION:

This Annual Report is presented in four parts as follows:

		PAGE
PART 1.	Evapotranspiration and energy balance of alfalfa	33-2
PART 2.	Evapotranspiration and energy balance of small grain	33-6
PART 3.	Evapotranspiration and energy balance of cotton.	33-10
PART 4.	Routine weather data	33-17

However, the Summary and Conclusions section applies to the experimental outline as a whole.

PART 1. EVAPOTRANSPIRATION AND ENERGY BALANCE OF ALFALFA

INTRODUCTION:

It was convincingly demonstrated during 1963 that the water losses from alfalfa, when well-watered, can be accurately predicted with a combination or modified Penman method. In this model, meteorological quantities are used without resort to empiricism, and we can expect this result to be generally applicable.

The effects of limited soil moisture supplies were also studied in 1963, but the data were not of ideal quality. Therefore, the investigation was continued during 1964 with the purpose of testing a revised form of the combination formula which accounts for stomatal resistance.

PROCEDURE:

Using the data from the weighable lysimeters and the routine weather station, the energy balance and other atmospheric factors were available on a continuous basis. A number of long irrigation cycles were imposed with the object of depleting soil moisture to the point of limiting transpiration. In addition to the atmospheric measurements, soil moisture content was monitored weekly inside and outside of the lysimeters and crop heights were recorded.

Data were analyzed by computing hourly potential evaporation and combining it with hourly actual evaporation to see if a measurable transpiration resistance had developed. This analysis has not been completed to date.

The following irrigation cycles were established; at the end of which the crop was mown close to the ground.

25 February	-	2 April		Cycle 1
10 April	-	13 May		Cycle 2
28 May	-	29 June		Cycle 3
8 July	-	3 September	-	Cycle 4

RESULTS AND DISCUSSION:

Data from the Cycle 1 have not been fully analyzed. However, on 28 March the actual evaporation was 69 percent of the potential one; thus, this series should give interesting data. It was discontinued because rainstorms had resulted in a ragged, irregular crop cover by 25 March.

At the end of Cycle 2 - on 11 May - evaporation was still close to the potential rate and thus, little information is to be expected from these data.

Cycle 3 was of considerable interest since evaporation went down to a negligible amount and weather conditions were ideal. Table 1-1 gives values of actual and potential evaporation on the days calculated, and also the value of the stomatal or leaf resistance at 1430. This summary table shows that evaporation at the potential rate prevails for a considerable period of time after irrigation (28 May). After about 20 days, evaporation is progressively reduced and appreciable surface resistance can be calculated from the data. This surface resistance - residing in the stomata - exhibits a typical diurnal pattern, exemplified in Figure 1-1.

Data from the last cycle of 1964 have not been fully elaborated, but show a pattern similar to that of Cycle 3. However, the latter data are the most informative since, during the entire period, weather conditions were ideal and nearly constant.

Table 1-1. Daily evaporation from alfalfa (1964) in mm and ratio to potential evaporation. Also, calculated surface resistance at 1430 in min cm^{-1}.

Date	Month	E	E/E_o	R_L'
		mm		min cm^{-1}
1	Jun	9.25	0.95	.000
5	Jun	9.09	1.00	.000
10	Jun	9.53	1.13	.000
16	Jun	9.65	1.04	.000
18	Jun	8.43	1.03	.000
20	Jun	7.11	0.86	.020
22	Jun	5.34	0.71	.070
24	Jun	4.60	0.47	.218
26	Jun	2.94	0.56	.280
28	Jun	2.53	0.29	.383
30	Jun	1.27	0.13	.480

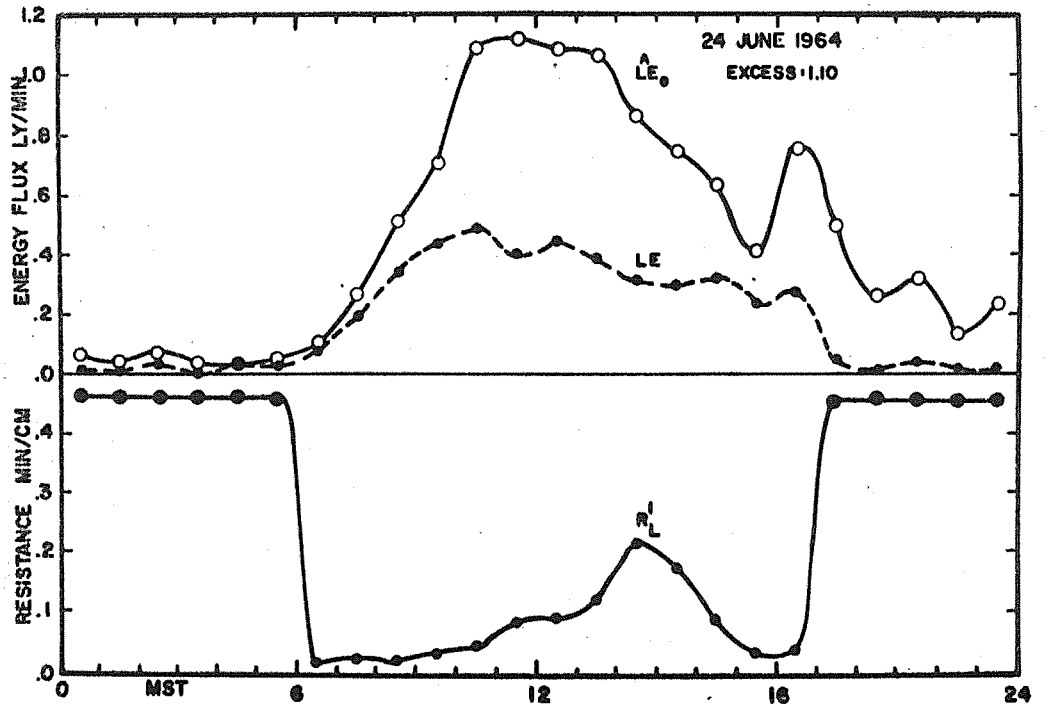

Figure 1-1. Potential (open circles) and actual (solid circles) evaporation from alfalfa on 24 June 1964. Also, calculated canopy resistance to evaporation.

PART 2. EVAPOTRANSPIRATION AND ENERGY BALANCE OF SMALL GRAIN

INTRODUCTION:

McIlroy has proposed a form of the combination method which is particularly adapted to the nature of most routine observations of humidity; that is, by wet bulb psychrometry or a hair hygrometer. The method requires the correlation of the vapor exchange coefficient to the windspeed by empirical means. Since the method is intended to apply to daily values of pertinent weather variables, additional empiricism is hidden in the wind function - inasmuch as the combination method applies strictly to short-time values only.

The adequacy of the McIlroy procedure was evaluated in 1964 on two small grain fields - one in oats and the other in wheat - during the period 1 April through 1 June.

PROCEDURE:

Air temperature and humidity were measured at a height of 40 cm over the crop with hygrothermographs. Windspeed was recorded at the same height with Casella anemometers; net radiation at 1 m over the crop with polyethylene net radiometers continuously recording.

The evaporation was determined from twice-weekly measurements of soil moisture using the neutron method. Attempts were made to measure the hydraulic gradient below the measurement zone, but were not successful due to lack of experience.

Irrigation of the fields was carried out by the management of the Cotton Research Center, where the plots were located.

Data were evaluated by summaries of irregular periods, usually overnight and 2-hour periods by day. On several days, detailed measurement of the evaporation was made using the Gradient Bowen Ratio method (see WCL 32). This provided an alternative method for finding the vapor transfer coefficient.

Although intended, a period of moisture stress never was developed because the farm management did not wish to postpone irrigation to the required date. Thus, the entire project was limited to a study of potential evaporation.

RESULTS AND DISCUSSION:

It turned out to be impossible to arrive at a reliable interpretation of the soil moisture data over short periods of time, as was more or less expected, with irrigations scheduled every 3 weeks and the precision of the neutron method being what it is. A brief summary of the data is as follows:

	Wheat	Oats
Irrigation	24 March	24 March
Daily Depletion 30 March - 13 April	6.3 mm	7.4 mm
Irrigation	14 April	15 April
Daily Depletion 20 April - 4 May	4.5 mm	7.8 mm
Irrigation	-	11 May
Daily Depletion		
4 May - 18 May	5.4 mm	-
18 May - 1 June	1.2 mm	6.1 mm
1 June - 15 June	-	1.0 mm

The 14-day values of soil moisture depletion established about a week or so after irrigation are reasonable and compare well with values obtained on single days by the Bowen Ratio method. However, having been taken over long periods of time, correlation with windspeed is impossible. This experience demonstrated again that soil moisture measurement cannot be employed to verify meteorological models or climatological formulas over periods of one or several days, even if a considerable period of time, say 8 to 10 days, is discounted following irrigation.

Correlation with hourly values from the Bowen Ratio method gave better results. Plots of the vapor transfer coefficient versus windspeed by the hour still gave very scattered relations, but the estimates of the vapor transfer coefficient based thereon resulted in reasonably close predictions. An example is shown in Figure 2-1, comparing measured values of ET with the McIlroy formula calculations. One should remember, however, that these data embody an automatic correlation through the empirical value of the transfer coefficient.

Further evaluation of the data is still pending, but the main conclusion is that the instrumentation used gave reasonable predictions of the evaporation, once the wind function was found or assumed from other work. Establishment of wind function for individual crops through standard soil moisture studies appears not feasible.

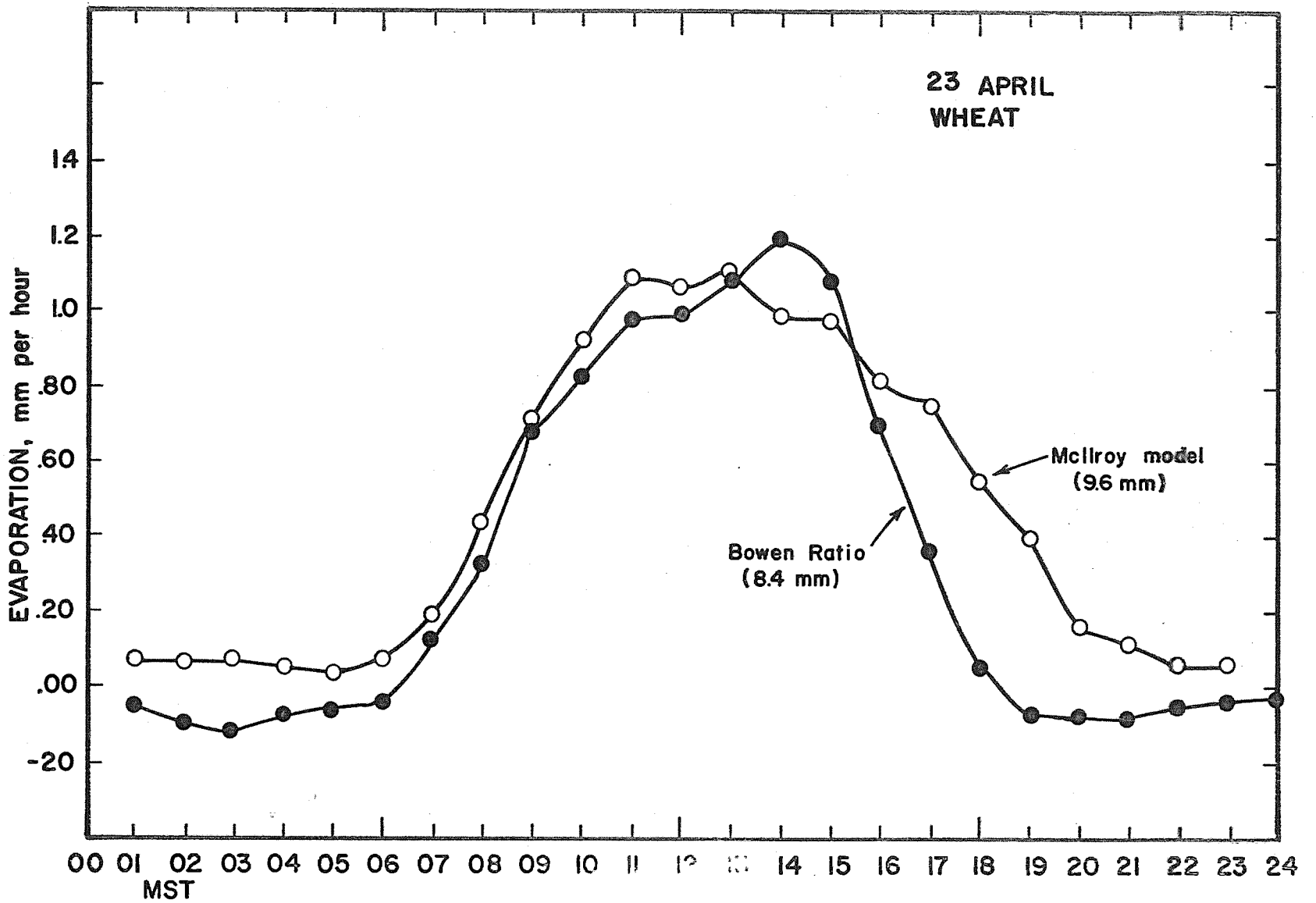

Figure 2-1. Evaporation from wheat on 23 April 1964 as found with the Gradient Bowen Ratio method and from the McIlroy model. Indicated totals are for daytime only.

Annual Report of the U.S. Water Conservation Laboratory

PART 3. EVAPOTRANSPIRATION AND ENERGY BALANCE OF COTTON

INTRODUCTION:

With much the same background as given under Part 2, a study was conducted in 1964 on an irrigated field of Deltapine cotton during the period 1 May - 14 September.

PROCEDURE:

The cotton study could be more completely instrumented than the corresponding one on small grain. Measurement of air temperature and relative humidity was done with hygrothermographs in insulated boxes with forced ventilation. Windspeed was measured with Casella anemometers and by photographing the registers every two hours. Net radiation was obtained with polyethylene-covered, insulated, miniature net radiometers.

A major improvement was the installation of 2 weighable lysimeters of the single load cell type (see Annual Report 1962). Each of these had 5 cotton plants in it. Neutron tubes were also installed and read twice weekly. Two differential tensiometers were installed at or near the lower boundary of the root zone to ascertain the moisture loss by seepage.

Cotton was planted on 30 March and the field installation was completed during April. The first irrigation was on 27 April and data were collected regularly following this irrigation.

Further irrigation dates were:

19 May

19 June

9 July

31 July

On 27 August the entire field (H-3) was irrigated except some 40 rows in which observations were made.

Meteorological measurements were reduced by 2-hour intervals, while lysimeter evaporation data and hydraulic gradients were measured daily. After 1 July, periodic measurements were made of the leaf diffusion resistance for correlation with decline in evaporation. These data are summarized in WCL-29 - Part 5.

RESULTS AND DISCUSSION:

At first, difficulty was encountered in establishing a stand in the lysimeters because the plants had to be transplanted. Later the plants in the lysimeters tended to be shorter than the surrounding ones, but as of 1 July a very representative stand was obtained. At the same time, plants in adjacent rows had effectively grown together.

Irrigations were scheduled too close together to permit any appreciable moisture deficit to develop, excepting the last period of observation. Also, the amount of water applied exceeded, in typical fashion, the requirement by a substantial margin. Thus, there is ample reason to doubt the validity of equating moisture depletion to evaporation. That this was indeed the case is illustrated by Figures 3-1 and 3-2. In Figure 3-1 the daily evaporation, averaged over "neutron periods" (3 or 4 days) as found from the lysimeters, is compared with soil moisture depletion. It may be seen that the soil moisture depletion values are more erratic than the lysimeter data, but also that they are badly off after the 9 July and 31 July irrigations. Agreement was better, but not satisfactory, after the 19 May and 19 June irrigation. However, during the latter part of August and early September, the two methods gave substantially the same answer.

The reason for disagreement is apparent from Figure 3-2, showing the hydraulic gradient at 135 cm depth. This gradient approaches unity for many days after irrigation and does not vanish until the 10th or 15th day. At the same time, moisture tension at that depth was estimated at about 100 mb and substantial seepage out of the root zone is implied.

The two independent sets of data bear out earlier contentions that soil moisture depletion cannot routinely be used to find evapotranspiration under a system of frequent irrigation.

In regard to evaluation of the McIlroy model, final analysis is not available. The instrumentation, upon comparison with other data, did give reliable primary data, but the correlation of the vapor transfer coefficient to windspeed proved to be inconclusive upon first

attempt. This is mainly ascribed to the fact that all manner of windspeeds occur in our climate during a 24-hour period, the shortest for which evaporation data were available. In contrast, daily averages for windspeed tend to be much the same.

The use of a wind function obtained from the alfalfa data (see Part 1) gave reasonable agreement between calculated and measured evaporation from the cotton. However, such a result would hardly answer the original intent of the investigation.

For some days, a detailed investigation using Bowen Ratio data could be made. This part of the study is incomplete as is an evaluation of the effect of declining soil moisture reserves on evaporation as found during the last irrigation cycle.

Figure 3-3 presents a summary record of soil moisture content (0 - 160 cm) and of measured evaporation. This record makes it obvious that moisture depletion in the first four irrigation cycles was only partial. Therefore, in the third and fourth cycle where the cover was complete, evaporation is not influenced by soil moisture. In the first two cycles, the effect of surface soil drying is apparent.

During the final cycle, the effect of soil moisture on evaporation became apparent around 29 August (see Figure 5-3, WCL 26), since potential evaporation was not attained. From the ratio of potential to actual evaporation, an approximate 24-hour value of the canopy resistance in min cm^{-1} may be computed. In Figure 3-4, this quantity has been plotted versus soil moisture tension in the top 100 cm and an apparently consistent relation emerges, roughly of the form

$$t^a + b = (R_L')^c + d$$

in which t is the soil moisture tension, R_L' the canopy resistance and a, b, c and d, constants. The data further suggest that at tension of 1 bar, R_L' becomes of equal magnitude as the aerodynamic transfer coefficient (designated as $1/B_v$ in WCL 33 - 1963, but here expressed in min cm^{-1}) and thus, begins to influence evaporation.

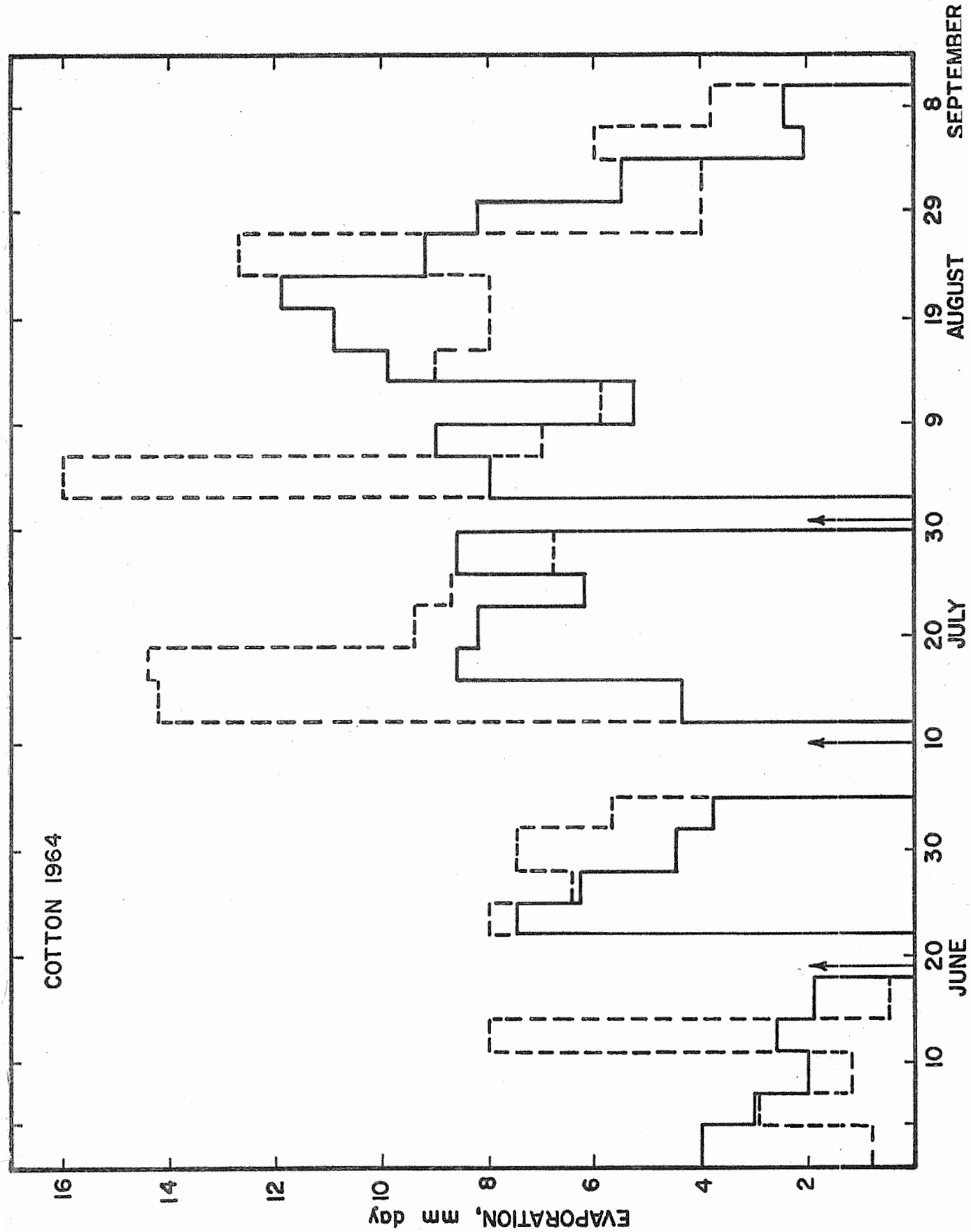

gure 3-1. Evaporation from cotton in 1964 as measured with single load cell lysimeters (solid histogram) and as calculated from twice-weekly soil moisture measurements (interrupted histogram). Arrows indicate time of irrigation.

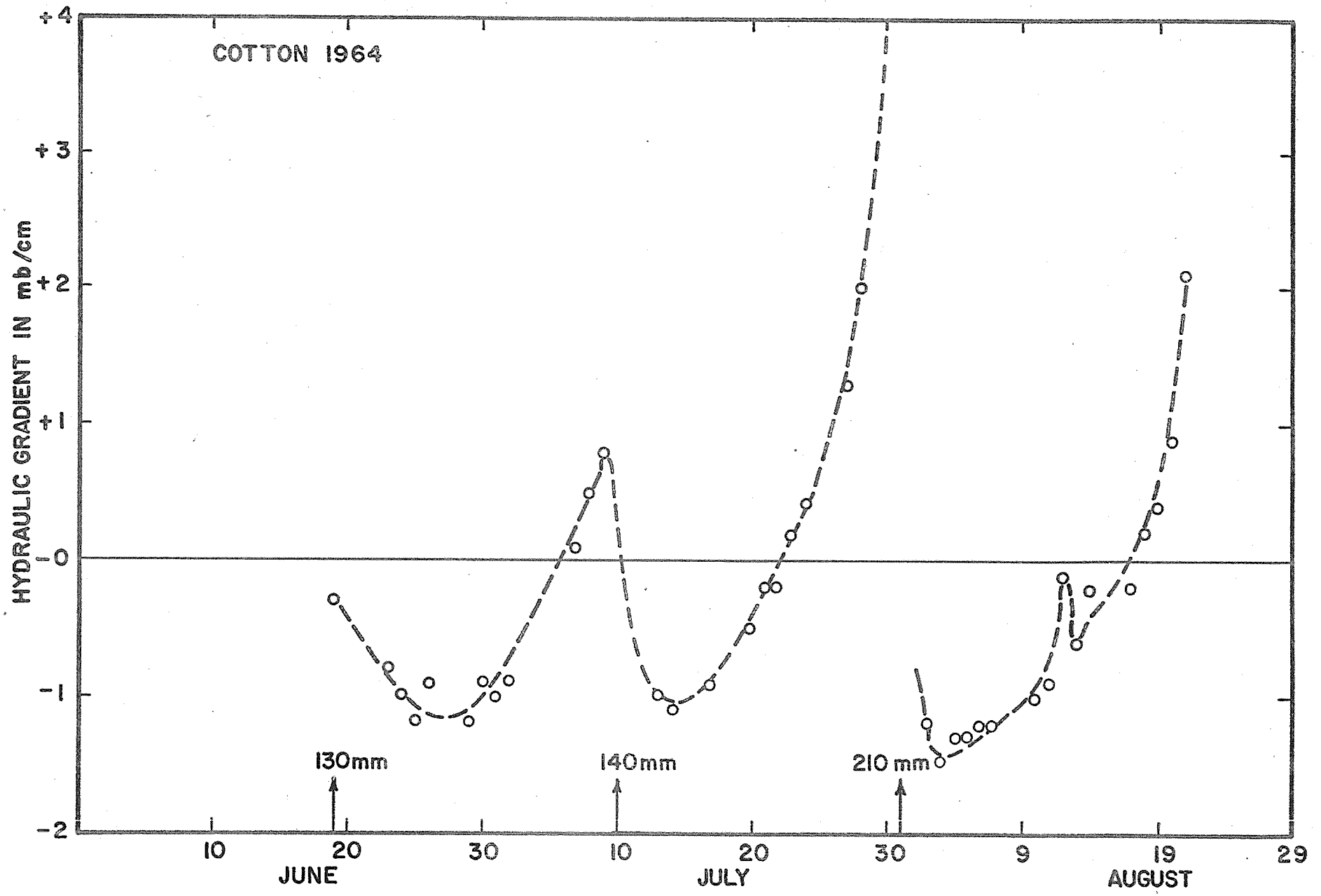

Figure 3-2. Hydraulic gradient at 135 cm depth as measured under an irrigated cotton field. Arrows indicate time and quantity of irrigation.

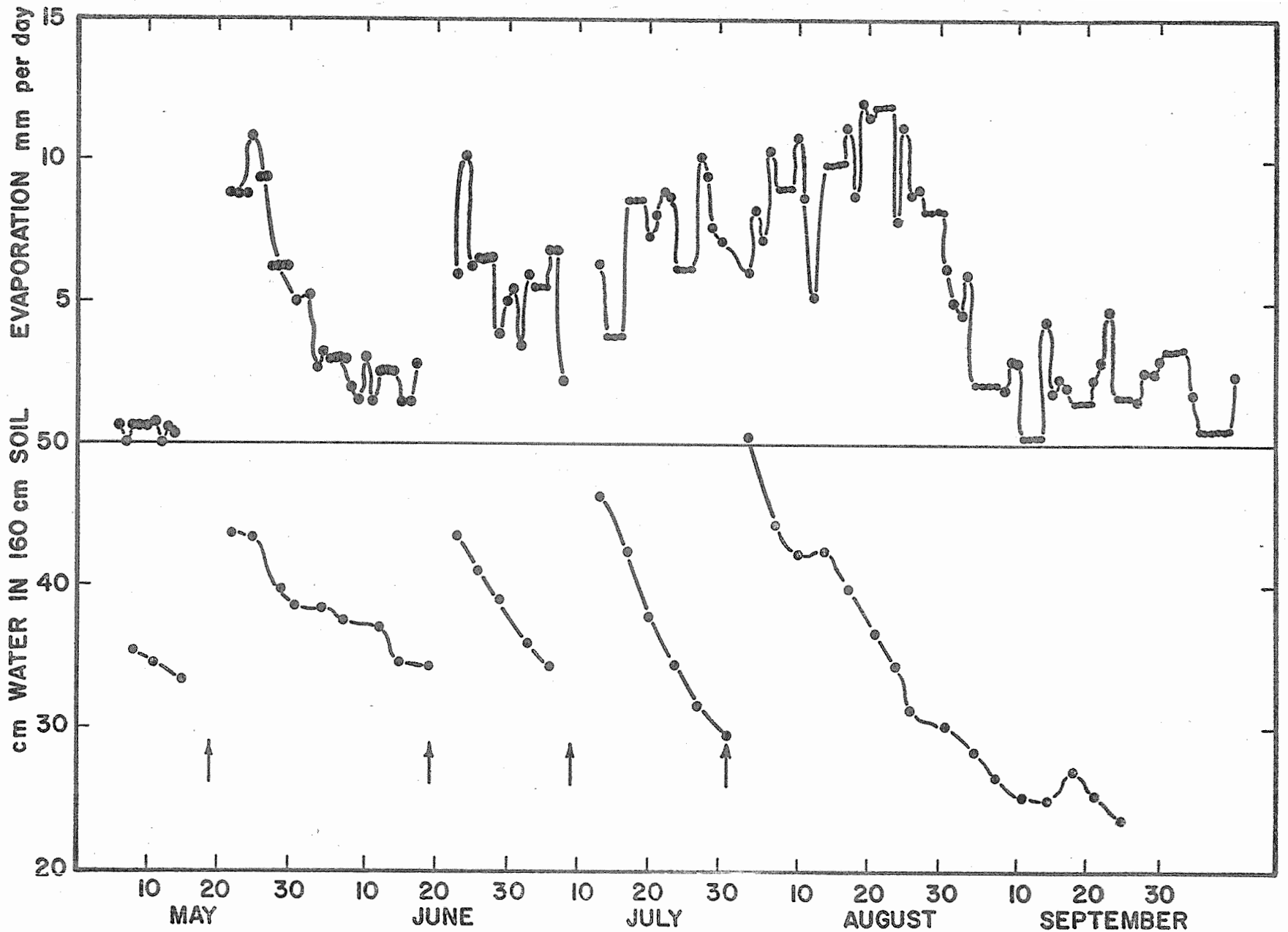

Figure 3-3. Daily evaporation from cotton in 1964 as measured with single load cell lysimeters and soil moisture content as measured twice-weekly. Arrows indicate time of irrigation.

Annual Report of the U.S. Water Conservation Laboratory

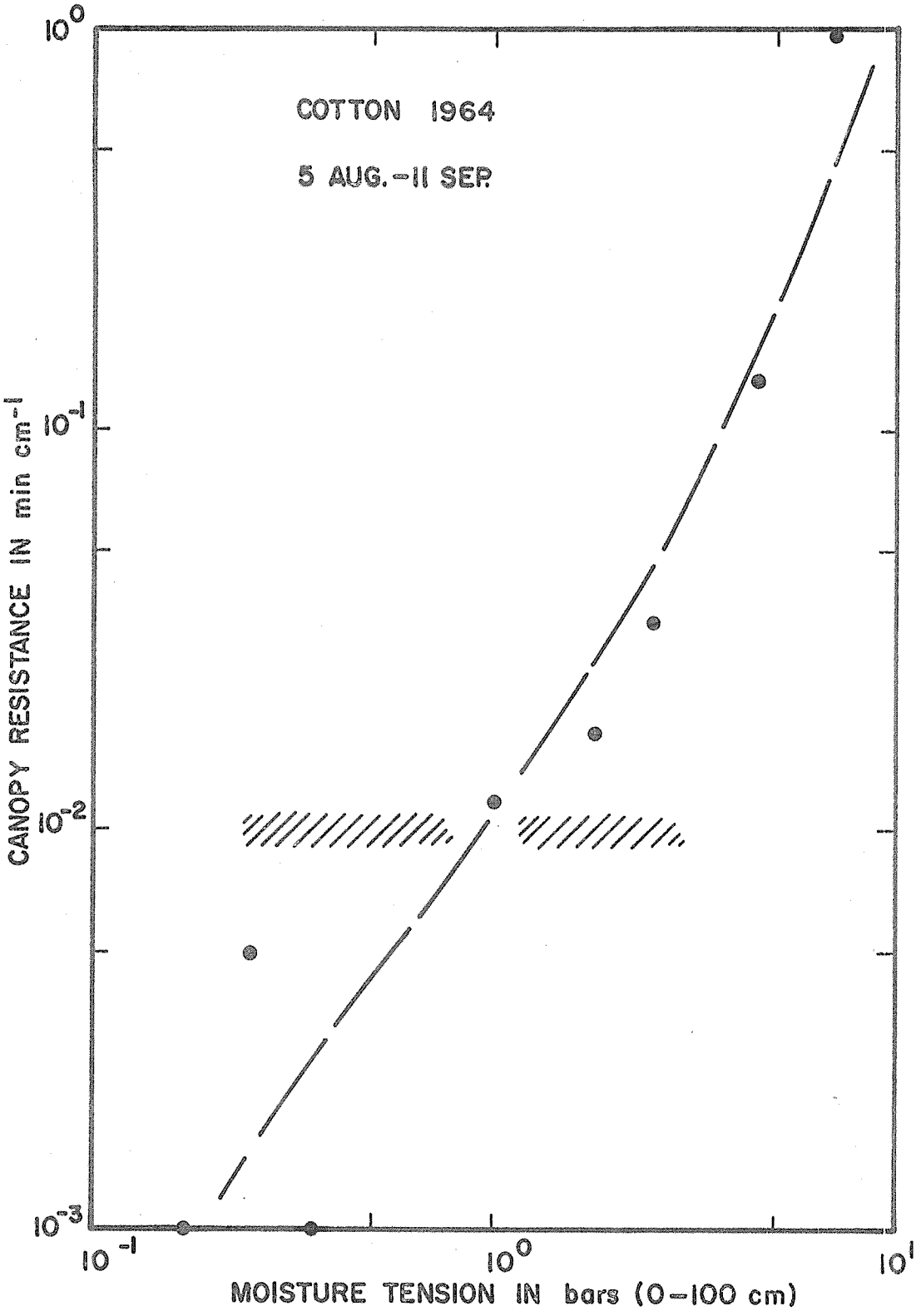

Figure 3-4. Relation between cotton canopy resistance as approximated from daily values of potential and actual evaporation, and soil moisture tension as approximated from soil moisture content. Shaded barrier indicates critical zone for effective transpiration reduction.

PART 4. COLLECTION OF ROUTINE WEATHER DATA

INTRODUCTION:

The methods whereby routine weather data over the lysimeter area were collected are described in WCL 33 - Part 6 - 1963. A major change was made in the method of recording, which is briefly described here.

PROCEDURE:

During 1963 and part of 1964, data were transcribed from an 11-inch recorder chart, 6 points every 30 minutes. Early in 1964 a Telechron shaft-mounted encoder was installed on the existing 6-point Honeywell recorder. The encoder had a span from -200 to +200 digits, corresponding to -2 to +2 millivolts.

In addition, a simple programmer, power supply and tape punch (Friden), were obtained with the encoder (all supplied by Hammarlund Corporation). From an external 30-minute timer, the output of all 6 channels is recorded in the punched tape, preceded by a carriage return and a sequential number. Thus, each period produces a single line that is typed onto a suitable form for each day. All data are directly accessible by channel, day and half-hourly period. Prepared digit-to-unit tables enable visual conversion of values where necessary. Direct records are obtained for radiation and windspeed.

RESULTS AND DISCUSSION:

In the first few months, many difficulties were encountered that were finally traced to faulty factory wiring of the tape punch. Minor defects in the external programming and the encoder mounting gave occasional flaws in the record until September. For the last 3 months of 1964, the system has turned out perfect daily statements that represent a great saving of time and effort compared to the visual chart readout.

The system could easily handle up to 24 data points and could be run at different frequencies. As such, it is well suited for routine weather data collection. The total investment is about $4,000 and therefore, preferable over the more sophisticated systems that we have. A disadvantage is the relatively large amount of space occupied

and the fact that some additional design and construction was required once the components were in hand.

A summary of the data for 1964 is shown in Table 4-1.

Table 4-1. Weather data at 2 m over alfalfa, U. S. Water Conservation Laboratory, Tempe, Arizona, 1964.

Month	Decade	R_s	R_n	Wind-Speed	Vapor Pressure	Air Temp. Ave. Max.	Air Temp. Ave. Min.	Air Temp. Ave.
		ly day^{-1}	ly day^{-1}	m sec^{-1}	mb	^{o}C	^{o}C	^{o}C
Jan	1	300	116	1.5	3.5	16.8	-0.7	7.2
	2	303	126	1.4	3.8	15.4	-2.7	5.8
	3	Hammarlund System Being Installed - No Data						
Feb	1	378	172	1.4	3.6	18.2	-1.6	7.8
	2	385	200	2.0	3.9	16.6	2.3	8.1
	3	418	243	2.2	4.3	16.9	-0.3	7.9
Mar	1	415	255	2.3	6.7	15.6	0.2	7.8
	2	493	303	2.5	6.6	21.9	5.4	13.8
	3	502	350	2.4	7.8	22.6	6.5	14.4
Apr	1	567	401	2.1	7.2	22.0	6.3	14.4
	2	611	436	2.3	7.0	28.7	9.9	20.1
	3	604	372	2.3	8.2	24.2	6.9	15.7
May	1	640	379	2.5	7.6	23.1	7.0	16.0
	2	653	382	1.8	8.0	35.5	11.9	24.3
	3	692	412	2.3	10.1	33.5	13.8	24.4
Jun	1	665	453	2.2	10.4	32.8	14.3	24.4
	2	687	463	1.8	10.5	34.4	13.4	24.8
	3	634	438	1.8	15.3	39.0	18.7	29.2
Jul	1	582	367	2.0	18.0	39.2	20.8	30.7
	2	561	403	2.0	24.1	38.4	22.8	30.6
	3	495	350	1.7	23.0	36.1	24.1	29.7
Aug	1	462	348	1.3	23.5	35.4	23.1	29.1
	2	497	371	1.5	22.7	35.7	22.3	28.6
	3	542	408	1.5	17.9	35.3	20.3	27.7
Sep	1	482	319	1.7	17.0	36.7	20.3	28.2
	2	445	311	1.5	16.9	34.2	19.0	25.5
	3	404	250	1.6	13.0	32.7	15.4	23.1
Oct	1	404	235	1.4	11.7	36.6	15.6	24.8
	2	357	203	1.6	11.1	31.1	13.8	21.7
	3	329	166	1.3	8.7	30.6	10.9	19.4
Nov	1	299	141	1.4	6.5	25.5	7.3	15.6
	2	231	103	1.5	5.4	14.9	2.2	7.8
	3	275	101	1.0	5.7	21.7	3.2	11.4
Dec	1	-	-	-	-	-	-	-
	2	-	-	-	-	-	-	-
	3	-	-	-	-	-	-	-

SUMMARY AND CONCLUSIONS:

During 1964, field studies were conducted concerning the relation between climatic variables and evapotranspiration when moisture was not limiting. These observations were made on alfalfa, wheat, oats and cotton.

The alfalfa data, based upon the use of weighable lysimeters, confirmed the applicability of the combination method for estimating evapotranspiration from single-level observations without empirical adjustment, as was already reported in 1963.

Tests of the McIlroy version of the combination method tended to give the same result, but it did not appear possible to find the empirical wind function without resorting to the use of hourly evaporation data, which were not routinely available for cotton and small grain. Sporadic tests were satisfactory, but insufficient to establish meaningful difference between crop covers.

Interpretation of soil moisture depletion data, as obtained in these studies by the neutron method, was not possible for the purpose of verifying any climatological method for estimating evapotranspiration. The cause - as demonstrated directly with differential tensiometers - was the considerable and unpredictable downward movement of moisture out of the root zone for as much as 10 days after irrigation. Conversely, any model empirically based on this type of data is subject to significant errors.

A second study, continued from 1963, was to quantitatively describe the effect of declining soil moisture reserves upon evapotranspiration. An analysis of data obtained from alfalfa showed the usefulness of the combination model in that it permitted a calculation of the canopy resistance. The latter value, being derived from the leaf diffusion resistance (stomatal aperture), shows typical diurnal as well as long-time effects.

A standard 11-inch, 6-point recorder was converted into a punched tape data logger by using commercial components at an added cost of $3,000. This system produces a daily printed sheet of half-hourly

weather data arranged in 6 columns. It is easily adaptable to other formats and performs reliably on a continuous basis.

PERSONNEL: C. H. M. van Bavel and I. C. McIlroy.

TITLE: EXCHANGE OF WATER VAPOR WITH PLANT LEAVES AND ITS RELATION TO STOMATAL DIFFUSIVE RESISTANCE

LINE PROJECT: SWC 11-gG 1 CODE NO.: Ariz.-WCL-34

INTRODUCTION:

The main features of this project, including the objective, theory and procedure, have been presented in the report of 1963. The project was terminated in 1964 and the reasons are presented in the Summary & Conclusions section.

If we assume that ordinary water vapor loss and tritiated water vapor gain in a leaf involve similar diffusive resistance processes, then the resistance can be measured by using the relation:

$$R_{H_2O \text{ or } THO} = \frac{\Delta C_{H_2O \text{ or } THO}}{E_{THO \text{ or } H_2O}}$$

where R is the stomatal resistance, ΔC is the vapor concentration difference between the inner stomatal cavity and the external atmosphere, and E is the rate of loss or gain of H_2O or THO. Previous study (1963 Annual Report: Ariz.-WCL-3, Soil Moisture Potentials and Water Uptake by Roots) showed that tritiated water and ordinary water diffused at different rates in soil material. The possibility that this might also occur with plant material was considered. For simplification, the comparison of THO and H_2O gain and loss was made with moist blotter paper instead of a leaf.

PROCEDURE:

Moist, 6 × 8 cm green blotter papers were exposed to tritiated water vapor for periods of 15 to 30 minutes in a Plexiglass chamber (50 × 25 × 50 cm), equipped with a 1.68 m^3 min^{-1} squirrel-cage blower. The THO vapor source (1 to 10μc ml^{-1}) was a mixture of THO and H_2O, or THO and NaCl-saturated solution. When the mixture of THO and NaCl-saturated solution was used as the THO source, the water vapor gradient was in the direction of the leaf to the solution, whereas, the THO vapor gradient was in the opposite direction.

The temperatures of the air and blotter paper were monitored with thermocouple and thermistor probes. Humidity in the chamber was measured with a lithium chloride resistance hygrometer.

Water loss from the evaporating material was measured gravimetrically. THO gain was determined by extracting the water from the sample by vacuum distillation and analyzing for THO in the extraction by liquid scintillation techniques (Annual Report WCL-3, 1960).

RESULTS AND DISCUSSION:

The results of the R_{THO} and R_{H_2O} measurements are presented in Table 1. It shows that the resistance values for THO and H_2O are different (Column 4). Furthermore, the resistance value of H_2O is about 0.01 cm^{-1} min and is essentially constant, being independent of the ratio of the source-to-sink. However, the resistance value associated with THO varied according to the relative proportion of absorbing and THO supplying surfaces. The results indicate strongly that isotopic exchange played a significant role in the overall flux of THO, which is not present in the transfer of ordinary water.

SUMMARY AND CONCLUSIONS:

Water loss and THO gain was determined simultaneously on moist blotter paper. Calculations for the experimental data show that the resistance values for H_2O and THO are different. Thus, it would be impractical to measure stomatal resistance of leaves by measuring the exchange of leaf water and atmospheric tagged water vapor.

PERSONNEL: F. S. Nakayama

TABLE 1. Relation between R_{THO} and R_{H_2O} for moist blotter paper.

Surface Area Ratio THO sink: source or H_2O source: sink	R_{H_2O} (cm^{-1} min)	R_{THO} (cm^{-1} min)	R_{THO}/R_{H_2O}
26:1	0.0079 ± 0.009	0.107 ± 0.007	13.6
1:1	.0111 ± .0001	.0531 ± 0.007	4.8
1:6	.0104 ± 0.0020	.0356 ± .00004	3.4

TITLE: WATER MANAGEMENT FOR THE EFFICIENT IRRIGATION OF SAFFLOWER

LINE PROJECT: SWC 5-g 2 CODE NO.: Ariz.-WCL-35

INTRODUCTION:

The objective of the experiment is to determine the irrigation requirements of safflower for maximum economic yield per unit of water applied.

Safflower has recently become an important economic crop in the Southwest with approximately 330,000 acres being grown in Arizona and California during 1963. This acreage represents about half of that grown in the United States. Many growers in the Southwest do not have sufficient water to allow the use of high irrigation rates recommended for maximum production per unit area of land.

Information concerning irrigation management for maximum production per unit of water is urgently needed, particularly in regard to the latter part of the safflower growing season when it must compete with cotton for available irrigation water. Yield must be considered in terms of saleable product and the relationships between oil content of seed and the percentage of hollow seed must be considered. There is evidence that the oil content of seed and the occurrence of hollow seed is directly influenced by water management.

PROCEDURE:

The experiment is located at the University of Arizona Experiment Farm, Mesa, Arizona.

Design and Procedure

Four borders, each 275 x 33 feet, were split into 12 plots containing six 20-inch rows approximately 40 feet long, establishing 48 plots. Eight irrigation treatments were replicated six times in a randomized block design. Beds were built with rows 20 inches apart and safflower planted 6 rows per plot on the flat the last week of December. A preplanting irrigation of at least one foot of water was given before the planting date. Border dikes were constructed around each plot. A pre-determined quantity of water was pumped and measured with a Sparling meter into the respective plots at each irrigation. Normal cultivation for weed control was conducted. A

newly-released, thin-hulled variety, A-104, was planted at 15 lbs per acre. Two hundred lbs of nitrate fertilizer were applied; 100 lbs previous to the pre-planting irrigation, and 50 lbs before the first irrigation and again before the second irrigation.

Treatments and Variables

A. Under investigation: (soil moisture)

Treatment 1 - irrigate when 50 percent of the available water has been depleted from the top three feet of soil.

1A - irrigate continuously until harvest.

1B - irrigate continuously until plants appear to be mature (leaves dry).

1C - irrigate continuously until the first blossoms commence to dry.

1D - irrigate continuously until the first blossoms open.

Treatment 2 - irrigate when 65 percent of the available water has been depleted from the top three feet of soil.

2E - irrigate until plants appear to be mature (leaves dry).

2F - irrigate until about one week after blossoming has commenced.

2G - irrigate until one week before blossoming commences.

2H - irrigate until one week before blossoming commences, then apply two additional irrigations, each given after plants have shown a definite visual moisture stress.

Treatment 2E is based on previous studies from which a mean consumptive use curve was developed. Treatment 1A is designed to create a more luxuriant moisture regime than 2E, especially during the peak consumptive use period. All other treatments are designed to obtain data on the optimum yield per unit of water and to create environments that might affect oil content and hollow seed.

Data to be Obtained.

1. Quantity of water by measurements with a Sparling meter.
2. Growth rate -- plant physiology pertaining to budding, blossoming, and maturing.
3. Oil content of seed.

4. Number of hollow seeds.

5. Soil moisture content by use of soil-moisture samples and neutron meter.

6. Yield of seed.

7. Occurrence date of blossoms associated with hollow seeds.

Methods of Interpreting Results

1. Analysis of variance

Source	DF
Total	47
Treatments	7
Replications	5
Error	35

Field Plan

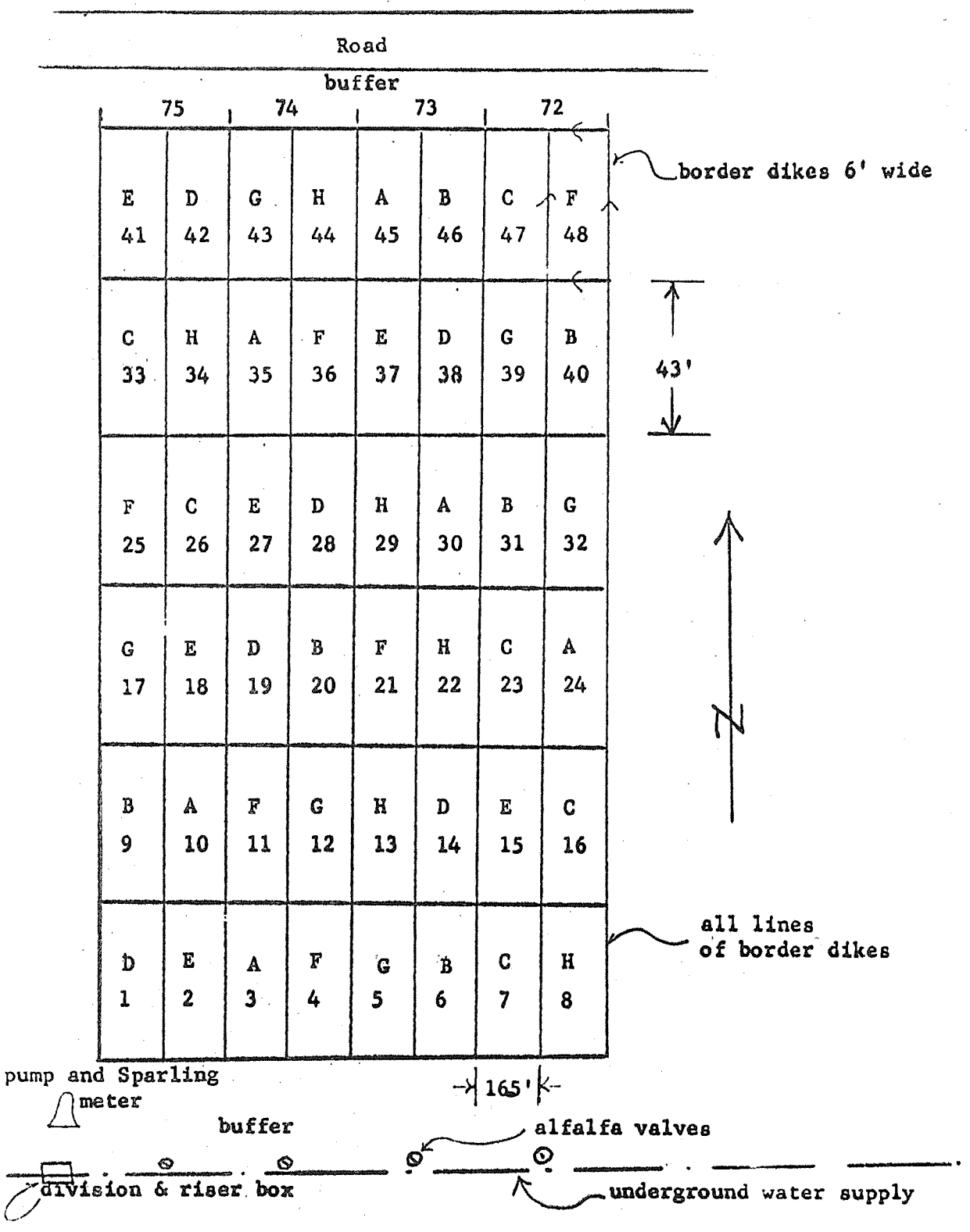
Road
buffer
75
74
73
72
border dikes 6' wide
E 41
D 42
G 43
H 44
A 45
B 46
C 47
F 48
C 33
H 34
A 35
F 36
E 37
D 38
G 39
B 40
43'
F 25
C 26
E 27
D 28
H 29
A 30
B 31
G 32
G 17
E 18
D 19
B 20
F 21
H 22
C 23
A 24
B 9
A 10
F 11
G 12
H 13
D 14
E 15
C 16
D 1
E 2
A 3
F 4
G 5
B 6
C 7
H 8
all lines of border dikes
N
pump and Sparling meter
165'
buffer
alfalfa valves
division & riser box
underground water supply

RESULTS AND DISCUSSION:

Safflower was planted December 26, 1963, about ten days after given a pre-planting irrigation. A good stand was obtained with plants emerging about January 13, 1964. All plants were hand-thinned in two rows, each twenty feet long, to approximately 4 inches between plants. Buffer rows were also thinned. Five plants were selected for hollow-seed information in treatments E, F, G and H.

The first flowers did not appear, except on treatment G, until May 20, approximately ten days late, at which time flowers were tagged every Tuesday and Friday until the end of the flowering period. Treatment "G" had open flowers by May 15. Each tagged head was harvested in July and processed.

Safflower was harvested from 40 lineal feet of row. Plants were counted in each plot when harvested. Seed was used to determine yield, oil content, iodine content, and weight per 500 seeds.

The first two irrigations were given March 13 and April 7. Water was not measured for these irrigations except by soil moisture sampling, and all plots were irrigated, regardless of treatments. Fifty pounds of nitrogen were applied with each of the first two irrigations.

IRRIGATION SCHEDULE

	TREATMENTS	3/13	4/7	4/21	4/23	4/30	5/7	5/11	5/18	5/22	6/1	6/15	7/1	No. of Irrigations
** 61% Wet	A	x	x	x		x		x		x	x	x	x	9
	B	x	x	x		x		x		x	x	x		8
	C	x	x	x		x		x		x				6
	D	x	x	x		x								4
** 72% Medium	E	x	x		x		x		x		x	x		7
	F	x	x		x		x							4
	G	x	x		x									3
	*H	x	x		x		x		x					5
	Inches of Water Applied			5	6	5	6	5	6	5	6	5	3	

* Treatment 'H' was changed from the original plan because of the late flowering date.

** Mean soil moisture percentage in the top four feet based on the following periods.

Wet	61% -- 4/20	→ 6/15
Medium	72% -- 4/23	→ 6/15

Plants were only 7 inches high by March 7. By April 3, they were 20 inches high. They were 40 inches high by April 24, and on May 7, they had reached their maximum height of 48 inches. Small buds were first observed on April 30, and on May 20, a few flowers showed on non-stressed treatments. Treatment "G" showed drought signs (grey, droopy lower leaves) by May 15, just when flowering started. Treatment "D" showed drought about May 25, and treatment "F" was showing yellow, droopy leaves on the lower part of the plant on June 1.

Soil moisture samples were taken on the planting date, at least every 10 days before and after irrigations, and on the harvest date. Samples were taken at two locations on two plots for each of the eight irrigation treatments. Soil samples were taken at 1-foot intervals through 6 feet.

No cultivations were accomplished after April 20, and no spraying for insects. A small amount of "yellows" was observed.

SUMMARY AND CONCLUSIONS:

There is a statistically significant difference in safflower yield for the irrigation regimes (Table 1). The variance is at the 1-percent level. There is no significant difference in yield between treatments "A", "E", and "B"; however, "E" was given only 7 irrigations and consumptively used about 10 inches less water (Table 1). Treatment "C" yielded over 700 pounds less safflower seed and was given one irrigation less than treatment "E". Treatment "C" consumptively used nearly 3 1/2 inches less water than Treatment "E". When the last irrigation was given on the date of the first major signs of blossoming, a reduction from the maximum potential of at least a thousand pounds of seed occurred (Treatments "C" and "H"). When irrigations were discontinued, 10 to 20 days before the first blossoms, reductions of over one-half, or approximately 2000 pounds, resulted (Treatments "D" and "G").

There is a statistically significant difference in the weights of 500 seeds and the oil content for the various irrigation regimes (Tables 2 and 3). The variance is at the 1-percent level. The trend in oil content and weight of 500 seeds is the same as for yield.

Differences between "B", "E", and "A" are not significant, and they are higher than other treatments. Late season moisture-stressed treatments are low, just as for yields.

There is no significance in iodine numbers between irrigation regimes (Table 4). There is a statistically significant difference in the number of seeds per head (Table 7). The variance is at the 1-percent level and the number of seeds per head are increased as the number of irrigations are increased. The number of seeds per head decreased as the season progressed for all treatments (Table 8). The total number of heads per plant as related to moisture did not follow a consistent trend. The data (Table 9) seems to indicate that a severe early stress, ten days or more, before flowering, caused a decrease in the number of heads.

The range in the number of hollow seeds is directly related to yields; however, the percent of hollow seed is the reverse (Table 6). When the weight of hollow seed is considered, the percent hollow is less for the high producing treatment "E". Hollow seed represents approximately 2 percent by weight of the total seed (Table 5). From 4.5 to 6.3 percent of the total number of seeds are hollow regardless of irrigation treatment (Table 6). Visual analysis of the data by weeks shows that hollow seeds occur throughout the flowering season for all irrigation treatments. Hollow seed is not necessarily associated with a specific time of flowering.

The correct irrigation schedule to obtain the most economical yield will depend upon the cost of water. The data indicates that 6 or 7 irrigations would be the most desirable since it would appear that 1 or 2 irrigations over 5 irrigations would mean about 1000 pounds of seed (Table 10). Reducing irrigations to 4 would not appear to be economically feasible.

PERSONNEL: Leonard J. Erie and Orrin F. French.

Table 1. Yield, Safflower. Mesa, Arizona. Pounds per Acre.

Treatment	Replications						Mean
	1	2	3	4	5	6	
A	4154	4445	5223	4135	4731	4570	4543
B	4340	3640	4302	4616	4970	4692	4427
C	3475	4734	3172	3037	4018	3852	3715
D	2189	2417	2440	2016	2022	2430	2252
E	4450	3804	4517	4871	4187	4789	4436
F	2353	2026	2121	1973	2721	3721	2486
G	2141	1561	1914	2593	1965	2049	2037
H	3484	2732	3281	3436	3339	3419	3282

		Sig. 1%		
A	4543	a		
E	4436	a		
B	4427	a		
C	3715		b	
H	3282		b	
F	2486			c
D	2252			c
G	2037			c

Table 2. Weight of 500 Seeds, Safflower (gm).

Treatment	Replications						Mean
	1	2	3	4	5	6	
A	18.75	18.99	18.62	18.44	17.89	18.77	18.58
B	19.28	18.61	18.50	19.16	19.50	18.44	18.92
C	17.42	18.59	17.14	16.94	16.36	17.02	17.25
D	16.22	17.13	16.99	16.01	16.69	16.95	16.67
E	17.78	19.01	19.17	18.97	18.49	18.84	18.71
F	16.10	16.89	15.52	16.73	17.16	17.66	16.68
G	15.92	15.78	16.41	17.09	16.23	15.84	16.21
H	19.24	17.57	16.58	17.84	17.19	17.14	17.59

Sig. 1%

B	18.92	a		
E	18.71	a		
A	18.58	a	b	
H	17.59		b	c
C	17.25			c	d
F	16.68			c	d
D	16.67			c	d
G	16.21				d

Table 3. Oil Content, Safflower.

Treatment	Replications						Mean
	1	2	3	4	5	6	
A	41.2	41.6	40.2	41.6	41.4	41.2	41.2
B	41.0	41.2	41.0	42.8	40.6	41.6	41.4
C	40.4	40.8	38.8	40.4	38.0	40.0	39.7
D	39.0	38.2	38.2	37.8	38.8	41.0	38.8
E	41.0	41.4	41.8	41.0	41.4	41.2	41.3
F	37.4	37.4	37.6	39.6	38.6	40.4	38.5
G	39.4	38.6	39.6	39.4	39.2	39.2	39.2
H	40.6	37.6	38.6	38.0	38.6	39.4	38.8

		Sig. 1%	
B	41.4	a	
E	41.3	a	
A	41.2	a	
C	39.7		b
G	39.2		b
D	38.8		b
H	38.8		b
F	38.5		b

Table 4. Iodine numbers, Safflower.

Treatment	Replications						Mean
	1	2	3	4	5	6	
A	146	145	146	147	147	147	146.3
B	146	145	145	147	147	147	146.2
C	146	146	146	145	146	146	145.8
D	144	145	146	145	145	146	145.2
E	146	146	147	147	147	147	146.7
F	143	144	144	145	145	146	144.5
G	145	144	145	146	145	144	144.8
H	145	145	145	146	145	145	145.2

No Sig.

Table 5. Weight of Hollow Seed, Safflower.

Treatment	Weight of Hollow Seed (gm)	Weight of Good Seed (gm)	Weight of Hollow and Good Seed (gm)	Percent of Total Weight Hollow
E	12.248	834.814	847.062	1.45
F	12.777	591.204	603.981	2.12
G	8.811	405.917	414.728	2.12
H	12.380	561.466	573.846	2.16

Table 6. Number of Hollow Seed, Safflower.

Treatment	Total Number of Hollow Seed	Total Number of Good Seed	Percent of Seed Hollow	Av. Seed Weight	
				Hollow	Good
E	165	3,472	4.53	.0119	.0394
F	161	2,745	5.55	.0132	.0358
G	134	1,999	6.27	.0113	.0333
H	156	2,763	5.36	.0126	.0336

Table 7. Seeds per Head, Safflower.

Treatment	Replications						Mean
E	47	43	50	59	34	44	46
F	30	35	32	48	42	24	35
G	35	38	30	33	31	23	32
H	33	35	36	44	41	41	38

	Sig. 1%		
E	46	a	
H	38	a	b
F	35		b
G	32		b

Table 8. Mean Seed per Head by Dates (6 replications)

Treatment	Tagging Dates							No Tags
	5/22	5/26	5/28	6/2	6/5	6/9	6/12	
E	56	56	55	45	33	24	13	28
F	51	45	37	30	14	13	11	20
G	45	36	25	19	11	14	---	17
H	58	54	46	31	16	5	2	24

Table 9. Number of Heads from 5 Plants. (6 replications)

	Tagging Dates								
Treatment	5/22	5/26	5/28	6/2	6/5	6/9	6/12	No Tag	Total
E	80	116	56	117	49	34	19	16	487
F	73	136	57	136	60	25	6	18	511
G	89	133	63	97	9	5	0	11	407
H	67	116	53	126	30	34	18	14	456

Table 10. Yield versus Water Use.

Treatment	No. Irrigations	Yield Lbs	Consumptive Use Water	Lbs/in. of Water
A	9	4543	52.9	85.9
E	7	4436	42.0	105.6
B	8	4427	50.0	88.5
C	6	3715	38.6	96.2
H	5	3282	33.0	99.5
F	4	2486	29.8	83.4
D	4	2252	29.7	75.8
G	3	2037	23.4	87.1

Table 11. Consumptive Use of Water by Safflower.

Treatment	Use (inches) Depth (feet)						Total Use
	0-1	1-2	2-3	3-4	4-5	5-6	
A	16.30	13.37	10.05	7.30	3.82	2.07	52.91
B	15.21	12.57	9.71	7.10	3.69	1.77	50.05
C	12.20	9.92	6.94	5.41	2.69	1.49	38.65
D	9.05	7.49	4.92	4.09	2.46	1.72	29.73
E	13.80	10.65	8.33	4.97	2.28	1.96	41.99
F	8.86	7.26	5.38	3.73	2.38	2.14	29.75
G	7.20	5.79	4.01	2.95	1.81	1.65	23.41
H	10.34	8.22	6.07	3.97	2.17	2.11	32.98

TITLE: CLAY DISPERSANTS FOR THE REDUCTION OF SEEPAGE LOSSES FROM RESERVOIRS

LINE PROJECT: SWC-4-gG1 CODE NO.: Ariz.-WCL-37

INTRODUCTION:

Observations and posttreatment soil analyses were made in May and September 1964 on two stock ponds treated with sodium salts. See Ariz.-WCL-8 Annual Report for 1963 for other details.

PROCEDURE:

No new procedures were adopted in 1964.

RESULTS AND DISCUSSION:

1. Dick Mason Pond.

This pond had a seepage rate of five inches per day prior to treating it in August 1962 with TSPP (tetrasodium pyrophosphate). There was very little sodium (ESP = 0.8) and naturally dispersed clay (2-3 percent) prior to treatment. One year after treatment the seepage rate was 0.3 inch per day. Two years after treatment, soil samples were taken and the seepage rate was measured at 1 inch per day.

The posttreatment physical analysis of soil samples taken in May 1964 showed a two-to-five-fold increase in the amount of dispersed clay over the pretreatment amount. This indicates the TSPP was effective in causing a partial dispersion of the clay fraction. The chemical analysis showed a fair amount of sodium on the exchange complex, ESP = 8 in the 0 to 2 inch layer, although this was less than the design ESP of 15. Obviously, the lower amount of sodium was effective in dispersing enough clay to reduce seepage.

At our request, the rancher measured the water loss from this pond in September 1964 at one inch per day, averaged over three days. The soil analysis of September 1964 (table 1) shows a marked decrease in the sodium remaining on the exchange complex, and in the amount of dispersed clay. ESP was 1.6 and dispersed clay 1-2 percent in the 0 to 2 inch depth. It appears that the calcium in the soil solution has increased to the point that it is replacing the sodium on the soil. The sodium has then been leached out of the profile, and the calcium has caused the clay to flocculate. This condition is reflected

in the increase in seepage rate from 0.3 inch per day in 1963 to 1 inch per day in September 1964.

2. House Mountain Tank #2.

The pretreatment seepage rate of this pond was never measured although it never held enough water to carry the cattle through the grazing season. Prior to treating the pond with sodium carbonate in July 1963, an analysis of the soil showed an ESP of 0.7 and the amount of naturally dispersed clay as 2.3 percent.

This pond contained approximately three feet of water in mid-June 1964 and had gone dry by mid-September 1964. This loss could be accounted for by 0.25 inch per day for evaporation and 0.25 inch per day for seepage.

The data given in Table 2 show an ESP of 1.7 in the 0 to 2 inch depth with 4.5 percent dispersed clay for the soil samples taken in May 1964. Both the ESP and dispersed clay increase down to the 10-inch depth. In September, however, the ESP increased to 3.9 in the 0 to 2 inch depth. The amount of dispersed clay decreased to 1-2 percent. It appears that the increase in sodium at the soil surface in 1964 was due to the evaporation of water (the pond was dry in September 1964). The increase in sodium at the lower depths was probably due to leaching. The data are not sufficiently complete to explain why a low ESP (1.7) is associated with 4.5 percent dispersed clay, and a higher ESP (3.9) is associated with less dispersed clay (2-3 percent). This question will be investigated.

SUMMARY:

Two ponds, apparently successfully treated with sodium salts to reduce seepage, were observed one and two years after treatment. House Mountain Tank #1 treated with sodium carbonate appears to be holding water one year after treatment with about 0.25 inch per day seepage loss. The amount of sodium remaining on the soil has apparently caused enough of the clay fraction to be dispersed to reduce the seepage rate to an acceptable level for the rancher's needs. A measured seepage loss next year will determine if the treatment is still effective.

In the Dick Mason pond, treated with tetrasodium pyrophosphate, the seepage rate has increased from 0.3 inch per day one year after treatment to 1 inch per day two years after treatment. Post-treatment analysis of the treated soil shows very little sodium remaining on the exchange complex (ESP = 1 to 2) and less than two percent of the clay fraction dispersed. Apparently, the calcium in the soil solution has increased enough to replace the sodium on the soil, the sodium has leached out of the profile, and the calcium has flocculated the soil, thereby causing an increased seepage rate.

PERSONNEL: Robert J. Reginato and Lloyd E. Myers.

Table 1. Pretreatment and posttreatment chemical and physical analyses of Dick Mason Pond.

Soil Depth - Inches		0-2			2-4		4-6		6-8		8-10	
Date Sampled		7/62 1/	5/64	9/64	5/64	9/64	5/64	9/64	5/64	8/64	5/64	9/64
Ca^{++}	meq/100g	29.3	25.2	24.5	25.6	24.4	23.0	26.9	20.7	30.7	29.7	23.6
Mg^{++}	meq/100g	24.4	22.0	19.6	21.3	20.0	19.0	26.1	21.7	36.6	19.7	26.4
Na^{+}	meq/100g	0.4	5.3	0.9	1.8	1.4	2.2	1.6	2.3	1.2	2.3	1.3
Cation Exchange Capacity	meq/100g	54.9	66.3	58.9	66.1	60.7	68.0	70.6	57.6	84.9	57.5	69.4
Exchangeable Sodium	%	0.8	8.0	1.6	2.7	2.2	3.2	2.2	4.0	1.4	4.0	1.8
Total Salts	ppm	619	1000	800	1090	850	933	970	700	1055	838	890
Sand > 50 μ	%	15	16	23	19	26	23	19	25	14	23	25
Coarse Silt 20 - 50 μ	%	9	9	11	9	8	15	7	17	2	10	6
Fine Silt 2 - 20 μ	%	27	24	25	22	22	15	22	13	18	17	24
Total Clay < 2 μ	%	49	51	42	50	44	47	52	45	66	50	45
Dispersed Clay < 2 μ	%	2-3	10	1-2	11	1-2	6	0.5	6	1-2	6	0

1/ This pretreatment analysis is from a composite sample and is applicable for all depths.

Soil Depth - Inches		0-2			2-4		4-6		6-8		8-10		10-12	
Date Sampled		7/62 1/	5/64	9/64	5/64	9/64	5/64	9/64	5/64	9/64	5/64	9/64	5/64	9/64
Ca^{++}	meq/100g	40.8	39.9	37.2	40.8	39.8	40.0	38.5	41.2	42.2	42.2	47.5	43.2	45.8
Mg^{++}	meq/100g	9.8	8.9	8.3	8.7	5.6	8.6	8.2	8.6	7.8	8.1	8.0	8.8	9.4
Na^{+}	meq/100g	0.3	0.9	2.0	1.6	1.0	1.6	1.0	2.2	1.4	2.0	2.2	1.3	3.2
Cation Exchange Capacity	meq/100g	61.9	50.5	51.7	49.8	46.2	50.9	-	49.3	50.0	52.1	54.5	52.5	-
Exchangeable Sodium	%	0.7	1.7	3.9	3.2	2.2	3.2	-	4.4	2.8	3.9	4.0	2.5	-
Total Salts	ppm	397	925	-	1017	-	989	-	1151	-	1151	-	1030	-
Sand > 50 μ	%	2	9	3	9	11	10	11	7	9	6	5	7	4
Coarse Silt 20-50 μ	%	17	11	20	13	23	12	18	13	18	12	19	12	16
Fine Silt 2-20μ	%	30	29	30	27	23	27	24	28	24	27	29	30	28
Total Clay < 2 μ	%	51	51	47	51	43	51	47	52	49	55	47	51	52
Dispersed Clay <2 μ	%	2-3	4.5	1-2	6	2-3	6.5	2-3	6.5	2-3	6.5	4	3	4

1/ This pretreatment analysis is from a composite sample and is applicable for all depths.

TITLE: WATERBORNE SEALANTS TO REDUCE SEEPAGE LOSSES FROM UNLINED CHANNELS AND RESERVOIRS

LINE PROJECT: SWC-4-gG1 CODE NO.: Ariz.-WCL-38

INTRODUCTION:

See 1963 Annual Report for WCL-8. During 1964, four different petroleum emulsions were investigated for suitability as water-borne seepage reducing agents.

PROCEDURES:

Procedures used have been previously described except for changes in the seepage cylinder equipment and the method of adding emulsions to field test ponds. The cylinder devices were modified to increase operating ease and to reduce airlocks in the discharge lines. Seepage rates are accurately controlled by changing the elevation of the flexible effluent tubes. Emulsions are added to test ponds with a venturi on the discharge line of a centrifugal pump. Low pressure created by the venturi draws emulsion from the supply barrels into the venturi where it is thoroughly mixed with water being discharged into the pond.

RESULTS AND DISCUSSION:

1. Emulsion A.

Emulsion A at a concentration of 1000 ppm emulsion was added to water ponded over soil packed in laboratory cylinders to determine the effect of pretreatment seepage rate on the amount of seepage reduction. Table 1 (figures are averages of duplicate cylinders) shows there is an effect of initial seepage rate on seepage reduction: the higher the rate, the greater the reduction. At 1 cm hr^{-1} the seepage reduction is only 4 percent, but increases to 86% reduction with an initial seepage rate of 13 cm hr^{-1}.

A field test with emulsion A was conducted on four ponds at Granite Reef. Table 2 shows consistent seepage reduction, 81, 75 and 80 percent on ponds 2, 3, and 4, respectively, 48 hours after treatment. The low reduction, 55 percent, noted on pond 5 was due to a contamination of emulsion A with a solvent. The solvent causes the emulsion to "break" and lose its effectiveness.

The probable explanations for ponds 2, 3, and 4 having good seepage reduction with low initial seepage rates, which is not consistent with the cylinder results, is that there was more asphalt on the soil in the ponds than on the soil in the cylinders. Twenty-four hours after the ponds were treated with 1000 ppm emulsion A in water, they were refilled to the original treatment depth with water containing 1000 ppm emulsion, resulting in an average of 0.15 gal emulsion per square yard of treated soil. The cylinder test applied only 0.095 gallons of emulsion per square yard of treated soil.

2. Emulsion B.

Emulsion B was added to water ponded over control soil packed in laboratory cylinders at a concentration of 1000 ppm emulsion, to determine the effect of pretreatment seepage rate on the amount of seepage reduction. Table 1 shows there is essentially no effect of initial rate on reduction. On rates from 1 to 13 cm hr^{-1} the reduction was 91-100 percent.

Two field soils were packed in cylinders and treated with 1000 ppm of emulsion B in water, the initial seepage rate was in the range 2-7 cm hr^{-1}. Seepage reduction of 80-92 percent for both soils was accomplished 48 hours after treatment.

Emulsion B was then obtained from a local oil company and tested on four field soils packed in cylinders. With 1000 ppm of this emulsion added to the soils, seepage reduction varied from 6 to 91 percent. It was observed in this test that the emulsion broke on the water surface and plated on the plastic cylinder walls. Also, the asphalt suspension cleared up in a much shorter time than the material supplied from the original manufacturer.

A 500-foot section of a canal with a 30-$foot^2$ cross section at a depth of 4.5 feet, holding about 1 acre-foot of water, was treated with 1000 ppm of emulsion B supplied by the local oil company. The pretreatment seepage rate was 1 cm hr^{-1} and 48 hours after treatment, there was no seepage reduction. As in the cylinders, the emulsion broke and came to the water surface. Investigation of the emulsion showed that it contained a large amount of solvent and was highly unstable.

It is concluded that the original emulsion B is very stable and will consistently reduce seepage, but the emulsion from the local oil company is not stable and does not consistently reduce seepage.

3. Emulsion C.

Emulsion C was added at 1000 ppm emulsion to water ponded over control soil packed in cylinders. Table 1 shows good seepage reduction, 89-99 percent at all initial seepage rates. However, emulsion C did not reduce seepage as much as did emulsion B.

4. Emulsion D.

Emulsion D was added in a concentration of 1000 ppm emulsion to water ponded over control soil to determine the effect of pretreatment seepage rate on seepage reduction. Table 1 shows the reduction increases 6 to 67 percent, with rates from 1 to 3 cm hr^{-1}, respectively, and then decreases to 28 percent as the rate increases to 13 cm hr^{-1}. This emulsion was not tested further because of its low seepage reduction in comparison to emulsion B.

SUMMARY:

Four different petroleum emulsions were investigated to determine their effectiveness as water-borne seepage reducing agents. Laboratory tests showed that emulsion D was inadequate. Similar tests showed that emulsion C could reduce seepage by 81 to 99 percent but was not as effective or consistent as emulsion B. Laboratory tests of emulsion A showed that it could reduce seepage about 80 percent at high seepage rates but that it was ineffective at low rates of 1 to 2 cm hr^{-1}. A field trial of emulsion A in small ponds at Granite Reef reduced seepage 75 to 81 percent except in one pond which was contaminated with solvents. The solvent caused the emulsion to break and flocculate before it reached the soil surface. These three emulsions were abandoned in favor of emulsion B.

Laboratory tests showed that emulsion B was very stable and reduced seepage by over 90 percent, even at the lowest seepage rates. Accordingly, a large quantity of emulsion B was prepared by a local company for field testing. Laboratory tests of the locally prepared emulsion showed that it was not stable and seepage reduction was erratic. The

emulsion failed to reduce seepage in a field trial on a canal near Beardsley, Arizona, and broken emulsion materials were observed floating on the water surface. An investigation revealed that the local company had not formulated emulsion B properly. In addition to using incorrect basic materials, they had incorporated about 12 percent solvent in the formulation. Reliably prepared emulsion B is now being obtained and additional field trials will be conducted.

PERSONNEL: Robert J. Reginato and Lloyd E. Myers.

Table 1. Seepage reduction after 48 hours treatment with four emulsions at five seepage rates.

Emulsion	Seepage rate - cm hr^{-1}				
	1	2	3	6	13
	Seepage reduction - percent				
A	4	30	78	82	86
B	91	99	100	98	98
C	81	99	96	97	93
D	6	54	67	27	28

Table 2. Seepage reduction on Granite Reef ponds 48 hours after treatment with 1000 ppm emulsion A.

Pond Number	Capacity Gallons	Seepage Rate - cm hr^{-1} Pretreatment	Posttreatment	Reduction Percent
2	4600	1.60	0.31	81
3	3300	2.00	0.51	75
4	3600	1.53	0.31	80
5	4100	1.48	0.66	55

TITLE: CRACK SEALANTS FOR CONCRETE LINED CANALS

LINE PROJECT: SWC 4-gG1 CODE NO.: Ariz.-WCL-39

INTRODUCTION:

Irrigation canals and farm ditches are lined with concrete for various reasons including seepage control. Almost all concrete linings crack. These cracks lose water and continue to deteriorate if they are not sealed. It is, therefore, necessary to find low-cost effective treatments to seal cracks in concrete lined canals and ditches. A good crack sealer should be able to span cracks up to 1/2 inch in width, have good cohesive and elastic properties, adhere to concrete surfaces having received a minimal amount of cleaning, have good strength, durability, weathering characteristics, and should be low in cost and easily applied. The sealer should be able to bridge cracks rather than fill them and should be suitable for application with spray equipment. Several sprayable, experimental sealants were tested by application to concrete linings in the field.

PROCEDURE:

Low-cost sprayable commercial crack sealers were not available when this study was initiated. Accordingly, we prepared a number of formulations using 70 to 90 percent asphalt, 5 to 20 percent butyl emulsion, 5 to 10 percent asbestos fibers, and 1 percent bentonite by weight of solids. Anionic and clay type asphalt emulsions were used for the asphalt components. Setting time, viscosity, ductility, and adhesive characteristics were observed in the laboratory. During March, five of the formulations using an anionic emulsion were sprayed on a local slip-form concrete lined ditch with a Lincoln Airless Sprayer Model 1934. To check sprayability and bonding to concrete, the concrete had received variations in the following treatments: no cleaning, sweeping with a fiber broom, wire brushing, no tack coat, a tack coat of cutback asphalt.

An experimental, commercial, sprayable crack sealer became available in May, and this plus two formulations of our own using asphalt-clay emulsion were sprayed on cracks in a concrete lined farm ditch. Cleaning and tack coat treatments were as outlined above.

During November a 500-foot reach of the Salt River Project's Tempe canal was treated with the commercial crack sealer. Cracks were cleaned by fiber broom sweeping, wire brushing, or washing with a high pressure water jet. Tack coat treatments were no tack coat and kerosene plus surfactant.

RESULTS:

Formulation of a sprayable crack sealer did not appear critical, but several formulations appeared satisfactory within the range of 85 to 90 percent asphalt, 5 to 10 percent butyl, 5 to 10 percent asbestos, and 1 percent bentonite (in the anionic asphalt emulsion) by weight of solids. These formulations and the commercial material were sprayable. Observations in December indicated no weathering damage to any of the materials except for minor cracking of the clay type asphalt emulsion material. Bonding to the concrete was excellent for all materials wherever the concrete had received any type of cleaning, even without a tack coat. Observation of the materials is continuing to detect differences in the field performance.

SUMMARY:

Several low-cost sprayable concrete crack sealers were developed and applied with apparent success. These materials should be able to span cracks up to 1/2 inch in width, have good cohesive and elastic properties, adhere to concrete surfaces having received a minimal amount of cleaning, have good strength, durability, weathering characteristics, and should be low in cost and easily applied. Several formulations were initially satisfactory which had the following proportions by weight: 85 to 90 percent asphalt, 5 to 10 percent butyl, 5 to 10 percent asbestos, and 1 percent bentonite. These materials, plus a commercial material which became available after the study was begun, were sprayed on cracks in a concrete lining of a farm ditch and in a canal during March, May, and November 1964. The concrete had received variations of the following treatments: no cleaning, sweeping with a fiber broom, wire brushing, no tack coat, and a tack coat of either cutback asphalt or kerosene plus surfactant. Observations in December indicated no weathering damage to any of the

materials except for minor cracking of the clay type asphalt emulsion material. Bonding to the concrete was excellent for all materials wherever the concrete had received any type of cleaning even without a tack coat. Observation of the materials is continuing to detect differences in the field performance.

PERSONNEL: R. J. Reginato and L. E. Myers

TITLE: DISPERSION AND FLOCCULATION OF SOIL AND CLAY MINERALS AS RELATED TO THE Na AND Ca STATUS OF THE AMBIENT SOLUTION

LINE PROJECT: SWC 4-gG3 CODE NO.: Ariz.-WCL-40

INTRODUCTION:

The use of chemicals to control water movement in soils is an important phase of water conservation. Practical experience and carefully conducted field and laboratory experiments have shown that water movement in the soil can be controlled with certain chemicals. This development has been furthered by a general understanding of the physicochemical behavior of the soil material and the interactions occurring between the chemical and the soil colloid. However, our knowledge in this area is not sufficiently adequate, as is evidenced by our inability to answer such questions as to what the best chemical to use and at what rate, and also to predict the effectiveness and the durability of a treatment.

A condition which has been closely related to water movement in the soil media is the dispersed or flocculated status of the soil colloidal material. Early studies give us an incomplete picture of this phenomenon with soils. In one way or another they have failed to take into account such factors as electrolyte concentration, type of anion, cation balance and particle-particle, particle-liquid interactions.

The objective of this study is then to investigate the dispersion and flocculation process of soil and clay materials by sodium and calcium ions in relation to the types of clay mineral, anions, and electrolyte concentrations. The phenomenon will be put on a more quantitative basis by use of more refined techniques of viscometric, turbimetric and electrophoretic mobility measurements.

PROCEDURE:

Bentonite clay (1 percent suspension), without any pretreatment, was passed through H-, Na- or Ca- saturated exchange resin (Amberlite IR 120, 20-50 mesh). The homoionic saturated exchange resins were prepared by passing 2N HCl, NaCl or $CaCl_2$ through the 1.25-inch D. × 10-inch L. column, followed by washing with distilled water until free of chlorides.

The viscosity of the clay suspensions was measured on a Brookfield Model LVT Viscometer with a U. L. adapter. Reproducibility of the equipment was 0.02 centipoise. The room temperature was 25 $\pm$ 0.5 degrees C except where noted. Exploratory study involved the preparation and measurement of viscosity of clay suspension at different concentrations. Only diluted (<1 percent) suspension could be passed through the resin column. Concentrated suspensions were obtained by evaporation of the water from the dilute sample at 25 to 45 degrees C over blowers.

Different Na-to-Ca saturated montmorillonites were prepared by proportionate mixing of the homoionic Na- and Ca-saturated montmorillonite clays. Viscosity of these mixtures at 0.005 and 0.0075 g ml^{-1} clay suspension was measured. In addition, the viscosities of H-, Ca- and Na-montmorillonite at 0.005 g ml^{-1} suspension concentration were measured at 10, 20, 25, 30 and 35 degrees C.

RESULTS AND DISCUSSION:

The viscosity data for H-, Ca-, and Na-montmorillonite as a function of the suspension concentration are presented in Figure 1. For the same clay concentration, the order of the viscosity value is Ca>H>Na.

The Ca-montmorillonite system has more particle-to-particle interaction and thus, a larger viscosity than the Na-montmorillonite where the particle-to-particle interaction is more in the nature of repulsion rather than attraction, thus causing a dispersed system.

The importance of the kind and degree of saturation of the exchange complex with Na or Ca is illustrated in Figure 2. A large change in viscosity occurred when only a few percent of the Ca in the Ca-saturated clay system is replaced by Na cations. For the 0.005 g ml^{-1} suspension, the viscosity changes from 5.3 cps at 100 percent Ca to 1.5 cps at a 90 percent Ca-10 percent Na saturation level. A large change of 16.0 to 1.7 cps was present in the 0.0075 suspension. In both cases, the affect of the Na on viscosity is noticeable up to 10 percent Na replacement. The flocculation-dispersion behavior appears to be independent of clay concentration

in this suspension concentration range. Beyond 10 percent Na-to-90 percent Ca-status of the ion on the exchange complex, the effect of Na on viscosity is negligible. The small amount of Na ions on the clay mineral have greatly affected the flocculation status of the Ca-montmorillonite system.

Preliminary results on the temperature dependence of viscosity of the various cation saturated clay minerals are presented in Figure 3. Na- and also H-montmorillonite behaved similar to water in regard to temperature dependence. The viscosity of Ca-montmorillonite, on the other hand, in the suspension concentration and temperature range was independent of temperature. More study to explain this behavior is needed.

SUMMARY AND CONCLUSIONS:

The viscosity of natural montmorillonite, passed through H-, Na- and Ca-exchange resins, was determined relative to that of suspension concentration, Na and Ca saturation percentage, and temperature. The viscosity for all clay materials increased with increasing suspension concentration. For the same amount of clay material, the viscosity value as related to cation saturation was in the order Ca>H>Na. A marked decrease in viscosity occurred in the Ca-montmorillonite suspension when from 1 to 10 percent of the Ca in the exchange complex is replaced by Na. The viscosity of Ca-montmorillonite, in which 10 percent of the Ca ions was replaced with Na, was about that of a 100% Na-saturated montmorillonite suspension. Viscosity measurement appears to be a sensitive method for determining the state of dispersion or flocculation of the dilute montmorillonite suspension system.

PERSONNEL: F. S. Nakayama

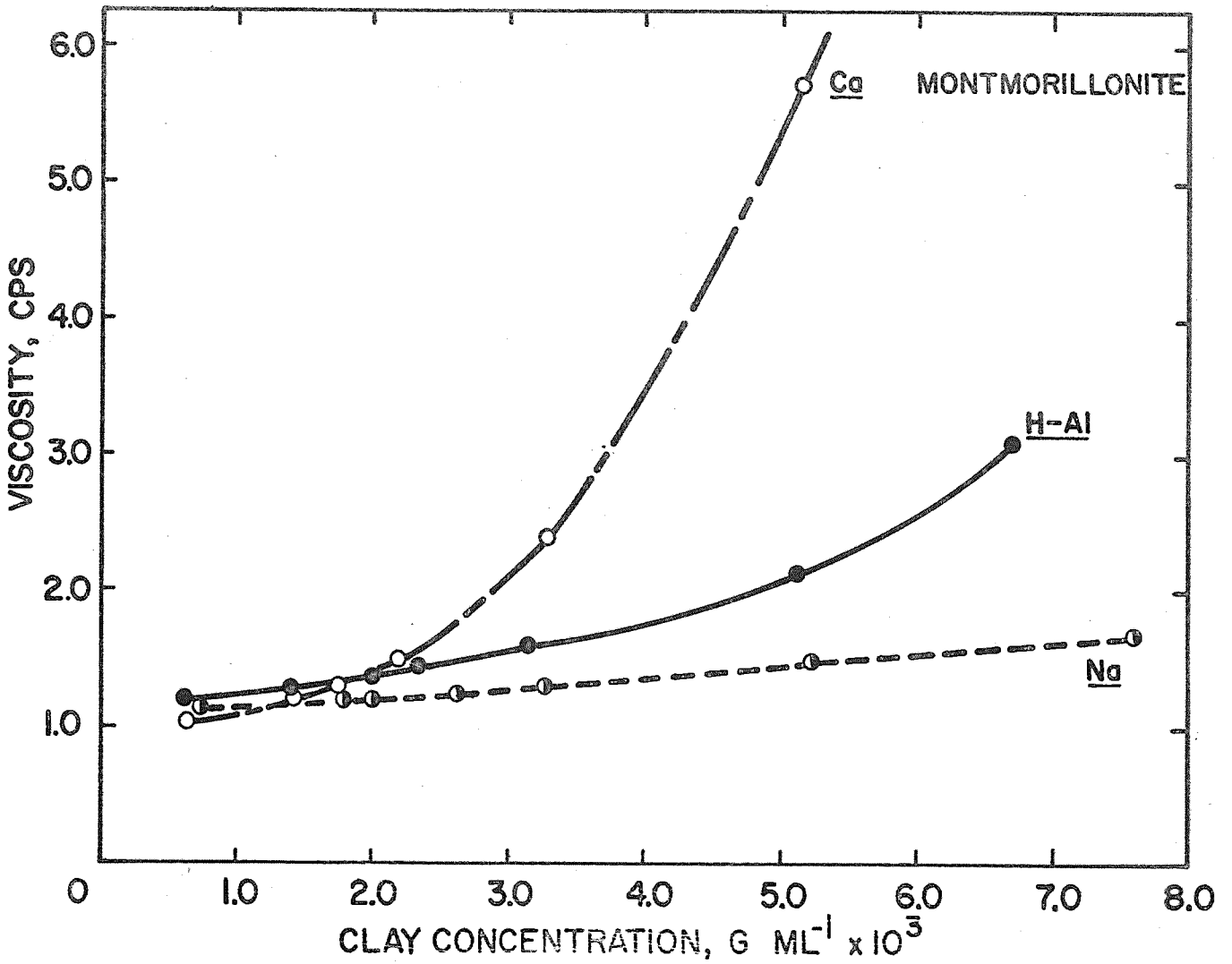

Figure 1. Viscosity of H-, Na-, & Ca-montmorillonite at different suspension concentrations at 25°C.

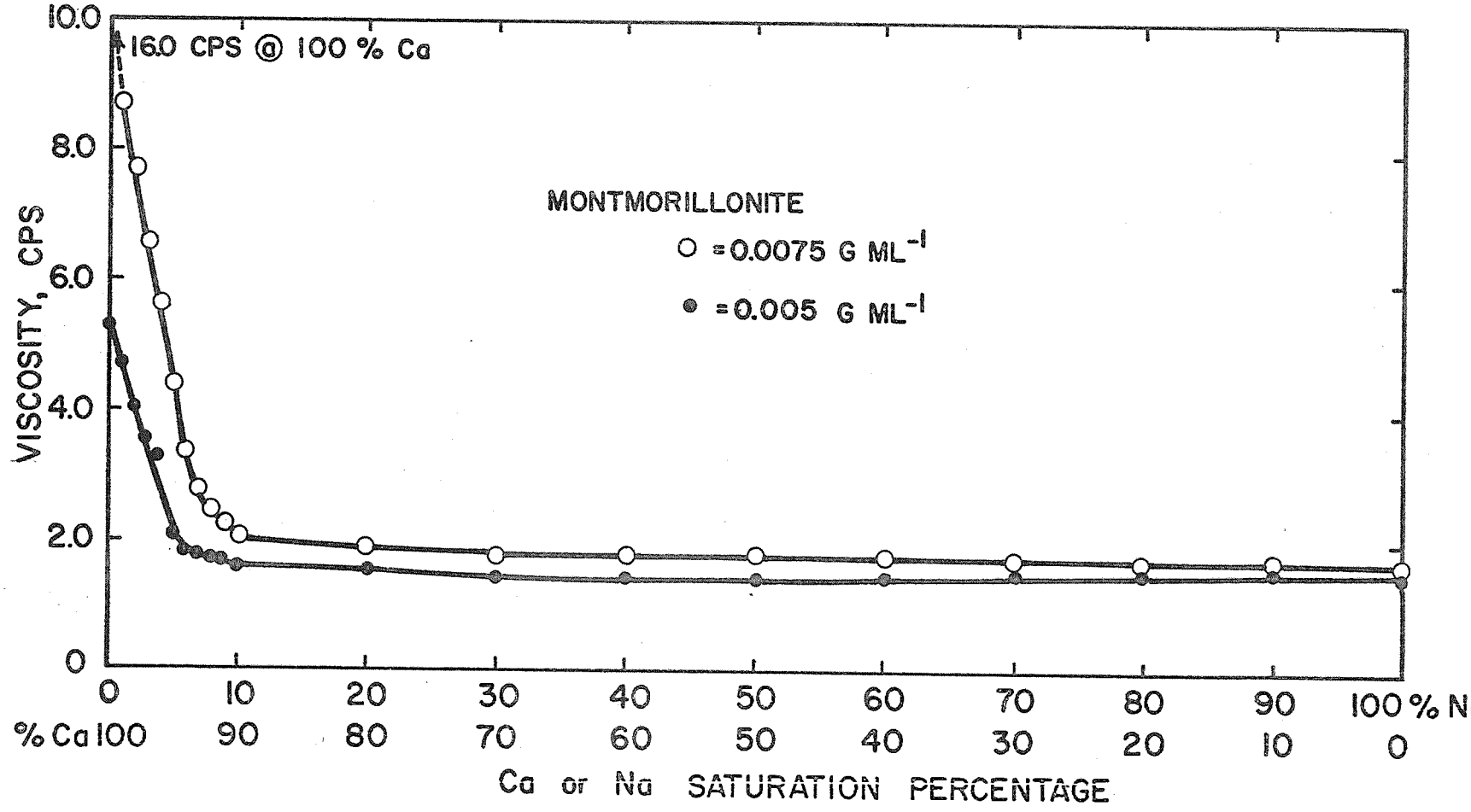

Figure 2. Viscosity of montmorillonite clay suspension at different Ca-to-Na-saturation percentage at 25°C.

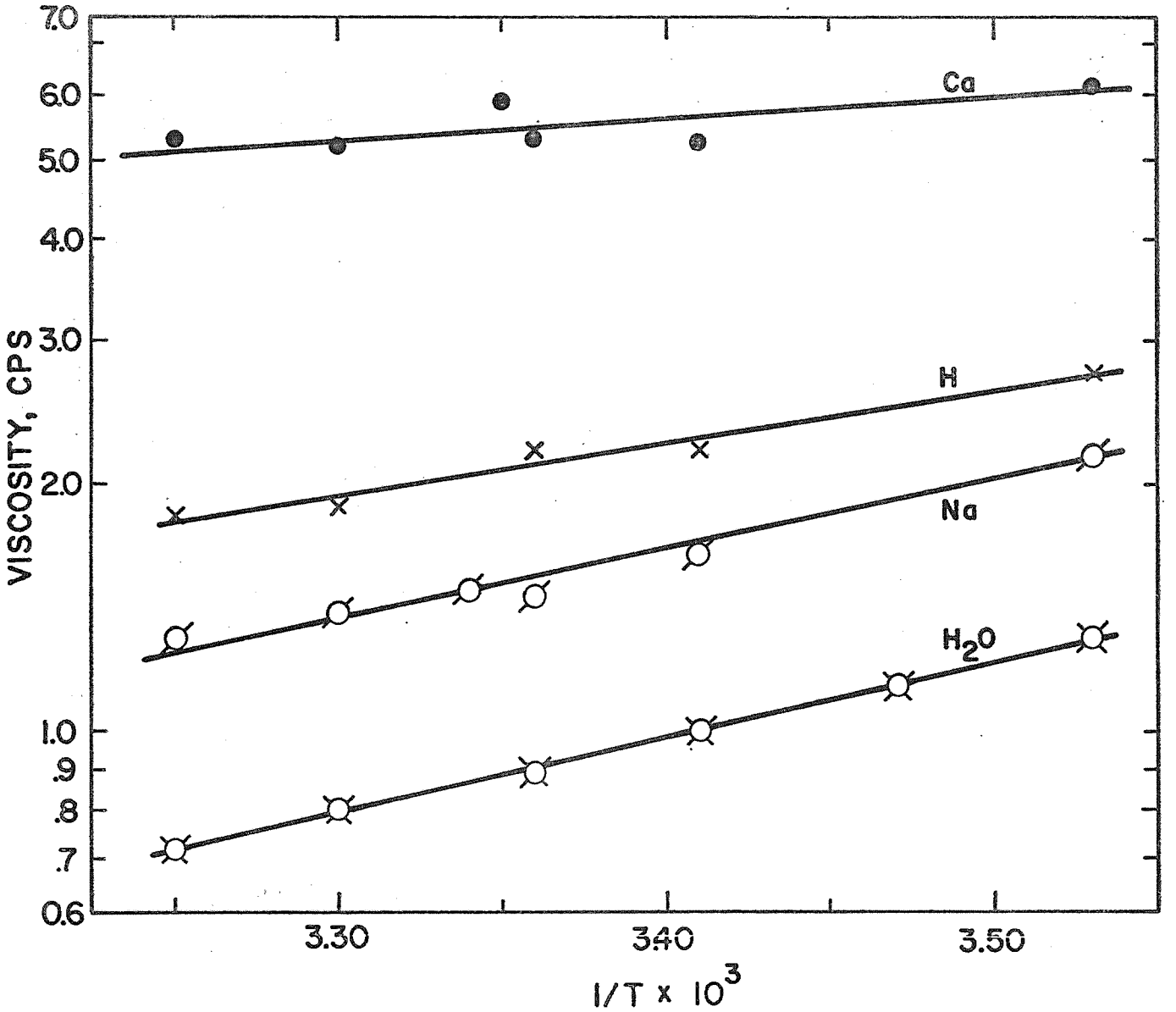

Figure 3. Temperature dependence of H-, Na- and Ca-montmorillonite suspensions.

APPENDIX I

MANUSCRIPTS APPROVED AND/OR PUBLISHED IN 1964	MS Number
Bouwer, Herman. Measuring horizontal and vertical hydraulic conductivity of soil with the double-tube method. Soil Sci. Soc. Amer. Proc. 28:19-23. 1964.	96
Bouwer, Herman, and Rice, R. C. Simplified procedure for calculation of hydraulic conductivity with the double-tube method. Soil Sci. Soc. Amer. Proc. (Note) 28:133-134. 1964.	97
Bouwer, Herman, and Rice, R. C. Seepage meters in seepage and recharge studies. Trans., Amer. Soc. Civ. Engin. 129:243-245. 1964.	118
Bouwer, Herman. Resistance network analogs for solving ground water problems. Ground Water 2(3):26-32. July, 1964.	120
Bouwer, Herman. Discussion: Seepage from Trapezoidal Channels, by El Nimr. Proc. ASCE, Jour. Engin. Mech. Div. 90(EM 2):241-243. April, 1964.	121
Bouwer, Herman. Unsaturated flow in ground water hydraulics. Proc. ASCE, Jour. Hydraul. Div. 90(HY 5):121-144. Sept. 1964.	127
Bouwer, Herman. Role of soil properties in the design and operation of surface irrigation systems.	129
Bouwer, Herman. Theoretical aspects of seepage from open channels.	131
Bouwer, Herman. Limitation of the Dupuit-Forchheimer assumption in recharge and seepage.	139
Ehrler, W. L., Van Bavel, C. H. M., and Nakayama, F. S. Transpiration, water absorption, and internal water balance of cotton plants as affected by light and changes in saturation deficit.	101
Ehrler, W. L., Nakayama, F. S., and Van Bavel, C. H. M. Cyclic changes in water balance and transpiration of cotton leaves in a steady environment.	126

	MS Number
Fritschen, Leo J., and Van Bavel, C. H. M. The energy balance as affected by height and maturity of Sudangrass. Agron. Jour. 56(2):201-204. 1964.	102
Fritschen, Leo J. Miniature net radiometer improvements.	137
Harris, K., Erie, L. J., and Fuller, W. H. Tillage in the Southwest.	107
Jackson, Ray D. Water vapor diffusion in relatively dry soil: I. Theoretical considerations and sorption experiments. Soil Sci. Soc. Amer. Proc. 28:172-176. 1964.	105
Jackson, Ray D. Water vapor diffusion in relatively dry soil: II. Desorption experiments. Soil Sci. Soc. Amer. Proc. 28:464-466. 1964.	116
Jackson, Ray D. Water vapor diffusion in relatively dry soil: III. Steady-state experiments. Soil Sci. Soc. Amer. Proc. 28:467-470. 1964.	119
Jackson, R. D., Reginato, R. J., and Van Bavel, C. H. M. Comparison of measured and calculated hydraulic conductivities of unsaturated soils.	130
Jackson, Ray D. Water vapor diffusion in relatively dry soil: IV. Temperature and pressure effects on sorption diffusion coefficients.	132
Jackson, R. D., Rose, D. A., and Penman, H. L. The circulation of water in soil under a temperature gradient.	136
Myers, Lloyd E. The conservation and beneficial use of water. Multilithed, 1964.	88
Myers, Lloyd E. Discussion: Australian policy for hydrologic education, by C. H. Munro.	124
Myers, Lloyd E. Research activities of the U. S. Water Conservation Laboratory. Minutes, 64-1 Meeting of the Pacific S. W. Inter-Agency Committee, Phoenix, Arizona, March 4, 1964.	125
Myers, Lloyd E. Potential of water salvage and re-use.	134

	MS Number
Myers, Lloyd E. Evaporation retardants: Application by means of a water soluble matrix.	140
Nakayama, F. S., and Ehrler, W. L. Beta ray gauging technique for measuring leaf water content changes and moisture status of plants. Plant Physiol. 39 (1):95-98. 1964.	100
Nakayama, F. S., Van Bavel, C. H. M., and Jackson, R. D. Tritiated water in the investigations of plant-soil-water relationships.	133
Reginato, Robert J. Evapotranspiration research at the U. S. Water Conservation Laboratory.	128
Replogle, John A., and Chow, Ven T. Tractive-force distribution in open channels.	138
Van Bavel, C. H. M. Water science needs more weather science. Crops and Soils 16(4-5):10. 1964.	114
Van Bavel, C. H. M. Letter to the editor. Scientific American 210 (2):14. 1964.	117
Van Bavel, C. H. M., Nakayama, F. S., and Ehrler, W. L. Measuring transpiration resistance of leaves.	135

Reports -- The following reports of the U. S. Water Conservation Laboratory were released during the year. Such reports are not considered as formal publications, are not distributed to libraries, and should not be cited:

Bouwer, Herman, Report of a Trip to Hawaii, Japan, Taiwan, and Australia, April 25 - June 20, 1963.

Van Bavel, C. H. M., and Fritschen, L. J., Interim Report for Meteorology Department, U. S. Army Electronics Research and Development Activity, Fort Huachuca, Arizona. Energy Balance Studies over Sudangrass, 1962. March 1964.

Bouwer, Herman, and Rice, Robert C., Basic Instructions for Falling-Head Seepage Meter Technique. WCL Report 1. 11 May 1964.

Van Bavel, C. H. M., Measuring Transpiration Resistance of Leaves. WCL Report 2. 1 December 1964.